

UNIVERSIDADE FEDERAL DE MINAS GERAIS

INSTITUTO DE CIÊNCIAS BIOLÓGICAS

PROGRAMA INTERUNIDADES DE PÓS-GRADUAÇÃO EM BIOINFORMÁTICA



Gabriel Quintanilha Peixoto

The virome of sisal (*Agave* spp.) and genomics aspects of its main pathogen, *Aspergillus welwitschiae* (Ascomycota, Trichocomaceae)

BELO HORIZONTE

2023

Gabriel Quintanilha Peixoto

The virome of sisal (*Agave* spp.) and genomics aspects of its main pathogen, *Aspergillus welwitschiae* (Ascomycota, Trichocomaceae)



Versão Final

Dissertação apresentada ao Programa Interunidades de Pós-Graduação em Bioinformática da Universidade Federal de Minas Gerais como requisito parcial para obtenção do título de Doutor em Bioinformática.

Orientador: Prof. Dr. Aristóteles Góes Neto

Coorientador: Prof. Dr. Eric R. G. R. Aguiar

BELO HORIZONTE

2023

043

Peixoto, Gabriel Quintanilha.

The virome of sisal (*Agave* spp.) and genomics aspects of its main pathogen, *Aspergillus welwitschiae* (Ascomycota, Trichocomaceae) [manuscrito] / Gabriel Quintanilha Peixoto. – 2023.

158 f. : il. ; 29,5 cm.

Orientador: Prof. Dr. Aristóteles Góes Neto. Coorientador: Prof. Dr. Eric R. G. R. Aguiar.

Tese (doutorado) – Universidade Federal de Minas Gerais, Instituto de Ciências Biológicas. Programa Interunidades de Pós-Graduação em Bioinformática.

1. Bioinformática. 2. Sisal. 3. Vírus. 4. *Aspergillus*. I. Góes Neto, Aristóteles. II. Aguiar, Eric Roberto Guimarães Rocha. III. Universidade Federal de Minas Gerais. Instituto de Ciências Biológicas. IV. Título.

CDU: 573:004



UNIVERSIDADE FEDERAL DE MINAS GERAIS
INSTITUTO DE CIÊNCIAS BIOLÓGICAS
PROGRAMA INTERUNIDADES DE PÓS-GRADUAÇÃO EM BIOINFORMÁTICA

ATA DE DEFESA DE TESE

GABRIEL QUINTANILHA PEIXOTO

Às treze horas e trinta minutos do dia **01 de agosto de 2023**, reuniu-se, no aplicativo Zoom, a Comissão Examinadora de Tese, indicada pelo Colegiado do Programa, para julgar, em exame final, o trabalho intitulado: "**The virome of sisal (*Agave spp.*) and genomics aspects of its main pathogen, *Aspergillus welwitschiae* (Ascomycota, Trichocomaceae)**", requisito para obtenção do grau de Doutor em **Bioinformática**. Abrindo a sessão, o Presidente da Comissão, **Dr. Aristóteles Góes Neto**, após dar a conhecer aos presentes o teor das Normas Regulamentares do Trabalho Final, passou a palavra ao candidato, para apresentação de seu trabalho. Seguiu-se a arguição pelos Examinadores, com a respectiva defesa do candidato. Logo após, a Comissão se reuniu, sem a presença do candidato e do público, para julgamento e expedição de resultado final. Foram atribuídas as seguintes indicações:

Professor(a)/Pesquisador(a)	Instituição	Indicação
Dr. Aristóteles Góes Neto - Orientador	UFMG	Aprovado
Dr. Eric Roberto Guimarães Rocha Aguiar - Coorientador	UESC	Aprovado
Dr. Thiago Motta Venancio	UENF	Aprovado
Dr. Rommel Thiago Juca Ramos	UFPA	Aprovado
Dr. Carlos Priminho Pirovani	UESC	Aprovado
Dra. Marcele Laux	LNCC	Aprovado
Dra. Renata Oliveira Batista	UFVJM	Aprovado

Pelas indicações, o candidato foi considerado: **Aprovado**.

O resultado final foi comunicado publicamente ao candidato pelo Presidente da Comissão. Nada mais havendo a tratar, o Presidente encerrou a reunião e lavrou a presente ATA, que será assinada por todos os membros participantes da Comissão Examinadora.

Belo Horizonte, 01 de agosto de 2023.



Documento assinado eletronicamente por **Rommel Thiago Jucá Ramos, Usuário Externo**, em 01/08/2023, às 16:43, conforme horário oficial de Brasília, com fundamento no art. 5º do [Decreto nº 10.543, de 13 de novembro de 2020](#).



Documento assinado eletronicamente por **Carlos Priminho Pirovani, Usuário Externo**, em 01/08/2023, às 17:14, conforme horário oficial de Brasília, com fundamento no art. 5º do [Decreto nº 10.543, de 13 de novembro de 2020](#).



Documento assinado eletronicamente por **Aristoteles Goes Neto, Professor do Magistério Superior**, em 01/08/2023, às 17:14, conforme horário oficial de Brasília, com fundamento no art. 5º do [Decreto nº 10.543, de 13 de novembro de 2020](#).



Documento assinado eletronicamente por **Renata Oliveira Batista, Usuário Externo**, em 01/08/2023, às 17:17, conforme horário oficial de Brasília, com fundamento no art. 5º do [Decreto nº 10.543, de 13 de novembro de 2020](#).



Documento assinado eletronicamente por **Eric Roberto Guimaraes Rocha Aguiar, Usuário Externo**, em 02/08/2023, às 07:35, conforme horário oficial de Brasília, com fundamento no art. 5º do [Decreto nº 10.543, de 13 de novembro de 2020](#).



Documento assinado eletronicamente por **Thiago Venancio, Usuário Externo**, em 04/08/2023, às 13:53, conforme horário oficial de Brasília, com fundamento no art. 5º do [Decreto nº 10.543, de 13 de novembro de 2020](#).



Documento assinado eletronicamente por **Marcele Laux, Usuário Externo**, em 09/08/2023, às 14:02, conforme horário oficial de Brasília, com fundamento no art. 5º do [Decreto nº 10.543, de 13 de novembro de 2020](#).



A autenticidade deste documento pode ser conferida no site https://sei.ufmg.br/sei/controlador_externo.php?acao=documento_conferir&id_orgao_acesso_externo=0, informando o código verificador **2495019** e o código CRC **92AEBB4F**.

ACKNOWLEDGEMENTS

O fio condutor deste trabalho teve a influência de tantas pessoas, mesmo antes do seu início. Peço perdão àqueles e àquelas que contribuíram e por acaso não forem mencionados aqui. Agradeço primeiramente à minha mãe, Danielle, e meu parceiro, Gabriel Bruno, pelo seu apoio incondicional e infinita paciência.

Agradeço ao Prof. Ari Góes Neto e Prof. Eric Aguiar, não só pela orientação, mas pelo exemplo de conhecimento, liderança, pelo respeito mútuo e profissionalismo que considero tão essenciais na ciência, e especialmente pelo apoio e compreensão para com todas as atividades de ensino e extensão em que decidi participar na UFMG, que me tornaram um profissional ainda mais sólido.

Às agências de fomento que permitiram a realização dessa pesquisa; FAPEMIG, CAPES e CNPq. Aos secretários do PPG Bioinformática, Tiago e Sheila, pelo seu trabalho excepcional.

Aos membros da banca por contribuírem neste este trabalho com suas diferentes expertises.

Na UENF, agradeço à Prof.^a Aline Intorne por ter indicado a bioinformática como uma carreira possível, e pelo seu apoio e credibilidade que me permitiram retornar à Texas A&M em 2022. Aos amigos queridos Sônia Guimarães, Anderson Ribeiro, Andressa Batista, Vitor Cyrino e Ronaldo Júnior. E também aos amigos Daniel Monteiro e Thiérri Araújo no Rio.

Aos chefes de equipe no Giz, Kênia Aulázia Herédia, Marcos Vinícius Tarquínio, e Rafaela Esteves Godinho Leal pelo conhecimento imensurável de educação superior e governança. Aos colegas do Curso de Verão em Bioinformática da UFMG e à Prof.^a Glória Regina Franco pelo espaço de criatividade. À colega de laboratório Paula Luize Fonseca por me introduzir à pesquisa com a podridão vermelha do sisal. Aos amigos da UFMG Stephane Tosta, Izabela Mamede, Daniela Pereira, Joicy Xavier, Henry Granger, e Wyll Nogueira. Aos amigos de república André Scodeler, André Fernandes, Catharina, Gabriel, Gabrielly, Gabriela, Maria Roberta, Victor, e é claro, ao melhor mascote de todos os tempos, nosso Chico Moleza.

Na Texas A&M, agradeço à Prof.^a Libo Shan e ao Prof. Ping He por me receberem em seu grupo de pesquisa mais uma vez, e por me permitirem colaborar nas pesquisas de ponta sob sua orientação. Aos colegas que confiaram em mim como colaborador; Guangchao, Yan, Sung-

Il, Liang, Catherine e F. Andres. Um agradecimento especial aos colegas Rachel Rivero e Brendan Mormile pela convivência.

Um agradecimento especial aos amigos que tornaram o Texas minha casa por 1 ano; Tatiane Cunha, Andresa Borges, Bibiana Petri, Cristiane Taniguti, Daniele Souto, Tessa Hochhaus, Tanja Stoll e Artem Bolshov. Aos amigos de Houston Ruth Barros e Luciano Branco.

Aos colegas sisaleiros Marina Marone, Fábio Raya, Juliana José, e aos produtores e trabalhadores que abriram as portas de seus sítios para nos receber, especialmente o Sr. Zé de Jorge. Um agradecimento especial à Prof.^a Ana Soares da UFRB pelo seu apoio com esta pesquisa.

*Pastora de nuvens, fui posta a serviço
por uma campina tão desamparada
que não principia e nem também termina,
e onde nunca é noite e nunca madrugada.*

– Cecília Meireles

*O que eu gosto mesmo é de já ter escrito.
E de ler, ouvir música de jazz, ficar vadiando pelo bairro onde moro
e principalmente de conversar fiado com meus amigos.*

– Fernando Sabino

RESUMO

Esta tese explora diferentes aspectos que afetam o cultivo do sisal no Brasil, com especial enfoque no viroma (conteúdo de espécies virais) das três principais variedades encontradas nos campos, e também vários aspectos genômicos do principal patógeno do sisal, *Aspergillus welwitschiae*, que podem estar relacionados com o progresso da doença. É apresentada uma descrição baseada em RNA-Seq do viroma associado a *Agave sisalana* (a principal variedade de sisal cultivada), *Agave fourcroydes* e *Agave Hybrid 11648*, duas variedades menos cultivadas, mas supostamente mais resistentes à podridão do caule de sisal. Vinte e cinco (25) espécies virais foram identificadas, sendo uma delas o *Cowpea Mild Mottle Virus* (CPMMV). As raízes geralmente são os tecidos vegetais mais diversos e ricos, provavelmente devido às associações planta-fungos. As relações filogenéticas de *A. welwitschiae* na seção Nigri do gênero *Aspergillus* foram descritas, bem como características evolutivas que afetam genes que podem desempenhar um papel relevante durante o estabelecimento e a progressão da podridão do caule do sisal. *A. welwitschiae* foi descrito como uma espécie polifilética (não foi possível definir um único ancestral comum), e diferentes genes no metabolismo primário e secundário foram identificados como estando sob seleção diversificadora. Foi desenvolvida uma patente com base na análise de ortologia do Capítulo II. Um gene codificante para uma $\Delta 1$ -pirrolina-5-carboxilato redutase (PC5R) contendo uma região única para *A. welwitschiae* foi encontrado, apesar de ser uma espécie polifilética, conforme descrito no Capítulo II. Discutimos a patogenicidade de *A. welwitschiae* através da análise do seu metabolismo secundário e seus possíveis papéis na progressão da doença, utilizando técnicas tanto moleculares como *in silico*. Vários metabólitos foram detectados através de cromatografia líquida de alto desempenho, incluindo moléculas típicas do metabolismo primário e secundário de fungos. Por fim, é apresentada uma discussão geral e observações conclusivas que combinam o conteúdo de todos os capítulos anteriores e perspectivas futuras para esta pesquisa.

Palavras-Chave: vírus, podridão vermelha do sisal, interação planta-patógeno, evolução, susceptibilidade.

ABSTRACT

This thesis examines diverse aspects impacting sisal cultivation in Brazil, with a particular focus on exploring the virome (viral species content) of the three main sisal varieties found in the fields. Additionally, it investigates various genomic facets of sisal's primary pathogen, *Aspergillus welwitschiae*, potentially linked to the progression of the bole rot disease. Utilizing an RNA-Seq-based approach, the study provides a comprehensive characterization of the virome associated with *Agave sisalana* (the main cultivated sisal variety), *Agave fourcroydes*, and *Agave* Hybrid 11648, two less cultivated varieties supposedly exhibiting higher resistance to bole rot disease. A noteworthy finding includes the identification of twenty-five (25) viral species, including the *Cowpea Mild Mottle Virus* (CPMMV), with roots demonstrating a particularly diverse and rich plant tissue attributed to plant-fungi associations. Furthermore, the research outlines the phylogenetic relationships of *A. welwitschiae* within the Nigri section of the *Aspergillus* genus, highlighting evolutionary traits impacting genes that may influence the establishment and progression of sisal's bole rot. The discovery that *A. welwitschiae* is polyphyletic (lacking a single common ancestor) and the identification of genes in primary and secondary metabolism under diversifying selection add new insights to the field. The thesis also includes the development of a patent based on the orthology analysis conducted in Chapter II, revealing a unique region in the gene coding for Δ 1-pyrroline-5-carboxylate reductase (PC5R) specific to *A. welwitschiae*, despite its polyphyletic nature. The study further investigates the pathogenicity of *A. welwitschiae* by examining its secondary metabolism and potential roles in disease progression through wet-bench and *in silico* techniques. Notably, high-performance liquid chromatography revealed various metabolites, including those typical of fungi's primary and secondary metabolism. Lastly, the thesis presents a comprehensive discussion and concluding remarks, integrating findings from all previous chapters and outlining future research perspectives in this domain.

Keywords: virus, red rot of sisal, plant-pathogen interaction, evolution, susceptibility.

LIST OF FIGURES

- Figure 1:** Sisal production (in tonnes) in the top 5 largest producers, worldwide. Records from 1961-2021. 10
- Figure 2:** Adapter from (SHAO et al., 2021). Schematic representation of effector functions during plant-fungal necrotroph interactions. 14
- Figure 3:** (A) Adapted from (GARCÍA-GUZMÁN; HEIL, 2014). Different lifestyles in plant associated fungi. (B) Adapted from (REDKAR et al., 2022). Conidia germination and plant infection by *Fusarium oxysporum*. 19

LIST OF ABBREVIATIONS AND ACRONYMS

CaM	Calmodulin
CAZy	Carbohydrate-Active Enzymes
CPMMV	<i>Cowpea Mild Mottle Virus</i>
DAMP	Damage-associated patterns
DNA	Deoxyribonucleic acid
ETI	Effector Triggered Immunity
FAOSTAT	Food and Agriculture Organization Corporate Statistical Database
HPLC-MS	High performance liquid chromatography-mass spectrometry
ITS	Nuclear ribosomal internal transcribed spacer
LysM	Lysin-rich motifs
PC5R)	Δ^1 -pyrroline-5-carboxylate reductase
PCD	Programmed cell death
PCR	Polymerase chain reaction
PTI	PAMP-Triggered Immunity
RNA	Ribonucleic acid
SMGC	Secondary Metabolite Gene Cluster
SPLD	Purple leafroll disease

TABLE OF CONTENTS

INTRODUCTION.....	12
Thesis organization	14
Chapter I – LITERATURE REVIEW	15
1.1 Plant-Pathogen Interactions.....	15
1.2 Plants as a repository for microbial and viral diversity	17
1.3 The bole rot of sisal and other diseases affecting sisal crops.....	18
1.4 <i>Aspergillus welwitschiae</i> , an opportunistic pathogen.....	19
OBJECTIVES	23
General aim.....	23
Specific aims	23
Chapter II – The Sisal Virome: Uncovering the Viral Diversity of <i>Agave</i> Varieties Reveals New and Organ-Specific Viruses.....	24
Chapter III – Phylogenomics and gene selection in <i>Aspergillus welwitschiae</i> : Possible implications in the pathogenicity in <i>Agave sisalana</i>	69
Chapter IV – Iniciadores, Kit e Método para Identificação de <i>Aspergillus Welwitschiae</i> e Diagnóstico Molecular da Podridão Vermelha de <i>Agave sisalana</i> e Seus Híbridos.	80
Chapter V – Calm Before the Storm: A Glimpse into the Secondary Metabolism of <i>Aspergillus welwitschiae</i> , the Etiologic Agent of the Sisal Bole Rot.....	117
Chapter VI – CONCLUSIONS AND PERSPECTIVES	138
REFERENCES.....	142
CURRICULUM VITAE (Lattes).....	149

INTRODUCTION

Plants are intrinsically associated with the neighboring organisms and environmental conditions in nature. When involving a plant host and one or more microorganisms, such associations are named “plant-microbe interactions” (CHENG; ZHANG; HE, 2019) or “plant-pathogen interactions” when referring specifically to the harmful effects of these microorganisms in plant hosts (ROJAS et al., 2014). Studying these associations is especially relevant in commercial crops, since the knowledge of plant-microbe interactions improves yielding by favoring beneficial interactions while avoiding pathogenic ones (MEENA et al., 2017). The lack of this knowledge increases the risks of yield losses, usually at a great economic cost (DAAMI-REMADI et al., 2011).

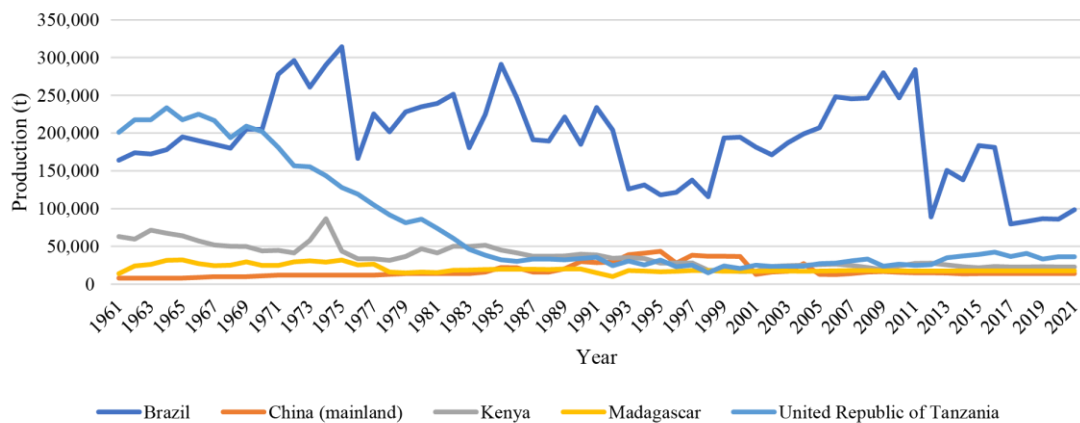


Figure 1: Sisal production (in tons) in the top 5 largest producers, worldwide. Records from 1961-2021.

Sisal is a common name for a few *Agave* species and hybrids used for the production of natural fibers deriving from their leaves (ANANDJIWALA; JOHN, 2010). *Agave sisalana* is the most widespread of these varieties, although other species such as *Agave fourcroydes* and hybrids like *Agave Hybrid 11648* and *Agave Hybrid 400 folhas* are available for cultivation (QUEIROGA et al., 2021). Since 1971, Brazil is the leading producer of sisal fibers, followed by Tanzania, Kenya, and Madagascar (East Africa), and China as the main producers (Figure 1). For its leading role as a sisal fiber producer worldwide, the Brazilian Enterprise of Agricultural Research (Embrapa) and the University of Campinas (Unicamp), maintain a sisal germplasm bank with sisal genotypes that are promising sources of disease resistance. This germplasm is mostly composed of plants with a particularly disease-resistant or unique phenotype, also deriving from small producers in Bahia, Paraíba, Pernambuco (States in

Northeast Brazil), and elsewhere. Considering the aforementioned knowledge of plant adaptation and interaction with their surrounding environment, and also the existing literature on viral diversity in plants such as pepper (JO et al., 2017), rubber tree (FONSECA et al., 2018), grapevine (COETZEE et al., 2010) and others, we hypothesized that the sisal varieties in the Embrapa germplasm plants could provide a relevant viral content that reflects its location history, pests, and associated microbiota.

Sisal fiber production is monitored by FAOSTAT (available at <<https://www.fao.org/>>), which has named it among the “Future Fibres” due to its varied uses (available at <<https://www.fao.org/economic/futurefibres/> available at <). The data compiled by FAOSTAT (Figure 1) shows a great drop in the Brazilian production of the fiber detected in 2012 and the following years as a result of a severe drought in the main sisal-producing region, in the State of Bahia (DE AZEVEDO et al., 2018; MENDONÇA, 2017). It is hypothesized that this drought has triggered an uncontrollable spread of the bole rot disease, which persists in the fields. Sisal production has never recovered to pre-2012 levels in Brazil (Figure 1). The bole rot was believed to be caused by various fungal species until 2018 when our research group confirmed *A. welwitschiae* was the true etiological agent (DUARTE et al., 2018). Two *A. welwitschiae* strains derived from this 2018 study were sequenced (CCMB 674 and CCMB 663), and have since based our research group’s research on the bole rot. *Aspergillus welwitschiae* is a common saprophytic species in stored produce, but it has also been described as a plant and human opportunistic pathogen (DE RIJK et al., 2015).

In this research, we combined different strategies, including high-throughput sequencing, -omics sciences, evolutionary models, and others to provide an overview of sisal as a plant host for neutral or pathogenic microorganisms and viruses. Our results include the first description of the virome of three different varieties of sisal (Chapter II), a new method for the detection of the pathogen in sisal samples (Chapter IV), important discoveries about the evolution of this pathogen (Chapter III), and possible strategies for fungal infection and colonization of the plant host (Chapter III, Chapter VI).

Thesis organization

This thesis explores different aspects affecting sisal cultivation in Brazil, especially the virome (viral species content) of the three main varieties found in the fields, and also various genomic aspects of sisal's main pathogen, *Aspergillus welwitschiae*, which could be related to the disease progress.

Chapter I outlines relevant scientific concepts and published research that lays the theoretical basis for the following chapters. This literature review is centered on the interactions of plants with biotic and abiotic factors and the implications of these interactions for plant susceptibility to diseases and yield loss.

Chapter II brings an RNA-Seq-based description of the virome associated with *Agave sisalana* (the main cultivated sisal variety), *Agave fourcroydes*, and *Agave* Hybrid 11648, two less cultivated varieties but supposedly more resistant to the bole rot disease. Twenty-five (25) viral species could be identified, one being the Cowpea Mild Mottle Virus (CPMMV). Roots are generally the most diverse and rich plant tissue, likely due to plant-fungi associations.

Chapter III describes the phylogenetic relationships of *A. welwitschiae* in the Nigri section of the genus *Aspergillus*, and also evolutionary traits affecting genes that could play a role during the establishment and progression of the bole rot of sisal. *A. welwitschiae* was found to be polyphyletic (a single common ancestor could not be defined), and different genes in the primary and secondary metabolism were detected to be under diversifying selection.

Chapter IV is a patent based on the orthology analysis of Chapter II. We found a gene coding for a Δ^1 -pyrroline-5-carboxylate reductase (PC5R) containing a region unique to *A. welwitschiae*, even though this is a polyphyletic species, as described in Chapter II.

Chapter V discusses the pathogenicity of *A. welwitschiae* through the lenses of its secondary metabolism and its possible roles in disease progression, using both wet-bench and *in silico* techniques. Various metabolites were detected through high-performance liquid chromatography, including typical molecules of the primary and secondary metabolism of fungi.

Finally, Chapter VI presents an overall discussion and conclusion remarks combining the content of all previous chapters and open perspectives for this research.

Chapter I – LITERATURE REVIEW

1.1 Plant-Pathogen Interactions

In nature, plants, like most organisms, do not live isolated but rather in association with other living organisms and the abiotic conditions that surround them. This delicate balance might either provide ideal conditions for plants to thrive or challenging conditions that might push them to decay (CHENG; ZHANG; HE, 2019). Microorganisms play a key role in interactions with plants. Beneficial interactions include microbes that form intricate symbiotic relationships with their plant hosts, such as rhizobia or ectomycorrhizal fungi (SANTOYO et al., 2016). In addition, neutral/beneficial interactions include the recycling of organic matter provided by saprophytic microorganisms, that feed off the dead plant matter (VAZ et al., 2020). Nonetheless, under specific host susceptibility or aggravating environmental conditions, pathogenic microorganisms thrive. These might be the same species that form either beneficial or neutral interactions with plant hosts, or strict pathogenic species and strains (DELAYE; GARCÍA-GUZMÁN; HEIL, 2013).

Symbiotic and pathogenic fungi share many similarities. Both use plants as a source of nutrients and a living environment (DUTTA et al., 2014), and both have to dodge the plant strategies for pathogen recognition and control (YAN et al., 2019). Even though symbionts might possess plant growth-promotion traits, some endophytes might be dormant, not contributing positively to the plant metabolism (SIEBER, 2007). Thus, the establishment of pathogenesis could be understood as the greatest divide between those two groups; while symbionts thrive in plant tissues while not causing visible symptoms (FESEL; ZUCCARO, 2016), pathogens are required to cause disease to complete their life cycle or to adequately exploit plant nutrients (RODRIGUEZ-MORENO et al., 2018). Pathogens are usually divided into three categories; Necrotrophs, which kill the infected plant tissue to feed off it, biotrophs, which feed on the living plant tissue, and hemibiotrophic species, which switch from a biotrophic lifestyle to necrotrophy at a given stage. In complementation to those, saprophytic fungi, which feed off dead plant matter, often switch to a pathogenic lifestyle in damaged or weak plants (HORBACH et al., 2011; LORANG, 2019).

To fight pathogens or even to keep symbionts under control, plants possess a complex immune system composed of broad and pathogen-specific receptors and signaling cascades with different outcomes, even though there are no mobile or immunity-specialized cells. In

summary, this immune response has been historically divided into a broad first line of response (PAMP-Triggered Immunity – PTI) and a second line, usually more specific, triggered by proteins from the pathogen that target the effect of the first line of defense (Effector Triggered Immunity – ETI). In the context of fungal pathogens, PTI is triggered by intrinsic fungal molecules like chitin, and plant molecules produced when the cell environment is disrupted, named damage-associated patterns (DAMPs).

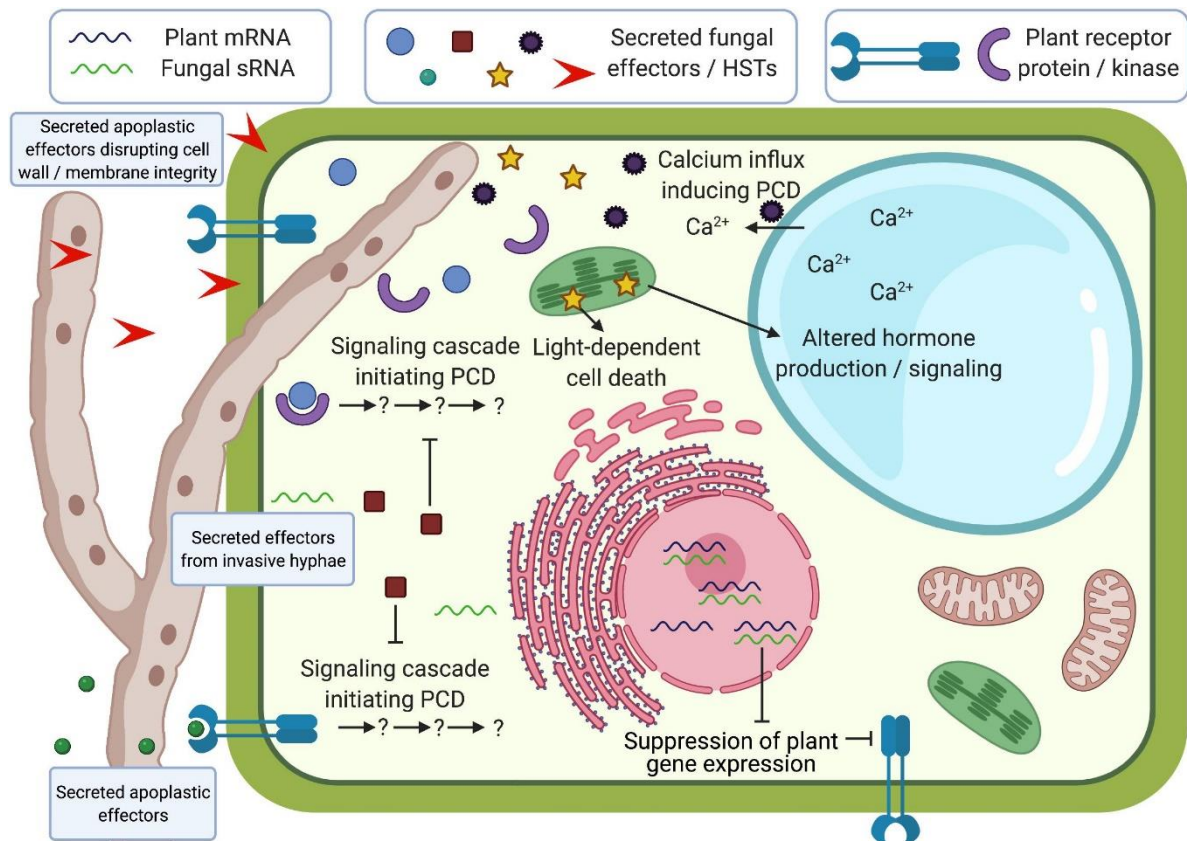


Figure 2: Adapter from (SHAO et al., 2021). Schematic representation of effector functions during plant-fungal necrotroph interactions.

Figure 2 provides a schematic overview of an interaction between a plant and a necrotrophic pathogen (SHAO et al., 2021). When infecting a host, fungi will secrete a broad set of proteins, including effectors and host-selective toxins (HSTs) targeting different regions of the plant cell environment, such as the apoplast (green dots) and the cell wall (red arrows). Such effectors include cellulases and pectin degrading enzymes (TAYI et al., 2016), and other proteins targeting the plant cytoplasm (other shapes). The main current effector protein predictor, EffectorP v3.0, is capable of differentiating between cytoplasmatic and apoplastic effectors (SPERSCHNEIDER; DODDS, 2021). Various fungal species form a specialized structure called appressoria to secrete proteins once the host cytoplasm is reached (DEMOOR;

SILAR; BRUN, 2019), but that is not the case in this example. The authors also highlight the delivery of non-coding small RNA molecules that will directly modulate plant transcription, which is a more recent discovery in comparison to the other strategies and responses shown in this scheme (SHAO et al., 2021). Fungal effectors will disrupt photosynthesis, the Ca^{2+} influx, and phytohormone production. Plant responses in ETI culminate with the hypersensitivity response, a type of localized programmed cell death (PCD) that is ideal for necrotrophic fungal pathogens, which will feed on the recently killed plant tissue (LI et al., 2015).

1.2 Plants as a repository for microbial and viral diversity

Considering the aforementioned settings in plant cell environments and their molecular response to the presence of microbes, why would it be advantageous for microorganisms to live inside a plant host? Microorganisms favor that interaction because a plant host provides much more favorable conditions than aquatic, air, or even soil environments. For instance: the microbial community in the rhizosphere (the area of influence of plant roots) is usually shaped through root exudates, meaning compounds such as sugars, amino acids, and organic compounds secreted from the roots to soil (CANARINI et al., 2019). On the other hand, the harsh conditions in the soil might lead to dormancy (LEBEIS, 2015). Thus, for soil microorganisms, being in the rhizosphere means greater nutrient availability. Nonetheless, under the incredibly large spectrum of interactions between plant hosts and microbes, there are a large number of dormant microorganisms and viruses that neither cause disease nor improve plant resistance or environmental adaptation (BOWSHER; KEARNS; SHADE, 2019). For being cryptic, these interactions often go unnoticed, which does not mean, necessarily, that these interactions do not provide the plant hosts with advantages or disadvantages (ESPERSCHÜTZ et al., 2009). As mentioned in the previous topics, associated microorganisms and viruses might help plants better adapt/resist pathogens or adverse conditions by conferring them with better access to water and minerals but also by causing pathogenesis in harmful microorganisms (MUÑOZ-ADALIA; FERNÁNDEZ; DIEZ, 2016). For instance, an associated mycovirus that does not harm a beneficial or neutral fungal species associated with a given plant host might affect a pathogen, thus, providing that plant species with higher resistance to that pathogen (LIU et al., 2019a). Even so, that still means that several microbial interactions will be neutral or even dispensable most of the time. Either way, those neutrally associated microorganisms and viruses help us understand plants as a possible harbor of microbial and

viral diversity, which might reflect the environment in which they occur, including biotic and abiotic factors, soil conditions, and vector occurrence.

Studying viromes in plant species comprises the obvious perspective of viruses as plant pathogens as they cause great losses in yield (COETZEE et al., 2010). Nonetheless, viruses affect all known clades, including bacteria, fungi, protists, and so on (CORREA et al., 2021). Hence, plant viromes might provide a broad description of a plant host as a microenvironment in which many types of different microbial interactions may occur. Some of those might not even be directly implicated with plant metabolism (CHIAPELLO et al., 2020).

1.3 The bole rot of sisal and other diseases affecting sisal crops

According to Embrapa, the only current relevant disease of sisal in Brazil is bole rot, caused by *Aspergillus welwitschiae*, and to a much less extent, the anthracnose caused by *Colletotrichum agaves* (SUINAGA; COUTINHO; SILVA, 2021). Bole rot (often referred to as red rot and variations of those names) is a fungal disease affecting the stems of sisal plants, especially *Agave sisalana*, which is currently the most widespread variety in the fields. The current hypothesis for infection is that the fungus invades the plant through wounds in the leaf basis (DUARTE et al., 2018) since the stem of *Agave sisalana* and similar species is mostly covered by the leaf's rosette, remaining covered by the dry leaf basis after excision. The publication that first described *A. welwitschiae* as the causative agent describes disease incidence of up to 40% in some farms (DUARTE et al., 2018), which highlights this as a relevant phytosanitary matter in sisal cultivation. As aforementioned, Tanzania and China are 2nd and 5th top sisal-producing nations worldwide (FAOSTAT, available at <<https://www.fao.org/>>). Although bole rot is also a limitation in those countries, other diseases affect their sisal farms and might eventually reach Brazilian fields.

The anthracnose caused by *C. agaves* has also been reported in *Agave angustifolia* in Brazil (ARAÚJO et al., 2021), of which *Agave fourcroydes* is a domesticated version (COLUNGA-GARCÍAMARÍN, 2015). Another publication studying Chinese sisal fields describes similar symptoms in *A. sisalana* caused by *Neoscytalidium dimidiatum* (XIE et al., 2021). According to both Brazilian and Chinese publications, the symptoms include a dark brown, circular, water-soaking spot.

Considering the rise of Hybrid 11648 as an alternative sisal variety due to its increased resistance to bole rot, research on the zebra stripe caused by *Phytophthora nicotianae* becomes especially relevant. Although there are no reports on the occurrence of *P. nicotianae* on sisal, this fungus occurs in Brazil as a pathogen in periwinkle (*Vinca rosea*) (REIS; HENRIQUE, 2007) and black wattle (SANTOS; LUZ; SOUZA, 2005). *Agave* Hybrid is already the main cultivar in China and Tanzania (GAO et al., 2014), which helps explain the low interest in the bole rot disease in these countries. In the zebra stripe of Hybrid 11648, dark spots in the leaf surface increase in size and spread toward the stem (GAO et al., 2012), which is also where *A. welwitschiae* concentrates. Nonetheless, the zebra stripe is associated with wet seasons (GAO et al., 2012, 2014) while the bole rot is associated with drought periods (DAMASCENO et al., 2019).

Two recent scientific publications research the sisal purple leafroll disease (SPLD) (WANG et al., 2022, 2023). According to the authors, this disease is very destructive in Chinese sisal crops due to a mealybug infestation (REN, 2013). In this disease, leaf tips turn purple or yellow, roll, and dry out. Although the etiology is not resolved, the authors have detected phytoplasmas in affected samples (WANG et al., 2022, 2023). Finally, sparse scientific research on the sisal fields of Tanzania describes a disease called “Korogwe Leaf Spot” (KIMARO; MSANYA, 1994). The etiological agent could be either a virus (MPUNAMI, 1986) or a fungal pathogen (MTUNG’E et al., 2014), and there is no further information publicly available online.

1.4 *Aspergillus welwitschiae*, an opportunistic pathogen

Aspergillus welwitschiae is a filamentous fungal species in the genus *Aspergillus* (Trichocomaceae, Ascomycota). This is an asexual species (anamorph), and like other black aspergilli, it does not have a known teleomorph stage (VARGA et al., 2014). Mating in this genus is often elusive (SEEKLES et al., 2022). *A. welwitschiae* is undistinguishable from various other black aspergilli, unless through the use of molecular techniques, such as PCR and DNA sequencing, which has led to years of misidentification of this species often confused with *Aspergillus niger*, which also shares an almost identical ecological niche (MASSI et al., 2016). Over the next paragraphs, we will review the published research on *A. welwitschiae* and its incredible niche plasticity, focusing on its role as an opportunistic pathogen in plants.

A. welwitschiae was named after its role as a pathogen in *Welwitschia mirabilis* in the Namib Desert (Namibia, Southwest Africa). The earliest mention of this nomenclature dates back to 1969, in a publication describing a disease associated with the female cones on the plant (*W. mirabilis* is a gymnosperm) (GIESS, 1969). Nonetheless, this scientific article was probably lost or inaccessible for years, and the fungus causing disease in *W. mirabilis* has been referred to as *A. niger* var. *phoenicis* (WHITAKER; PAMMENTER; BERJAK, 2008) or simply *A. niger* (PEKAREK; JACOBSON; DONOVAN, 2006). *A. welwitschiae* has also been referred to by the synonym *Aspergillus awamori* (PERERA et al., 2021), especially in biotechnology research, which we will discuss later. Under its current name, *A. welwitschiae* is known for its post-harvest occurrence in food stocks, affecting a vast array of produce including nuts, coffee, grapes, cocoa (LAMBONI et al., 2016; MASSI et al., 2016), onions (MASSI et al., 2020), cabbage (LI et al., 2023b), and corn (SUSCA et al., 2014). Saprotrophy is a common trait of species in the genus *Aspergillus* (CLEVELAND et al., 2009; LIU et al., 2017; PFLIEGLER et al., 2020) and in the family Trichocomaceae (BEULE et al., 2017; DISKIN et al., 2017). This lifestyle switch that categorizes *A. welwitschiae* as an opportunistic pathogen in sisal (DUARTE et al., 2018) is also discussed elsewhere (LIU et al., 2017; PFLIEGLER et al., 2020).

It is also important to make a brief note on the application of *A. welwitschiae* as a biofactory. This use of this fungal species dates as far back as 1966 (WANG, 1966), and is especially common under the synonym “*Aspergillus awamori*”, being in use to this day (LI et al., 2023a). The application of *A. welwitschiae* in biotechnology studies is usually related to the optimization of the degradation of complex carbon molecules and raw waste (BASHEER et al., 2011; BOTELLA et al., 2005; SHIN et al., 2019) or to the production of enzymes serving that purpose, such as amylases, proteases (NEGI; BANERJEE, 2009), and xylanases (SOLÓRZANO LEMOS et al., 2000). There is also research on phosphate solubilization by *A. welwitschiae* (MITTAL et al., 2008), which is related to its role as an endophyte, described in more detail later in this topic. There is also research on the benefits of *A. welwitschiae* as a replacement for antibiotics in poultry (SALEH et al., 2011, 2014).

Besides the genus *Aspergillus*, some other opportunistic fungal pathogens are included in the genera *Fusarium* (MADRIZ-ORDEÑANA et al., 2019; SOLÍS-GARCÍA et al., 2021), *Alternaria* (TAHERI; KAKOOEE, 2017), *Lasiodiplodia* (SOLÍS-GARCÍA et al., 2021), and *Corynespora* (MADRIZ-ORDEÑANA et al., 2019). An opportunistic pathogen could be an endophyte or saprotroph that switches to a pathogenic lifestyle under specific conditions, meaning that they are not obligate pathogens. In sisal, this is associated with abiotic stresses

that weaken the plants (DUARTE et al., 2018). Nonetheless, while in field work, our research group noticed that the disease also affects mature plants in blooming stages and large complexes of mother plants and suckers (sisal also propagates asexually through rhizomes) (DEBNATH et al., 2010). Such plants are discarded from our experimental designs since this presents a clear selection bias.

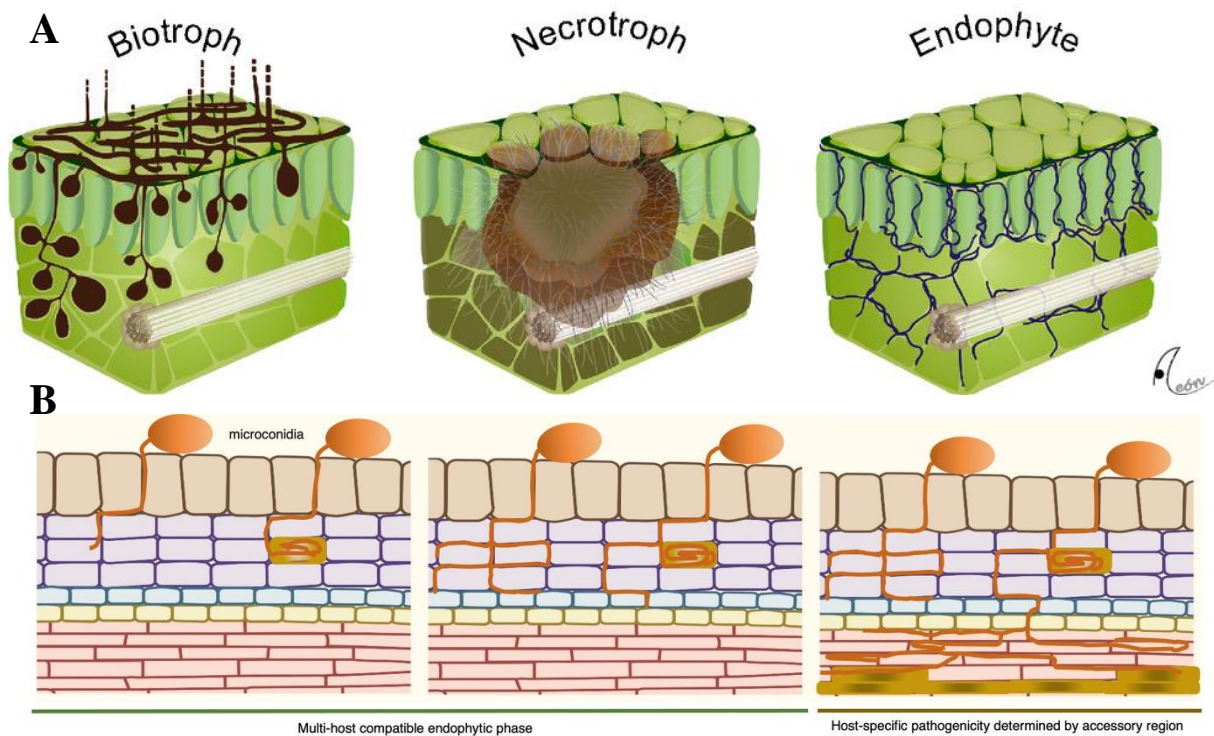


Figure 3: (A) Adapted from (GARCÍA-GUZMÁN; HEIL, 2014). Different lifestyles in plant associated fungi. (B) Adapted from (REDKAR et al., 2022). Conidia germination and plant infection by *Fusarium oxysporum*.

Not surprisingly, all aforementioned opportunistic pathogens are necrotrophic (Figure 3A) such as *A. welwitschiae* (CIPRIANO et al., 2015; COLOU et al., 2019; RIBEIRO et al., 2021; STONE et al., 2000). Although elusive and multifaceted, the link between saprotrophy and necrotrophy is not new (LEWIS, 1973), and it seems to be connected with the content of carbohydrate metabolism-related enzymes (ZHAO et al., 2013). Carbohydrate-Active Enzymes (CAZy) and Secondary Metabolite Gene Clusters (SMGCs) are two examples of strategic groups of proteins that are required throughout different life stages and trophic modes in fungi, which makes those proteins a common research target. Classic examples of those enzyme classes are cell wall-degrading enzymes (including ligninases, cellulases, and pectate lyases) (KUBICEK; STARR; GLASS, 2014) and mycotoxins clusters (WU et al., 2011), for CAZy and SMGCs, respectively. Sometimes the concepts of CAZy and SMGCs is overlapped and mixed

with the concept of effector proteins, which are any protein that modulates, directly or indirectly, the plant immune responses. Classical fungal effectors include chitinases, lysin-rich motifs (LysM), and others (CEN et al., 2017; PRITSCH; GARBAYE, 2011).

A. welwitschiae has also been described in the literature as an endophyte in three of the most relevant commercial crops; rice (LIU et al., 2019b; XIANG et al., 2020), soybean (HUSNA et al., 2022), and maize (GUL et al., 2023). This reinforces the genome plasticity in this species. Even though Duarte et al. (2018) managed to isolate *A. welwitschiae* from the soil around the root zone of *Agave sisalana* and also proved that the disease can be established from wounds in the leaf basis, it would not be mutually exclusive that *A. welwitschiae* is part of the healthy microbiota of sisal and is also switching from an endophytic to a necrotrophic lifestyle besides switching from saprotrophy in the soil (Figure 3A). The presence of *A. welwitschiae* in the soil would also agree with the model for *Fusarium oxysporum* presented by Redkar et al. (2022) (Figure 3B). In this hypothesis, the fungal spores around the root surface start developing hyphae toward the root center, triggered by root signals (1st figure). An endophytic phase follows, in which the fungus survives in the apoplast and explores the plant tissue using CAZy (2nd figure). Finally, a necrotrophic phase is established when the fungus reaches the epidermis and the xylem (3rd figure). In the case of *A. welwitschiae* in sisal, we also know that there is a tropism to the bole (stem), which is sugar-rich, and that disease symptoms are delimited to that tissue.

OBJECTIVES

General aim

This research aimed to describe new and known species directly and indirectly associated with sisal (*Agave sisalana*, *Agave fourcroydes*, and *Agave* Hybrid 11648), and bring relevant aspects of its main pathogen, *Aspergillus welwitschiae* through *in silico* and molecular techniques.

Specific aims

- Describe the viral content associated with sisal plants through transcriptomics (RNA-Seq);
- Understand the intra- and interspecies relationships of the sisal pathogen *Aspergillus welwitschiae* through phylogenomics;
- Screen genes under positive selection in this fungal pathogen that could have a role in disease progression through functional annotation and adequate evolutionary models;
- Create a molecular marker for the presence of the pathogen based on unique genomic regions through orthology tests;
- Describe the secondary metabolism gene clusters in the genome of the pathogen, highlighting shared and unique clusters through functional annotation;
- Verify secondary metabolites produced under common cultivation conditions through high-performance liquid chromatography (HPLC).

Chapter II – The Sisal Virome: Uncovering the Viral Diversity of *Agave* Varieties Reveals New and Organ-Specific Viruses.

RESUMO: Sisal é um nome comum para diferentes variedades de plantas do gênero *Agave* (especialmente *Agave sisalana*) usadas para a extração de fibras naturais de folhas de alta qualidade. Apesar do valor econômico dessas plantas, ainda falta informação sobre a diversidade de vírus (viroma) em espécies não-*tequilana* do gênero *Agave*. Neste trabalho, por meio da associação de sequenciamento profundo de RNA e DNA, fomos capazes de identificar 25 espécies virais putativas infectando *A. sisalana*, *A. fourcroydes* e *Agave* Híbrido 11648, incluindo uma cepa de *Cowpea Mild Mottle Virus* (CPMMV) e 24 elementos provavelmente representando novos vírus. A análise filogenética indicou que eles pertencem a pelo menos seis famílias virais: Alphaflexiviridae, Betaflexiviridae, Botourmiaviridae, Closteroviridae, Partitiviridae, Virgaviridae, e três grupos distintos não classificados. Observamos maior riqueza de táxons virais nas raízes em comparação com folhas e caules. Além disso, folhas e caules são muito semelhantes em termos de diversidade, com um número menor de táxons e predominância de uma única espécie viral. Finalmente, aproximadamente 50% dos vírus identificados foram encontrados em todos os órgãos de *Agave* investigados, o que sugere que provavelmente causam uma infecção sistêmica. Este é o primeiro estudo de metatranscriptômica focado na identificação viral em espécies do gênero *Agave*. Apesar de termos analisado indivíduos assintomáticos, identificamos diversos vírus que supostamente infectam espécies de *Agave*, incluindo espécies específicas de órgãos e sistêmicas. Surpreendentemente, alguns desses vírus putativos provavelmente estão infectando microrganismos que compõem a microbiota da planta. Como um todo, nossos resultados reforçam a importância de estratégias imparciais para a identificação e monitoramento de vírus em espécies vegetais, inclusive aquelas com fenótipos assintomáticos.

Palavras-chave: viroma; metatranscriptômica; *Agave*.



Article

The Sisal Virome: Uncovering the Viral Diversity of *Agave* Varieties Reveals New and Organ-Specific Viruses

Gabriel Quintanilha-Peixoto ¹, Paula Luize Camargos Fonseca ¹ , Fábio Trigo Raya ² , Marina Pupke Marone ² , Dener Eduardo Bortolini ¹, Piotr Mieczkowski ³, Roenick Proveti Olmo ^{1,4} , Marcelo Falsarella Carazzolle ², Christian A. Voigt ⁵, Ana Cristina Fermino Soares ⁶, Gonçalo Amarante Guimarães Pereira ², Aristóteles Góes-Neto ^{1,*} and Eric Roberto Guimarães Rocha Aguiar ^{7,*}

¹ Institute of Biological Sciences, Universidade Federal de Minas Gerais, Belo Horizonte 31270-901, Brazil; gabrielqpx@ufmg.br (G.Q.-P.); camargos.paulaluize@gmail.com (P.L.C.F.); gigatonn@gmail.com (D.E.B.); Roenick@gmail.com (R.P.O.)

² Department of Genetics and Evolution, Institute of Biology, Universidade Estadual de Campinas, Campinas 13083-872, Brazil; fabioraya@gmail.com (F.T.R.); marina.marone@gmail.com (M.P.M.); mcarazzo@unicamp.br (M.F.C.); goncalo@unicamp.br (G.A.G.P.)

³ High-Throughput Sequencing Facility, School of Medicine, University of North Carolina at Chapel Hill, Chapel Hill, NC 27516, USA; Piotr_Mieczkowski@med.unc.edu

⁴ CNRS UPR9022, INSERM U1257, Université de Strasbourg, 67084 Strasbourg, France

⁵ BASF Innovation Center Gent, 9052 Gent, Belgium; christian.voigt@basf.com

⁶ Center of Agricultural, Environmental and Biological Sciences, Universidade Federal do Recôncavo da Bahia, Cruz das Almas 44380-000, Brazil; acsoares@ufrb.edu.br

⁷ Center of Biotechnology and Genetics, Department of Biological Science, Universidade Estadual de Santa Cruz, Ilhéus 45662-900, Brazil

* Correspondence: arigoesneto@icb.ufmg.br (A.G.-N.); ericgdp@gmail.com (E.R.G.R.A.)



Citation: Quintanilha-Peixoto, G.; Fonseca, P.L.C.; Raya, F.T.; Marone, M.P.; Bortolini, D.E.; Mieczkowski, P.; Olmo, R.P.; Carazzolle, M.F.; Voigt, C.A.; Soares, A.C.F.; et al. The Sisal Virome: Uncovering the Viral Diversity of *Agave* Varieties Reveals New and Organ-Specific Viruses. *Microorganisms* **2021**, *9*, 1704. <https://doi.org/10.3390/microorganisms9081704>

Academic Editors: Dániel Cadar and Krisztián Bányai

Received: 31 May 2021

Accepted: 1 August 2021

Published: 10 August 2021

Publisher's Note: MDPI stays neutral with regard to jurisdictional claims in published maps and institutional affiliations.



Copyright: © 2021 by the authors. Licensee MDPI, Basel, Switzerland. This article is an open access article distributed under the terms and conditions of the Creative Commons Attribution (CC BY) license (<https://creativecommons.org/licenses/by/4.0/>).

Abstract: Sisal is a common name for different plant varieties in the genus *Agave* (especially *Agave sisalana*) used for high-quality natural leaf fiber extraction. Despite the economic value of these plants, we still lack information about the diversity of viruses (virome) in non-*tequilana* species from the genus *Agave*. In this work, by associating RNA and DNA deep sequencing we were able to identify 25 putative viral species infecting *A. sisalana*, *A. fourcroydes*, and *Agave* hybrid 11648, including one strain of *Cowpea Mild Mottle Virus* (CPMMV) and 24 elements likely representing new viruses. Phylogenetic analysis indicated they belong to at least six viral families: Alphaflexiviridae, Betaflexiviridae, Botourmiaviridae, Closteroviridae, Partitiviridae, Virgaviridae, and three distinct unclassified groups. We observed higher viral taxa richness in roots when compared to leaves and stems. Furthermore, leaves and stems are very similar diversity-wise, with a lower number of taxa and dominance of a single viral species. Finally, approximately 50% of the identified viruses were found in all *Agave* organs investigated, which suggests that they likely produce a systemic infection. This is the first metatranscriptomics study focused on viral identification in species from the genus *Agave*. Despite having analyzed symptomless individuals, we identified several viruses supposedly infecting *Agave* species, including organ-specific and systemic species. Surprisingly, some of these putative viruses are probably infecting microorganisms composing the plant microbiota. Altogether, our results reinforce the importance of unbiased strategies for the identification and monitoring of viruses in plant species, including those with asymptomatic phenotypes.

Keywords: virome; metatranscriptomics; *Agave*

1. Introduction

Sisal is a common name for different species and hybrid varieties in the genus *Agave* (especially *Agave sisalana*) cultivated worldwide for the production of hard natural fibers [1,2]. In Brazil, the greatest producer of sisal fibers, sisal-producing areas are concentrated in the Northeastern region of the country, especially in the state of Bahia [3],

followed by the states of Paraíba and Pernambuco [4]. The semi-arid portion of this region, known as the *Caatinga* biome, bears a high richness of highly adapted species, in all the domains of life [5,6]. Although the cultivated *Agave* species are not native to that region, they are adapted to the specific environmental conditions of this area, including low rainfall, high temperatures, and low aboveground biomass coverage [7]. These traits of resistance to abiotic stresses make sisal one of the few cultivation options available in the *Caatinga* biome, historically neglected in infrastructure projects.

Viral infections in plants may cause damage to specific structures, such as the photosynthetic apparatus in the leaves [8], the roots system [9], and also in growth and development, as in early flowering, often used to accelerate yielding [10]. In sisal, these forms of damage could harm fiber quality, which is the main commercial and valuable trait in these *Agave* species. Studies in other economically important plants, such as grapevine, revealed that the viral diversity goes beyond pathogenic species, which broadens our knowledge of plant viruses [11,12]. Therefore, the study of neglected cultures could provide not only a better perspective of viral diversity in economically relevant individuals and related species but also a glimpse of the real circulation of viruses in the region where it is grown.

Sisal and other plants, as all known domains of life, are susceptible to viral infection. Nonetheless, the knowledge on viruses infecting non-*tequilana* species in the genus *Agave* is very scarce and restricted to low-throughput strategies, with only a few published articles describing infections on sisal until this date. Pinkerton and Bock (1969) [13] indicated (but did not confirm) viruses as the causative agent of the parallel streak of sisal in Kenya; Galvez et al. (1977) [14] described the *Necrotic streak virus* in the genus *Furcraea* (not to be confused with *Agave fourcroydes*, one of the plant taxa in the present study), later described in-depth by Morales et al. (1992) [15]; and Izaguirre-mayoral et al. (1995) [16], which described the infection of *Cactus X virus* on *A. sisalana*. In a more recent record, Chabi-Jesus et al. (2019) [17] described the presence of the *Citrus Chlorotic Spot virus* in *Agave desmettiana* individuals. Hence, the real diversity of viruses associated with sisal and its respective associated In these cases, different metagenomics strategies have been applied, including small RNA (sRNA) sequencing [18–21], DNA sequencing [22], simultaneous extraction of microorganisms and surroundings is still unclear. As mentioned before, different works in other plant species show an abundant viral diversity, such as those observed in lilies [20], grapevines [23], and peaches [24], including those of viruses infecting plant-associated microorganisms [25,26]. DNA and RNA followed by digestion with RNases/DNases [27], and even amplification-based methods [28]. Among them, the next-generation sequencing of RNA (metatranscriptomics) has been consolidated as an important unbiased strategy for virome studies [23,29,30]. Indeed, this strategy allows the detection of almost all viral species, since most of the viruses are made of or produce RNA molecules during replication, which would not be detected using DNA deep sequencing.

Therefore, our study focused on uncovering the viral diversity of *Agave* species using metatranscriptomics. We investigate three different *Agave* cultivars used for fiber extraction (*A. fourcroydes*, *A. sisalana* and *Agave* Hybrid 11648) collecting samples from three different organs (leaves, stems, and roots) in biological triplicates. Using this approach in association with DNA deep sequencing to filter out endogenous elements, we identified 25 putative viral species in asymptomatic *Agave* individuals, including the known species *Cowpea Mild Mottle Virus* (CPMMV) and 24 previously unknown viral species, belonging to at least six viral families: *Alphaflexiviridae*, *Betaflexiviridae*, *Botourmiaviridae*, *Closteroviridae*, *Partitiviridae*, *Virgaviridae* and three distinct unclassified viruses. *A. fourcroydes* displayed the highest diversity among the three *Agave* taxa while the roots were the plant organ with the highest viral diversity. We also observed discrepant abundance for the same virus among different organs, highlighting replication strategy preferences, such as observed for *Sisal-associated Closterovirus A* (higher in leaves and stems) and *Sisal-associated Virgavirus C* (higher in roots). Altogether, our results highlight both the importance of unbiased high-throughput strategies for the discovery of new viral species and also the relevance of screening asymptomatic plants for obtaining a more realistic viral diversity scenario.

2. Materials and Methods

2.1. Sample Origin, Transcriptome Sequencing, Assembly, and Quantification

In this study, we investigated the sisal virome using transcriptomic datasets previously generated by Raya et al. (2020) [29]. Our samples were extracted from sections of the leaves, stems, and roots from three different seven-year-old adult plants of *A. sisalana*, *A. fourcroydes*, and the *Agave* hybrid 11648 (*(A. amaniensis x A. angustifolia) x A. amaniensis*) collected at the EMBRAPA collection in Monteiro, in the state of Paraíba, Brazil (07°53' S; 37°07' W, elevation: 619 m). For all cultivars, leaves (central fraction of the proximal-distal axis), roots, and stems were sampled from seven-year-old healthy adult plants. For each cultivar, three biological replicates growing side-by-side were sampled. To maintain leaf maturity equivalency within the cultivars, we sampled the fifth leaf counted from the central spike of each plant. Although the plants were maintained in the field and exposed to long drought periods typical of the Caatinga biome, all the collected individuals were healthy, with the leaves showing homogenous green coloration, with no visible symptoms of diseases (necrosis, chlorosis, spots, etc.). Total RNA was extracted according to the protocol described by Zeng and Yang, (2002), with the modifications proposed by Le Provost et al. (2003) [30]. mRNA library preparation and sequencing were done at the High-Throughput Sequencing Facility of the Carolina Center for Genome Sciences (University of North Carolina at Chapel Hill, NC, USA). The libraries were prepared using the KAPA Stranded mRNA-Seq kit (07962193001) for Illumina platforms following the manufacturer's protocol, using 1 µg total RNA. The sequencing was done on the Illumina HiSeq 4000 system, generating 50 bp paired-end reads. More details can be found in Raya et al. (2020) [29]. The DNA Libraries, one for each *Agave* taxon, were prepared using the KAPA Hyper Prep Kit (07962312001) following the manufacturer's instructions. For the library preparation, 1000 ng of fragmented DNA (average size ~280 bp) was used. Subsequently, the three DNA libraries were pooled together and sequenced with the Illumina HiSeq 4000 system. The transcriptome was de novo assembled using Trinity v. 2.5.1 for each species separately [31]. Transcript quantification was performed using kallisto v 0.44.0 [32], and ORF prediction was carried out with TransDecoder v. 5.0.2 [33]. An overview of the methods can be found in Figure 1.

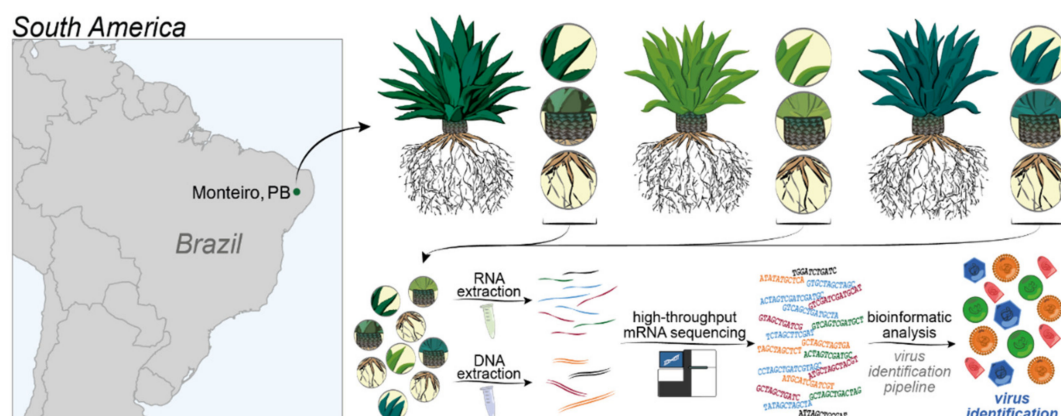


Figure 1. Strategy applied to uncover the virome of *Agave* species. The dot in the map indicates the localization of Monteiro, in the state of Paraíba. *Agave fourcroydes*, *Agave sisalana* and *Agave* Hybrid 11648 (and their respective organ samples) are indicated in different tones of green, for differentiation purposes. The following methods are indicated in the lower portion of the figure; RNA extraction, DNA extraction, high-throughput sequencing in the Illumina platform, and bioinformatics analysis (see further details in the Material and Methods section).

2.2. Identification of Virus-Derived Sequences

Sequence similarity searches were performed similarly for all the *Agave* transcriptomes. Assembled transcripts were aligned to the nucleotide (NT) database of GenBank

(available online: <ftp://ftp.ncbi.nlm.nih.gov/blast/db/>, accessed on 14 April 2020) using BLASTn [34], keeping only the best hit (with the `-max_target_seqs` flag set to 1) for each sequence. Viral hits were used to identify transcripts possibly derived from viruses present in the samples. The closest reference viral genomes whose transcripts displayed similarity at nucleotide level were obtained from GenBank and used to align the transcripts back using BLASTn to assess genome coverage. To create coverage plots, those transcripts were sampled with *sample.py* (available on Supplementary Materials) and aligned to a full viral genome with Bowtie2 [35], and, subsequently, formatted with Samtools [36] and visualized with IGV [37] and Mauve [38]. The plant variety containing the largest number of transcripts aligned to the reference viral genome was chosen to obtain a full consensus-based genome. Pre-processed reads were aligned to the reference viral genome with Bowtie2 as previously described, and the output SAM file was analyzed with both Samtools and BCFtools to generate a consensus sequence in FASTA format file representing the reconstituted viral genome.

Contigs that did not exhibit significant similarity with reference genomes in public databases, at the nucleotide level (BLASTn requiring e -value $< 1 \times 10^{-5}$ against NCBI NT database), were compared against the non-redundant (NR) database of GenBank (available online: <ftp://ftp.ncbi.nlm.nih.gov/blast/db/>, accessed on 14 April 2020) with the BLASTx module of Diamond [39], and viral hits were selected considering E -value $< 1 \times 10^{-3}$. Contigs from different libraries that displayed matching regions with the same viral sequences were submitted to redundancy removal and contig extension using CAP3 [40]. Non-redundant contigs were further analyzed to investigate possible conserved domains using HMMER [41].

2.3. Manual Curation and Detection of Endogenous Viral Elements

In order to distinguish whether viral sequences were derived from an endogenous or exogenous origin, we sequenced three (one for each *Agave* taxa) DNA libraries from the leaves of the same individuals from which we produced the transcriptomes. Genomic DNA was prepared using the KAPA Hyper Prep Kit (07962312001) following the manufacturer's instructions. For the library preparation, 1 μ g of fragmented DNA with an average length of 280 bp was used as input material, and then four PCR cycles were used for amplification. Libraries were sequenced with Illumina HiSeq 4000 platform. Finally, to investigate the origin of possible viral sequences, raw genomic reads were aligned to the candidate viral genomes using Bowtie2 allowing zero mismatches. Removal of false-positive results was adapted from Aguiar et al. (2015) [42]. Briefly, we removed sequences presenting similarity with retroviral elements, containing truncated ORFs and viral transcripts assigned to non-retroviral families that presented alignment from DNA sequencing libraries (at least 10 reads covering 70% sequence) were considered derived from endogenous viral elements (EVEs).

2.4. Phylogenetic Analysis

A classification-based method was developed to stipulate the confidence levels of the detected species, and those sequences suitable for phylogenetic analysis. From lower confidence to higher confidence: Class 0 would comprise viral species with no RNA-dependent RNA polymerase (RdRp) sequence detected, Class 1 would comprise elements in which a partial RdRp sequence (< 500 bp) was found accompanied or not by other viral proteins, Class 2 would encompass viruses with large fragments (> 500 bp) of RdRp, while Class 3 would consist of viral species containing a large fragment (> 500 bp) of RdRp and some other viral protein (except for the coat protein). Finally, Class 4 consists of viral species with a large fragment (> 500 bp) of RdRp and the coat protein detected, with the facultative presence of other viral proteins. The species classified within Classes 2–4, were then selected for phylogenetic analysis. Then, assembled contigs that showed similarity with RdRp were translated into amino acid sequences and aligned with related viral sequences available in NCBI public protein database [43] using MAFFT [44]. The accession numbers of the viral sequences used in this study are listed in Table S1. The protein best-fit model

was selected for each alignment file using ProtTest 3.2, considering the Akaike information criterion (AIC) [45]. Maximum likelihood (ML) trees were constructed in MEGA X [46] with 1000 bootstrap replicates for evaluating branch support. The trees were mid-point rooted and edited in FigTree (available online: <http://tree.bio.ed.ac.uk/software/figtree/>, accessed on 14 April 2020) and Geneious Prime 2020 1.2. (available online: <https://www.geneious.com>, accessed on 14 April 2020).

2.5. Diversity Analysis

The quantification metrics for selected viral contigs (in tpm—transcripts per million) were obtained from kallisto [32]. The resulting expression matrix was analyzed with the packages *vegan* and *vegetarian* from R [47], while PCA analysis and diversity indices were produced with PAST [48] using as variables the viral expression of our 25 species on the three analyzed organs (leaves, stems, and roots) for each of the three *Agave* taxa. For the PCA analysis, quantitative data from kallisto were used, while for the diversity indices, a presence-absence matrix was generated.

3. Results

3.1. Identification of Virus-Derived Sequences

In this study, we took advantage of RNA deep sequencing to identify and characterize the virome of *Agave* taxa. We deep sequenced 27 RNA libraries from two plant species, and a hybrid variety (three plant taxa \times three organs \times three replicates for leaf, stem, and root tissues), totalizing 559,267,611 raw reads (Table S2). Transcriptome assemblies produced 251,953 contigs, considering all libraries. Sequence similarity searches revealed that the percentage of viral sequences (not considering contig extension with CAP3) represented $\sim 0.02\%$ of all transcripts assembled for almost all the organs and varieties, with exception of the roots of *Agave fourcroydes* (0.04%) and *Agave* Hybrid 11648 (0.03%) and the leaves of *Agave* Hybrid 11648 (0.01%) (Figure 2). From the total, 10 contigs showed similarity with viruses at the nucleotide level (Tables S3 and S4), and 80 contigs (extended with CAP3) showed similarity with viral sequences at amino acid level, compared against NCBI sequence databases NT and NR, respectively (Tables S3 and S5). These initial 90 viral contigs identified by sequence similarity suggested the presence of 28 viral species associated with the sisal samples, including one known species (CPMMV) and 27 new viral species, which were assigned to at least seven viral families; Alphaflexiviridae (three species, four contigs), Betaflexiviridae (seven species, 22 contigs), Botourmiaviridae (two species, two contigs), Closteroviridae (one species, eight contigs), Mitoviridae (one species, five contigs), Partitiviridae (one species, one contig), Virgaviridae (three species, 19 contigs), and Unclassified species including Unclassified dsRNA (four species, 12 contigs), Unclassified Riboviria (one species, two contigs), or simply Unclassified (four species, 13 contigs). Details about sequence similarity searches can be visualized in Table S5.

3.2. Manual Curation and Detection of Endogenous Viral Elements

In our analysis, we took different precautions to avoid the occurrence of false-positive sequences, a major problem in virome studies, which usually corresponds to either poorly assembled/annotated sequences and/or endogenous viral elements (EVEs) (detailed in methods). Firstly, we sequenced genomic DNA from all three plant taxa to verify if any of our contigs assigned to viruses would be derived from EVEs. We also analyzed top similarity hits considering the online version of NCBI Blast (which uses the most updated versions of amino acid databases), the ORF profile, the existence of conserved domains, the contig length, and the presence of proteins encoding to polymerase and coat proteins.

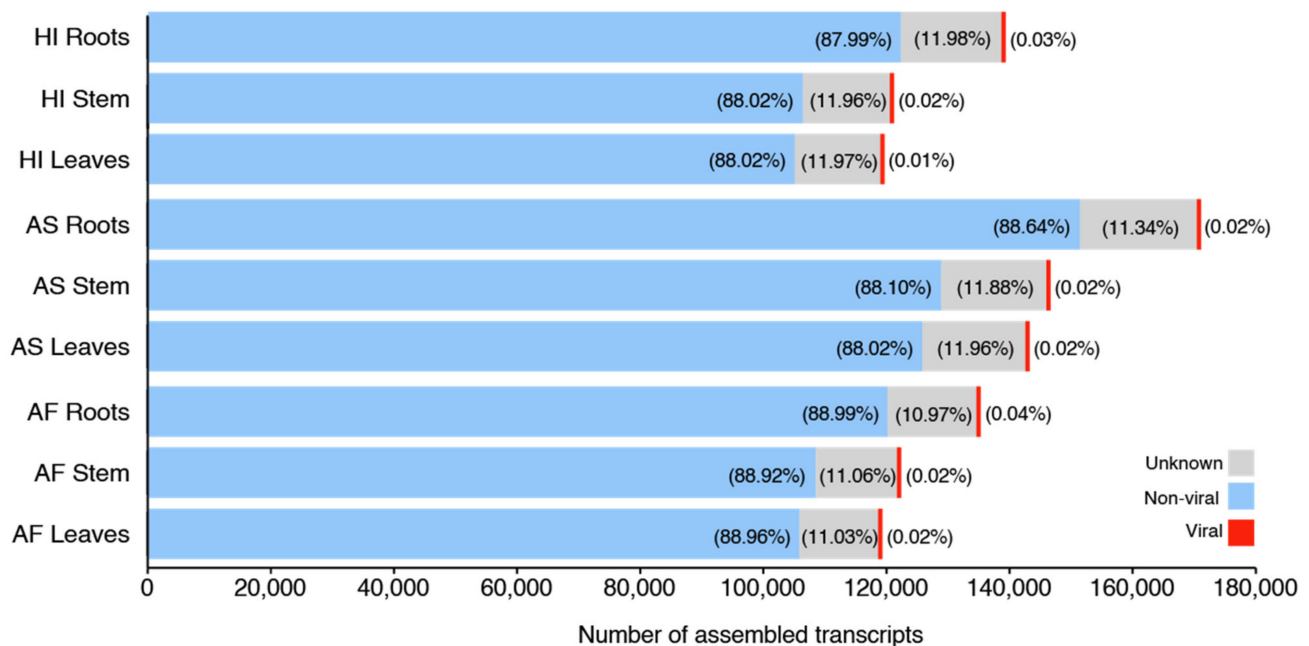


Figure 2. Overview of sequence similarity searches. The bar plots indicate the non-normalized values of viral, unknown, and other (non-viral) contigs in the nine analyzed samples. Color keys are indicated in the figure. Percentages are indicated inside color bars or on the right side, for viral contigs values. “Unknown” represents sequences with no significant hit at NCBI nucleotide and protein databases, while “non-viral” indicates sequences with hits with any other organism but viral.

Our manual curation discarded 13 contigs initially detected as viral, which were named with the prefix *disc* plus a number for identification (Table S6), three of which (*disc1*, *disc2*, and *disc3*, showing similarity with the RdRp of *Macrophomina phaseolina tobamo-like virus* (*disc1*) and the putative proteins P31 and P33 of *Pistachio ampelovirus A* (*disc2* and *disc3*), respectively). These transcripts presented counts in the genomic DNA sequencing and/or the presence of non-viral domains. One contig was discarded based solely on the detection of non-viral protein domains (originally showing similarity with a movement protein of *Podosphaera prunicola tobamo-like virus*), and the three remaining contigs with neither protein domains nor hits with viral sequences using the web version of NCBI BLASTx (originally showing similarity with a hypothetical protein of *Aspergillus foetidus dsRNA mycovirus*, and the RdRp of *Aspergillus mycovirus 341* and *Helicobasidium mompa partitivirus V1-2*). Five other contigs putatively derived from mitoviruses displayed counts on DNA sequencing and were also discarded. Twenty-four possible new viral species were left after false-positive results were removed. To stipulate the confidence levels of the species detected in our analyses, we developed a classification-based system consisting of five classes and used this method to select species for further phylogenetic characterization (Table S7). From lower confidence to higher confidence: Class 0 comprises viral species with no RdRp sequence detected (two viral species), Class 1 comprises elements in which a partial RdRp sequence (<500 bp), found accompanied or not by other viral proteins (10 viral species), Class 2 encompasses viruses with large fragments (>500 bp) of RdRp (eight viral species), while Class 3 consists of viral species containing a large fragment (>500 bp) of RdRp and some other viral protein (except for the coat protein) (one viral species), and finally, Class 4 is made up of viral species with a large fragment (>500 bp) of RdRp and the coat protein detected, with other viral proteins being facultative (four viral species) (Table S7). The species classified within Classes 2–4 (13 viral species) were selected for phylogenetic analysis.

3.3. Reconstitution of Cowpea Mild Mottle Virus (CPMMV) Strain Associated with Agave Species

Sequence similarity searches revealed 10 contigs showing high similarity and identity with CPMMV at the nucleotide level, of which one of them (assembled from *Agave fourcroydes*) was 3600 nt-long. Thus, we decided to apply a reference-based strategy to reconstruct the whole genome of this *Agave*-derived lineage (Figure S1, Tables S3 and S4) taking advantage of the libraries derived from *Agave fourcroydes* to obtain the full viral genome of the sisal isolate of CPMMV. As seen in Figure S2, raw RNA reads covered 100% of the closest reference genome, with some genetic variability between the reference and our isolate, which probably reflects the real variation between strains but did not impact the structural annotation of our CPMMV strain (Table S4, Figure S3). The full genome sequence (8193 nt) of the sisal *Cowpea mild mottle virus* isolate PB:AF (*Carlavirus*, *Betabreviviridae*) is available on GenBank under the accession code MZ329767.

3.4. Phylogenetic Characterization of New Viral Sequences

In order to further assess the phylogenetic relationship between *Agave*-associated viruses and related species in public reference databases, we selected all the species belonging to Classes 2–4 to perform phylogeny, which included 13 putative viral species (Figure 3A–C). Among these 13 species, five were assigned to the family *Betaflexiviridae* (Figure 3A): *Sisal-associated Betaflexivirus A* (phylogenetically closer to *Cowpea mild mottle virus*, a broad-host-range plant-infecting species also found in our samples); *Sisal-associated Betaflexivirus B* and *Sisal-associated Betaflexivirus C* formed a separate clade, phylogenetically closer to a clade including the *Grapevine Pinot gris virus* and others, all of which characterized as plant-infecting species; *Sisal-associated Betaflexivirus E* was closer to a clade including the *Agave tequilana leaf virus* (virus identified in a species related to the *Agave* species investigated in our study), *Heracleum latent virus*, and seven other viral species infecting grapevine. Three viral species were assigned to the family *Virgaviridae* (Figure 3B): *Sisal-associated virgavirus A* was closer to *Luckshill virus*, a virus found in *Drosophila suzukii*, according to Medd et al. (2018) [49]; *Sisal-associated Virgavirus B* (closer to two grapevine viruses), and *Sisal-associated Virgavirus C* (closer to oomycete-infecting viruses and mycoviruses). Three species were designed to clades containing viruses described solely as ‘Unclassified’, besides one *Unclassified dsRNA virus* (Figure 3C): *Sisal-associated Unclassified virus B*, *Sisal-associated Unclassified virus C*, *Sisal-associated Unclassified virus E*, and *Sisal-associated Unclassified dsRNA virus C*. The family *Closteroviridae* were represented by one species (Figure 3B): *Sisal-associated Closterovirus A*. Usually, viral species were assigned to the same family of its closest related virus identified by sequence similarity searches, except for *Sisal-associated Virgavirus B*, which was initially described as unclassified, but further phylogenetic analysis indicates it is an element from the *Virgaviridae* family, similarly to *Sisal-associated Unclassified dsRNA virus*, initially only classified as *Riboviria*. After performing the phylogeny, based on phylogenetic relationships and sequence similarity results we settled the identity and named our 24 putative new viral species, as described in Table 1. We also constructed a phylogenetic tree to analyze the obtained CPMMV isolate, which is available in Figure S4. Interesting, we observed the CPMMV identified in *Agave* species is closely related to other isolates identified in Brazilian samples. Furthermore, we observed a great number of CPMMV isolates derived from different species, indicating the broad range of hosts that the virus can infect. The accession codes for other viral sequences are available in Table S8.

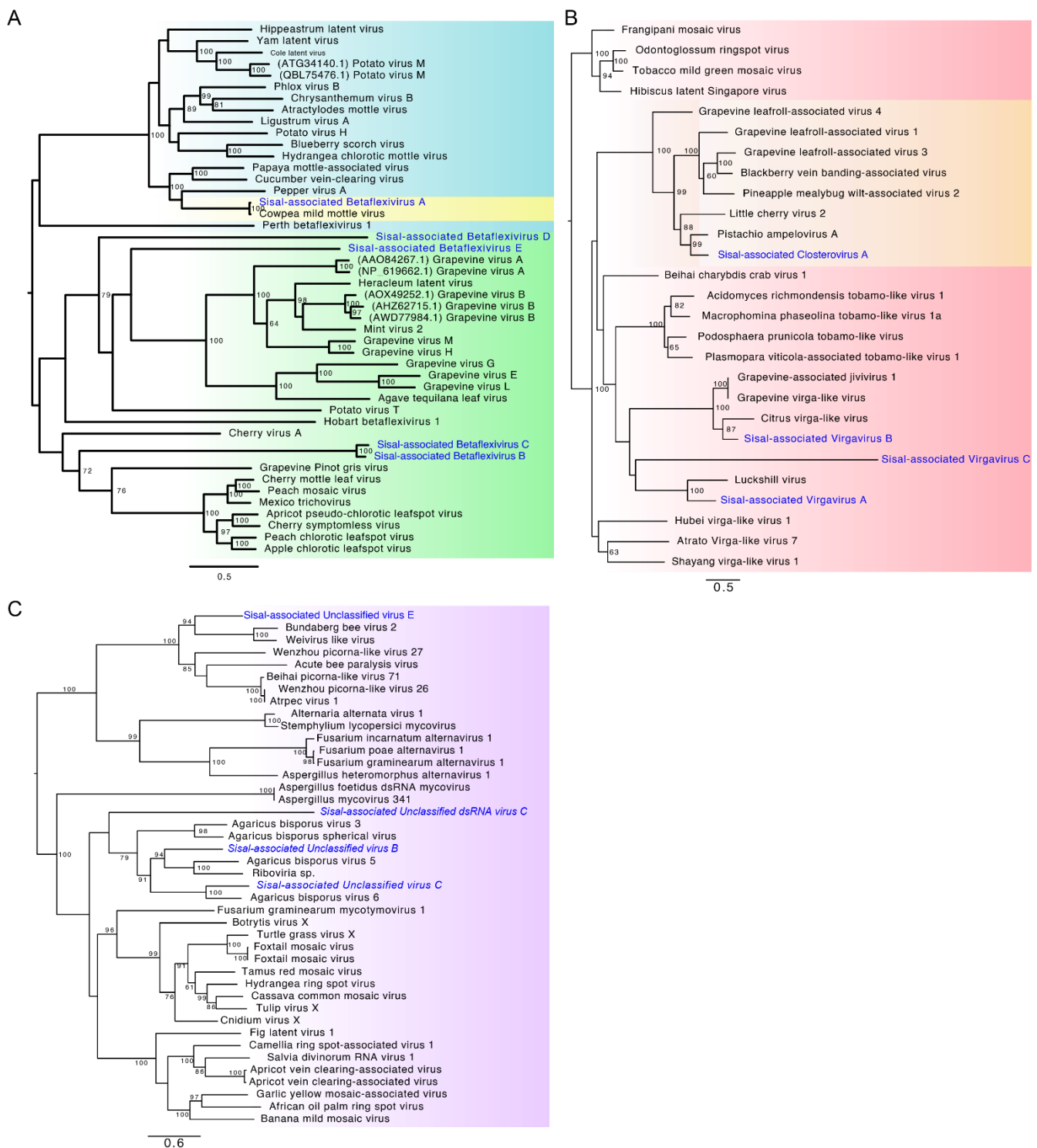


Figure 3. Phylogenetic analysis of high-confidence viral sequences identified in *Agave* species. Phylogenetic trees contain 13 selected species, highlighted in blue. (A) Family Betaflexiviridae. In blue; Carlavirus. In green; Trivirusinae. In yellow; unclassified Betaflexivirus. (B) +ssRNA (positive sense, single-stranded RNA), in red. In orange; Ampelovirus. (C) Riboviria (in violet). Node support values were determined using 1000 pseudoreplicates where values over 60% of confidence are shown.

Table 1. Viral species assignments according to sequence similarity searches and phylogeny. Columns indicate (i) the family indicated by phylogeny, (ii) the family of the best BLASTx hit (columns merged when results are identical), (iii) the species of the best BLASTx hit, and (iv) the new species name.

Family (BLAST)	Family (Phy)	Species Hit (BLASTx)	New Name	
Unclassified	-	Actinidia seed-borne latent virus	Sisal-associated Unclassified virus A	
	Unclassified	Agaricus bisporus virus 5	Sisal-associated Unclassified virus B	
Alphaflexiviridae	Unclassified	Agaricus bisporus virus 6	Sisal-associated Unclassified virus C	
	-	Alternanthera mosaic virus	Sisal-associated Alphaflexivirus A	
Unclassified dsRNA	-	Alternaria alternata virus 1	Sisal-associated Unclassified dsRNA virus A	
Unclassified dsRNA	Betaflexiviridae	Apple stem pitting virus	Sisal-associated Betaflexivirus A	
	-	Aspergillus foetidus dsRNA mycovirus	Sisal-associated Unclassified dsRNA virus B	
Unclassified	-	Aspergillus heteromorphus alternavirus 1	Sisal-associated Unclassified virus D	
Alphaflexiviridae	Virgaviridae	Botryosphaeria dothidea tobamo-like virus	Sisal-associated Virgavirus A	
	-	Cassia mild mosaic virus	Sisal-associated Alphaflexivirus B	
Unclassified	Virgaviridae	Citrus virga-like virus	Sisal-associated Virgavirus B	
Unclassified Riboviria	Betaflexiviridae	Diuris virus A	Sisal-associated Betaflexivirus B	
	Betaflexiviridae	Grapevine Pinot gris virus	Sisal-associated Betaflexivirus C	
	-	Grapevine virga-like virus	Sisal-associated Ribovirus A	
	Betaflexiviridae	Grapevine virus G	Sisal-associated Betaflexivirus D	
	Betaflexiviridae	Grapevine virus H	Sisal-associated Betaflexivirus E	
	Unclassified	Halhan virus 3	Sisal-associated Unclassified virus E	
	Virgaviridae	Macrophomina phaseolina tobamo-like virus	Sisal-associated Virgavirus C	
	Alphaflexiviridae	-	Nerine virus X	Sisal-associated Alphaflexivirus C
	-	Pistachio ampelovirus A	Sisal-associated Closterovirus A	
	Botourmiaviridae	-	Plasmopara viticola associated ourmia-like virus 29	Sisal-associated Botourmiavirus A
Botourmiaviridae	-	Plasmopara viticola associated ourmia-like virus 6	Sisal-associated Botourmiavirus B	
Virgaviridae	-	Podosphaera prunicola tobamo-like virus	Sisal-associated Virgavirus D	
Unclassified Riboviria	Unclassified dsRNA	Stemphylium lycopersici mycovirus	Sisal-associated Unclassified dsRNA virus C	

3.5. Viral Diversity in *Agave* Species

In order to further investigate and better understand the viral diversity in our samples, we performed diverse statistical tests (Appendix A). First, we analyzed data normality with Shapiro–Wilk tests and assessed statistical differences among organs with the Kruskal–Wallis test, considering both individual differences in viral diversity and whole viral composition considering viral abundance. Our results (available on Supplementary Materials) indicate that there is no significant difference when comparing the same organs (leaves, stems, roots) among the three sisal taxa. Nonetheless, when comparing the diversity of the organs in the same plant taxa, different patterns could be observed. In *Agave fourcroydes*, the roots displayed a significant difference from the leaves (Kruskal–Wallis test p -value 0.003377) and stems (Kruskal–Wallis test p -value 0.003723), while in *Agave* Hybrid 11648 the leaves were statistically different from the other organs (Kruskal–Wallis test p -values 0.03518 and 0.006339, when comparing against stems and roots, respectively). In *Agave sisalana*, no statistical differences were detected among distinct organs. Considering these results, we decided to portray the results at the organ level, instead of the plant taxa level. Our gamma diversity was 25 viral species, divided with an average alpha species richness of 10.66 species per sample (Table S9). The entropy (Shannon diversity index) in our samples varied greatly. Low values, such as seen in the leaves and stems of *A. sisalana*, and the leaves of *Agave* Hybrid 11648, indicated low richness (in the leaves) or a high dominance of a single species, in this case, the *Sisal-associated Closterovirus A*. The average dominance was lower in the roots, which exhibited a higher richness of species more equally distributed, represented here by the values of evenness (a value based on how similar are the abundance of each species in a sample and the equitability (Simpson’s Diversity Index, a value between 0 and 1 based on the richness and relative abundances in a sample). These values, followed by high dominance, were higher in the leaves and stems of *A. sisalana*. Our principal component analysis (PCA, Figure 4) allowed us to assess the divergence among viral profiles for the three distinct organs analyzed for each of the three *Agave* taxa. We noticed that roots showed the highest divergence among samples, followed by *A. sisalana* leaves and stems. On the other hand, all the other samples displayed a similar

profile, clustering together (Figure 4). Table S10 shows the raw expression table for each species according to each sample (and the annotated protein domains for each species).

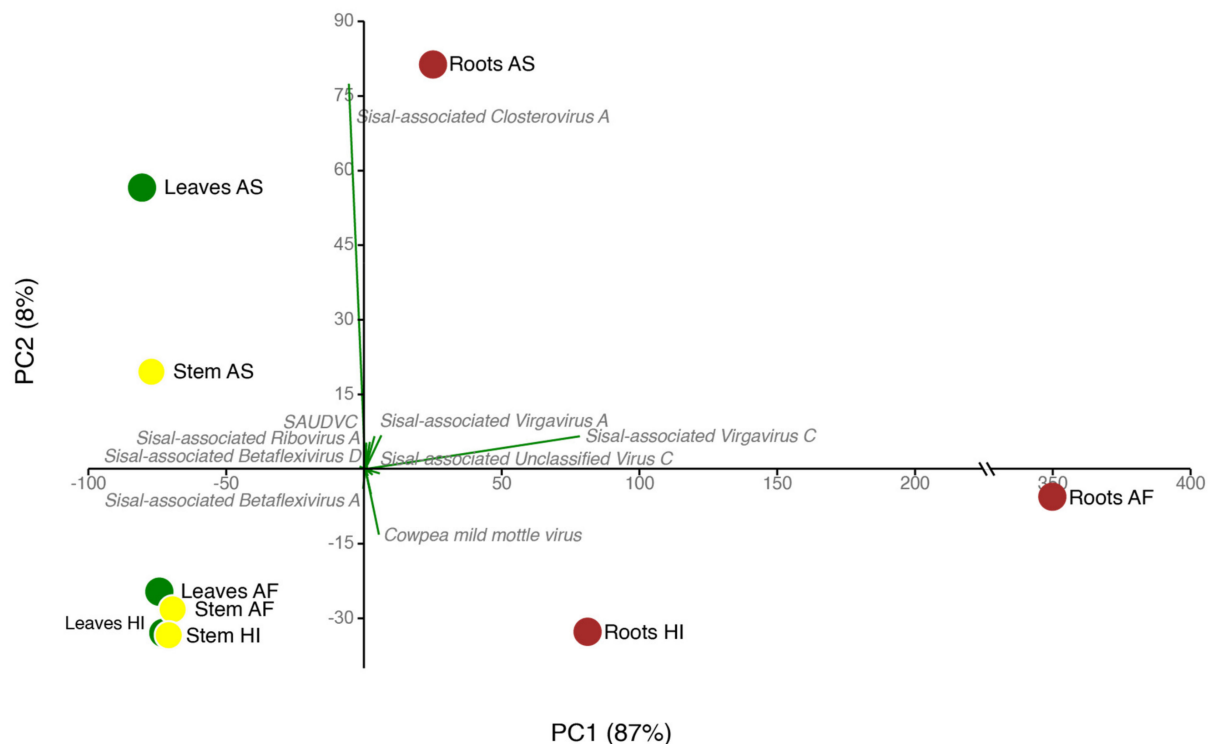


Figure 4. Principal component analysis of virus abundance in *Agave* organs. Viral species were used according to their abundance (green arrows) and presence in organs; Each organ (dots) is represented by a color: leaves (green dots), stems (yellow dots), and roots (brown dots).

The richness of viral families varied in all the three organs; however, two viral families represent over 50% of richness in leaves and stems (Figure 5A,B): Betaflexiviridae (represented by five viral species) and Closteroviridae, which was represented by a single species (*Sisal-associated Closterovirus A*). The roots (Figure 5C) were dominated by viruses from Virgaviridae and exhibited the highest proportion of Unclassified viral species reaching up to 17.5%. We also noted that the roots were the most diverse organ (Figure 6, Table S9), with the number of taxa in all the three plant varieties above the mean *alpha* species richness of 11.66 species per sample. In addition, roots formed a separate clade based on viral species presence/absence (Figure 6), especially due to the *Agave fourcroydes* roots, which possessed the greatest richness of all the organs (19 species) with a low dominance (0.3983).

3.6. Organ Tropism of *Agave*-Infecting Viruses

Abundance assessment of the viral species in each organ showed that a few viral species seem to present systemic infection while others seem to be restricted to a specific organ (Figure 5E). *Sisal-associated Closterovirus A* dominates all leaves and stems, and also the roots of *A. sisalana*, in which it shares dominance with *Sisal-associated Virgavirus C* that has the major contribution in the other root samples, of *A. fourcroydes* and *Agave Hybrid 11648*. The top 12 species with higher transcriptional activity, shown in Figure 5E, represent most of the total abundance in all the organs, while the other 13 species are responsible only for a small portion of viral abundance including the roots of *Agave Hybrid 11648*, where this group of species displays higher abundance than all the other organs. Figure 6 also shows that fewer viral species can be identified in leaves and stems, with only one species exclusively restricted to leaves (*Sisal-associated Unclassified virus A*), two species uniquely found in the stems (*Sisal-associated Botourmiavirus A* and *Sisal-associated*

Botourmiavirus B), and other five viral species were restricted to the roots (*Sisal-associated Unclassified dsRNA virus A*, *Sisal-associated Unclassified virus C*, *Sisal-associated Virgavirus D*, *Sisal-associated Alphaflexivirus C*, and *Sisal-associated Alphaflexivirus B*). It is relevant to point out that we observed a high number of putative viruses, 12 species, in co-infection in all three distinct plant organs, which likely indicate they can produce systemic infection.

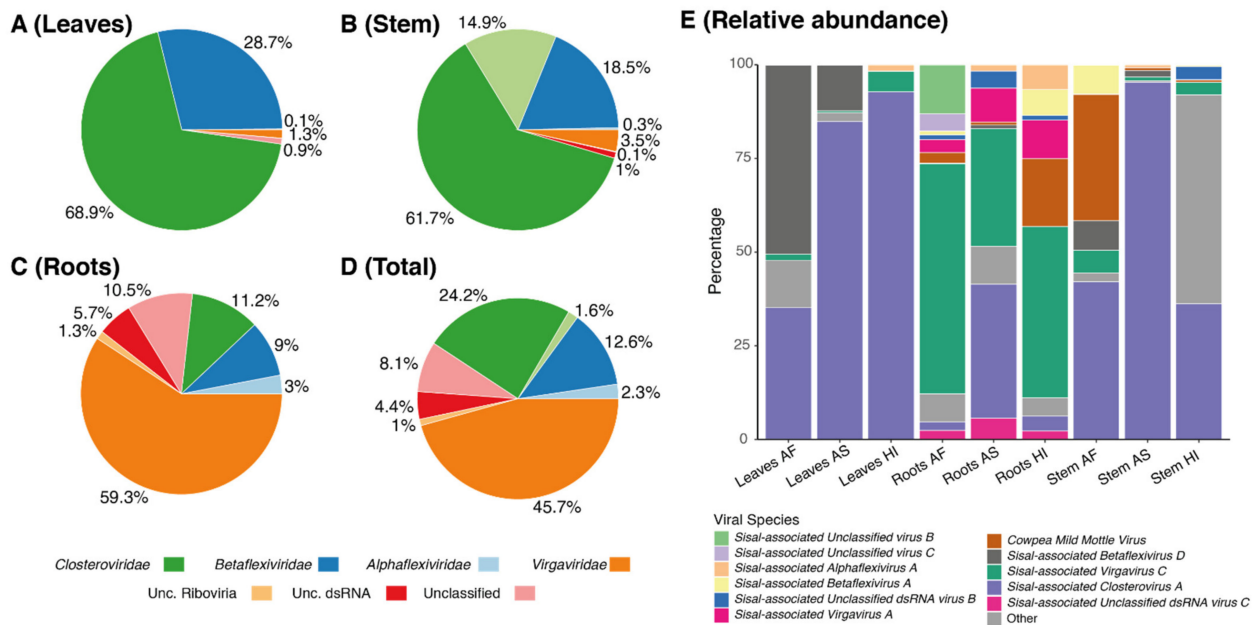


Figure 5. Viral abundance of Agave-associated viruses by organ. Pie charts indicate viral family abundance by expression in tpm, in (A): leaves, (B): stems, (C): roots, and (D): in total. Values are summed for all plants. (E): The stacked bar plot indicates the relative abundance of the top 12 expressed viral species in each organ.

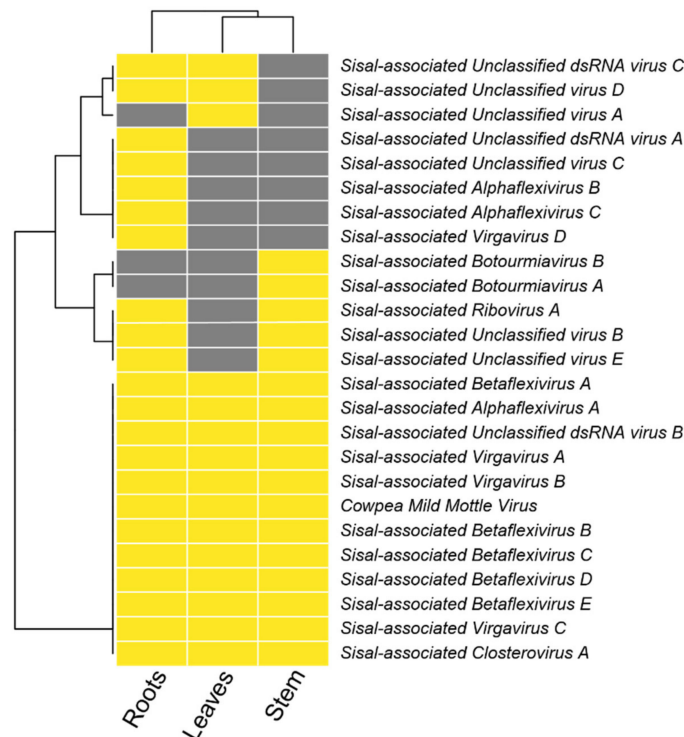


Figure 6. Organ tropism of Agave-infecting viruses. Colors indicate the presence (yellow) or absence (grey) of viral species over plant organs.

4. Discussion

Plants, such as all the known living organisms, are susceptible to viral infections. Some viral infections are cryptic, i.e., a given virus infects a host with no apparent symptoms [50,51]. In this study, we have described 25 cryptical viral species associated with three plant taxa in the genus *Agave*: *Agave fourcroydes*, *Agave sisalana* and *Agave* hybrid 11648 using RNA-sequencing and genomic DNA sequencing for curation. The use of metagenomics-based approaches for the discovery of viral species is seen in research conducted by Charon et al. [52], and Wolf et al. [53], and also reviewed by Greninger [54], Maclot et al. [55], and Shi et al. [56]. In our methods, we also discarded false-positive results and endogenous elements (EVEs). The plants were grown in a genetic collection, located in an area with very typical climatic and soil conditions of the sisal producing areas in Brazil. To the best of our knowledge, this is the first unbiased virome study in the genus *Agave*, the first virology study in *A. fourcroydes* and *A. hybrid* 11648, as well as the first virology study in *A. sisalana* since the 1995 study by Izaguirre-mayoral et al. [16], with another two earlier studies on the viral streak of sisal [13,14]. Among the 25 total species described in our study, only one is a known species, *Cowpea mild mottle virus* (CPMMV), and all the other 24 are new viral species. Our approach was based on the similarity of transcripts detected in leaf, stem, and root samples from these three plant taxa to viral nucleotide sequences and protein domains in public databases, followed by the verification of the origin of those sequences via genomic DNA sequencing, removal of false positives, and identity confirmation via phylogeny, when possible.

CPMMV was the only viral species detected in our samples through sequence similarity search at the nucleotide level (Figures S1–S3, Tables S3 and S4). On the other hand, searches at the protein level were able to find sequences (our remaining 24 viral species) sharing lower similarity with known references, thus being considered a new species. CPMMV was first identified by Brunt and Kenten in 1973 [57], infecting the Cowpea (*Vigna unguiculata*, hence the name) in Ghana, and after that in a broad range of other species (*Phaseolus vulgaris*, *Glycine max*, *Nicotiana clevelandii*, *Theobroma cacao*, among others) in vitro. Symptoms included mild to severe mottle chlorosis followed by leaf necrosis, however, visually symptomless individuals, as in our case with the *Agave* species, have been described in this same study. Brunt and Kenten also described how this virus was spread by sap-feeding aphids, however, their results indicate that spreading was dependent on other viruses, such as the *Potato Y virus* or *Pepper Veinal Mottle virus*. Following their discovery, the whitefly (*Bemisia tabacci*) is now widely accepted as the sole vector of CPMMV [58], and the occurrence of the whitefly in the state of Paraíba is also described in the literature [59–61], which is suggestive that this insect might also act as the vector for CPMMV in this environment. Nonetheless, CPMMV is more expressed in the stems and roots in all three *Agave* species, not being detected at any levels in the leaves of *A. sisalana* or *A. hybrid* 11648, and very low levels in the leaves of *A. fourcroydes*, which is in opposition to earlier findings for this species, considering the interaction of its vector (the whitefly) with plant leaves. The isolate PB:AF is also phylogenetically closer to other Brazilian isolates (highlighted in blue), considering all genomes available for this species so far (Figure S4). Of note, CPMMV seems to be a broad range of hosts, since isolates have been identified in many hosts, such as soybean, the common bean, and papaya.

On average, each of our samples contains around 11 species unevenly distributed (Table S9), indicating the presence of dominating species, which we describe in detail in the next paragraphs. In all the three sisal taxa, the roots were the organ with the highest number of species (richness), ranging from 12 species in the root of *A. Hybrid* 11648 and 13 in the roots of *A. sisalana* up to 18 species in the roots of *A. fourcroydes*, the richest sample in our analysis (Table S9). We believe this pattern is due to the diversity of associated microorganisms in the root system [62,63], which are, as the host plant, susceptible to viral infections. Our species have shown similarity with nine mycoviral species at the amino acid level with BLASTx. Indications that these species are also mycoviruses include not only their similarity with known species and phylogeny but also their distribution

in plant organs, which is especially higher in roots for such species, making the roots significantly distinct from stem and leaf samples (Figure 5E). The mycoviruses sharing similarities with our species are *Agaricus bisporus virus 5* and *Agaricus bisporus virus 6* [64], *Alternaria alternata virus 1* [65], *Aspergillus foetidus dsRNA mycovirus* [66], *Aspergillus heteromorphus alternavirus 1* [67], *Podosphaera prunicola tobamo-like virus* [68], *Macrophomina phaseolina tobamo-like virus* [69], *Botryosphaeria dothidea tobamo-like virus* (unpublished), and *Stemphylium lycopersici mycovirus* (unpublished) (Table 1). The occurrence of viral species showing similarity with *Aspergillus* mycoviruses, and their pattern of expression (higher in stems and roots, but also present in leaves) leads us to hypothesize that *Aspergillus welwitschiae*, a fungal species which causes the bole rot of sisal [70,71] is also part of the healthy microbiome of sisal, causing disease through imbalances in plant metabolism, rather than infecting vulnerable plants from spores in the environment. Such a pattern has been described in peppermint by Dakin et al. (2010) [72]. Nonetheless, it is also possible that this species is infecting the plant host, and not some associated fungal species, following the theories that mycoviruses originated from plant viruses [73] and that these mycoviruses can replicate in plant cells [74]. We can also hypothesize that such an infection in *A. welwitschiae* could modulate pathogenicity by stimulating it, or causing hypovirulence, as seen in Nuss (2005) [75]. The latter could be a highly promising treatment to the bole rot of sisal if properly managed.

Identification of our likely mycoviral species reveals four species, out of nine, belonging to the family Virgaviridae, the family with the second-highest number of represented contigs (Figure 5E). This viral family is commonly described as only infecting plants [76]; however, the first mycovirus belonging to this family was described by [69] and later by Pandey et al. (2018) [68], and, thus, corroborating our findings. As also described by Pandey et al. (2018) [68], *Podosphaera prunicola tobamo-like virus* shows similarity with *Macrophomina phaseolina tobamo-like virus*, such as our proposed new species, *Sisal-associated Virgavirus C*, which is one of the most highly expressed and dominating viral species in our samples (Figures 5E and 6), especially in the roots (Figure 5E), while *Sisal-associated Virgavirus D* shares similarity with *Podosphaera prunicola tobamo-like virus*, unique to the roots. These results reinforce the assertion that the higher species richness in the root system is related to the microbial species associated with sisal varieties. Furthermore, in the family Virgaviridae, *Sisal-associated Virgavirus B* shares similarity with “*Citrus virga-like virus*” [77], which is a plant-infecting species, and is expressed in stems and roots of *A. sisalana* and *A. hybrid 11648* and leaves of *A. sisalana*. This viral species was, as seen in Matsumura et al. (2017) [77], isolated from the city of Comendador Gomes, in the state of Minas Gerais, Brazil. This location is in the Cerrado biome, another endangered Brazilian biome that shares similarities with the Caatinga biome where our samples came from, including moderately low rainfall and low aboveground biomass [78].

Besides the aforementioned *Citrus virga-like virus* and *Cowpea Mild Mottle virus*, the other 12 species sharing similarity with our discoveries are plant-infecting viruses. The most prominent of those species, as seen in Figure 5E, is *Sisal-associated Closterovirus A*, the only representative species of the family Closteroviridae, which is the most represented viral family in our samples, sharing similarity with *Pistachio ampelovirus A*, first described by Al Rwahnih et al. (2018) [79]. This species is present in all the samples and plant taxa (Figures 5E and 6) but is especially highly expressed in *A. sisalana* (Figure 5E). This +ssRNA family has been described by Rubio et al. (2013) [80] as transmitted through mealybugs, aphids, or the whitefly, which is also likely responsible for the presence of CPMMV in our samples. The occurrence of mealybugs is described by da Silva et al. in the state of Paraíba, affecting cultivation of cotton (2013) [81] and peanuts (2018) [82], reinforcing the role of this insect in the transmission of viral infections in this region. Our results also revealed six viral species sharing similarities with viruses initially described in grapevines, three of which belonging to the family Betaflexiviridae (the third most represented family in the stems, and fourth most represented in leaves and roots); *Sisal-associated Betaflexivirus C*, sharing similarity with *Grapevine Pinot gris virus*, as seen in Giampetruzzi et al. (2012) [51]

and *Sisal-associated Betaflexivirus E*, sharing similarity with *Grapevine virus H*, as seen in Candresse et al. (2018) [50], both of which are unique to *A. fourcroydes*, with higher expression in the leaves. *Sisal-associated Betaflexivirus D*, sharing similarity with *Grapevine virus G* as seen in Blouin et al. (2018) [83], which was absent in the organs of *A. hybrid* 11648, and *Sisal-associated Ribovirus A*, sharing similarity with *Grapevine virga-like virus* (unpublished), which is unique to the stems and roots of *A. sisalana* and *A. hybrid* 11648. The family Betaflexiviridae, which also includes CMMV, affects exclusively plants [84], and also includes the *Sisal-associated Betaflexivirus A* (sharing similarity with *Apple stem pitting virus*), not expressed in *A. sisalana*, and *Sisal-associated Betaflexivirus B* (sharing similarity with *Diuris virus A*), not expressed in *A. hybrid* 11648. Taking together, our findings indicate that there is no organ tropism for the family Betaflexiviridae in our samples, even though some species seem to favor the leaves or roots. Other two species (*Sisal-associated Botourmiavirus A* and *Sisal-associated Botourmiavirus B*) share similarities with the oomycete-infecting viral species, *Plasmopara viticola associated ourmia-like virus 29* and *Plasmopara viticola associated ourmia-like virus 6*, respectively, both of which were described by Chiapello et al. (2020) [85]. Since the production of grapes in the state of Paraíba [86] and the *caatinga* biome [87] is limited, with a local study by Medeiros et al. (2017) [88] considering the climate conditions unsuitable for the cultivation of vines, the similarity of some of our new viral species to grapevine-infecting viruses suggests that these species have a broader host range than just the species from which they were originally isolated.

The family Alphaflexiviridae includes three species in our samples, sharing similarities on BLASTx with plant-infecting species in this same family; *Alternanthera mosaic virus* [89], *Cassia mild mosaic virus* [90], and *Nerine virus X* [91]. As well as Betaflexiviridae, this family does not display an expression pattern to the family level. *Sisal-associated Alphaflexivirus A* is expressed only in the stems and roots of *A. sisalana* and the hybrid, and in the leaves of *A. sisalana* while *Sisal-associated Alphaflexivirus B* is exclusive of the roots of *A. fourcroydes* and *A. sisalana*, and *Sisal-associated Alphaflexivirus C* is unique to the roots of *A. fourcroydes*. *Sisal-associated Unclassified virus A* is also unique to *A. fourcroydes* but to leaves instead of roots.

Finally, a curious result is the detection of *Sisal-associated Unclassified virus E*, which shares similarity on BLASTx with *Halhan virus 3*, described by Rosani et al. (2019) [92]. This viral species was infecting the bivalve *Haliotis discus*, a sea snail species. By contrast with the aforementioned fungal and plant species, the occurrence of sea snails in the Brazilian *caatinga* is virtually impossible. Thus, considering the expression of *Sisal-associated Unclassified virus E* only in the stems and roots of *A. fourcroydes*, we hypothesize that other *Gastropoda* species inhabiting the roots of this plant, as described by Pearce and Örstan (2006) [93] and Pratt (1971) [94], might have left viable viral RNA on the organs where it was detected, and that this group of species occurs in a broader range of environments than previously thought.

5. Conclusions

This is the first study using an unbiased high-throughput sequencing strategy to investigate the viral diversity in the genus *Agave*. According to our initial hypothesis that *Agave* species could act as a reservoir of plant viruses even with no apparent infection, in our study we were able to identify 25 species associated with three sisal taxa, of which 24 likely represent new viral species. Most of the species displayed high transcriptional activity in the roots, the plant organ with the highest viral diversity. At the species level, *Agave fourcroydes* is the variety with a higher abundance of viral species. A total of 11 new viral species shares similarities with known mycoviruses and oomycete-infecting viral species, reinforcing the effects of the associated microbiota in viral diversity.

Supplementary Materials: The following are available online at <https://www.mdpi.com/article/10.3390/microorganisms9081704/s1>, Table S1: Species names and respective accession numbers of the viral sequences used for phylogenetic analysis in Figure 3; Table S2: General description of deep sequenced libraries and virus detection strategy. Raw counts of RNA and DNA libraries as well as

metrics related to transcript assembly and sequence similarity searches are presented in the rows. *Agave* species are indicated in the columns; Table S3: Similarity of *Agave*-derived contigs against known CPMMV genomes. Analysis was performed using Blast with the variant BLASTn; Table S4: Quantitative metrics for the reference genome of CPMMV (CPMMV:BR:MG:09:3) and the genome obtained from the RNA-seq data of *Agave fourcroydes*; Table S5: BLASTx best hits for each viral contig, and their respective alignment metrics; Table S6: Transcripts discarded as false positives (rows) and associated data. Columns indicate transcript name, length (in base pairs), the protein and species hit on BLASTx, their respective accession code, detected protein domains, and finally, the reason for discard; Table S7: A classification scheme for phylogeny. Columns indicate: Class name, the requisites for that given class (characteristics of the viral species, concerning contig length and type), the number of species included in that category, and their correspondent percentage; Figure S1: Alignment of detected transcripts (arrows in the lower portion) of the three plant varieties sharing similarity with the genome of *Cowpea Mild Mottle virus* (KC884245.1), in the upper half of the figure, using IGV. Colorful lines inside arrows indicate genetic variation in comparison with the reference; Figure S2: Raw sequencing reads (with length >50 bp) coverage of the reference genome of CPMMV using IGV. Each arrow in the lower part indicates a single sequencing read. In those arrows, colorful regions indicate genetic variation in comparison to the reference. As seen in the middle section, coverage is deeper in the end on the transcript; Figure S3: ORF pattern in CPMMV:BR:MG:09:3 (upper) and CPMMV isolate PB:AF (lower). Figure S4: Phylogenetic analysis of Cowpea Mild Mottle virus isolate PB:AF. Accession numbers in blue indicate samples from Brazil, while green indicates the isolate assembled in this work; Table S8: The accession codes and descriptions to each viral contig and their respective viral species. “RdRp” stands for RNA-dependent RNA polymerase, and, in this table, is a synonym to “Replicase”; Table S9: Diversity indices for the organs and species analyzed; Table S10: Viral species and their respective detected protein domains (with Pfam/HMMER) and their expression (in tpm, *transcripts per million*) in each analyzed sample, representing the average expression of the three technical replicates.

Author Contributions: Conceptualization, E.R.G.R.A. and A.G.-N.; methodology, E.R.G.R.A., G.Q.-P., P.L.C.F., F.T.R., M.P.M. and P.M.; software, E.R.G.R.A., G.Q.-P., D.E.B. and P.L.C.F.; validation, F.T.R., M.P.M. and G.Q.-P.; formal analysis, G.Q.-P., P.L.C.F., F.T.R. and M.P.M.; investigation, G.Q.-P., P.L.C.F., F.T.R. and M.P.M.; resources, M.F.C., C.A.V., A.C.F.S., G.A.G.P. and A.G.-N.; data curation, G.Q.-P., P.L.C.F., F.T.R. and M.P.M.; writing—original draft preparation, E.R.G.R.A., G.Q.-P., P.L.C.F., R.P.O. and A.G.-N.; writing—review and editing, E.R.G.R.A., G.Q.-P., P.L.C.F., R.P.O. and A.G.-N.; visualization, E.R.G.R.A., G.Q.-P., P.L.C.F. and A.G.-N.; supervision, E.R.G.R.A. and A.G.-N.; project administration, A.C.F.S., G.A.G.P. and A.G.-N.; funding acquisition, A.C.F.S., G.A.G.P. and A.G.-N. All authors have read and agreed to the published version of the manuscript.

Funding: This research was funded by FAPESP (Fundação de Amparo a Pesquisa do Estado de São Paulo), grant numbers 16/05396-8 and 17/04900-7.

Institutional Review Board Statement: Not applicable.

Informed Consent Statement: Not applicable.

Data Availability Statement: The data supporting the reported results in this research can be found under the accession code PRJNA746623 in SRA and under accession codes MZ329754-MZ329767 and MZ599598-MZ599651 in the Nucleotide Database of NCBI.

Acknowledgments: We would like to thank all the members of the research groups of Eric Aguiar, Aristoteles Góes-Neto and Gonçalo Pereira for their support in the execution of this research, and the secretariat of the Graduate Program of Bioinformatics of UFMG, for their exceptional work.

Conflicts of Interest: The authors declare no conflict of interest.

Appendix A

Statistical Analysis among Organs Samples.

Part I: Comparing the same tissue type in the three plant varieties

1. Leaves

1.1. Normality Tests

Test	Leaves AF	Leaves AS	Leaves HI
N	25	25	25
Shapiro–Wilk W	0.842	0.2534	0.2256
p(normal)	3.217×10^{-9}	2.845×10^{-10}	1.764×10^{-10}
p (Monte Carlo)	0.0001	0.0001	0.0001

Conclusion: The three distribution are not Gaussian (normal). We must use a non-parametric test.

1.2. Kruskal–Wallis Test

H (chi2):	2.25
Hc (tie corrected):	3.477
p (same):	0.1758

Conclusion: There is no significant difference between sample medians.

2. Stem

2.1. Normality Tests

Test	Stem AF	Stem AS	Stem HI
N	25	25	25
Shapiro–Wilk W	0.438	0.2153	0.4168
p(normal)	9.652×10^{-9}	1.484×10^{-10}	6.209×10^{-9}
p (Monte Carlo)	0.0001	0.0001	0.0001

Conclusion: the three distribution are not Gaussian (normal). We must use a non-parametric test.

2.2. Kruskal–Wallis Test

H (chi2):	0.2957
Hc (tie corrected):	0.3705
p (same):	0.8309

Conclusion: There is no significant difference between sample medians.

3. Roots

3.1. Normality Tests

Test	Roots AF	Roots AS	Roots HI
N	25	25	25
Shapiro–Wilk W	0.3351	0.4847	0.4686
p(normal)	1.246×10^{-9}	2.65×10^{-8}	1.858×10^{-8}
p (Monte Carlo)	0.0001	0.0002	0.0001

Conclusion: the three distribution are not Gaussian (normal). We must use a non-parametric test.

3.2. Kruskal–Wallis Test

H (chi2):	2.254
Hc (tie corrected):	2.443
p (same):	0.2948

Conclusion: There is no significant difference between sample medians.

Part II: Comparing all tissue in of a same plant variety

4. *Agave fourcroydes*

4.1. Normality Tests

Test	Leaves	Stem	Roots
N	25	25	25
Shapiro–Wilk W	0.842	0.438	0.3351
p(normal)	3.217×10^{-9}	9.652×10^{-9}	1.246×10^{-9}
p (Monte Carlo)	0.0001	0.0002	0.0001

Conclusion: the three distribution are not Gaussian (normal). We must use a non-parametric test.

4.2. Kruskal–Wallis Test

H (chi2):	10.52
Hc (tie corrected):	11.96
p (same):	0.002533

Conclusion: There is a significant difference on viral diversity among distinct tissues in AF.

4.3. Mann–Whitney Pairwise Test

Test	Leaves	Stem	Roots
Leaves		0.9041	0.003377
Stem	0.9041		0.003723
Roots	0.003377	0.003723	

Conclusion: Viral diversity of the roots is statistically significant different from both the diversity in leaf and stem, but there is no significant difference between leaf and stem viral diversity.

5. *Agave sisalana*

5.1. Normality Tests

Test	Leaves	Stem	Roots
N	25	25	25
Shapiro–Wilk W	0.2534	0.2153	0.4847
p(normal)	2.85×10^{-7}	1.48×10^{-7}	2.65×10^{-8}
p (Monte Carlo)	0.0001	0.0001	0.0001

Conclusion: the three distribution are not Gaussian (normal). We must use a non-parametric test.

5.2. Kruskal–Wallis Test

H (chi2):	4.006
Hc (tie corrected):	5.019
p (same):	0.0813

Conclusion: There is no significant difference on viral diversity among the three distinct tissues in *Agave sisalana*.

6. Agave Hybrid 11648

6.1. Normality Tests

Test	Leaves	Stem	Roots
N	25	25	25
Shapiro–Wilk W	0.2256	0.4168	0.4686
p(normal)	1.76×10^{-7}	6.21×10^{-6}	1.86×10^{-5}
p (Monte Carlo)	0.0001	0.0002	0.0001

Conclusion: the three distribution are not Gaussian (normal). We must use a non-parametric test.

6.2. Kruskal–Wallis Test

H (chi2):	6.226
Hc (tie corrected):	8.437
p (same):	0.01472

Conclusion: There is a significant difference between sample medians.

6.3. Mann–Whitney Pairwise Test

Test	Leaves	Stem	Roots
Leaves		0.03518	0.006339
Stem	0.03518		0.2202
Roots	0.006339	0.2202	

Conclusion: The viral diversity in the leaf is statistically significant different from both stem and roots, but there is no significant difference between the viral diversities of stem and roots.

References

1. Brown, K. *Agave sisalana* Perrine. *Wildl. Weeds* **2002**, *5*, 18–21.
2. González-Iturbe, J.A.; Olmsted, I.; Tun-Dzul, F. Tropical dry forest recovery after long term Henequen (sisal, *Agave fourcroydes* Lem.) plantation in northern Yucatan, Mexico. *For. Ecol. Manag.* **2002**, *167*, 67–82. [CrossRef]
3. Santos, E.M.C.; Silva, O.A. Da Sisal in Bahia—Brazil. *Mercator* **2017**, *16*, 1–13. [CrossRef]
4. De Andrade Santos, R.; Brandão, W. ÁRVORE DO CONHECIMENTO: Território Sisal. EMBRAPA. Available online: https://www.agencia.cnptia.embrapa.br/gestor/territorio_sisal/arvore/CONT000ghou0b0002wx5ok05vadr1fx7pyzy.html (accessed on 31 May 2021).
5. Alves, J.J.A.; de Araújo, M.A.; do Nascimento, S.S. Degradação da caatinga: Uma investigação ecogeográfica. *Rev. Caatinga* **2009**, *22*, 126–135.
6. Guedes, T.B.; Sawaya, R.J.; De C. Nogueira, C. Biogeography, vicariance and conservation of snakes of the neglected and endangered Caatinga region, north-eastern Brazil. *J. Biogeogr.* **2014**, *41*, 919–931. [CrossRef]
7. Debnath, M.; Pandey, M.; Sharma, R.; Thakur, G.S.; Lal, P. Biotechnological intervention of *Agave sisalana*: A unique fiber yielding plant with medicinal property. *J. Med. Plants Res.* **2010**, *4*, 177–187.
8. Gonçalves, M.C.; Vega, J.; Oliveira, J.G.; Gomes, M.M.A. Sugarcane yellow leaf virus infection leads to alterations in photosynthetic efficiency and carbohydrate accumulation in sugarcane leaves. *Fitopatol. Bras.* **2005**, *30*, 10–16. [CrossRef]
9. Adams, I.P.; Skelton, A.; Macarthur, R.; Hodges, T.; Hinds, H.; Flint, L.; Nath, P.D.; Boonham, N.; Fox, A. Carrot yellow leaf virus is associated with carrot internal necrosis. *PLoS ONE* **2014**, *9*, e109125. [CrossRef]
10. Yuan, C.; Li, H.; Qin, C.; Zhang, X.; Chen, Q.; Zhang, P.; Xu, X.; He, M.; Zhang, X.; Tör, M.; et al. Foxtail Mosaic Virus-induced Flowering Assays in Monocot Crops. *J. Exp. Agric. Int.* **2020**, *71*, 3012–3023. [CrossRef]
11. Al Rwahnih, M.; Daubert, S.; Úrbez-Torres, J.R.; Cordero, F.; Rowhani, A. Deep sequencing evidence from single grapevine plants reveals a virome dominated by mycoviruses. *Arch. Virol.* **2011**, *156*, 397–403. [CrossRef]
12. Dolja, V.V.; Meng, B.; Martelli, G.P. Evolutionary Aspects of Grapevine Virology. In *Grapevine Viruses: Molecular Biology, Diagnostics and Management*; Springer: New York, NY, USA, 2017; pp. 659–688. ISBN 9783319577067.
13. Pinkerton, A.; Bock, K.R. Parallel streak of sisal (*Agave sisalana*) in kenya. *Exp. Agric.* **1969**, *5*, 9–16. [CrossRef]
14. Galvez, G.E.; Castano, M.; Vesga, B. Purification and serology of the necrotic streak mosaic virus of sisal. *Fitopatol. Colomb.* **1977**, *6*, v.139(2).
15. Morales, F.; Castaño, M.; Calvert, L.; Arroyave, J.A. Furcraea Necrotic Streak Virus: An Apparent New Member of the Dianthovirus Group. *J. Phytopathol.* **1992**, *134*, 247–254. [CrossRef]
16. Izaguirre-Mayoral, M.L.; Marys, E.; Olivares, E.; Oropeza, T. Effect of seasonal drought and cactus x virus infection on the crassulacean acid metabolism of *Agave sisalana* plants growing in a neotropical savanna. *J. Exp. Bot.* **1995**, *46*, 639–646. [CrossRef]
17. Chabi-Jesus, C.; Ramos-González, P.L.; Tassi, A.D.; Barguil, B.M.; Beserra, J.E.A., Jr.; Harakava, R.; Kitajima, E.W.; Freitas-Astúa, J. First report of citrus chlorotic spot virus infecting the succulent plant *Agave desmettiana* Jacob. *Plant Dis.* **2019**, *103*, 1438. [CrossRef]
18. Turco, S.; Golyaev, V.; Seguin, J.; Gilli, C.; Farinelli, L.; Boller, T.; Schumpp, O.; Pooggin, M.M. Small RNA-omics for virome reconstruction and antiviral defense characterization in mixed infections of cultivated solanum plants. *Mol. Plant Microbe Interact.* **2018**, *31*, 707–723. [CrossRef]
19. Golyaev, V.; Candresse, T.; Rabenstein, F.; Pooggin, M.M. Plant virome reconstruction and antiviral RNAi characterization by deep sequencing of small RNAs from dried leaves. *Sci. Rep.* **2019**, *9*, 1–10. [CrossRef]
20. Li, Y.; Jia, A.; Qiao, Y.; Xiang, J.; Zhang, Y.; Wang, W. Virome analysis of lily plants reveals a new potyvirus. *Arch. Virol.* **2018**, *163*, 1079–1082. [CrossRef]
21. Fonseca, P.L.C.; Badotti, F.; De Oliveira, T.F.P.; Fonseca, A.; Vaz, A.B.M.; Tomé, L.M.R.; Abrahão, J.S.; Marques, J.T.; Trindade, G.S.; Chaverri, P.; et al. Virome analyses of *Hevea brasiliensis* using small RNA deep sequencing and PCR techniques reveal the presence of a potential new virus. *Virol. J.* **2018**, *15*, 1–9. [CrossRef]
22. Ng, T.F.F.; Duffy, S.; Polston, J.E.; Bixby, E.; Vallad, G.E.; Breitbart, M. Exploring the diversity of plant DNA viruses and their satellites using vector-enabled metagenomics on whiteflies. *PLoS ONE* **2011**, *6*, e19050. [CrossRef] [PubMed]
23. Coetzee, B.; Freeborough, M.J.; Maree, H.J.; Celton, J.M.; Rees, D.J.G.; Burger, J.T. Deep sequencing analysis of viruses infecting grapevines: Virome of a vineyard. *Virology* **2010**, *400*, 157–163. [CrossRef]
24. Jo, Y.; Lian, S.; Chu, H.; Cho, J.K.; Yoo, S.H.; Choi, H.; Yoon, J.Y.; Choi, S.K.; Lee, B.C.; Cho, W.K. Peach RNA viromes in six different peach cultivars. *Sci. Rep.* **2018**, *8*, 1–14. [CrossRef]
25. Kotta-Loizou, I.; Coutts, R.H.A. Studies on the Virome of the Entomopathogenic Fungus *Beauveria bassiana* Reveal Novel dsRNA Elements and Mild Hypervirulence. *PLoS Pathog.* **2017**, *13*, 1–19. [CrossRef]
26. Velasco, L.; Arjona-Girona, I.; Cretazzo, E.; López-Herrera, C. Viromes in Xylariaceae fungi infecting avocado in Spain. *Virology* **2019**, *532*, 11–21. [CrossRef] [PubMed]
27. Calusinska, M.; Marynowska, M.; Goux, X.; Lentzen, E.; Delfosse, P. Analysis of dsDNA and RNA viromes in methanogenic digesters reveals novel viral genetic diversity. *Environ. Microbiol.* **2016**, *18*, 1162–1175. [CrossRef] [PubMed]
28. Phan, T.G.; da Costa, A.C.; del Valle Mendoza, J.; Bucardo-Rivera, F.; Nordgren, J.; O’Ryan, M.; Deng, X.; Delwart, E. The fecal virome of South and Central American children with diarrhea includes small circular DNA viral genomes of unknown origin. *Arch. Virol.* **2016**, *161*, 959–966. [CrossRef]

29. Raya, F.T.; Marone, M.P.; Carvalho, L.M.; Rabelo, S.C. Transcriptome analysis of three Agave fiber-producing cultivars suitable for biochemicals and biofuels production in semiarid regions. *BioRxiv* **2020**. [[CrossRef](#)]
30. Le Provost, G.; Paiva, J.; Pot, D.; Brach, J.; Plomion, C. Seasonal variation in transcript accumulation in wood-forming tissues of maritime pine (*Pinus pinaster* Ait.) with emphasis on a cell wall glycine-rich protein. *Planta* **2003**, *217*, 820–830. [[CrossRef](#)]
31. Grabherr, M.; Haas, B.J.; Yassour, M.; Levin, J.Z.; Thompson, D.; Amit, I.; Adiconis, X.; Fan, L.; Raychowdhury, R.; Zeng, Q.; et al. Trinity: Reconstructing a full-length transcriptome without a genome from RNA-Seq data. *Nat. Biotechnol.* **2013**, *29*, 644–652. [[CrossRef](#)]
32. Bray, N.L.; Pimentel, H.; Melsted, P.; Pachter, L. Near-optimal probabilistic RNA-seq quantification. *Nat. Biotechnol.* **2016**, *34*, 525–527. [[CrossRef](#)]
33. Haas, B.J.; Papanicolaou, A.; Yassour, M.; Grabherr, M.; Blood, P.D.; Bowden, J.; Couger, M.B.; Eccles, D.; Li, B.; Lieber, M.; et al. De novo transcript sequence reconstruction from RNA-seq using the Trinity platform for reference generation and analysis. *Nat. Protoc.* **2013**, *8*, 1494–1512. [[CrossRef](#)]
34. Camacho, C.; Coulouris, G.; Avagyan, V.; Ma, N.; Papadopoulos, J.; Bealer, K.; Madden, T.L. BLAST+: Architecture and applications. *BMC Bioinform.* **2009**, *10*, 421. [[CrossRef](#)] [[PubMed](#)]
35. Langmead, B.; Wilks, C.; Antonescu, V.; Charles, R. Scaling read aligners to hundreds of threads on general-purpose processors. *Bioinformatics* **2019**, *35*, 421–432. [[CrossRef](#)] [[PubMed](#)]
36. Li, H.; Handsaker, B.; Wysoker, A.; Fennell, T.; Ruan, J.; Homer, N.; Marth, G.; Abecasis, G.; Durbin, R. The Sequence Alignment/Map format and SAMtools. *Bioinformatics* **2009**, *25*, 2078–2079. [[CrossRef](#)]
37. Robinson, J.T.; Thorvaldsdóttir, H.; Winckler, W.; Guttman, M.; Lander, E.S.; Getz, G.; Mesirov, J.P. Integrative Genome Viewer. *Nat. Biotechnol.* **2011**, *29*, 24–26. [[CrossRef](#)] [[PubMed](#)]
38. Darling, A.C.E.; Mau, B.; Blattner, F.R.; Perna, N.T. Mauve: Multiple Alignment of Conserved Genomic Sequence with Rearrangements. *Genome Res.* **2004**, *14*, 1394–1403. [[CrossRef](#)] [[PubMed](#)]
39. Buchfink, B.; Xie, C.; Huson, D.H. Fast and sensitive protein alignment using DIAMOND. *Nat. Methods* **2014**, *12*, 59–60. [[CrossRef](#)]
40. Huang, X.; Madan, A. CAP3: A DNA sequence assembly program. *Genome Res.* **1999**, *9*, 868–877. [[CrossRef](#)]
41. Finn, R.D.; Clements, J.; Eddy, S.R. HMMER web server: Interactive sequence similarity searching. *Nucleic Acids Res.* **2011**, *39* (Suppl. S2), 29–37. [[CrossRef](#)]
42. Aguiar, E.R.G.R.; Olmo, R.P.; Paro, S.; Ferreira, F.V.; De Faria, I.J.D.S.; Todjro, Y.M.H.; Lobo, F.P.; Kroon, E.G.; Meignin, C.; Gatherer, D.; et al. Sequence-independent characterization of viruses based on the pattern of viral small RNAs produced by the host. *Nucleic Acids Res.* **2015**, *43*, 6191–6206. [[CrossRef](#)]
43. Geer, L.Y.; Marchler-Bauer, A.; Geer, R.C.; Han, L.; He, J.; He, S.; Liu, C.; Shi, W.; Bryant, S.H. The NCBI BioSystems database. *Nucleic Acids Res.* **2009**, *38* (Suppl. S1), 492–496. [[CrossRef](#)]
44. Katoh, K.; Rozewicki, J.; Yamada, K.D. MAFFT online service: Multiple sequence alignment, interactive sequence choice and visualization. *Brief. Bioinform.* **2018**, *20*, 1160–1166. [[CrossRef](#)]
45. Akaike, H. A New Look at the Statistical Model Identification. *IEEE Trans. Automat. Contr.* **1974**, *19*, 716–723. [[CrossRef](#)]
46. Kumar, S.; Stecher, G.; Li, M.; Nkya, C.; Tamura, K. MEGA X: Molecular Evolutionary Genetics Analysis across Computing Platforms. *Mol. Biol. Evol.* **2018**, *35*, 1547–1549. [[CrossRef](#)]
47. R Core Team. R: A Language and Environment for Statistical Computing. 2013. Available online: <https://doi.org/10.1108/eb003648> (accessed on 14 April 2021).
48. Hammer, Ø.; Harper, D.A.; Ryan, P.D. PAST Paleontological Statistics Reference manual. *Palaeontol. Electron.* **1999**, *4*, 9.
49. Medd, N.C.; Fellous, S.; Waldron, F.M.; Xuéreb, A.; Nakai, M.; Cross, J.V.; Obbard, D.J. The virome of *Drosophila suzukii*, an invasive pest of soft fruit. *Virus Evol.* **2018**, *4*, vey009. [[CrossRef](#)] [[PubMed](#)]
50. Candresse, T.; Theil, S.; Faure, C.; Marais, A. Determination of the complete genomic sequence of grapevine virus H, a novel vitivirus infecting grapevine. *Arch. Virol.* **2018**, *163*, 277–280. [[CrossRef](#)]
51. Giampetruzzi, A.; Roumi, V.; Roberto, R.; Malossini, U.; Yoshikawa, N.; La Notte, P.; Terlizzi, F.; Credi, R.; Saldarelli, P. A new grapevine virus discovered by deep sequencing of virus- and viroid-derived small RNAs in Cv Pinot gris. *Virus Res.* **2012**, *163*, 262–268. [[CrossRef](#)] [[PubMed](#)]
52. Charon, J.; Marcelino, V.R.; Wetherbee, R.; Verbruggen, H.; Holmes, E.C. Metatranscriptomic identification of diverse and divergent RNA viruses in green and chlorarachniophyte algae cultures. *Viruses* **2020**, *12*, 1180. [[CrossRef](#)] [[PubMed](#)]
53. Wolf, Y.I.; Silas, S.; Wang, Y.; Wu, S.; Bocek, M.; Kazlauskas, D.; Krupovic, M.; Fire, A.; Dolja, V.V.; Koonin, E.V. Doubling of the known set of RNA viruses by metagenomic analysis of an aquatic virome. *Nat. Microbiol.* **2020**, *5*, 1262–1270. [[CrossRef](#)] [[PubMed](#)]
54. Greninger, A.L. A decade of RNA virus metagenomics is (not) enough. *Virus Res.* **2018**, *244*, 218–229. [[CrossRef](#)]
55. Maclot, F.; Candresse, T.; Filloux, D.; Malmstrom, C.M.; Roumagnac, P.; van der Vlugt, R.; Massart, S. Illuminating an Ecological Blackbox: Using High Throughput Sequencing to Characterize the Plant Virome Across Scales. *Front. Microbiol.* **2020**, *11*, 1–16. [[CrossRef](#)] [[PubMed](#)]
56. Shi, M.; Lin, X.D.; Tian, J.H.; Chen, L.J.; Chen, X.; Li, C.X.; Qin, X.C.; Li, J.; Cao, J.P.; Eden, J.S.; et al. Redefining the invertebrate RNA virosphere. *Nature* **2016**, *540*, 539–543. [[CrossRef](#)]
57. Brunt, A.A.; Kenten, R.H. Cowpea mild mottle, a newly recognized virus infecting cowpeas (*Vigna unguiculata*) in Ghana. *Ann. Appl. Biol.* **1973**, *74*, 67–74. [[CrossRef](#)] [[PubMed](#)]

58. Zanardo, L.G.; Carvalho, C.M. Cowpea mild mottle virus (Carlavirus, Betaflexiviridae): A review. *Trop. Plant Pathol.* **2017**, *42*, 417–430. [[CrossRef](#)]
59. De Oliveira, R.; Oliveira, G.M.; dos Santos de Souza, M.; Borba, M.A.; Vendruscolo, J.; da Silva Nunes, G.; Nascimento, I.N.; de Luna Batista, J. Development and parasitism of *Encarsia hispida* (Hymenoptera: Aphelinidae) on *Bemisia tabaci* biotype B in cotton. *Afr. J. Agric. Res.* **2016**, *11*, 2266–2270. [[CrossRef](#)]
60. Queiroz, P.R.; Lima, L.H.; Martins, É.S.; Sujii, E.R.; Monnerat, R.G. Description of the molecular profiles of *Bemisia tabaci* (Hemiptera: Aleyrodidae) in different crops and locations in Brazil. *J. Entomol. Nematol.* **2017**, *9*, 36–45. [[CrossRef](#)]
61. Torres, J.B.; Silva-Torres, C.S.A.; Barros, R. Relative effects of the insecticide thiamethoxam on the predator *Podisus nigrispinus* and the tobacco whitefly *Bemisia tabaci* in nectaried and nectariless cotton. *Pest Manag. Sci.* **2003**, *59*, 315–323. [[CrossRef](#)] [[PubMed](#)]
62. Prashar, P.; Kapoor, N.; Sachdeva, S. Rhizosphere: Its structure, bacterial diversity and significance. *Rev. Environ. Sci. Biotechnol.* **2014**, *13*, 63–77. [[CrossRef](#)]
63. Shi, S.; Nuccio, E.E.; Shi, Z.J.; He, Z.; Zhou, J.; Firestone, M.K. The interconnected rhizosphere: High network complexity dominates rhizosphere assemblages. *Ecol. Lett.* **2016**, *19*, 926–936. [[CrossRef](#)]
64. Deakin, G.; Dobbs, E.; Bennett, J.M.; Jones, I.M.; Grogan, H.M.; Burton, K.S. Multiple viral infections in *Agaricus bisporus*—Characterisation of 18 unique RNA viruses and 8 ORFans identified by deep sequencing. *Sci. Rep.* **2017**, *7*, 1–13. [[CrossRef](#)] [[PubMed](#)]
65. Aoki, N.; Moriyama, H.; Kodama, M.; Arie, T.; Teraoka, T.; Fukuhara, T. A novel mycovirus associated with four double-stranded RNAs affects host fungal growth in *Alternaria alternata*. *Virus Res.* **2009**, *140*, 179–187. [[CrossRef](#)] [[PubMed](#)]
66. Kozlakidis, Z.; Herrero, N.; Ozkan, S.; Kanhayuwa, L.; Jamal, A.; Bhatti, M.F.; Coutts, R.H.A. Sequence determination of a quadripartite dsRNA virus isolated from *Aspergillus foetidus*. *Arch. Virol.* **2013**, *158*, 267–272. [[CrossRef](#)]
67. Gilbert, K.B.; Holcomb, E.E.; Allscheid, R.L.; Carrington, J.C. Hiding in plain sight: New virus genomes discovered via a systematic analysis of fungal public transcriptomes. *PLoS ONE* **2019**, *14*, e0219207. [[CrossRef](#)]
68. Pandey, B.; Naidu, R.A.; Grove, G.G. Next generation sequencing analysis of double-stranded RNAs from sweet cherry powdery mildew fungus *Podosphaera prunicola*. *J. Plant Pathol.* **2018**, *100*, 435–446. [[CrossRef](#)]
69. Marzano, S.-Y.L.; Nelson, B.D.; Ajayi-Oyetunde, O.; Bradley, C.A.; Hughes, T.J.; Hartman, G.L.; Eastburn, D.M.; Domier, L.L. Identification of Diverse Mycoviruses through Metatranscriptomics: Characterization of the Viromes of Five Major Fungal Plant Pathogens. *J. Virol.* **2016**, *90*, 6846–6863. [[CrossRef](#)] [[PubMed](#)]
70. Duarte, E.A.; Damasceno, C.L.; Oliveira, T.A.; Barbosa, L.D.; Martins, F.M.; Silva, J.R.; Lima, T.E.; Silva, R.M.; Kato, R.B.; Bortoline, D.E.; et al. Putting the mess in order: *Aspergillus welwitschiae* (and not *A. niger*) is the etiologic agent of the sisal bole rot disease. *Front. Microbiol.* **2018**, *9*, 1227. [[CrossRef](#)] [[PubMed](#)]
71. Quintanilha-Peixoto, G.; Torres, R.O.; Reis, I.M.A.; De Oliveira, T.A.S.; Bortolini, D.E.; Duarte, E.A.A.; De Carvalho Azevedo, V.A.; Brenig, B.; Aguiar, E.R.G.R.; Soares, A.C.F.; et al. Calm before the storm: A glimpse into the secondary metabolism of *aspergillus welwitschiae*, the etiologic agent of the sisal bole rot. *Toxins* **2019**, *11*, 631. [[CrossRef](#)] [[PubMed](#)]
72. Dakin, N.; White, D.; Hardy, G.E.S.J.; Burgess, T.I. The opportunistic pathogen, *Neofusicoccum australe*, is responsible for crown dieback of peppermint (*Agonis flexuosa*) in Western Australia. *Australas. Plant Pathol.* **2010**, *39*, 202–206. [[CrossRef](#)]
73. Son, M.; Yu, J.; Kim, K.H. Five Questions about Mycoviruses. *PLoS Pathog.* **2015**, *11*, 5–11. [[CrossRef](#)]
74. Nerva, L.; Varese, G.C.; Falk, B.W.; Turina, M. Mycoviruses of an endophytic fungus can replicate in plant cells: Evolutionary implications. *Sci. Rep.* **2017**, *7*, 1–11. [[CrossRef](#)]
75. Nuss, D.L. Hypovirulence: Mycoviruses at the fungal-plant interface. *Nat. Rev. Microbiol.* **2005**, *3*, 632–642. [[CrossRef](#)]
76. Adams, M.J.; Adkins, S.; Bragard, C.; Gilmer, D.; Li, D.; MacFarlane, S.A.; Wong, S.M.; Melcher, U.; Ratti, C.; Ryu, K.H. ICTV virus taxonomy profile: Virgaviridae. *J. Gen. Virol.* **2017**, *98*, 1999–2000. [[CrossRef](#)] [[PubMed](#)]
77. Matsumura, E.E.; Coletta-Filho, H.D.; Nourin, S.; Falk, B.W.; Nerva, L.; Oliveira, T.S.; Dorta, S.O.; Machado, M.A. Deep sequencing analysis of RNAs from citrus plants grown in a citrus sudden death-affected area reveals diverse known and putative novel viruses. *Viruses* **2017**, *9*, 92. [[CrossRef](#)]
78. Noojipady, P.; Morton, C.D.; Macedo, N.M.; Victoria, C.D.; Huang, C.; Gibbs, K.H.; Bolfe, L.E. Forest carbon emissions from cropland expansion in the Brazilian Cerrado biome. *Environ. Res. Lett.* **2017**, *12*, 025004. [[CrossRef](#)]
79. Al Rwahnih, M.; Rowhani, A.; Westrick, N.; Stevens, K.; Diaz-Lara, A.; Trouillas, F.P.; Preece, J.; Kallsen, C.; Farrar, K.; Golino, D. Discovery of viruses and virus-like pathogens in pistachio using high-throughput sequencing. *Plant Dis.* **2018**, *102*, 1419–1425. [[CrossRef](#)]
80. Rubio, L.; Guerri, J.; Moreno, P. Genetic variability and evolutionary dynamics of viruses of the family Closteroviridae. *Front. Microbiol.* **2013**, *4*, 1–15. [[CrossRef](#)]
81. Da Silva, C.A.D. Occurrence of new species of mealybug on cotton fields in the states of Bahia and Paraíba, Brazil. *Bragantia* **2013**, *71*, 467–470. [[CrossRef](#)]
82. Da Silva, C.A.D.; Vasconcelos, E.D.; De Almedia, R.P. Impact of different pineapple mealybug densities in a peanut crop. *Rev. Colomb. Entomol.* **2018**, *44*, 8–11. [[CrossRef](#)]
83. Blouin, A.G.; Keenan, S.; Napier, K.R.; Barrero, R.A.; MacDiarmid, R.M. Identification of a novel vitivirus from grapevines in New Zealand. *Arch. Virol.* **2018**, *163*, 281–284. [[CrossRef](#)] [[PubMed](#)]

84. Adams, M.J.; Candresse, T.; Hammond, J.; Kreuze, J.F.; Martelli, G.P.; Mamba, S.; Pearson, M.N.; Ryu, K.H.; Saldarelli, P.; Yoshikawa, N. Betaflexiviridae. In *Virus Taxonomy: Ninth Report of the International Committee on Taxonomy of Viruses*; Elsevier: Amsterdam, The Netherlands, 2012; pp. 920–941.
85. Chiapello, M.; Rodríguez-Romero, J.; Ayllón, M.A.; Turina, M. Analysis of the virome associated to grapevine downy mildew lesions reveals new mycovirus lineages. *Virus Evol.* **2020**, *6*, veaa058. [[CrossRef](#)] [[PubMed](#)]
86. Da Costa, C.R.G.; de Lima Marques, A.; de Moura, D.C.; Linhares, A.C.M.; de Sousa Silva, S.; Cavalcanti, M.I.P.; de Meireles, D.A.; de Melo Lucena, A.L. Post-harvest Quality of Table Grapes Marketed in the Municipality of Areia in the State of Paraíba. *J. Exp. Agric. Int.* **2020**, *42*, 56–59. [[CrossRef](#)]
87. Pereira-Stamford, N.; Pereira-Andrade, I.; da Silva-Junior, S.; Lira-Junior, M.; Silva-Santos, C.; Santiago de Freitas, A.; Van-Straaten, P. Soil properties and grape yield affected by rock biofertilisers with earthworm compound. *J. Soil Sci. Plant Nutr.* **2011**, *11*, 15–25. [[CrossRef](#)]
88. De Medeiros, R.M.; de Matos, R.M.; Saboya, L.M.F.; da Silva, P.F. Aptidão agroclimática para o cultivo da videira (*Vitis vinifera* L.) no estado da paraíba. *Rev. Bras. Agric. Irrig.* **2017**, *11*, 1492–1499. [[CrossRef](#)]
89. Geering, A.D.W.; Thomas, J.E. Characterisation of a virus from Australia that is closely related to papaya mosaic potexvirus. *Arch. Virol.* **1999**, *144*, 577–592. [[CrossRef](#)]
90. Beserra, J.E.A., Jr.; de Carvalho, M.G.; Barguil, B.M.; Zerbini, F.M. Partial genome sequence of a Potyvirus and of a virus in the order Tymovirales found in *Senna macranthera* in Brazil. *Trop. Plant Pathol.* **2011**, *36*, 116–120. [[CrossRef](#)]
91. Fuji, S.; Shinoda, K.; Furuya, H.; Naito, H.; Fukumoto, F. Complete nucleotide sequence of Nerine virus X (NVX-J) isolated from the African lily plant (*Agapanthus campanulatus*) in Japan. *Arch. Virol.* **2006**, *151*, 205–208. [[CrossRef](#)]
92. Rosani, U.; Shapiro, M.; Venier, P.; Allam, B. A needle in a haystack: Tracing bivalve-associated viruses in high-throughput transcriptomic data. *Viruses* **2019**, *11*, 205. [[CrossRef](#)]
93. Pearce, T.A.; Örstan, A. Terrestrial gastropoda. In *The Mollusks: A Guide to Their Study, Collection, and Preservation*; Universal-Publishers: Irvine, CA, USA, 2006; pp. 262–285.
94. Pratt, W.L. *Humboldtiana agavophila*, a New Helminthoglyptid Land Snail from the Chisos Mountains, Big Bend National Park, Texas. *Southwest. Nat.* **1971**, *15*, 429–435. [[CrossRef](#)]

Supplementary Data

Table S1: Species names and respective accession numbers of the viral sequences used for phylogenetic analysis in Fig. 3.

Virus name	Accession
<i>Acidomyces richmondensis</i> tobamo-like virus 1	AZT88673
Acute bee paralysis virus	QGL51678
African oil palm ring spot virus	YP_002776347
<i>Agaricus bisporus</i> spherical virus	AQM32769
<i>Agaricus bisporus</i> virus 3	AQM49919
<i>Agaricus bisporus</i> virus 5	AQM49927
<i>Agaricus bisporus</i> virus 6	AQM49948
<i>Agave tequilana</i> leaf virus	YP_009373228
<i>Alternaria alternata</i> virus 1	YP_001976150
Apple chlorotic leaf spot virus	AOF42977
Apple chlorotic leaf spot virus	NP_040551
Apple stem grooving virus	NP_044335
Apple stem pitting virus	NP_604464
Apricot pseudo-chlorotic leaf spot virus	BCA25706
Apricot vein clearing associated virus	YP_008997790
Apricot vein clearing associated virus	BCA25721
<i>Aspergillus foetidus</i> dsRNA mycovirus	YP_007353985
<i>Aspergillus heteromorphus</i> alternavirus 1	AZT88576
<i>Aspergillus</i> mycovirus 341	ABX79997
Atractylodes mottle virus	YP_009508317
Atrato Virga-like virus 7	QHA33778
Atrpec virus 1	AYN75539
<i>Auricularia heimuier</i> myco virgavirus 1	QIM57886
Banana mild mosaic virus	NP_112029
Beihai charybdis crab virus 1	YP_009333242
Beihai picorna-like virus 71	YP_009333456
Betavulgaris mito virus 1	QBN22178
Blackberry vein banding-associated virus	YP_008411010
Blueberry scorch virus	AAV18409
<i>Botrytis</i> virus X	NP_932306
Bundaberg bee virus 2	AWK77852
Camellia ring spot associated virus 1	QEJ80622
<i>Cannabis sativa</i> mitovirus 1	DAB417542
Carrot Ch virus 1	NP_009103999
Cassava common mosaic virus	NP_042695
<i>Chenopodium quinoa</i> mitovirus 1	YP_009551903
Cherry mottle leaf virus	AOY07776
Cherry rusty mottle associated virus	YP_007761581
Cherry symptomless virus	QIA61761
Cherry virus A	ATJ05013
Chrysanthemum virus B	CAO78688
Citrus chlorotic leaf spot virus	QOQ52500
Citrus leaf blotch virus	NP_624333
Citrus virga-like virus	ARO38275
Cnidium virus X	BBI37360
Cole latent virus	QGN03507
Cowpea mild mottle virus	AGS13088

Cucumber vein-clearing virus	YP_009664734
Diuris virus A	YP_006905850
Fig latent virus 1	CAY32622
Fox tail mosaic virus	AWT40556
Fox tail mosaic virus	ABW25054
Frangipani mosaic virus	AEW67306
<i>Fusarium graminearum</i> alternavirus 1	YP_009449446
<i>Fusarium graminearum</i> mycotymo virus 1	YP_009553357
<i>Fusarium incarnatum</i> alternavirus 1	AYJ09266
<i>Fusarium poae</i> alternavirus 1	YP_009272949
Garlic yellow mosaic-associated virus	AZM69107
Grapevine associated jivivirus 1	QIJ25699
Grapevine leafroll-associated virus 1	QBZ78645
Grapevine leafroll-associated virus 3	AXI82159
Grapevine leafroll-associated virus 4	ARP51817
Grapevine Pinotgris virus	QEQ50023
Grapevine virga-like virus	QCF47402
Grapevine virus A	NP_619662
Grapevine virus A	AAO84267
Grapevine virus B	AHZ62715
Grapevine virus B	AWD77984
Grapevine virus B	AOX49252
Grapevine virus E	YP_002117775
Grapevine virus G	ATV81261
Grapevine virus G	YP_009551946
Grapevine virus H	YP_009551905
Grapevine virus L	QBM91193
Grapevine virus M	QCF24338
<i>Haemonchus contortus</i> virus	CDJ82925
Heracleum latent virus	QIQ28218
Hibiscus latent Singapore virus	ARM71140
Hippeastrum latente virus	YP_002308447
Hobart betaflexivirus 1	AWK77906
Hubei virga-like virus 1	YP_009337423
<i>Humulus lupulus</i> mitovirus 1	DAB41749
Hydrangea chlorotic mottle virus	YP_002985636
Hydrangea ring spot virus	BAU45634
Ligustrum virus A	YP_009288956
Little cherry virus 2	ATB18128
Luckshill virus	AWA82251
<i>Macrophomina phaseolina</i> tobamo-like virus 1A	ALD891032
Mexico tricho virus	QDR50348
Mint virus 2	YP_009664761
Odonto glossum rings potvirus	AAZ81884
<i>Oxybasis rubra</i> mitovirus 1	DAB41745
Papaya mottle associated virus	QIJ97108
Peach chlorotic leaf spot virus	AYA62500
Peach mosaic virus	YP_002308565
Pepper virus A	YP_009357230
Perth betaflexivirus 1	AWK77908
<i>Petunia exserta</i> mitovirus 1	DAB41750
Phlox virus B	YP_001552317
Pineapple mealy bug wilt-associated virus 2	QCC20262
Pistachio ampelo virus A	AVN99305
<i>Plasmopara viticola</i> associated tobamo-like virus 1	QIP68002
<i>Podosphaera prunicola</i> tobamo-like virus	ATS94407

Potato vírus H	AYV96574
Potato virus M	QBL75476
Potato virus M	ATG34140
Potato virus M	NP_056767
Potato virus T	AFV39891
Potato virus T	YP_002019748
Potato vírus T	AFV39891
Riboviria sp	QDH89210
<i>Salvia divinorum</i> RNA virus 1	YP_009553026
Shayang virga-like vírus 1	YP_009333208
<i>Solanum chacoense</i> mitovirus 1	DAB41743
<i>Stemphylium lycopersici</i> mycovirus	YP_009551661
Tamus red mosaic virus	YP_004849314
Tobacco mild green mosaic virus	QIM41095
Tulip virus X	NP_702988
Turtle grass vírus X	YP_009552762
Weivirus-like virus	QJI53767
Wenzhou picorna-like vírus 26	YP_009337682
Wenzhou picorna-like vírus 27	YP_009336706
Yam latente virus	YP_009134730

Table S2: General description of deep sequenced libraries and virus detection strategy. Raw counts of RNA and DNA libraries as well as metrics related to transcript assembly and sequence similarity searches are presented in the rows. *Agave* species are indicated in the columns.

	<i>A. fourcroydes</i>	<i>A. sisalana</i>	<i>A. hybrid 11648</i>	Sum
Raw RNAseq reads	200,498,222	208,260,315	150,509,074	559,267,611
Assembled Transcripts	81,190	93,569	77,194	251,953
Mean contig length	599	575	584	1758
Min. contig length	168	171	171	510
Viral Transcripts BLASTN	4	1	5	10
Viral Transcripts BLASTX	49	34	28	79*
Raw DNAseq reads	131,365,537	118,820,218	119,180,610	369,366,365

Table S3: Similarity of *Agave*-derived contigs against known CPMMV genomes. Analysis was performed using Blast with the variant BLASTn.

	Plant	AF				AS	HI				
	Contig	DN22786	DN53839	DN59783	DN97584	DN6612	DN10130	DN110105	DN114005	DN42686	DN55516
	Length	270	3600	369	362	867	867	264	387	315	285
KC774019.1	Sim. (%)	97.41	98.31	98.37	98.34	98.62	98.73	98.49	95.87	98.41	98.25
	Length	269	3599	368	361	866	866	263	386	314	284
KC774020.1	Sim. (%)	97.78	98.08	97.29	97.21	98.85	98.96	98.86	95.35	98.73	97.54
	Length	269	3599	368	358	866	866	263	386	314	284
KC884245.1	Sim. (%)	97.05	98.42	98.37	98.62	98.85	98.96	99.24	95.87	97.46	96.49
	Length	270	3599	368	361	866	866	263	386	314	284
MK202583.1	Sim. (%)	98.52	96.25	98.37	96.41	90.31	90.43	99.24	94.32	96.19	
	Length	269	3595	368	361	866	866	263	386	314	
KC884248.1	Sim. (%)	98.15	98.28	98.65	98.34			99.24	95.87	97.46	
	Length	269	3599	368	361			263	386	314	

Table S4: Quantitative metrics for the reference genome of CPMMV (CPMMV:BR:MG:09:3) and the genome obtained from the RNA-seq data of *Agave fourcroydes*.

Name	CPMMV:BR:MG:09:3	CPMMV isolate PB:AF
Contigs	1	1
Length	8196	8193
N50	8196	8193
L50	1	1
GC	0.403	0.4
For runs of Ns (>= 10 Ns):		
Num	0	2
Span	0	47

Table S5: BLASTx best hits for each viral contig, and their respective alignment metrics.

qseqid (TRINITY_DN...)	sseqid	percent	length	mismatch	gapopen	qstart	qend	sstart	send	evalue	bitscore	qlen	species
61147	YP_009553503.1	50.9	55	27	0	4	168	1915	1969	8.10E-14	65.9	213	Actinidia seed-borne latent virus
49676	AQM49927.1	39.7	662	384	7	4	1953	1742	2400	5.2E-124	435.3	2163	Agaricus bisporus virus 5
16142	AQM49927.1	32.7	431	252	8	115	1356	1259	1668	1.90E-60	223.4	1359	Agaricus bisporus virus 5
44352	AQM49927.1	30.8	347	226	6	4	1008	1742	2086	2.20E-37	146.4	1011	Agaricus bisporus virus 5
83710	AQM49927.1	46.3	188	100	1	1	564	2214	2400	1.40E-42	163.3	774	Agaricus bisporus virus 5
19804	AQM49927.1	52.9	140	66	0	7	426	2076	2215	4.30E-38	147.5	435	Agaricus bisporus virus 5
24880	AQM32763.1	54.5	411	187	0	37	1269	2132	2542	1.3E-139	486.5	1404	Agaricus bisporus virus 6
27401	AQM49948.1	47.3	281	145	3	1	843	1815	2092	2.10E-68	249.2	846	Agaricus bisporus virus 6
77293	AQM49948.1	59.5	121	47	2	4	366	1700	1818	1.60E-41	158.7	366	Agaricus bisporus virus 6
55189	AQM32763.1	41.1	112	58	3	7	324	642	751	4.70E-21	90.5	327	Agaricus bisporus virus 6
Contig17	YP_459948.1	32.8	186	121	3	271	825	11	193	1.50E-26	110.2	867	Alternanthera mosaic virus
63052	YP_459944.1	43	114	64	1	1	339	1023	1136	1.40E-20	89	342	Alternanthera mosaic virus
81586	YP_001976142.1	85.5	110	16	0	1	330	441	550	3.10E-52	194.1	330	Alternaria alternata virus 1
61614	YP_001976151.1	75	80	20	0	7	246	21	100	1.30E-34	135.2	246	Alternaria alternata virus 1
Contig7	NP_604464.1	49.9	1001	477	6	607	3588	1193	2175	1.80E-286	975.7	3600	Apple stem pitting virus
83885	NP_604464.1	42.8	201	112	3	10	606	1652	1851	8.50E-40	153.7	609	Apple stem pitting virus
Contig14	YP_007353983.1	53.2	538	250	1	1	1614	191	726	2.10E-170	589	1617	Aspergillus foetidus dsRNA mycovirus

73798	YP_007353985.1	76.3	97	23	0	10	300	637	733	3.50E-39	150.6	300	Aspergillus foetidus dsRNA mycovirus
116043	YP_007353985.1	75.9	79	19	0	4	240	307	385	1.20E-34	135.2	240	Aspergillus foetidus dsRNA mycovirus
72309	YP_007353983.1	55.4	56	25	0	64	231	6	61	2.60E-13	64.3	231	Aspergillus foetidus dsRNA mycovirus
Contig19	AZT88576.1	49.6	514	255	3	1	1530	319	832	9.90E-138	480.3	1533	Aspergillus heteromorphus alternavirus 1
83752	AZT88575.1	55.4	112	50	0	1	336	159	270	4.70E-40	153.7	336	Aspergillus heteromorphus alternavirus 1
Contig5	QED22727.1	54.6	1124	502	5	31	3384	13	1134	0.00E+00	1201.8	3387	Botryosphaeria dothidea tobamovirus-like virus
Contig12	ADD65542.1	41.2	148	82	1	1	444	525	667	6.50E-32	127.1	465	Cassia mild mosaic virus
100760	ARO38275.1	56.7	838	353	3	544	3036	1	835	4.70E-280	954.1	3069	Citrus virga-like virus
26278	ARO38274.1	50.4	125	61	1	4	378	1168	1291	1.00E-31	126.3	432	Citrus virga-like virus
133840	ARO38274.1	62.3	114	42	1	1	339	369	482	9.20E-36	139.4	339	Citrus virga-like virus
88105	YP_006905850.1	32.6	218	120	8	1	612	1107	1311	1.40E-18	83.2	615	Diuris virus A
86319	YP_006908997.1	66.7	105	28	3	1	309	258	357	5.10E-33	130.2	309	Diuris virus A
44239	YP_004732978.2	36.7	256	139	13	7	744	1221	1463	1.10E-25	107.1	765	Grapevine Pinot gris virus
3617	QCF47403.1	38.4	739	391	12	70	2268	25	705	1.80E-138	483.4	2310	Grapevine virga-like virus
65779	QCF47402.1	63.4	134	49	0	1	402	368	501	1.60E-42	162.2	402	Grapevine virga-like virus
52979	YP_009552539.1	26.6	872	538	26	31	2406	16	865	2.30E-73	267.3	2619	Grapevine virus G
46510	YP_009552539.1	25	680	408	23	1	1806	210	865	8.50E-41	158.7	1965	Grapevine virus G
40814	YP_009552542.1	38.3	128	79	0	16	399	74	201	7.60E-21	90.1	402	Grapevine virus G
65618	YP_009552542.1	35.9	128	82	0	10	393	74	201	2.20E-20	88.6	396	Grapevine virus G

42135	YP_009551905.1	54.9	255	115	0	82	846	1368	1622	6.20E-81	290.8	846	Grapevine virus H
52810	YP_009552715.1	38.4	482	281	7	91	1521	1232	1702	3.40E-87	313.9	4224	Halhan virus 3
99951	YP_009552715.1	48.6	72	34	3	1	216	445	513	1.10E-13	65.5	222	Halhan virus 3
Contig9	YP_009109559.1	27.4	1644	930	51	1093	5370	2	1600	3.90E-136	476.9	5397	Macrophomina phaseolina tobamo-like virus
Contig6	YP_009109559.1	32.9	140	77	4	2419	2838	1314	1436	4.50E-10	57.4	3309	Macrophomina phaseolina tobamo-like virus
30831	YP_009109561.1	41.6	370	182	6	1	1110	40	375	1.40E-64	236.9	1110	Macrophomina phaseolina tobamo-like virus
38090	YP_009109562.1	46.1	332	169	2	43	1008	2	333	7.30E-84	300.8	1038	Macrophomina phaseolina tobamo-like virus
Contig8	YP_009109562.1	36.9	293	178	6	31	888	7	299	3.20E-44	169.1	1011	Macrophomina phaseolina tobamo-like virus
105616	YP_009109562.1	36.1	299	180	4	16	891	7	301	2.20E-45	172.9	1005	Macrophomina phaseolina tobamo-like virus
72996	YP_009109559.1	84.3	70	11	0	1	210	1962	2031	1.60E-33	131.3	213	Macrophomina phaseolina tobamo-like virus
26423	YP_009109559.1	48.5	68	35	0	1	204	1766	1833	3.70E-16	73.6	204	Macrophomina phaseolina tobamo-like virus
75281	YP_009109561.1	68.3	63	20	0	13	201	221	283	3.30E-20	87	204	Macrophomina phaseolina tobamo-like virus
85955	YP_009109559.1	84.1	63	10	0	7	195	1351	1413	2.00E-27	110.9	198	Macrophomina phaseolina tobamo-like virus
38752	YP_446996.1	33.8	201	132	1	148	747	16	216	1.20E-33	133.7	774	Nerine virus X
59050	AVN99304.1	41.6	1634	766	18	1	4899	1	1446	0.00E+00	1148.3	4902	Pistachio ampelovirus A
49906	AVN99304.1	42.4	1603	762	17	1	4794	1	1446	0.00E+00	1160.2	4797	Pistachio ampelovirus A
Contig16	AVN99304.1	34.8	1246	655	16	1	3729	1	1091	1.00E-191	661	3732	Pistachio ampelovirus A

59050	AVN99304.1	43.4	670	378	1	1	2010	1	669	8.20E-159	551.6	3561	Pistachio ampelovirus A
2548	AVN99305.1	63.6	453	165	0	1	1359	33	485	3.30E-177	611.3	1362	Pistachio ampelovirus A
Contig15	AVN99306.1	39.1	207	126	0	292	912	150	356	4.10E-38	148.7	924	Pistachio ampelovirus A Plasmopara viticola
75741	QGY72559.1	46.6	131	66	3	7	390	459	588	1.60E-28	115.5	390	associated ourmia-like virus 29
110665	QGY72536.1	61.8	68	26	0	1	204	76	143	2.30E-21	90.9	204	Plasmopara viticola associated ourmia-like virus 6
83949	ATS94408.1	46.4	207	107	3	10	621	614	819	2.90E-43	165.2	621	Podosphaera prunicola tobamo-like virus
77371	ATS94409.1	40.9	171	101	0	61	573	98	268	6.80E-39	150.6	576	Podosphaera prunicola tobamo-like virus
69322	ATS94408.1	49.4	85	42	1	7	261	821	904	3.00E-18	80.9	264	Podosphaera prunicola tobamo-like virus
Contig20	YP_009551663.1	64	339	114	2	4	1011	423	756	2.90E-125	438.3	1014	Stemphylium lycopersici mycovirus
Contig1	YP_009551661.1	68.5	308	87	3	1	924	545	842	8.70E-113	396.7	927	Stemphylium lycopersici mycovirus
17344	YP_009551660.1	64.3	252	90	0	1	756	897	1148	9.70E-102	359.8	759	Stemphylium lycopersici mycovirus
Contig10	YP_009551661.1	56.5	239	98	1	4	702	305	543	1.10E-75	273.1	702	Stemphylium lycopersici mycovirus
Contig11	YP_009551661.1	64.8	128	45	0	1	384	170	297	1.70E-41	158.7	387	Stemphylium lycopersici mycovirus
92324	YP_009551660.1	68	100	32	0	1	300	799	898	3.30E-40	154.1	306	Stemphylium lycopersici mycovirus

Table S6: Overview of the transcripts assigned as false positives (rows) and associated data. Columns indicate transcript name, length (in base pairs), the protein and species hit on BLASTx, their respective accession code, detected protein domains and finally, the reason for discard.

Protein Domain	Discarded by	ORF Pattern
AAA domain	Present in genomic DNA, protein domain not viral	non-fragmented
Cation efflux family, Dimerisation domain of Zinc Transporter	Present in genomic DNA, protein domain not viral	
Thaumatin family	Present in genomic DNA, protein domain not viral	
<i>none identified</i>	<i>no relevant hits</i>	
<i>none identified</i>	<i>no relevant hits</i>	non-fragmented
<i>none identified</i>	<i>no relevant hits</i>	non-fragmented
Cas3	Protein domain not viral	
Viral methyltransferase	CPMMV	
<i>none identified</i>	Present in genomic DNA	non-fragmented
<i>none identified</i>	Present in genomic DNA	non-fragmented
Mitovirus RdRp	Present in genomic DNA	non-fragmented
<i>none identified</i>	Present in genomic DNA	non-fragmented
<i>none identified</i>	Present in genomic DNA	non-fragmented

Name	Length	Protein hit	Species	Accession code
<i>disc1</i>	813	RdRp	Macrophomina phaseolina tobamo-like virus	YP_009109559.1
<i>disc2</i>	1197	Putative Protein P31	Pistachio ampelovirus A	AVN99313.1
<i>disc3</i>	762	Putative Protein P33	Pistachio ampelovirus A	AVN99309.1
<i>disc4</i>	201	Hypothetical Protein	Aspergillus foetidus dsRNA mycovirus	YP_007353982.1
<i>disc5</i>	1809	Putative RdRp	Aspergillus mycovirus 341	ABX79997.1
<i>disc6</i>	222	RdRp	Helicobasidium mompa partitivirus V1-2	BAD32678.1
<i>disc7</i>	792	Movement Protein	Podosphaera prunicola tobamo-like virus	ATS94408.1
<i>disc8</i>	369	RdRp	Apple stem pitting virus	NP_604464.1
<i>disc9</i>	693	RdRp	Beta vulgaris mitovirus 1	DAB41759.1
<i>disc10</i>	309	RdRp	Beta vulgaris mitovirus 1	DAB41759.1
<i>disc11</i>	435	RdRp	Beta vulgaris mitovirus 1	DAB41759.1
<i>disc12</i>	207	RdRp	Beta vulgaris mitovirus 1	DAB41759.1
<i>disc13</i>	228	RdRp	Beta vulgaris mitovirus 1	DAB41759.1

Table S7: Classification scheme for the phylogenetic analysis. Columns indicate: Class name, the requisites for that given class (characteristics of the viral species, concerning contig length and type), the number of species included in that category, and their correspondent percentage.

Class	Requisites	Number	(%)
0	No RdRp sequence detected	2	9.52
1	Partial RdRp sequence (<500 bp) accompanied by other transcripts or not	10	40.00
2	Large fragment (>500 bp) of RdRp	8	32.00
3	Large fragment (>500 bp) of RdRp and some other viral protein (except for the coat protein)	1	4.00
4	Large fragment (>500 bp) of RdRp and the coat protein detected, other viral protein facultative	4	16.00

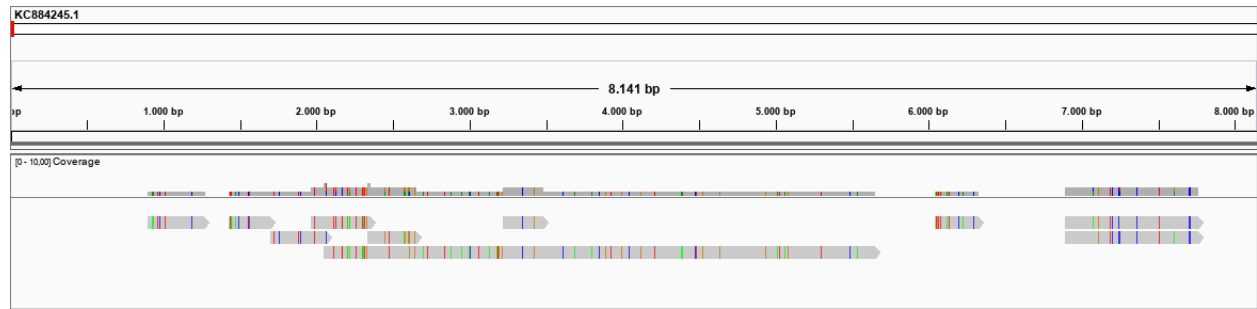


Figure S1: Distribution of the assembled transcript on the genome of *Cowpea mild mottle virus* (KC884245.1). Figure as produced using IGV. Colorful lines inside arrows indicate genetic variation in comparison with the reference.

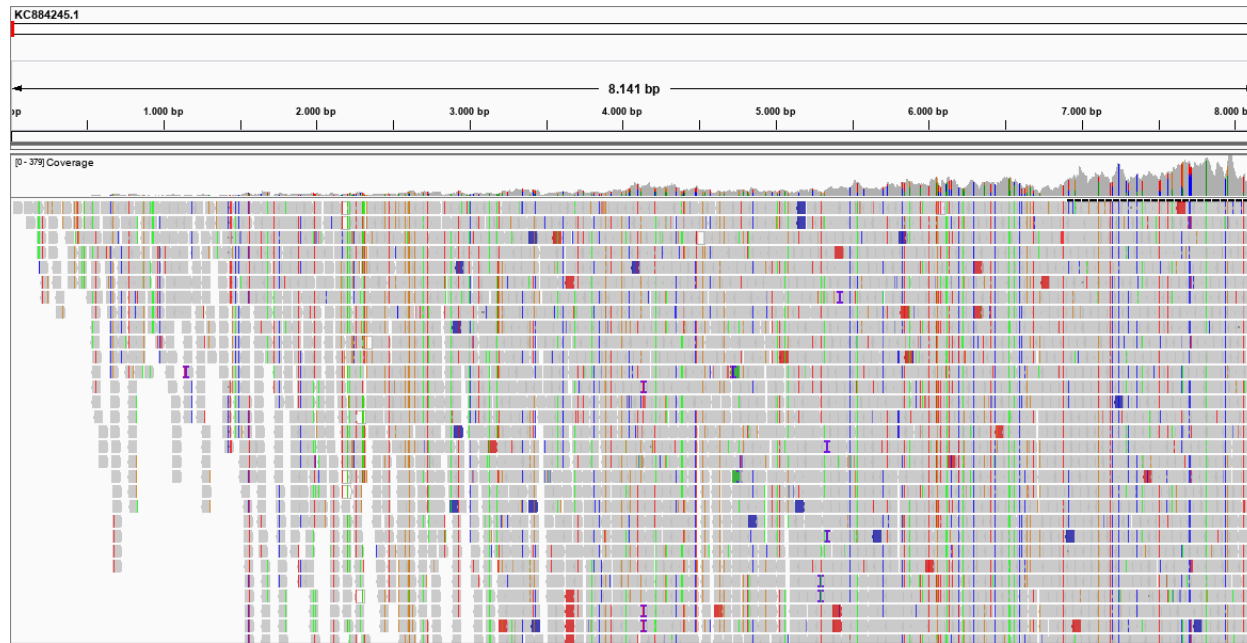


Figure S2: Coverage of raw sequencing reads along CPMMV reference genome. Only reads over 50 bp were used in this analysis. The visualization was generated using IGV. Each arrow in the lower part indicates a single sequencing read. In those arrows, colorful regions indicate genetic variation in comparison to the reference. As seen in the middle section, coverage is deeper in the end on the transcript.

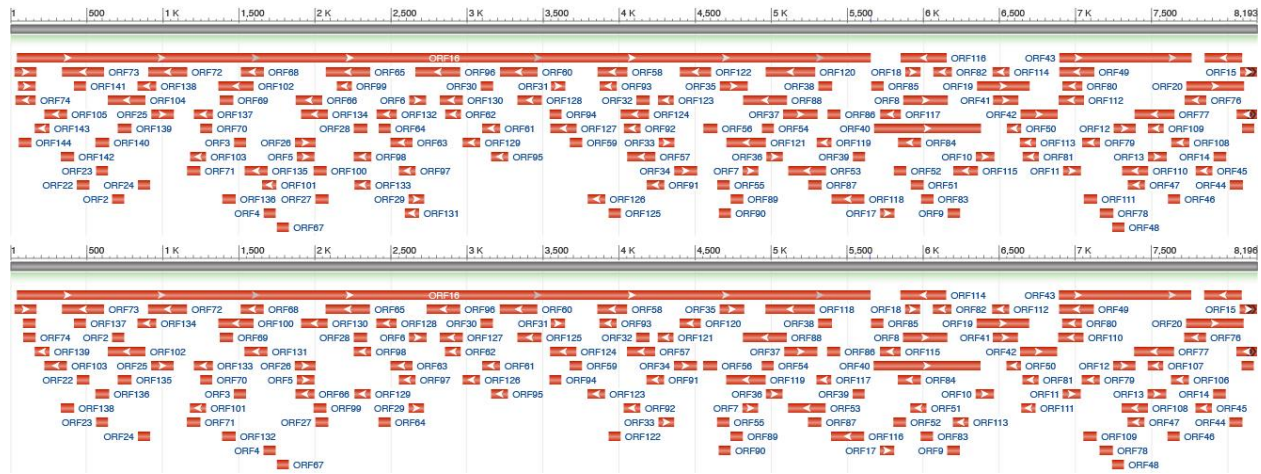


Figure S3: Structural annotation of CPPMV strains. ORF profile in CPMMV:BR:MG:09:3 (upper) and CPMMV isolate PB:AF (lower). The visualization was produced using orffinder (<https://www.ncbi.nlm.nih.gov/orffinder/>) from NCBI portal. The arrow direction indicates the strand which the ORF was identified.

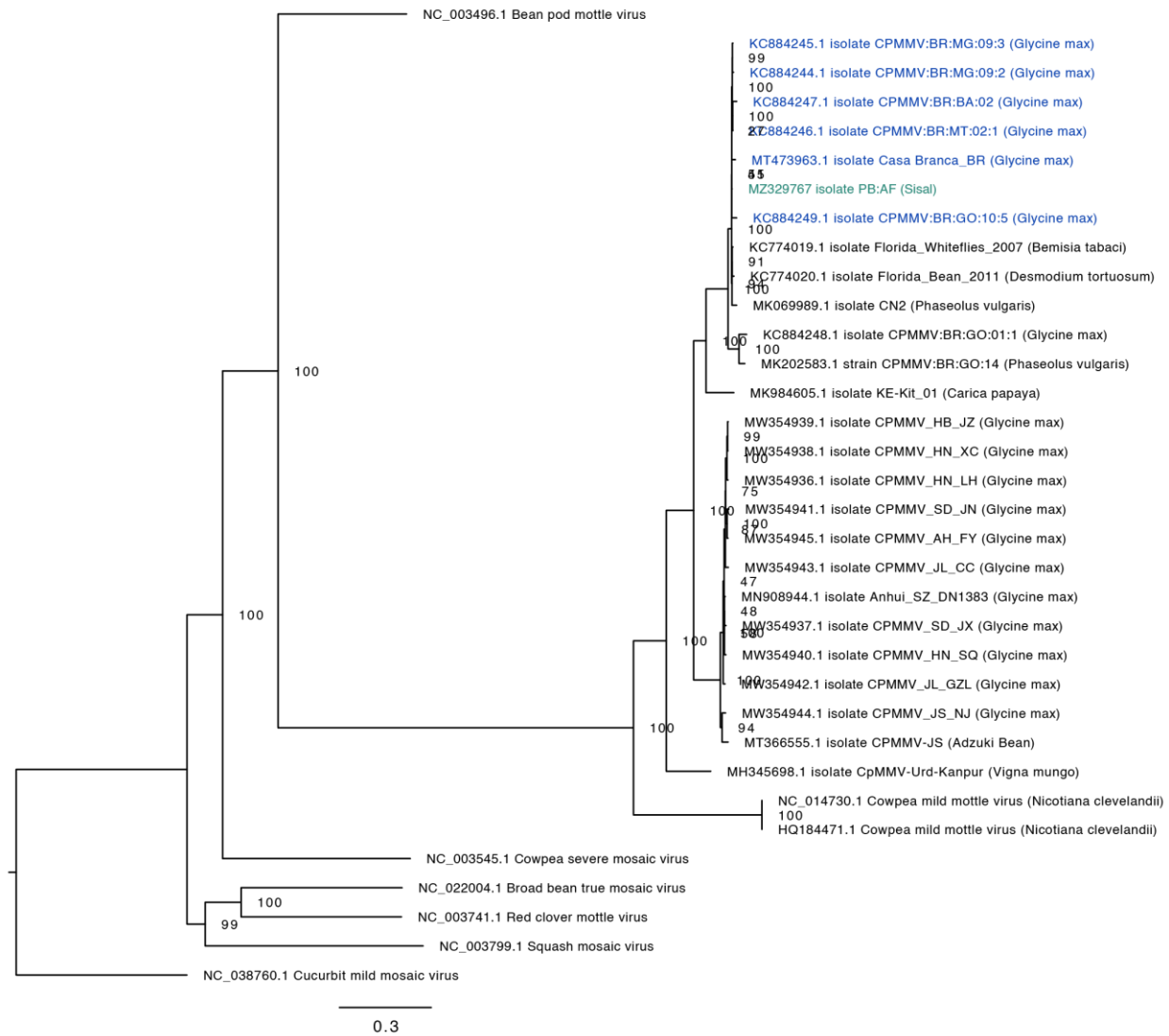


Figure S4: Phylogenetic analysis of Cowpea Mild Mottle virus isolate PB:AF. Accession numbers in blue indicate samples from Brazil, while green indicates the isolate assembled in this work.

Table S8: The accession codes and descriptions to each viral contig and their respective viral species. “RdRp” estands for RNA-dependent RNA polymerase, and, in this table, is a synonym to “Replicase”.

Species Name	Contig Name	Acc Code	Protein Type
Cowpea Mild Mottle Virus	Cowpea	MZ329767	Genome
Sisal-associated Alphaflexivirus A	Contig17	MZ599622	Putative coat protein
Sisal-associated Alphaflexivirus A	TRINITY_DN63052_c0_g1_i1	MZ599634	Putative Replicase
Sisal-associated Alphaflexivirus B	Contig12	MZ599625	Putative Replicase
Sisal-associated Alphaflexivirus C	TRINITY_DN38752_c0_g1_i1	MZ599621	Putative coat protein
Sisal-associated Betaflexivirus A	Contig7	MZ329756	RdRp
Sisal-associated Betaflexivirus A	TRINITY_DN83885_c0_g1_i1	MZ599608	Putative Replicase
Sisal-associated Betaflexivirus B	TRINITY_DN88105_c0_g1_i1	MZ329759	RdRp
Sisal-associated Betaflexivirus B	TRINITY_DN86319_c0_g1_i1	MZ599609	Putative Replicase
Sisal-associated Betaflexivirus C	TRINITY_DN44239_c0_g1_i1	MZ329760	RdRp
Sisal-associated Betaflexivirus D	TRINITY_DN52979_c0_g1_i1	MZ329761	RdRp
Sisal-associated Betaflexivirus D	TRINITY_DN46510_c0_g1_i1	MZ599640	Putative Replicase
Sisal-associated Betaflexivirus D	TRINITY_DN40814_c0_g1_i1	MZ599610	Putative coat protein
Sisal-associated Betaflexivirus D	TRINITY_DN65618_c0_g1_i1	MZ599641	Putative coat protein
Sisal-associated Betaflexivirus E	TRINITY_DN42135_c0_g1_i1	MZ329762	RdRp
Sisal-associated Botourmiavirus A	TRINITY_DN75741_c0_g1_i1	MZ599649	Putative Replicase
Sisal-associated Botourmiavirus B	TRINITY_DN110665_c0_g1_i1	MZ599650	Putative Replicase
Sisal-associated Closterovirus A	TRINITY_DN2548_c0_g1_i1	MZ329764	RdRp
Sisal-associated Closterovirus A	TRINITY_DN59050_c1_g1_i1	MZ599642	hypothetical protein
Sisal-associated Closterovirus A	TRINITY_DN49906_c0_g1_i3	MZ599616	hypothetical protein
Sisal-associated Closterovirus A	Contig16	MZ599628	hypothetical protein
Sisal-associated Closterovirus A	TRINITY_DN59050_c1_g1_i2	MZ599643	hypothetical protein
Sisal-associated Closterovirus A	Contig15	MZ599629	Putative coat protein
Sisal-associated Ribovirus A	TRINITY_DN3617_c0_g1_i1	MZ599639	hypothetical protein
Sisal-associated Ribovirus A	TRINITY_DN65779_c0_g1_i1	MZ599646	Putative Replicase
Sisal-associated Unclassified dsRNA virus A	TRINITY_DN81586_c0_g1_i1	MZ599606	Putative Replicase

Sisal-associated Unclassified dsRNA virus A	TRINITY_DN61614_c0_g1_i1	MZ599607	hypothetical protein
Sisal-associated Unclassified dsRNA virus B	Contig14	MZ599623	hypothetical protein
Sisal-associated Unclassified dsRNA virus B	TRINITY_DN73798_c0_g1_i1	MZ599644	Putative Replicase
Sisal-associated Unclassified dsRNA virus B	TRINITY_DN116043_c0_g1_i1	MZ599635	Putative Replicase
Sisal-associated Unclassified dsRNA virus B	TRINITY_DN72309_c0_g1_i1	MZ599636	hypothetical protein
Sisal-associated Unclassified dsRNA virus C	TRINITY_DN17344_c0_g1_i1	MZ329765	RdRp
Sisal-associated Unclassified dsRNA virus C	Contig20	MZ599630	hypothetical protein
Sisal-associated Unclassified dsRNA virus C	Contig1	MZ599631	Putative coat protein
Sisal-associated Unclassified dsRNA virus C	Contig10	MZ599632	Putative coat protein
Sisal-associated Unclassified dsRNA virus C	Contig11	MZ599633	Putative coat protein
Sisal-associated Unclassified dsRNA virus C	TRINITY_DN92324_c0_g1_i1	MZ599619	Putative Replicase
Sisal-associated Unclassified virus A	TRINITY_DN61147_c0_g1_i1	MZ599598	Putative Replicase
Sisal-associated Unclassified virus B	TRINITY_DN49676_c0_g1_i2	MZ329754	RdRp
Sisal-associated Unclassified virus B	TRINITY_DN16142_c0_g1_i1	MZ599599	Putative Replicase
Sisal-associated Unclassified virus B	TRINITY_DN44352_c0_g1_i1	MZ599600	Putative Replicase
Sisal-associated Unclassified virus B	TRINITY_DN83710_c0_g1_i1	MZ599601	Putative Replicase
Sisal-associated Unclassified virus B	TRINITY_DN19804_c0_g1_i1	MZ599602	Putative Replicase
Sisal-associated Unclassified virus C	TRINITY_DN24880_c0_g1_i1	MZ329755	RdRp
Sisal-associated Unclassified virus C	TRINITY_DN27401_c0_g1_i1	MZ599603	Putative Replicase
Sisal-associated Unclassified virus C	TRINITY_DN77293_c0_g1_i1	MZ599604	Putative Replicase
Sisal-associated Unclassified virus C	TRINITY_DN55189_c0_g1_i1	MZ599605	Putative Replicase
Sisal-associated Unclassified virus D	Contig19	MZ599624	hypothetical protein
Sisal-associated Unclassified virus D	TRINITY_DN83752_c0_g1_i1	MZ599637	Putative Replicase
Sisal-associated Unclassified virus E	DN52810	MZ329766	RdRp
Sisal-associated Unclassified virus E	TRINITY_DN99951_c0_g1_i1	MZ599611	Putative Replicase
Sisal-associated Virgavirus A	Contig5	MZ329757	RdRp
Sisal-associated Virgavirus B	TRINITY_DN100760_c0_g1_i1	MZ329758	RdRp
Sisal-associated Virgavirus B	TRINITY_DN26278_c0_g1_i1	MZ599645	hypothetical protein
Sisal-associated Virgavirus B	TRINITY_DN133840_c0_g1_i1	MZ599638	hypothetical protein
Sisal-associated Virgavirus C	Contig9	MZ329763	RdRp

Sisal-associated Virgavirus C	Contig6	MZ599626	Putative Replicase
Sisal-associated Virgavirus C	TRINITY_DN30831_c0_g1_i1	MZ599612	hypothetical protein
Sisal-associated Virgavirus C	TRINITY_DN38090_c0_g1_i1	MZ599620	Putative coat protein
Sisal-associated Virgavirus C	Contig8	MZ599627	Putative coat protein
Sisal-associated Virgavirus C	TRINITY_DN105616_c0_g1_i1	MZ599647	Putative coat protein
Sisal-associated Virgavirus C	TRINITY_DN72996_c0_g1_i1	MZ599613	Putative Replicase
Sisal-associated Virgavirus C	TRINITY_DN26423_c0_g1_i1	MZ599614	Putative Replicase
Sisal-associated Virgavirus C	TRINITY_DN75281_c0_g1_i1	MZ599621	hypothetical protein
Sisal-associated Virgavirus C	TRINITY_DN85955_c0_g1_i1	MZ599615	Putative Replicase
Sisal-associated Virgavirus D	TRINITY_DN83949_c0_g1_i1	MZ599651	hypothetical protein
Sisal-associated Virgavirus D	TRINITY_DN77371_c0_g1_i1	MZ599617	Putative coat protein
Sisal-associated Virgavirus D	TRINITY_DN69322_c0_g1_i1	MZ599618	hypothetical protein

Table S9: Diversity indices for the organs and species analyzed.

Index	Leaves AF	Leaves AS	Leaves HI	Stem AF	Stem AS	Stem HI	Roots AF	Roots AS	Roots HI
Number of Taxa (S)	10	8	4	10	10	11	18	13	12
Dominance (D)	0,3837	0,7361	0,8649	0,3072	0,9094	0,3317	0,401	0,2444	0,2648
Simpson Index (1-D)	0,6163	0,2639	0,1351	0,6928	0,09059	0,6683	0,599	0,7556	0,7352
Shannon Index (H)	1,185	0,5205	0,3017	1,414	0,2622	1,323	1,534	1,756	1,747
Evenness (e^{H/S})	0,3271	0,2104	0,338	0,4112	0,13	0,3413	0,2576	0,4452	0,4782
Equitability	0,5147	0,2503	0,2176	0,6141	0,1139	0,5516	0,5307	0,6845	0,7031

Table S10: Viral species and their respective detected protein domains (with Pfam/HMMER) and their expression (in tpm, *transcripts per million*) in each analyzed sample, representing the average expression of the three technical replicates.

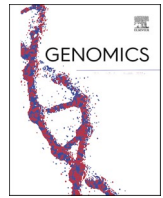
Viral Species	Proteic Domains Detected	Leaves AF	Leaves AS	Leaves HI	Stem AF	Stem AS	Stem HI	Roots AF	Roots AS	Roots HI
Sisal-associated Unclassified virus A	none	1.79	0.00	0.00	0.00	0.00	0.00	0.00	0.00	0.00
Sisal-associated Unclassified virus B	RdRP, Viral_helicase1	0.00	0.00	0.00	0.01	0.00	0.00	87.08	0.00	0.00
Sisal-associated Unclassified virus C	RdRP, Viral_helicase1, Viral methyltransferase	0.00	0.00	0.00	0.00	0.00	0.00	30.17	0.00	0.00
Sisal-associated Alphaflexivirus A	Viral coat protein	0.00	0.00	0.32	0.00	0.56	0.09	0.00	5.65	21.86
Sisal-associated Unclassified dsRNA virus A	none	0.00	0.00	0.00	0.00	0.00	0.00	6.02	0.00	0.00
Sisal-associated Betaflexivirus A	RdRP	0.01	0.00	0.00	4.94	0.00	0.15	7.33	0.00	23.02
Sisal-associated Unclassified dsRNA virus B	none	0.00	0.01	0.00	0.00	0.01	1.82	7.64	15.29	4.05
Sisal-associated Unclassified virus D	RdRP	0.00	0.25	0.00	0.00	0.00	0.00	0.00	5.30	3.26
Sisal-associated Virgavirus A	none	0.03	0.03	0.02	0.09	0.03	0.04	23.26	30.74	34.15
Sisal-associated Alphaflexivirus B	none	0.00	0.00	0.00	0.00	0.00	0.00	4.09	1.62	0.00
Sisal-associated Virgavirus B	RdRP, Viral_helicase1	0.00	0.02	0.00	0.00	0.01	0.13	0.00	13.10	4.76
Cowpea Mild Mottle Virus	none	0.01	0.00	0.00	21.42	0.56	0.32	18.66	2.66	59.78
Sisal-associated Betaflexivirus B	RdRP	0.00	2.79	0.00	0.00	0.30	0.00	3.85	0.32	0.00
Sisal-associated Betaflexivirus C	Viral_helicase1	4.35	0.00	0.00	0.55	0.00	0.00	0.55	0.00	0.00
Sisal-associated Ribovirus A	RdRP, Viral_helicase1	0.00	0.00	0.00	0.00	0.01	0.20	0.00	13.71	3.94
Sisal-associated Betaflexivirus D	Trichovirus coat protein, Viral_helicase1, Viral methyltransferase	38.15	15.98	0.00	4.97	1.30	0.00	1.14	3.11	0.00

Sisal-associated Betaflexivirus E	RdRP	3.47	0.00	0.00	0.91	0.00	0.00	0.09	0.00	0.00
Sisal-associated Unclassified virus E	RdRP, RNA helicase	0.00	0.00	0.00	0.01	0.00	0.00	14.45	0.00	0.00
Sisal-associated Virgavirus C	DEAD/DEAH box helicase, RdRP, Viral_helicase1, Viral methyltransferase	1.24	0.62	1.06	3.86	0.76	1.75	407.81	106.22	151.75
Sisal-associated Alphaflexivirus C	Viral coat protein	0.00	0.00	0.00	0.00	0.00	0.00	6.59	0.00	0.00
Sisal-associated Closterovirus A	Closterovirus coat protein, RdRP, Viral methyltransferase	26.52	110.78	18.15	26.7 6	72.6 5	18.7 6	15.28	120.90	13.18
Sisal-associated Botourmiavirus A	none	0.00	0.00	0.00	0.00	0.00	6.39	0.00	0.00	0.00
Sisal-associated Botourmiavirus B	none	0.00	0.00	0.00	0.00	0.00	22.1 4	0.00	0.00	0.00
Sisal-associated Virgavirus D	none	0.00	0.00	0.00	0.00	0.00	0.00	14.03	0.00	4.13
Sisal-associated Unclassified dsRNA virus C	none	0.07	0.00	0.00	0.00	0.00	0.00	15.95	19.12	7.53
Mean Sequencing Depth		117.85	131.02	107.70	152. 24	131. 30	107. 42	141.55	124.35	118.69

Chapter III – Phylogenomics and gene selection in *Aspergillus welwitschiae*: Possible implications in the pathogenicity in *Agave sisalana*.

RESUMO: *Aspergillus welwitschiae* causa a doença da podridão do caule no sisal (*Agave sisalana* e espécies relacionadas), afetando a produção de fibras naturais no Brasil, o principal produtor mundial de fibras de sisal. Esse fungo é um saprófito com uma ampla variedade de hospedeiros. Pesquisas anteriores estabeleceram *A. welwitschiae* como o único agente causador da podridão do caule no campo, mas pouco se sabe sobre a evolução dessa espécie e suas cepas. Neste trabalho, realizamos uma análise genômica comparativa de 40 cepas de *Aspergillus*. Mostramos a identidade molecular conflitante desta espécie, com uma cepa que infecta o sisal compartilhando seu ancestral comum mais recente com *Aspergillus niger*, tendo divergido apenas 833 mil anos atrás. Além disso, nossa análise de seleção positiva revela locais sob seleção em genes que codificam transportadores de sideróforos, trocadores de sódio-cálcio e proteínas de ligação a fosfatidiletanolamina (PEBPs). Neste estudo, discutimos os possíveis impactos dessas funções gênicas na patogenicidade no sisal.

Palavras-chave: Sideróforo, Trocadores de sódio-cálcio, Doença da podridão do caule, Genômica comparativa, Saprófito.



Phylogenomics and gene selection in *Aspergillus welwitschiae*: Possible implications in the pathogenicity in *Agave sisalana*

Gabriel Quintanilha-Peixoto ^{a,1}, Marina Püpke Marone ^{b,1}, Fábio Trigo Raya ^b, Juliana José ^b, Adrielle Oliveira ^b, Paula Luize Camargos Fonseca ^a, Luiz Marcelo Ribeiro Tomé ^a, Dener Eduardo Bortolini ^a, Rodrigo Bentes Kato ^a, Daniel S. Araújo ^c, Ruth B. De-Paula ^d, Yesid Cuesta-Astroz ^e, Elizabeth A.A. Duarte ^{f,g}, Fernanda Badotti ^h, Vasco Ariston de Carvalho Azevedo ^a, Bertram Brenig ⁱ, Ana Cristina Fermينو Soares ^g, Marcelo Falsarella Carazzolle ^b, Gonçalo Amarante Guimarães Pereira ^b, Eric Roberto Guimarães Rocha Aguiar ^{a,j}, Aristóteles Góes-Neto ^{a,*}

^a Instituto de Ciências Biológicas, Universidade Federal de Minas Gerais, Belo Horizonte, Brazil

^b Department of Genetics, Evolution, Microbiology, and Immunology, University of Campinas, Campinas, São Paulo, Brazil

^c Program in Bioinformatics, Loyola University Chicago, Chicago, United States

^d Department of Neurology, Baylor College of Medicine, Houston, United States

^e Instituto Colombiano de Medicina Tropical, Universidad CES, Medellín, Colombia

^f Centro Universitário Maria Milza, Cruz das Almas, Brazil

^g Center of Agricultural, Environmental and Biological Sciences, Universidade Federal do Recôncavo da Bahia, Cruz das Almas, Brazil

^h Department of Chemistry, Federal Center of Technological Education of Minas Gerais, Belo Horizonte, Brazil

ⁱ Institute of Veterinary Medicine, University of Göttingen, Göttingen, Germany

^j Center of Biotechnology and Genetics, Department of Biological Science, Universidade Estadual de Santa Cruz, Ilhéus, Brazil

ARTICLE INFO

Keywords:

Siderophore
Sodium-calcium exchangers
Bole rot disease
Comparative genomics
Saprotroph

ABSTRACT

Aspergillus welwitschiae causes bole rot disease in sisal (*Agave sisalana* and related species) which affects the production of natural fibers in Brazil, the main worldwide producer of sisal fibers. This fungus is a saprotroph with a broad host range. Previous research established *A. welwitschiae* as the only causative agent of bole rot in the field, but little is known about the evolution of this species and its strains. In this work, we performed a comparative genomics analysis of 40 *Aspergillus* strains. We show the conflicting molecular identity of this species, with one sisal-infecting strain sharing its last common ancestor with *Aspergillus niger*, having diverged only 833 thousand years ago. Furthermore, our analysis of positive selection reveals sites under selection in genes coding for siderophore transporters, Sodium-calcium exchangers, and Phosphatidylethanolamine-binding proteins (PEBPs). Herein, we discuss the possible impacts of these gene functions on the pathogenicity in sisal.

1. Introduction

Aspergillus welwitschiae is a fungal species of the phylum Ascomycota [1], named after *Welwitschia mirabilis*, a peculiar plant species endemic to the Namib desert, where the fungus was first reported [2,3]. *A. welwitschiae* naturally inhabits the soil and spreads its spores in the air, and may cohabit with plants and cause primary pathology, followed by plant death [4,5]. *A. welwitschiae* is a saprotroph and also an

opportunistic pathogen with necrotrophic behavior [6]. The current research discusses some aspects of *A. welwitschiae* in the context of the red rot (or bole rot) disease of *Agave sisalana*.

Agave sisalana and some varieties of the *Agave* genus, commonly known as “sisal” [7,8], are plants of economic interest associated with the natural fibers extracted from their leaves [9]. Brazil is the largest producer of these fibers, with the cultivation areas mostly concentrated in the semiarid region of Brazil, mainly in the state of Bahia, which

* Corresponding author.

E-mail address: arigoesneto@icb.ufmg.br (A. Góes-Neto).

¹ These authors have contributed equally to this work and share the first authorship.

accounts for 93% of national production and 40% of world production of sisal, and, to a lesser extent, in Paraíba and other states in the North-eastern region of Brazil [10,11]. The sisal culture is essential for the population living in this region, as it is one of the few and main sources of income [12]. The bole rot is one of the most relevant limiting factors for the cultivation of sisal in these regions and the consequent production of natural fibers, causing great production losses. This disease affects the plant stems and is characterized by an intense red color in affected stems and leaf basis, followed by chlorosis (yellowing of the leaves) and subsequently death [13].

The bole rot disease is caused by *A. welwitschiae*, which was assigned in a study published in 2018, after decades of isolated and incomplete studies of this pathosystem [13]. Before that study, the etiologic agent of the bole rot was thought to be *A. niger* while some other species were also assigned [14,15]. A possible explanation for this misclassification would be that both *A. welwitschiae* and *A. niger* belong to section Nigri of the genus *Aspergillus*, which is a non-formal name for a group of closely related species, undistinguishable by almost any morphological features, and forming a monophyletic clade [16]. Few studies focus on the evolution and phylogenomics of some sections of the genus *Aspergillus* [17,18]. None of these studies, however, perform a broad analysis of the genus, approach the evolution of pathogenicity in *A. welwitschiae*, or

even include this species. There are currently five available assemblies of *Aspergillus welwitschiae*, for the following strains; CBS 139.54 [1], CCMB 674 [19], CCMB 663 (this study), ITEM 11945 [20], and IHEM 2864 (unpublished). Only the first three of them are annotated and were, thus, used in this study. Two of these genomes were obtained from *A. sisalana*, and the strain CCMB 663 is presented in this current study.

In this context, we present a comparative genomic study of several *Aspergillus* species, comprising species in the section Nigri of *Aspergillus*, focusing on the unique characteristics that evolved in *A. welwitschiae*, including a new strain from sisal. In addition, we aimed to analyze effector proteins (predicted by their corresponding enzyme-coding genes), hypothesized to play a key role in colonization and intracellular interaction between plant and fungus [19], culminating in the apparent and typical symptoms that give rise to the popular name of this plant disease. The broad spectrum of living and decomposing hosts and its consequent broad range of metabolic strategies summarizes the relevance of the genomics and evolution of *A. welwitschiae*.

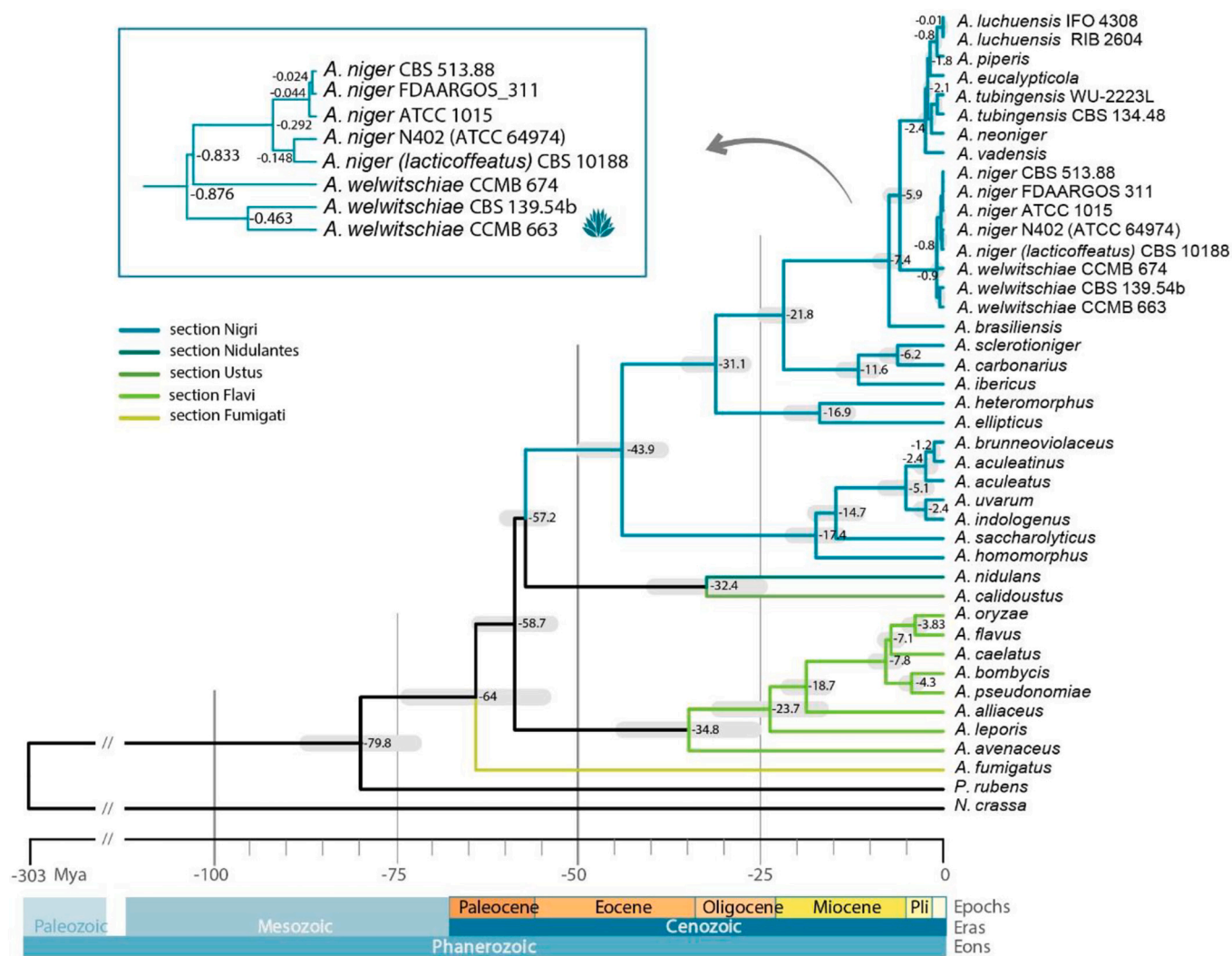


Fig. 1. Phylogenomic tree of *Aspergillus* species. Maximum likelihood reconstruction using 1842 single copy orthogroups alignment matrix. Branch support is 100% for all branches, obtained with 1000 bootstraps. Tree dating used the two calibration points of nodes in bold, and other node ages were estimated by the least-squares method in IQtree. Branches are colored by section as described in Vesth et al. (2018) [1]. *Neurospora crassa* and *Penicillium rubens* are used as outgroups. The *A. niger*/*A. welwitschiae* clade is zoomed in the detail box showing the paraphyletic status and the node ages of *A. welwitschiae* lineages.

2. Results

2.1. Homology assignment and phylogenomic reconstruction

We used 42 fungal genomes for ortholog assignment; 40 *Aspergillus* genomes distributed among sections Nigri (21 species), Flavi (8 species), Nidulantes, Ustus, and Fumigati (one species each), plus 2 outgroups, *Penicillium rubens* and *Neurospora crassa*. Species in the section Nigri helped increase the resolution of our analysis, while further distant species in the genus *Aspergillus* and other species outside of this genus helped for a broader perspective of gene conservation (Table S1). For this dataset, we found 1842 families of single-copy ortholog (SCO) genes (Supplementary data). We used SCO to reconstruct the phylogeny of this species, obtaining 100% of bootstrap support for all branches (Fig. 1). The three *A. welwitschiae* genomes are positioned in the section Nigri, in the same clade as *A. niger*, which was expected since *A. welwitschiae* is a morphological cryptic species of *A. niger*. Nonetheless, interestingly, the three *A. welwitschiae* strains are polyphyletic: *A. welwitschiae* CCMB 663 and *A. welwitschiae* CBS 139.54 are in a monophyletic clade whereas *A. welwitschiae* CCMB 674 is clustered with the other *A. niger* species (Fig. 1, detail).

Time calibration estimated a divergence time of 463 thousand years (326–659C.I.) for the CCMB 663 and CBS 139.54 lineages of *A. welwitschiae*, which is longer than the divergence times among *A. niger* lineages. An even greater timespan was estimated for the MRCA of *A. welwitschiae* CCMB 674 and *A. niger*, dated 833 thousand years (609–1088C.I.). The MRCA of the *A. niger/A. welwitschiae* clade dated 876 thousand years (609–1293C.I.), which is much more recent than the ones separating other *Aspergillus* species, for instance, the MRCAs of *A. brunneoviolaceus/A. aculeatinus* (1.2Mya), and *A. sclerotioniger/A. ibericus* (6.2Mya) (Fig. 1).

2.2. Prospecting for positive selection evidences in *A. welwitschiae* strains

As described by the developers of HyPhy [21], BUSTED [22] “provides a gene-wide (not site-specific) test for positive selection by asking whether a gene has experienced positive selection in at least one site on at least one branch”, while MEME [23] “aims to detect sites evolving under positive selection under a proportion of branches”. In our study, these two methods for inferring positive selection pressure are combined with the purpose of (i) detecting genes that are under positive selection in *A. welwitschiae* but not in any other species in our analysis, and consequently, (ii) differentiating the gene usage and presumably pathogenicity strategies in *A. welwitschiae* that differ from those other species. From 1842 SCO orthogroups tested using the BUSTED model, 64 presented evidence of positive selection when comparing the three *A. welwitschiae* strains to the other 39 fungal species [22]. These 64 orthogroups were also tested using the MEME branch-site model that confirmed positive selection evidence in the same 64 orthogroups. Among them, 28 families presented a *p*-value <0.0001 and were chosen for further annotation with InterPro and Pfam using GoFeat [24]. The consensus terms of InterPro and Pfam (meaning terms showed in all three strains) were obtained for the *A. welwitschiae* genes in 25 gene families, out of which 10 gene families have been previously described in the literature with roles in pathogenicity (Table 1). The other 15 gene families under positive selection have no specific effects on pathogenicity described in the literature (Table S2).

Guided by the strong literature support for the role of their detected domains in pathogenicity, we decided to further investigate two ortholog families under positive selection (OG3308 and OG4361), by checking sites under selection (detected with the MEME model). The OG3308, which contains a Major Facilitator Superfamily domain according to InterProscan and Pfam, was annotated as an iron transporter protein (Fig. 2A). In this gene family, two mutations were detected in *A. welwitschiae* strain CCMB 674 (ON695840) and one mutation in strain CBS 139.54 (RDH30067.1). In the latter, the glycine in site 738 is

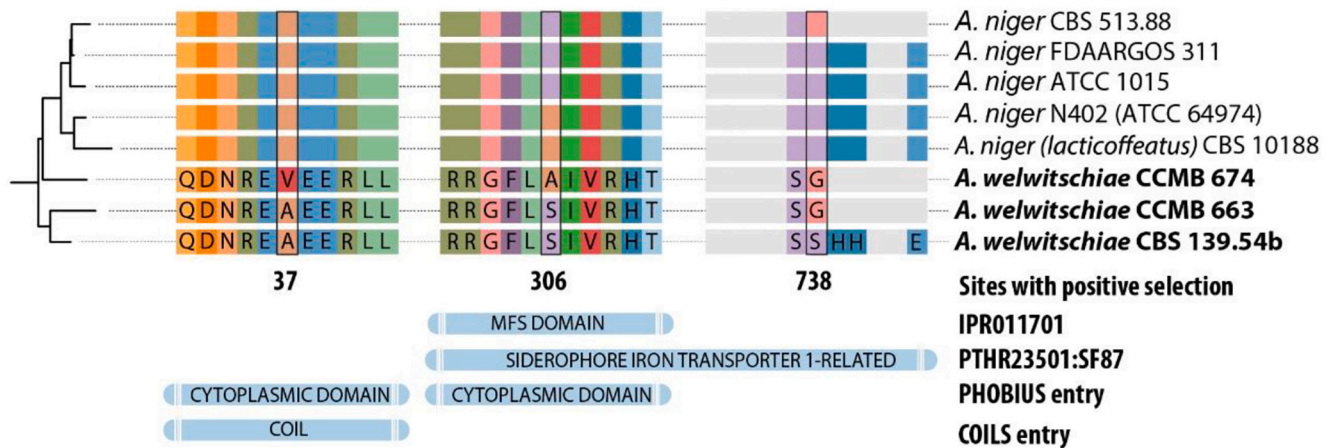
Table 1

Gene clusters with positive selection evidence and previously associated with pathogenicity, and their detected InterPro and Pfam codes (with respective descriptions) present in all three *A. welwitschiae* strains.

Cluster	Protein families and domains
OG3308	IPR020846: Major facilitator superfamily domain
	IPR036259: MFS transporter superfamily
	IPR011701: Major facilitator superfamily
	PF07690: <i>MFS_1</i> (Major Facilitator Superfamily)
	References: Pel et al., 2007 [25]; Roohparvar et al., 2007 [26]; Wang et al., 2012 [27]; Menke et al., 2013 [28]; Natesan et al., 2013 [29]; Che et al., 2018 [30].
	IPR003163: Transcription regulator HTH, APSES-type DNA-binding domain
OG3525	IPR018004: Kila, N-terminal/APSES-type HTH, DNA-binding
	IPR020683: Domain of unknown function DUF3447
	IPR036770: Ankyrin repeat-containing domain superfamily
	IPR036887: HTH APSES-type DNA-binding domain superfamily
	References: Donaldsson et al., 2013 [31]; Zhao et al., 2014 [32]; Rath et al., 2020 [33]; Xin et al., 2020 [34];
OG3961	IPR027267: AH/BAR domain superfamily
	IPR028245: Eicosome component PIL1/LSP1
	PF13805: <i>Pil1</i> (Eicosome component PIL1)
	References: Suh et al., 2012 [35]; Athanasopoulos et al., 2013 [36]; Zhang et al., 2017 [37]; Colou et al., 2019 [38];
OG4087	IPR002110: Ankyrin repeat
	IPR020683: Domain of unknown function DUF3447
	IPR036770: Ankyrin repeat-containing domain superfamily
	IPR036887: HTH APSES-type DNA-binding domain superfamily
	IPR018004: Kila, N-terminal/APSES-type HTH, DNA-binding
	IPR029793: MBF transcription factor complex subunit Mbp1/Res1/Res2
	IPR003163: Transcription regulator HTH, APSES-type DNA-binding domain
	PF00023: <i>Ank</i> (Ankyrin repeat)
	PF04383: <i>Kila-N</i> (Kila-N domain)
	References: Medina et al., 2019 [39]; Hussein et al., 2011 [40].
OG4150	IPR018327: Rad4 beta-hairpin domain 2
	IPR004583: DNA repair protein Rad4
	IPR038765: Papain-like cysteine peptidase superfamily
	IPR018325: Rad4/PNGase transglutaminase-like fold
	IPR018326: Rad4 beta-hairpin domain 1
	References: Li et al., 2010 [41]; Feng et al., 2020 [42]; Paul et al., 2021 [43].
OG4361	IPR004837: Sodium/calcium exchanger membrane region
	IPR005185: Inner membrane component domain
	PF01699: <i>Na₂Ca₂ex</i> (Sodium/calcium exchanger protein)
	PF03733: <i>YccF</i> (Inner membrane component domain)
	References: Kmetzsch et al., 2010 [44]; Hu et al., 2014 [45]; Klukovich et al., 2016 [46]; Qi et al., 2022 [47].
OG4394	IPR034753: hSac2 domain
	IPR022158: Inositol phosphatase
	IPR002013: SAC domain
	PF12456: <i>hSac2</i> (Inositol phosphatase)
	PF02383: <i>Syja_N</i> (<i>SacI</i> homology domain)
	References: Sheng et al., 2015 [48]; Zhang et al., 2015 [49].
OG4836	IPR029058: Alpha/Beta hydrolase fold
	IPR002921: Fungal lipase-like domain
	PF01764: <i>Lipase_3</i> (Lipase (class 3))
	References: Stehr et al., 2003 [50]; Brunke & Hube, 2006 [51]; Gupta et al., 2015 [52].
OG4911	IPR000961: AGC-kinase, C-terminal
	IPR011009: Protein kinase-like domain superfamily
	IPR000719: Protein kinase domain
	PF00069: <i>Pkinase</i> (Protein kinase domain)
	References: C. Wang et al., 2019 [53]; Y. Wang et al., 2019 [54]; Fabri et al., 2019 [55].
OG4981	IPR008937: Ras-like guanine nucleotide exchange factor
	IPR000651: Ras-like guanine nucleotide exchange factor, N-terminal
	IPR019804: Ras guanine-nucleotide exchange factor, conserved site
	IPR023578: Ras guanine nucleotide exchange factor domain superfamily
	IPR001895: Ras guanine-nucleotide exchange factors catalytic domain
	References: Gu et al., 2017 [56]; Martin-Vicente et al., 2019 [57].

present in the other *A. welwitschiae* strains, and in an *A. niger* strain is exchanged for a serine, as so happens in other *A. niger* strains. In the MFS domain, which is also part of the siderophore domain, strain CCMB 674 and two other *A. niger* strains exchange the typical serine for alanine. Finally, in site 37 (cytoplasmatic domain/coil) strain CCMB 674 contains a valine instead of the alanine seen elsewhere. No mutations were

A OG3308



B OG4361

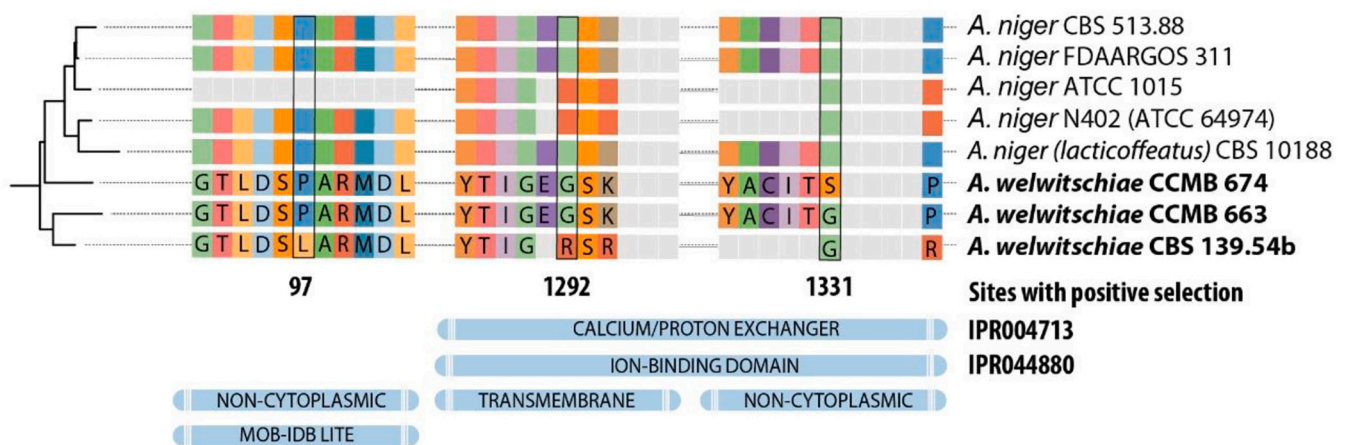


Fig. 2. Sites with positive selection for OG3308 (A), coding an iron transporter protein, and OG4361 (B), coding for a $\text{Na}^+/\text{Ca}^{2+}$ exchanger. The figure shows a 10-amino acid region around three alignment sites with positive selection evidence ($p < 0.05$). The corresponding Interproscan hits for *A. welwitschiae* proteins are shown below the alignment.

detected in the gene of strain CCMB 663 (ON695834).

In OG4361 (Fig. 2B), three amino acid exchanges were detected; sites 97 and 1292 in strain CBS 139.54 (RDH27708.1), and site 1331 in strain CCMB 674 (ON695839). No mutations were detected in the gene of strain CCMB 663 (ON695835). The mutation in site 97 (non-cytoplasmic domain) is unique to CBS 139.54, where the typical proline is exchanged for a leucine. The mutation in site 1331 is unique to CCMB 674, in which the typical glycine is exchanged for serine. The mutation in site 1292 is also seen in two strains of *A. niger*, where the glycine is exchanged for an arginine. Both affect the proton exchanger domain, in a non-cytoplasmic and transmembrane domain, respectively.

2.3. Putative effectors in *A. welwitschiae* and their adaptive role

The content of effector proteins in *Aspergillus welwitschiae* was described in a workflow of five software aiming to remove non-effector proteins; DeepSig [58], SignalP v4.1 [59], TargetP v1.1 [60], TMHMM v2.0 [61], and EffectorP v3.0 [62]. In total, we identified 660 candidate effector proteins; 231 in *A. welwitschiae* strain CCMB 674, 188 in strain CCMB 663, and 241 candidates in strain CBS 139.54. They were divided into 263 orthogroups, of which 9 were exclusive of CCMB 663 and CBS 139.54 and 1 exclusive of CCMB 663 and CCMB 674 (families containing only genes of these strains). The orthogroups containing candidate effectors were aligned and tested for positive selection evidences, using

HyPhy with BUSTED and MEME models as previously mentioned. Our positive selection analysis obtained 12 gene families positively selected, one of which is positively selected in *A. welwitschiae* strains CCMB 663 and CCMB 674, with no orthologs in strain CBS 139.54.

Orthogroup OG1694 was identified as a putative effector protein with positive selection on four amino acid sites (Fig. 3). It contains two CCMB 674 genes, one CCMB 663 gene, and two CBS 139.54 genes. Interproscan identified a signal peptide and a PEBP domain in this family, although neither could be detected on the strain CCMB 674 gene ON695837. Three of these genes were clustered in a clade (ON695838 from CCMB 674, ON695836 from CCMB 663, and RDH30697.1 from CBS 139.54) and the only mutation between them is a change of leucine to phenylalanine in the signal peptide of CBS 149 (gene RDH30697.1). As for the other two genes clustered separately in another clade, ON695837 from CCMB 674 has a gap in the signal peptide, while the pattern in RDH34005.1 is seen elsewhere.

3. Discussion

In this study, we aimed to understand the phylogenetic relationship of *Aspergillus welwitschiae* in comparison with other fungal species, and prospect genes likely involved in the infection, disease progression, and other pathogenicity traits in this species that might help in the epidemiological management of the bole rot of sisal. Our results show that

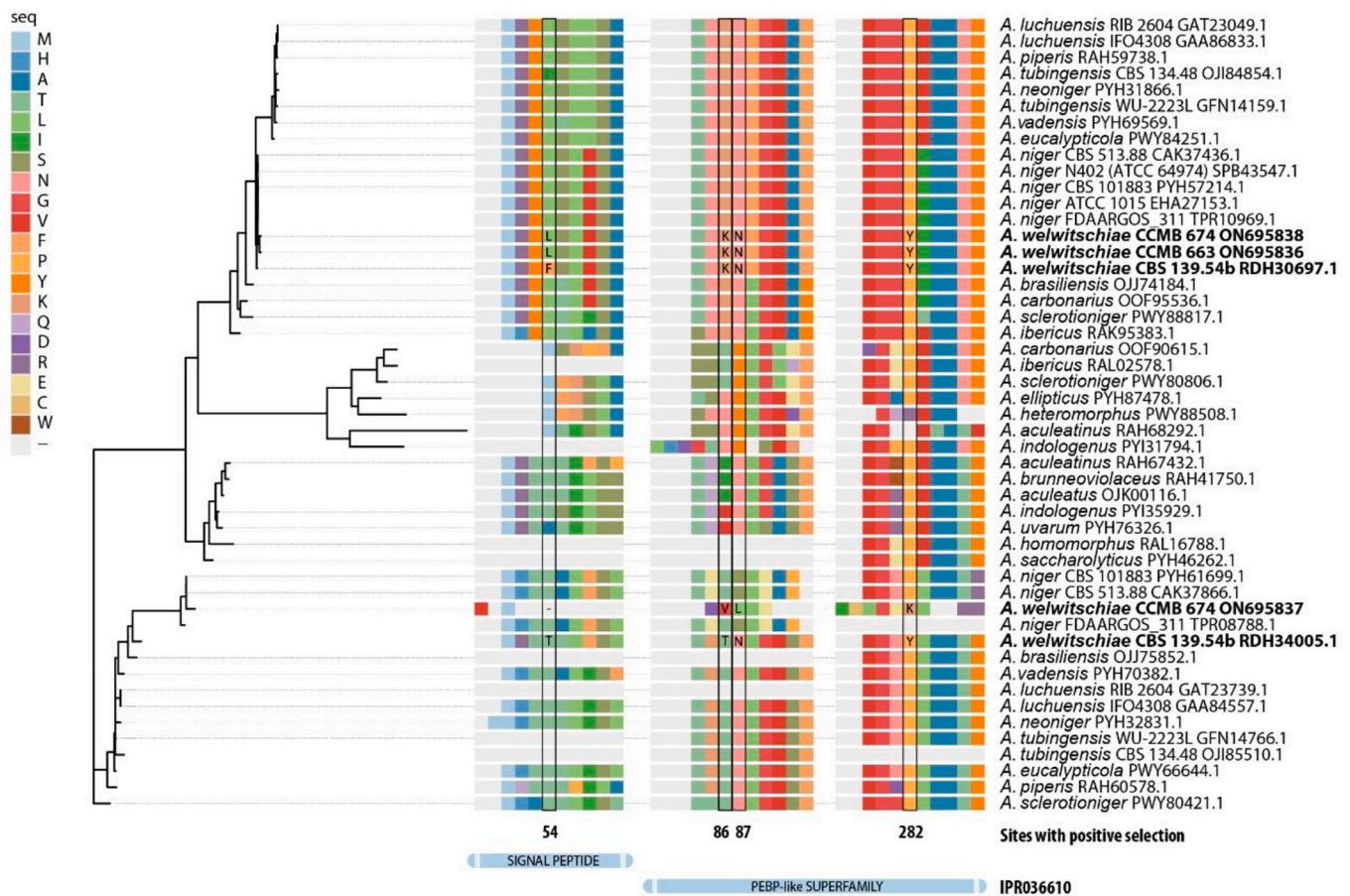


Fig. 3. Sites with positive selection for OG1694, coding a putative effector protein. The figure shows a 10-amino acid region around three alignment sites with positive selection evidence ($p < 0.05$). The corresponding Interproscan hit for *A. welwitschiae* proteins is shown below the alignment.

phylogenomic relationships differ from our early thoughts, indicating *A. welwitschiae* is still not well-defined taxonomically. Investigating the evolution of gene families, we were able to reveal positive selection evidence at the sequence level that might play a role in *A. welwitschiae* pathogenicity. With the appropriate methods, we show that 28 *A. welwitschiae* orthologs differ from all other analyzed species with a p -value < 0.0001 , including those orthologs of *A. niger*. 15 of those orthologs have previously-described roles in pathogenicity. The detection of diversifying selection in these orthologs suggests that such genes are relevant to the metabolism of *A. welwitschiae* in a different form than other species, and when related to pathogenicity, that suggests that these genes have a more crucial role in *A. welwitschiae* than it does in the other species.

Our data shows that the clade including the three strains of *Aspergillus welwitschiae* does not possess a single common ancestor, but it rather looks tangled with its closest, morphological cryptic species, *Aspergillus niger* (Fig. 1). *A. welwitschiae* CCMB 674 escapes the clade containing the other two strains of *A. welwitschiae*, sharing its closest ancestor with the *A. niger* clade instead. Nonetheless, it diverged early from the MRCA relative to the monophyletic *A. niger* clade. It might indicate an ongoing process of speciation, meaning that strain CCMB 674 is a different phylogenetic lineage both from the *A. niger* and *A. welwitschiae*. While this indicates a conflicting identity for *A. welwitschiae* CCMB 674, deeper analysis is required to state whether it is a separate species or not. Giraud et al. (2010) [63] describe that substrate and host affinity might be a condition for this sympatric speciation, as well as mating inside the host plant. Mating, however, remains elusive in *A. welwitschiae*, *A. niger*, and many other species in this genus [64] since they appear to be asexual/clonal species.

Furthermore, both CCMB 674 and CCMB 663 affect the same host (*Agave sisalana*), and *Aspergillus* species, in general have a broad range of hosts and niches, with niche/host switching as a common trait [65–67]. Since *Aspergillus* spores are ubiquitous in the air [64], different species are commonly found in close areas [68,69]. Kollár et al. (2022) [70] reinforce the idea of species as a spatiotemporal entity, rather than a terminal state. According to the authors, the present time state (T_0) is preceded by two separately evolving stories (T_{-1}) which is then preceded by a period of restrictions in gene flow, gradually leading to their divergence (T_{-2}). We hypothesize that *A. welwitschiae* CCMB 674 is between T_{-2} and T_{-1} in comparison to the other strains of *A. niger*. Hence, the driving forces behind the differentiation among *A. welwitschiae* and *A. niger* could be restricted to the genetic drive and the lack of gene flow [64].

Looking at specific gene functions and sequence similarities (Figs. 2–4) gave us a more detailed understanding of how the *A. welwitschiae* strains differ. Our diversifying selection analysis detected different mutations that might confer advantages to various sites in different domains, especially for *A. welwitschiae* CCMB 674, which reinforces the differentiation of this strain, but also for CCMB 663 and CBS 139.54 in some cases. Mutations with the strongest impact on the protein function are those in which the amino acid polarity, charge, or size, is altered. A Glycine is exchanged for a Serine in two sites; in the side-phore domain of OG3308 (Table 1, Fig. 2A) in *A. welwitschiae* CCMB 674 and CCMB 663, and in the $\text{Na}^+/\text{Ca}^{2+}$ exchanger region of OG4361 (Table 1, Fig. 2B), only in *A. welwitschiae* CCMB 674. Glycine is a nonpolar amino acid while Serine is polar neutral. In the $\text{Na}^+/\text{Ca}^{2+}$ exchanger region of strain CBS 139.54, a glycine, which is a nonpolar amino acid, is replaced with an Arginine, which is a polar, positively

charged amino acid.

The genes in OG3308 (Fig. 2A) code for proteins containing MFS domains, more specifically for the transport of siderophores (PTHR23501:SF87). Siderophores are iron-chelating compounds, usually small secreted proteins. Saha et al. (2013) [71] pointed out that only the export of siderophores can be achieved via MFS, while the import of Fe ions or the Fe-siderophore complex is usually performed by ABC transporters or permeases. As for pathogenicity, the presence of a siderophore-based iron acquisition system is typical of pathogenic microorganisms, and a requirement for successful pathogenicity [72]. The positive selection/selective sweep of fungal MFS transporters is described in a few articles, such as in *Rhynchospirium commune* [73], *Sclerotinia sclerotiorum* [74], and *Zymoseptoria tritici* [75]. Nonetheless, none of these works go into detail about the modifications of these transporters.

Genes in OG4361 (Fig. 2B) code for a calcium efflux pump; the Na⁺/Ca²⁺ exchanger protein. In *Cryptococcus neoformans*, a mutation in a similar protein disrupts the Ca²⁺-calcineurin signaling pathway, decreasing pathogenicity (measured by survival rate in contact with mice macrophages). This mutation also increased sensitivity to Ca²⁺ ions under CaCl₂ stress [44]. Nonetheless, in plants, CaCl₂ is related to drought resistance [76,77] but it might also cause osmotic stress [78]. For this reason, although Kmetzsch et al. (2010) [44] describe an ortholog of their exchanger protein in *A. fumigatus*, the role of such protein in plant pathogens such as *A. welwitschiae* is still unclear.

A set of mutations are also present in effector genes (OG1694, Fig. 3), especially in *A. welwitschiae* CCMB 674 (Fig. 3). Except for a mutation in the signal peptide, in which leucine is exchanged for phenylalanine in *A. welwitschiae* CBS 139.54, all other sites refer to the gene ON695837 of strain CCMB 674. In this gene, no signal peptide was detected, nor was the PEBP domain found in other genes, which might indicate that this effector gene is prone to duplications and mutation, as so happens in other effector genes [79–81]. This gene was likely included in this gene family because it shares similarities with the other genes later in the sequence, in an area not shown in the positively selected sites. Therefore, we hypothesize that this specific gene could be originated from an event of duplication, and following the theory of birth-and-death of gene evolution [79], it might have a different function (since the PEBP domain is undetectable) or be affected by consecutive mutations to the point it becomes completely uncharacterized. In fungi, PEBP has been described as a protease inhibitor [82,83]. In plants, however, it is well-studied as a florigen [84–86]. As it is a secreted protein, we believe that fungi-synthesized PEBP could mimic plant PEBP and induce the transition from vegetative to reproductive states. In *Agave*, flowering mobilizes fructan polymers, degrading complex structures to oligofructans [87]. Hence, we hypothesize that fungal PEBP could trigger fructan degradation typical of flowering stages in *Agave* to then feed off simpler sugar molecules that would be addressed to the flowering structures.

Among other gene families previously described as participating in pathogenicity, we found some with positive selection in *A. welwitschiae* (Table 1). Family OG3525 includes proteins in the APSES-type DNA-binding domain superfamily and Kila-N and Ankyrin repeats. APSES proteins are transcription factors in the topology HTH (winged helix-turn-helix family of proteins). They commonly contain Kila-N domain, described in the literature as laterally transferred from DNA viruses [88] and Ankyrin repeats. Despite their broad spectrum of functions, they have been described as regulators of the production of secondary metabolites in some fungal species. In *Ustilago maydis*, an APSES-type protein was shown to be increasingly expressed 14 days after infection in corn, repressing the formation of teliospores (spores that give rise to basidia) during the biotrophic stage [31]. APSES-mutants in *Fusarium verticillioides* were shown to decrease the production of fumonisin and fusarin C, and decrease the efficiency in the infection of maize seedlings [33]. In the entomopathogenic fungal species *Metarhizium rileyi*, the mutation of APSES-like transcription factors impaired the pathogenicity and increased the sensitivity to thermal stress [34]. Similarly, family

OG4087 was annotated as an MBF transcription factor complex, containing the subunit Mbp1/Res1/Res2, which also derives from viral Kila-N repeats [39] and also presents Ankyrin domains. Despite the scarcity of literature exploring MBF in pathogenicity, it has been described that this transcription factor is crucial during the transition from cell division stages G1 to S [40], which indicates that MBF might have similar effects to APSES. Although *A. welwitschiae* does not produce asci (the Ascomycota meiosporangia, homologous to Basidiomycota basidia) or any kind of sexual sporoma (in fact, mating in *A. welwitschiae* remains undescribed), fumonisins or fusarin C, as seen in our 2019 study [19], suggests that these protein domains and families are involved in lifestyle switching and the production of secondary metabolites.

Various gene families detected to be positively selected in our *A. welwitschiae* strains might operate on pathogenicity via the metabolism of lipids and regulation of the fungal cell wall (Table 1). The component PIL1/LSP1 is included in OG3961, and the protein coded by these genes is part of the eisosome, a domain of the plasmatic membrane with diverse functions, including regulation of sphingolipids and lipid homeostasis as well as cell wall morphogenesis [89–91]. PIL1/LSP1 forms filaments that bend the membrane into the typical furrow shape of the eisosome [89]. In the genus *Aspergillus*, there are a few studies on the role of the eisosome on conidiation in *Aspergillus nidulans* [36,92,93] and *Aspergillus fumigatus* [35]. Nonetheless, some research in fungal species phylogenetically distant from *A. welwitschiae* describe the role of eisosomes in *Alternaria brassicicola* [38] and *Beauveria bassiana* [37]. In *Alternaria brassicicola*, Colou et al. [38] have described that eisosome components are overexpressed when the spores were exposed to common plant defense mechanisms (phytoalexins, osmotic stress); however, mutations in Pil1A and Pil1B did not increase susceptibility to those conditions. The authors [38] then hypothesize that eisosomes are involved in appressoria formation, a structure used to invade the plant host cell, usurp nutrients and deliver toxic compounds. Appressoria were never described in *A. welwitschiae*, and a study including *A. fumigatus* [94] could not find this structure in this species either, although that does not harm their ability to invade the host cells. In *B. bassiana*, an entomopathogen, mutations in Pil1A and Pil1B have disrupted the expression of autophagy-related genes, the formation of autophagosomes, and decreased pathogenicity by making the fungus unable to deliver proteases into the host, which could be viewed as an equivalent to the eisosome role in toxin delivery via appressoria [37].

Another family with positive selection and related to lipid metabolism was annotated as AGC Kinase. The role of AGC Kinases in the metabolism of sphingolipids and pathogenicity have been described in the literature. While in *A. fumigatus* the silencing of ypkA, an AGC Kinase, causes a series of growth defects [55], its mutation also causes decreased pathogenicity in plant and insect fungal pathogens [53,54]. The SAC1 protein (OG4394) and the Ras-like guanine nucleotide exchange factor (OG4981) might also play a role in pathogenicity via the maintenance of cell wall integrity, biofilm formation, and chitin deposition [49,56,57]. Still from the perspective of lipid metabolism and appressoria formation, the lipases (OG4836) act as important pathogenicity factors in fungi, both for human pathogens [50,51] and for plant pathogens [95]. In the latter, lipases were shown to be highly expressed in early infections, while their repression significantly decreases disease progression.

4. Conclusions

In this paper, we performed a comparative genomics study of 40 *Aspergillus* species and 2 outgroups, including three strains of *A. welwitschiae*, a saprotroph/opportunistic pathogen. Among these, two strains were isolated from *Agave sisalana* affected with the bole rot disease (CCMB 663 and CCMB 674). Previous research of our research group [13] indicated that these two strains belong to two different haplotypes, but our current study shows that CCMB 674 shared its last common ancestor with *A. niger*, while its last common ancestor with the

clade including CCMB 663 dates back to 833 thousand years ago. We found point mutations in the genomes of *A. welwitschiae* that could be related to pathogenicity. These mutations affect both primary metabolism genes, such as membrane transporters and efflux pumps, and specific traits, such as effector proteins that might disrupt sugar metabolism in the host plant. With these results, we hope to expand the knowledge on the evolution of the *Aspergillus* genus and improve disease management through the dispersion of healthy individuals. *Aspergillus welwitschiae* is a saprotroph/opportunistic pathogen.

5. Materials and methods

5.1. Genomic data

In addition to various species in the sections Nigri and Flavi of the genus *Aspergillus* and other fungal species, which are listed in detail in Table S1, this study comprises a new strain of *Aspergillus welwitschiae*: CCMB 663, which was directly isolated from the stem of a field-collected *Agave sisalana* plant in Conceição do Coité, State of Bahia, Brazil, and belongs to the same haplotype as *A. welwitschiae* strain CBS 139.54, as determined in Duarte et al., (2018) [13]. Briefly, the stem sample from which CCMB 663 was obtained was surface-sterilized and then plated on PDA with chloramphenicol. *Aspergillus* CFUs were then cultivated onto a new PDA plate. The identity of this strain was confirmed through Sanger sequencing, and haplotypes were determined with adequate statistical tests using all available *A. welwitschiae* barcoding sequences (calmodulin gene) in public databases. For the WGS, the mycelia of *A. welwitschiae* strain CCMB 663 was grown on potato dextrose agar medium (PDA – Sigma-Aldrich, Missouri, USA) and incubated at 25 °C for 5 days, or until covering the surface of a 9-cm Petri dish. Subsequently, the mycelium was scrapped for genomic DNA extraction, which was performed with FastDNA™ for Soil kit (MP Biomedicals – California, USA). Genomic DNA quality and quantity were assessed by agarose gel electrophoresis and fluorometric analysis, respectively. A 450-bp library was prepared with NEBNext Fast DNA Fragmentation and Library Preparation Kit (New England Biolabs, Nebraska, USA) following the manufacturer's instructions. Library quality was evaluated with a 2100 Bioanalyzer (Agilent – California, USA), and whole-genome sequencing was performed on a HiSeq 2500 platform with the paired-end strategy and estimated fragment size of 450 bp (Illumina – California, USA) in the Georg August University Göttingen (Göttingen, Germany).

5.2. Genome assembly, annotation, and quality control of *Aspergillus welwitschiae* CCMB 663

Genome assembly for *Aspergillus welwitschiae* strain CCMB 663 was performed as in Quintanilha-Peixoto et al., (2019) [19]. Briefly, raw reads were trimmed (Phred score > 20) with BBDuk and normalized with BBNorm, both being components of the BBTools v.36.86 software package [96]. Normalized reads were assembled with SPAdes v. 3.11.1, and assembly metrics were assessed using the Perl script scaffold_stats.pl [97] and BUSCO v. 3.1 [98]. Short contigs (< 800 nt) were removed without any impact on ORF (open reading frame, coding) content (according to BUSCO results). Non-annotated scaffolds of *A. welwitschiae* CBS 139.54 were obtained from the Joint Genome Institute portal (JGI; <https://jgi.doe.gov/>). Assembly QC was analyzed with Perl script scaffold_stats.pl and BUSCO v.3, using the Ascomycota lineage dataset. The resulting assemblies were annotated with MAKER2 v2.31.9 [99], with support from ab initio predictors SNAP [100], GeneMark [101], and Augustus [102], as seen in Masonbrink et al. (2019) [103]. To improve gene prediction, a protein set containing sequences from *Aspergillus welwitschiae* and *Aspergillus niger*, the phylogenetically closest species to *Aspergillus welwitschiae* [16], was also used.

5.3. Effector protein detection

Our approach to identifying secreted proteins was modified from Cuesta-Astroz et al. [104]. All annotated proteins in *Aspergillus welwitschiae* strains CBS 139.54, CCMB 663, and CCMB 674 were submitted to DeepSig [58] and SignalP v4.1 [59], both of which identify classical secretory proteins. Following that, possible mitochondrial proteins were removed by using TargetP v1.1 [60], and sequences containing transmembrane domains were removed using TMHMM v2.0 [61], using default parameters for the three applications. For our effector proteins analysis, it is worth noting that we considered classical effectors, that is, proteins acting directly on the host, addressed outside of the fungal cell via a signal peptide. The three predicted secretomes were submitted to EffectorP v3.0 [62]. Putative effectors were also annotated with Localizer (for the prediction of subcellular localization in the host plant). Finally, candidate effectors were annotated with InterPro and Pfam using GO Feat [24].

5.4. Homology assignment and phylogenetic inferences

Homology assignment of gene families was performed using OrthoFinder v2.5.2 [105]. The species used in this analysis comprise the three aforementioned strains of *A. welwitschiae*, 37 other *Aspergillus* species from sections Nigri, Flavi, and other sections, as well as *Neurospora crassa* and *Penicillium rubens* as outgroups, all with public genomes (Table S1). The species phylogenomics was inferred using 1842 single-copy orthologous gene families, whose proteins were aligned using the built-in MAFFT module in OrthoFinder with default parameters and then concatenated in a supermatrix. We used IQ-TREE v. 2.1.2 [106] for phylogenetic inference with the parameter “-m TEST” to calculate the best fitting model using BIC criteria, which was JTT + F + I + G4, with 1000 ultra-fast bootstrap replicates for branch support. IQ-TREE was also used for the time calibration of the tree with the least-squares analysis and two calibration points obtained from the TimeTree database [107]: 64 Mya for the *Aspergillus* genera MRCA, and 3.8 Mya for *A. oryzae* and *A. flavus* MRCA. For the phylogenetic inference of individual gene families including paralogs, we used PRANK v.150803 [108] for the alignment using the parameter “-codon”, and, to obtain the alignments in protein sequences, we used the parameters “-translate” and “-convert”. IQTREE was used with the same settings as aforementioned.

5.5. Detection of positive selection and expression in the predicted coding sequences

For all single-copy gene families, we searched for evidence of episodic positive (diversifying) selection using the BUSTED model [22] implemented in HyPhy v.2.5.32 [21]. Families where a positive selection was detected with *p*-values < 0.001, were also tested by the branch-test of the MEME model [22] implemented in HyPhy, using genes from the three *A. welwitschiae* strains marked as the foreground to be contrasted with the rest of the tree.

Availability of data and materials

The datasets generated and analyzed during the current study are available in the GenBank repository, under accession codes ON695834-ON695840.

Funding

This work was supported by Coordenação de Aperfeiçoamento de Pessoal de Nível Superior - Brazil (CAPES) [grant number 88887.373979/2019-00]; Fundação de Amparo à Pesquisa do Estado de Minas Gerais (FAPEMIG) [grant number 5.18/2022, quote 439]; Conselho Nacional de Desenvolvimento Científico e Tecnológico (CNPq)

[Nexus Project: Integration Caatinga-Sisal n. 441625/2017-7].

CRedit authorship contribution statement

Gabriel Quintanilha-Peixoto: Conceptualization, Methodology, Software, Validation, Formal analysis, Investigation, Data curation, Writing – original draft, Writing – review & editing, Visualization. **Marina Püpke Marone:** Conceptualization, Methodology, Software, Validation, Formal analysis, Investigation, Data curation, Writing – original draft, Writing – review & editing, Visualization. **Fábio Trigo Raya:** Conceptualization, Methodology, Validation, Formal analysis, Investigation, Data curation, Writing – original draft, Writing – review & editing, Visualization. **Juliana José:** Conceptualization, Methodology, Software, Formal analysis, Investigation, Data curation, Writing – original draft, Writing – review & editing, Visualization, Supervision. **Adriele Oliveira:** Methodology, Validation, Formal analysis. **Paula Luize Camargos Fonseca:** Methodology, Investigation. **Luiz Marcelo Ribeiro Tomé:** Methodology, Investigation. **Dener Eduardo Bortolini:** Software. **Rodrigo Bentes Kato:** Methodology. **Daniel S. Araújo:** Formal analysis. **Ruth B. De-Paula:** Formal analysis. **Yesid Cuesta-Astroz:** Software. **Elizabeth A.A. Duarte:** Formal analysis. **Fernanda Badotti:** Conceptualization. **Vasco Ariston de Carvalho Azevedo:** Resources, Funding acquisition. **Bertram Brenig:** Resources, Funding acquisition. **Ana Cristina Fermino Soares:** Resources, Project administration, Funding acquisition. **Marcelo Falsarella Carazzolle:** Resources. **Gonçalo Amarante Guimarães Pereira:** Resources, Project administration, Funding acquisition. **Eric Roberto Guimarães Rocha Aguiar:** Conceptualization, Supervision. **Aristóteles Góes-Neto:** Conceptualization, Resources, Supervision, Project administration, Funding acquisition.

Declaration of Competing Interest

None of the authors have any competing interests.

Data availability

Data will be made available on request.

Acknowledgments

We would like to thank Dr. Aline C. Intorne, Dr. Carlos P. Pirovani, Dr. F. Murilo Zerbinini and Dr. Luiz E. V. Del-Bem for their suggestions to this work. We would also like to thank all the members of the research groups of Eric Aguiar, Aristoteles Góes-Neto, and Gonçalo Pereira for their support in the execution of this research, and the Funding Agencies for the possibility of this research.

Appendix A. Supplementary data

Supplementary data to this article can be found online at <https://doi.org/10.1016/j.ygeno.2022.110517>.

References

- [1] T.C. Vesth, et al., Investigation of inter- and intraspecies variation through genome sequencing of *Aspergillus* section *Nigri*, *Nat. Genet.* 50 (December) (2018) 1688–1695, <https://doi.org/10.1038/s41588-018-0246-1>.
- [2] D. Perera, S. Savocchia, P.D. Prenzler, P.C. Thomson, C.C. Steel, Occurrence of fumonisin-producing black aspergilli in Australian wine grapes: effects of temperature and water activity on fumonisin production by *A. niger* and *A. welwitschiae*, *Mycotoxin Res.* 37 (4) (2021) 327–339, <https://doi.org/10.1007/s12550-021-00438-8>.
- [3] J. Varga, et al., New and revisited species in *Aspergillus* section *Nigri*, *Stud. Mycol.* 69 (June 2014) (2011) 1–17, <https://doi.org/10.3114/sim.2011.69.01>.
- [4] K. Hanif, N. Akhtar, R. Hafeez, First report of *Aspergillus welwitschiae* as a postharvest pathogen of *Brassica campestris* seeds in Pakistan, *J. Plant Pathol.* 98 (1) (2016) 185, <https://doi.org/10.4454/JPP.V98I1.070>.
- [5] F.P. Massi, et al., Molecular analysis of *Aspergillus* section *Nigri* isolated from onion samples reveals the prevalence of *A. welwitschiae*, *Braz. J. Microbiol.* (2020), <https://doi.org/10.1007/s42770-020-00390-2>.
- [6] L. Rodriguez-Moreno, M.K. Ebert, M.D. Bolton, B.P.H.J. Thomma, Tools of the crook- infection strategies of fungal plant pathogens, *Plant J.* 93 (4) (2018) 664–674, <https://doi.org/10.1111/tpj.13810>.
- [7] G. Quintanilha-peixoto, et al., The sisal Virome: uncovering the viral diversity of *Agave* varieties reveals new and organ-specific viruses, *Microorganisms* 9 (1704) (2021) 1–21.
- [8] Y.M. Zhang, X. Li, Z. Chen, J.F. Li, J.Y. Lu, W.Z. Zhou, Shoot organogenesis and plant regeneration in *Agave* hybrid, No. 11648, *Sci. Hortic. (Amsterdam)*. 161 (2013) 30–34, <https://doi.org/10.1016/j.scienta.2013.06.047>.
- [9] K. Brown, *Agave sisalana* Perrine, *Wildl. Weeds* 5 (2002) 18–21.
- [10] Food and Agriculture Organizations of the United Nations, FAOSTAT, FAOSTAT. Food and Agriculture Organizations of the United Nations, 2022 [Online]. Available, <http://www.fao.org/faostat/en/#data/QC>.
- [11] E.M.C. Santos, O.A. da Silva, *Sisal* in Bahia - Brazil, *Mercator* 16 (12) (2017) 1–13, <https://doi.org/10.4215/rm2017.e16029>.
- [12] M.L.M. Broeren, S.N.C. Dellaert, B. Cok, M.K. Patel, E. Worrell, L. Shen, Life cycle assessment of sisal fibre – exploring how local practices can influence environmental performance, *J. Clean. Prod.* 149 (2017) 818–827, <https://doi.org/10.1016/j.jclepro.2017.02.073>.
- [13] E.A. Duarte, et al., Putting the mess in order: *Aspergillus welwitschiae* (and not *A. niger*) is the etiologic agent of the sisal bole rot disease, *Front. Microbiol.* 9 (1227) (2018), <https://doi.org/10.3389/fmicb.2018.01227>.
- [14] J.T. De Souza, E.S. Jesus, A.F. De Jesus Santos, Putative pathogenicity genes of *Aspergillus Niger* in sisal and their expression in vitro, *Rev. Bras. Cienc. Agrar.* 12 (4) (2017) 441–445, <https://doi.org/10.5039/agraria.v12i4a5475>.
- [15] P.O. dos Santos, A.C.M. da Silva, É.B. Corrêa, V.C. Magalhães, J.T. de Souza, Additional species of *Aspergillus* causing bole rot disease in *Agave sisalana*, *Trop. Plant Pathol.* 39 (4) (2014) 331–334, <https://doi.org/10.1590/s1982-56762014000400008>.
- [16] J.D. Palumbo, T.L. O’Keeffe, Detection and discrimination of four *aspergillus* section *Nigri* species by PCR, *Lett. Appl. Microbiol.* 60 (2) (2015) 188–195, <https://doi.org/10.1111/lam.12358>.
- [17] I. Kjørboelling, et al., A comparative genomics study of 23 *aspergillus* species from section *Flavi*, *Nat. Commun.* 11 (1) (2020), <https://doi.org/10.1038/s41467-019-14051-y>.
- [18] R.P. de Vries, et al., Comparative genomics reveals high biological diversity and specific adaptations in the industrially and medically important fungal genus, *Aspergillus* 18 (1) (2017).
- [19] G. Quintanilha-Peixoto, et al., Calm before the storm: a glimpse into the secondary metabolism of *aspergillus welwitschiae*, the etiologic agent of the sisal bole rot, *Toxins (Basel)*. 11 (11) (2019), <https://doi.org/10.3390/toxins11110631>.
- [20] A. Susca, et al., Variation in the fumonisin biosynthetic gene cluster in fumonisin-producing and nonproducing black aspergilli, *Fungal Genet. Biol.* 73 (2014) 39–52, <https://doi.org/10.1016/j.fgb.2014.09.009>.
- [21] S.L. Kosakovsky Pond, S.D.W. Frost, S.V. Muse, HyPhy: hypothesis testing using phylogenies, *Bioinformatics* 21 (5) (2005) 676–679, <https://doi.org/10.1093/bioinformatics/bti079>.
- [22] B. Murrell, et al., Gene-wide identification of episodic selection, *Mol. Biol. Evol.* 32 (5) (2015) 1365–1371, <https://doi.org/10.1093/molbev/msv035>.
- [23] B. Murrell, J.O. Wertheim, S. Moola, T. Weighill, K. Scheffler, S.L. Kosakovsky Pond, Detecting individual sites subject to episodic diversifying selection, *PLoS Genet.* 8 (7) (2012), <https://doi.org/10.1371/journal.pgen.1002764>.
- [24] F.A. Araujo, D. Barh, A. Silva, L. Guimarães, R.T.J. Ramos, GO FEAT: a rapid web-based functional annotation tool for genomic and transcriptomic data, *Sci. Rep.* 8 (1) (2018) 8–11, <https://doi.org/10.1038/s41598-018-20211-9>.
- [25] H.J. Pel, et al., Genome sequencing and analysis of the versatile cell factory *aspergillus niger* CBS 513.88, *Nat. Biotechnol.* 25 (2) (2007) 221–231, <https://doi.org/10.1038/nbt1282>.
- [26] R. Roohparvar, M.A. De Waard, G.H.J. Kema, L.H. Zwierts, Mgmfs1, a major facilitator superfamily transporter from the fungal wheat pathogen *Mycosphaerella graminicola*, is a strong protectant against natural toxic compounds and fungicides, *Fungal Genet. Biol.* 44 (5) (2007) 378–388, <https://doi.org/10.1016/j.fgb.2006.09.007>.
- [27] Ji-ye Wang, Pdmfs1, a major facilitator superfamily transporter from *Penicillium digitatum*, is partially involved in the imazalil-resistance and pathogenicity, *Afr. J. Microbiol. Res.* 6 (1) (2012) 95–105, <https://doi.org/10.5897/ajmr11.1045>.
- [28] J. Menke, J. Weber, K. Broz, H.C. Kistler, Cellular development associated with induced mycotoxin synthesis in the filamentous fungus *fusarium graminearum*, *PLoS One* 8 (5) (2013), <https://doi.org/10.1371/journal.pone.0063077>.
- [29] S.K. Natesan, A.K. Lamichchane, S. Swaminathan, W. Wu, Differential expression of ATP-binding cassette and/or major facilitator superfamily class efflux pumps contributes to voriconazole resistance in *aspergillus flavus*, *Diagn. Microbiol. Infect. Dis.* 76 (4) (2013) 458–463, <https://doi.org/10.1016/j.diagmicrobio.2013.04.022>.
- [30] H.C. Lin, P.L. Yu, L.H. Chen, H.C. Tsai, K.R. Chung, A major facilitator superfamily transporter regulated by the stress-responsive transcription factor yap1 is required for resistance to fungicides, xenobiotics, and oxidants and full virulence in *Alternaria alternata*, *Front. Microbiol.* 9 (SEP) (2018) 1–11, <https://doi.org/10.3389/fmicb.2018.02229>.
- [31] M.E. Donaldson, et al., Investigating the *Ustilago maydis/Zea mays* pathosystem: transcriptional responses and novel functional aspects of a fungal calcineurin

- regulatory B subunit, *Fungal Genet. Biol.* 58–59 (2013) 91–104, <https://doi.org/10.1016/j.fgb.2013.08.006>.
- [32] Y. Zhao, H. Su, J. Zhou, H. Feng, K.Q. Zhang, J. Yang, The APSES family proteins in fungi: characterizations, evolution and functions, *Fungal Genet. Biol.* 81 (2014) 271–280, <https://doi.org/10.1016/j.fgb.2014.12.003>.
- [33] M. Rath, N.J. Crenshaw, L.W. Lofton, A.E. Glenn, S.E. Gold, FvSTUA is a key regulator of sporulation, toxin synthesis, and virulence in *Fusarium verticillioides*, *Mol. Plant-Microbe Interact.* 33 (7) (2020) 958–971, <https://doi.org/10.1094/MPMI-09-19-0271-R>.
- [34] C. Xin, et al., Analogous and diverse functions of APSES-type transcription factors in the morphogenesis of the entomopathogenic fungus *metarhizium rileyi*, *Appl. Environ. Microbiol.* 86 (8) (2020), <https://doi.org/10.1128/AEM.02928-19>.
- [35] M.J. Suh, et al., Development stage-specific proteomic profiling uncovers small, lineage specific proteins most abundant in the *Aspergillus fumigatus* conidial proteome, *Proteome Sci.* 10 (1) (2012) 1–13, <https://doi.org/10.1186/1477-5956-10-30>.
- [36] A. Athanasopoulos, H. Boleti, C. Scazzocchio, V. Sophianopoulou, Eisosome distribution and localization in the meiotic progeny of *aspergillus nidulans*, *Fungal Genet. Biol.* 53 (2013) 84–96, <https://doi.org/10.1016/j.fgb.2013.01.002>.
- [37] L. Bin Zhang, L. Tang, S.H. Ying, M.G. Feng, Two eisosome proteins play opposite roles in autophagic control and sustain cell integrity, function and pathogenicity in *Beauveria bassiana*, *Environ. Microbiol.* 19 (5) (2017) 2037–2052, <https://doi.org/10.1111/1462-2920.13727>.
- [38] J. Colou, et al., Role of membrane compartment occupied by Can1 (MCC) and eisosome subdomains in plant pathogenicity of the necrotrophic fungus *Alternaria brassicicola*, *BMC Microbiol.* 19 (1) (2019) 1–14, <https://doi.org/10.1186/s12866-019-1667-4>.
- [39] E.M. Medina, E. Walsh, N.E. Buchler, Evolutionary innovation, fungal cell biology, and the lateral gene transfer of a viral KILa-N domain, *Curr. Opin. Genet. Dev.* 58–59 (2019) 103–110, <https://doi.org/10.1016/j.gde.2019.08.004>.
- [40] B. Hussein, et al., G1/S transcription factor orthologues Swi4p and Swi6p are important but not essential for cell proliferation and influence hyphal development in the fungal pathogen *Candida albicans*, *Eukaryot. Cell* 10 (3) (2011) 384–397, <https://doi.org/10.1128/EC.00278-10>.
- [41] Y. Li, J. Yan, I. Kim, C. Liu, K. Huo, H. Rao, Mutant SOD1 and attenuates mutant SOD1-induced reactive oxygen species generation, *Mol. Biol. Cell* 21 (2010) 177–185, <https://doi.org/10.1091/mbc.E09>.
- [42] J. Feng, S. Yao, Y. Dong, J. Hu, M. Whiteway, J. Feng, Nucleotide excision repair protein Rad23 regulates cell virulence independent of Rad4 in *Candida albicans*, *mSphere* 5 (1) (2020), <https://doi.org/10.1128/mSphere.00062-20>.
- [43] D. Paul, et al., Tethering-facilitated DNA ‘opening’ and complementary roles of β -hairpin motifs in the Rad4/XPC DNA damage sensor protein, *Nucleic Acids Res.* 48 (21) (2021) 12348–12364, <https://doi.org/10.1093/nar/gkaa909>.
- [44] L. Kmetzsch, et al., The vacuolar Ca²⁺ exchanger vcx1 is involved in calcineurin-dependent Ca²⁺ tolerance and virulence in *Cryptococcus neoformans*, *Eukaryot. Cell* 9 (11) (2010) 1798–1805, <https://doi.org/10.1128/EC.00114-10>.
- [45] Y. Hu, J. Wang, S.H. Ying, M.G. Feng, Five vacuolar Ca²⁺ exchangers play different roles in calcineurin-dependent Ca²⁺/Mn²⁺ tolerance, multistress responses and virulence of a filamentous entomopathogen, *Fungal Genet. Biol.* 73 (2014) 12–19, <https://doi.org/10.1016/j.fgb.2014.09.005>.
- [46] R. Klukovich, W.E. Courchesne, Functions of *Saccharomyces cerevisiae* Ecm27p, a putative Na⁺/Ca²⁺ exchanger, in calcium homeostasis, carbohydrate storage and cell cycle reentry from the quiescent phase, *Microbiol. Res.* 186–187 (2016) 81–89, <https://doi.org/10.1016/j.micres.2016.03.007>.
- [47] Z. Qi, et al., The sodium/calcium exchanger PnCX1-mediated Ca²⁺ efflux is involved in Cinnamaldehyde-induced Cell-Wall defects of *Phytophthora capsici*, *Agronomy* 12 (8) (2022) 1763, <https://doi.org/10.3390/agronomy12081763>.
- [48] F.S. Hsu, F. Hu, Y. Mao, Spatiotemporal control of phosphatidylinositol 4-phosphate by Sac2 regulates endocytic recycling, *J. Cell Biol.* 209 (1) (2015) 97–110, <https://doi.org/10.1083/jcb.201408027>.
- [49] B. Zhang, et al., The actin-related protein Sac1 is required for morphogenesis and cell wall integrity in *Candida albicans*, *Fungal Genet. Biol.* 81 (2015) 261–270, <https://doi.org/10.1016/j.fgb.2014.12.007>.
- [50] F. Stehr, M. Kretschmar, C. Kröger, B. Hube, W. Schäfer, Microbial lipases as virulence factors, *J. Mol. Catal. B Enzym.* 22 (5–6) (2003) 347–355, [https://doi.org/10.1016/S1381-1177\(03\)00049-3](https://doi.org/10.1016/S1381-1177(03)00049-3).
- [51] S. Brunke, B. Hube, MfLIP1, a gene encoding an extracellular lipase of the lipid-dependent fungus *Malassezia furfur*, *Microbiology* 152 (2) (2006) 547–554, <https://doi.org/10.1099/mic.0.28501-0>.
- [52] R. Gupta, A. Kumari, P. Syal, Y. Singh, Molecular and functional diversity of yeast and fungal lipases: their role in biotechnology and cellular physiology, *Prog. Lipid Res.* 57 (2015) 40–54, <https://doi.org/10.1016/j.plipres.2014.12.001>.
- [53] C. Wang, et al., An AGC kinase, PgAGC1 regulates virulence in the entomopathogenic oomycete *Pythium guiyangense*, *Fungal Biol.* 123 (1) (2019) 87–93, <https://doi.org/10.1016/j.funbio.2018.11.006>.
- [54] Y. Wang, et al., The AGC kinase SsAgc1 regulates sporisorium *scitamineum* mating/Filamentation and pathogenicity, *mSphere* 4 (e00259–19) (2019) 1–15, <https://doi.org/10.1128/mSphere.00259-19>.
- [55] J.H.T.M. Fabri, et al., The AGC kinase YpkA regulates sphingolipids biosynthesis and physically interacts with SakA MAP kinase in *Aspergillus fumigatus*, *Front. Microbiol.* 10 (JAN) (2019) 1–19, <https://doi.org/10.3389/fmicb.2018.03347>.
- [56] Q. Gu, M. Chen, J. Huang, Y. Wei, T. Hsiang, L. Zheng, Multifaceted roles of the ras guanine-nucleotide exchange factor ChRgf in development, pathogenesis, and stress responses of *colletotrichum higginsianum*, *Phytopathology* 107 (4) (2017) 433–443, <https://doi.org/10.1094/PHYTO-03-16-0137-R>.
- [57] A. Martin-Vicente, A.C.O. Souza, Q. Al Abdallah, W. Ge, J.R. Fortwendel, SH3-class Ras guanine nucleotide exchange factors are essential for *Aspergillus fumigatus* invasive growth, *Cell. Microbiol.* 21 (6) (2019) 1–16, <https://doi.org/10.1111/cmi.13013>.
- [58] C. Savojardo, P.L. Martelli, P. Fariselli, R. Casadio, DeepSig: deep learning improves signal peptide detection in proteins, *Bioinformatics* 34 (10) (2018) 1690–1696, <https://doi.org/10.1093/bioinformatics/btx818>.
- [59] T.N. Petersen, S. Brunak, G. von Heijne, H. Nielsen, SignalP 4.0: discriminating signal peptides from transmembrane regions, *Nat. Methods* 8 (10) (2011) 785–786, <https://doi.org/10.1038/nmeth.1701>.
- [60] O. Emanuelsson, S. Brunak, G. Von Heijne, H. Nielsen, Locating proteins in the cell using TargetP, SignalP and related tools, *Nat. Protoc.* 2 (4) (2007) 953–971, <https://doi.org/10.1038/nprot.2007.131>.
- [61] A. Krogh, B. Larsson, G. Von Heijne, E.L.L. Sonnhammer, Predicting transmembrane protein topology with a hidden Markov model: application to complete genomes, *J. Mol. Biol.* 305 (2001) 567–580, <https://doi.org/10.1006/jmbi.2000.4315>.
- [62] J. Sperschneider, P. Dodds, EffectorP 3.0: prediction of apoplastic and cytoplasmic effectors in fungi and oomycetes, *Mol. Plant-Microbe Interact.* (2021) 1–28, <https://doi.org/10.1094/mpmi-08-21-0201-r>.
- [63] T. Giraud, P. Gladieux, M. Hood, The origin of species in Fungi, *Fungi* 3 (4) (2010) 23–27, <https://doi.org/10.1086/279246>.
- [64] J. Varga, G. Szigeti, N. Baranyi, S. Kocsubé, C.M. O’Gorman, P.S. Dyer, *Aspergillus*: sex and recombination, *Mycopathologia* 178 (5–6) (2014) 349–362, <https://doi.org/10.1007/s11046-014-9795-8>.
- [65] F. Tekaiia, J.P. Latgé, *Aspergillus fumigatus*: saprophyte or pathogen? *Curr. Opin. Microbiol.* 8 (4) (2005) 385–392, <https://doi.org/10.1016/j.mib.2005.06.017>.
- [66] J.O. Masanga, J.M. Matheka, R.A. Omer, S.C. Ommeh, E.O. Monda, A. E. Alakonya, Downregulation of transcription factor aRfR in *aspergillus flavus* confers reduction to aflatoxin accumulation in transgenic maize with alteration of host plant architecture, *Plant Cell Rep.* 34 (8) (2015) 1379–1387, <https://doi.org/10.1007/s00299-015-1794-9>.
- [67] M. Ismail, A. Hamayun, A. Hussain, S.A. Khan Iqbal, I.-J. Lee, Endophytic fungus *aspergillus japonicus* mediates host plant growth under normal and heat stress conditions, *Biomed. Res. Int.* 2018 (2018) 1–11, <https://doi.org/10.1155/2018/7696831>.
- [68] Y. Lamboni, et al., Diversity in secondary metabolites including mycotoxins from strains of *aspergillus section nigri* isolated from raw cashew nuts from Benin, West Africa, *PLoS One* 11 (10) (2016) 1–14, <https://doi.org/10.1371/journal.pone.0164310>.
- [69] F.P. Massi, et al., Prospecting for the incidence of genes involved in ochratoxin and fumonisin biosynthesis in Brazilian strains of *aspergillus Niger* and *Aspergillus welwitschiae*, *Int. J. Food Microbiol.* 221 (2016) 19–28, <https://doi.org/10.1016/j.ijfoodmicro.2016.01.010>.
- [70] J. Kollár, A. Poulíčková, P. Dvořák, On the relativity of species, or the probabilistic solution to the species problem, *Mol. Ecol.* 31 (2) (2022) 411–418, <https://doi.org/10.1111/mec.16218>.
- [71] R. Saha, N. Saha, R.S. Donofrio, L.L. Bestervelt, Microbial siderophores: a mini review, *J. Basic Microbiol.* 53 (4) (2013) 303–317, <https://doi.org/10.1002/jobm.201100552>.
- [72] A. Rakin, L. Schneider, O. Podladchikova, Hunger for iron: the alternative siderophore iron scavenging systems in highly virulent *Yersinia*, *Front. Cell. Infect. Microbiol.* 2 (November) (2012) 151, <https://doi.org/10.3389/fcimb.2012.00151>.
- [73] N. Mohd-Assaad, B.A. McDonald, D. Croll, Genome-wide detection of genes under positive selection in worldwide populations of the barley scald pathogen, *Genome Biol. Evol.* 10 (5) (2018) 1315–1332, <https://doi.org/10.1093/gbe/evy087>.
- [74] M.C. Derbyshire, et al., A whole genome scan of SNP data suggests a lack of abundant hard selective sweeps in the genome of the broad host range plant pathogenic fungus *Sclerotinia sclerotiorum*, *PLoS One* 14 (3) (2019) 1–24, <https://doi.org/10.1371/journal.pone.0214201>.
- [75] F.E. Hartmann, B.A. McDonald, D. Croll, Genome-wide evidence for divergent selection between populations of a major agricultural pathogen, *Mol. Ecol.* 27 (12) (2018) 2725–2741, <https://doi.org/10.1111/mec.14711>.
- [76] A.A. Nessem, W.A. Kasim, Physiological impact of seed priming with CaCl₂ or carrot root extract on *lupinus termis* plants fully grown under salinity stress, *Egypt. J. Bot.* 59 (3) (2019) 763–777, <https://doi.org/10.21608/ejbo.2019.8026.1289>.
- [77] C. Xu, X. Li, L. Zhang, The effect of calcium chloride on growth, photosynthesis, and antioxidant responses of *Zoysia japonica* under drought conditions, *PLoS One* 8 (7) (2013) 1–10, <https://doi.org/10.1371/journal.pone.0068214>.
- [78] B.J. Jam, F. Shekari, M.R. Azimi, E. Zangani, Effect of priming by salicylic acid on germination and seedling growth of safflower seeds under CaCl₂ stress E Effect of priming by salicylic acid on germination and seedling growth of safflower seeds under CaCl₂ stress, *Int. J. Agric. Res. Rev.* 2 (5) (2012) 1097–1105.
- [79] I. Stergiopoulos, Y.A.I. Kourmpetis, J.C. Slot, F.T. Bakker, P.J.G.M. De Wit, A. Rokas, In silico characterization and molecular evolutionary analysis of a novel superfamily of fungal effector proteins, *Mol. Biol. Evol.* 29 (11) (2012) 3371–3384, <https://doi.org/10.1093/molbev/mss143>.
- [80] K. Guyon, C. Balagué, D. Roby, S. Raffaele, Secretome analysis reveals effector candidates associated with broad host range necrotrophy in the fungal plant pathogen *Sclerotinia sclerotiorum*, *BMC Genomics* 15 (1) (2014) 1–18, <https://doi.org/10.1186/1471-2164-15-336>.
- [81] M. Franceschetti, A. Maqbool, M.J. Jiménez-Dalmaroni, H.G. Pennington, S. Kamoun, M.J. Banfield, Effectors of filamentous plant pathogens: commonalities amid diversity, *Microbiol. Mol. Biol. Rev.* 81 (2) (2017) 1–17, <https://doi.org/10.1128/mbr.00066-16>.

- [82] R.M. De Miccolis Angelini, L. Landi, C. Raguseo, S. Pollastro, F. Faretra, G. Romanazzi, Tracking of diversity and evolution in the Brown rot Fungi *Monilinia fructicola*, *Monilinia fructigena*, and *Monilinia laxa*, *Front. Microbiol.* 13 (March) (2022), <https://doi.org/10.3389/fmicb.2022.854852>.
- [83] D.G.O. Saunders, J. Win, L.M. Cano, L.J. Szabo, S. Kamoun, S. Raffaele, Using hierarchical clustering of secreted protein families to classify and rank candidate effectors of rust fungi, *PLoS One* 7 (1) (2012), <https://doi.org/10.1371/journal.pone.0029847>.
- [84] J. Khosa, F. Bellinazzo, R. Kamenetsky Goldstein, R. Macknight, R.G.H. Immink, Phosphatidylethanolamine-binding proteins: the conductors of dual reproduction in plants with vegetative storage organs, *J. Exp. Bot.* 72 (8) (2021) 2845–2856, <https://doi.org/10.1093/jxb/erab064>.
- [85] O. Tsoy, A. Mushegian, Florigen and its homologs of FT/CETS/PEBP/RKIP/Ybhb family may be the enzymes of small molecule metabolism: review of the evidence, *BMC Plant Biol.* 22 (1) (2022) 1–16, <https://doi.org/10.1186/s12870-022-03432-z>.
- [86] M. Ksiazkiewicz, S. Rychel, M.N. Nelson, K. Wyrwa, B. Naganowska, B. Wolko, Expansion of the phosphatidylethanolamine binding protein family in legumes: a case study of *Lupinus angustifolius* L. flowering Locus T homologs, LanFTc1 and LanFTc2, *BMC Genomics* 17 (1) (2016) 1–21, <https://doi.org/10.1186/s12864-016-3150-z>.
- [87] A.V. Pérez-López, J. Simpson, The sweet taste of adapting to the desert: Fructan metabolism in Agave species, *Front. Plant Sci.* 11 (March) (2020) 1–5, <https://doi.org/10.3389/fpls.2020.00324>.
- [88] M.S. Iyer, K. Bhargava, M. Pavalam, R. Sowdhamini, GenDiS database update with improved approach and features to recognize homologous sequences of protein domain superfamilies, *Database* 2019 (1) (2019) 1–11, <https://doi.org/10.1093/database/baz042>.
- [89] L.M. Douglas, J.B. Konopka, Fungal membrane organization: the eisosome concept, *Annu. Rev. Microbiol.* 68 (2014) 377–393, <https://doi.org/10.1146/annurev-micro-091313-103507>.
- [90] J.E. Foderaro, L.M. Douglas, J.B. Konopka, MCC/eisosomes regulate cell wall synthesis and stress responses in fungi, *J. Fungi* 3 (4) (2017) 1–18, <https://doi.org/10.3390/jof3040061>.
- [91] J. Zahumensky, J. Malinsky, Role of MCC/eisosome in fungal lipid homeostasis, *Biomolecules* 9 (8) (2019) 1–20, <https://doi.org/10.3390/biom9080305>.
- [92] C. Scazzocchio, I. Vangelatos, V. Sophianopoulou, Eisosomes and membrane compartments in the ascomycetes: a view from *aspergillus nidulans*, *Commun. Integr. Biol.* 4 (1) (2017) 64–68, <https://doi.org/10.4161/cib.13764>.
- [93] I. Vangelatos, K. Roumelioti, C. Gournas, T. Suarez, C. Scazzocchio, V. Sophianopoulou, Eisosome organization in the filamentous ascomycete *aspergillus nidulans*, *Eukaryot. Cell* 9 (10) (2010) 1441–1454, <https://doi.org/10.1128/EC.00087-10>.
- [94] A. Demoor, P. Silar, S. Brun, Appressorium: the breakthrough in Dikarya, *J. Fungi* 5 (3) (2019), <https://doi.org/10.3390/jof5030072>.
- [95] C.A. Voigt, W. Schäfer, S. Salomon, A secreted lipase of fusarium graminearum is a virulence factor required for infection of cereals, *Plant J.* 42 (3) (2005) 364–375, <https://doi.org/10.1111/j.1365-3113X.2005.02377.x>.
- [96] B. Bushnell, BBTools: A Suite of Fast, Multithreaded Bioinformatics Tools Designed for Analysis of DNA and RNA Sequence Data, *Jt. Genome Institute*, 2018. <https://jgi.doe.gov/data-and-tools/bbtools>.
- [97] P. Thorpe, C.M. Escudero-Martinez, P.J.A. Cock, S. Eves-Van Den Akker, J.I. B. Bos, Shared transcriptional control and disparate gain and loss of aphid parasitism genes, *Genome Biol. Evol.* 10 (10) (2018) 2716–2733, <https://doi.org/10.1093/gbe/evy183>.
- [98] F.A. Simão, R.M. Waterhouse, P. Ioannidis, E.V. Kriventseva, E.M. Zdobnov, BUSCO: assessing genome assembly and annotation completeness with single-copy orthologs, *Bioinformatics* 31 (19) (2015) 3210–3212, <https://doi.org/10.1093/bioinformatics/btv351>.
- [99] M. Yandell, C. Holt, MAKER2: an annotation pipeline and genome-database management tool for second-generation genome projects, *BMC Bioinformatics* 12 (1) (2011) 491, <https://doi.org/10.1186/1471-2105-12-491>.
- [100] I. Korf, Gene finding in novel genomes, *BMC Bioinformatics* 5 (2004) 1–9, <https://doi.org/10.1186/1471-2105-5-59>.
- [101] A.V. Lukashin, M. Borodovsky, GeneMark.Hmm: new solutions for gene finding, *Nucleic Acids Res.* 26 (4) (1998) 1107–1115, <https://doi.org/10.1093/nar/26.4.1107>.
- [102] M. Stanke, R. Steinkamp, S. Waack, B. Morgenstern, Augustus: a web server for gene finding in eukaryotes, *Nucleic Acids Res.* 32 (WEB SERVER ISS) (2004) 309–312, <https://doi.org/10.1093/nar/gkh379>.
- [103] R.E. Masonbrink, et al., An annotated genome for *haliothis rufescens* (red abalone) and resequenced green, pink, pinto, black, and white abalone species, *Genome Biol. Evol.* 11 (2) (2019) 431–438, <https://doi.org/10.1093/gbe/evz006>.
- [104] Y. Cuesta-Astroz, et al., Helminth secretomes reflect different lifestyles and parasitized hosts, *Int. J. Parasitol.* 47 (9) (2017) 529–544, <https://doi.org/10.1016/j.ijpara.2017.01.007>.
- [105] D.M. Emms, S. Kelly, OrthoFinder: phylogenetic orthology inference for comparative genomics, *bioRxiv* (2018) 1–14, <https://doi.org/10.1101/466201>.
- [106] B.Q. Minh, et al., IQ-TREE 2: new models and efficient methods for phylogenetic inference in the genomic era, *Mol. Biol. Evol.* 37 (5) (2020) 1530–1534, <https://doi.org/10.1093/molbev/msaa015>.
- [107] S. Kumar, G. Stecher, M. Suleski, S.B. Hedges, TimeTree: a resource for timelines, timetrees, and divergence times, *Mol. Biol. Evol.* 34 (7) (2017) 1812–1819, <https://doi.org/10.1093/molbev/msx116>.
- [108] A. Löytynoja, Phylogeny-aware alignment with PRANK, *Methods Mol. Biol.* 1079 (2014) 155–170, https://doi.org/10.1007/978-1-62703-646-7_10.

Chapter IV – Iniciadores, Kit e Método para Identificação de *Aspergillus Welwitschiae* e Diagnóstico Molecular da Podridão Vermelha de *Agave sisalana* e Seus Híbridos.

RESUMO: A presente tecnologia oferece um método inovador para a detecção molecular do fungo *Aspergillus welwitschiae*, causador da podridão vermelha em plantas de *Agave sisalana* (sisal) e seus híbridos. O sisal é amplamente cultivado no Brasil, mas a produção tem sido afetada por essa doença que causa o avermelhamento e morte dos caules das plantas. Atualmente, a detecção da doença é difícil, pois só pode ser observada quando os sintomas externos se manifestam, momento em que a extração de fibras com qualidade é inviável. Os métodos existentes para o diagnóstico são complexos, caros e dependem de mão-de-obra altamente especializada. A nova tecnologia propõe o uso de iniciadores e um kit de diagnóstico baseado na técnica de reação em cadeia da polimerase (PCR), que permite um diagnóstico rápido e preciso da podridão vermelha. Esse método possibilita o manejo fitossanitário adequado do cultivo, bem como a propagação de plantas saudáveis. Ao contrário de outras patentes que tratam de inibir o desenvolvimento da doença, a presente tecnologia concentra-se no diagnóstico de plantas possivelmente já infectadas. Ela oferece uma solução simples, prática e de baixo custo para a identificação de *Aspergillus welwitschiae*, permitindo um controle mais efetivo da doença e a proteção das culturas de sisal. Com o uso dessa inovação, os produtores de sisal no Brasil podem adotar medidas preventivas e de manejo mais eficientes, garantindo a obtenção de mudas saudáveis e a identificação precoce da doença. Isso tem o potencial de aumentar a produtividade do sisal e fortalecer a indústria nacional de fibras naturais.

Palavras-chave: Patente, PCR, detecção, infecção.



Pedido nacional de Invenção, Modelo de Utilidade, Certificado de Adição de Invenção e entrada na fase nacional do PCT

Número do Processo: BR 10 2022 018126 8

Dados do Depositante (71)

Depositante 1 de 2

Nome ou Razão Social: UNIVERSIDADE FEDERAL DE MINAS GERAIS

Tipo de Pessoa: Pessoa Jurídica

CPF/CNPJ: 17217985000104

Nacionalidade: Brasileira

Qualificação Jurídica: Instituição de Ensino e Pesquisa

Endereço: Av. Antônio Carlos, 6627 - Unidade Administrativa II - 2º andar- sala 2011

Cidade: Belo Horizonte

Estado: MG

CEP: 31270-901

País: Brasil

Telefone: (31) 3409-6430

Fax:

Email: patentes@ctit.ufmg.br

Depositante 2 de 2

Nome ou Razão Social: UNIVERSIDADE ESTADUAL DE CAMPINAS

Tipo de Pessoa: Pessoa Jurídica

CPF/CNPJ: 46068425000133

Nacionalidade: Brasileira

Qualificação Jurídica: Instituição de Ensino e Pesquisa

Endereço: Cidade Universitária Zeferino Vaz, Distrito de Barão Geraldo

Cidade: Campinas

Estado: SP

CEP:

País: BRASIL

Telefone:

Fax:

Email: patentes@inova.unicamp.br

Dados do Pedido

Natureza Patente: 10 - Patente de Invenção (PI)

Título da Invenção ou Modelo de Utilidade (54): INICIADORES, KIT E MÉTODO PARA IDENTIFICAÇÃO DE ASPERGILLUS WELWITSCHIAE E DIAGNÓSTICO MOLECULAR DA PODRIDÃO VERMELHA DE AGAVE SISALANA E SEUS HÍBRIDOS, E USOS

Resumo: A presente tecnologia trata de dois iniciadores, definidos pelas SEQ ID N° 1 e 2, um kit contendo os iniciadores e um método para detecção molecular de *Aspergillus welwitschiae*, agente etiológico da podridão vermelha da espécie vegetal *Agave sisalana* e seus híbridos, conhecidos como sisal, baseado na técnica de reação em cadeia da polimerase (PCR). A tecnologia se refere ainda ao uso dos iniciadores e do kit para o diagnóstico da podridão vermelha do sisal.

Figura a publicar: 1

Dados do Inventor (72)

Inventor 1 de 8

Nome: GABRIEL QUINTANILHA PEIXOTO,

CPF: 13401940740

Nacionalidade: Brasileira

Qualificação Física: Pesquisador

Endereço: Av. Pres. Antônio Carlos, 6627 - Pampulha

Cidade: Belo Horizonte

Estado: MG

CEP: 31270-901

País: BRASIL

Telefone: (31) 340 93932

Fax:

Email: patentes@ctit.ufmg.br

Inventor 2 de 8

Nome: ERIC ROBERTO GUIMARÃES ROCHA AGUIAR

CPF: 02502164508

Nacionalidade: Brasileira

Qualificação Física: Professor do ensino superior

Endereço: Av. Pres. Antônio Carlos, 6627 - Pampulha

Cidade: Belo Horizonte

Estado: MG

CEP: 31270-901

País: BRASIL

Telefone: (31) 340 93932

Fax:

Email: patentes@ctit.ufmg.br

Inventor 3 de 8

Nome: ARISTÓTELES GÓES NETO

CPF: 54434882520

Nacionalidade: Brasileira

Qualificação Física: Professor do ensino superior

Endereço: Av. Pres. Antônio Carlos, 6627 - Pampulha

Cidade: Belo Horizonte

Estado: MG

CEP: 31270-901

País: BRASIL

Telefone: (31) 340 93932

Fax:

Email: patentes@ctit.ufmg.br

Inventor 4 de 8

Nome: FÁBIO TRIGO RAYA

CPF: 41852315806

Nacionalidade: Brasileira

Qualificação Física: Pesquisador

Endereço: Cidade Universitária Zeferino Vaz, Distrito de Barão Geraldo

Cidade: Campinas

Estado: SP

CEP:

País: BRASIL

Telefone:

Fax:

Email: patentes@inova.unicamp.br

Inventor 5 de 8

Nome: MARINA PUPKE MARONE

CPF: 35303055884

Nacionalidade: Brasileira

Qualificação Física: Pesquisador

Endereço: Cidade Universitária Zeferino Vaz, Distrito de Barão Geraldo

Cidade: Campinas

Estado: SP

CEP:

País: BRASIL

Telefone:

Fax:

Email: patentes@inova.unicamp.br

Inventor 6 de 8

Nome: ADRIELE BARBARA DE OLIVEIRA

CPF: 44314238852

Nacionalidade: Brasileira

Qualificação Física: Pesquisador

Endereço: Cidade Universitária Zeferino Vaz, Distrito de Barão Geraldo,
Campinas

Cidade: Campinas

Estado: SP

CEP:

País: BRASIL

Telefone:

Fax:

Email: patentes@inova.unicamp.br

Inventor 7 de 8

Nome: GONÇALO AMARANTE GUIMARÃES PEREIRA

CPF: 28987039587

Nacionalidade: Brasileira

Qualificação Física: Professor do ensino superior

Endereço: Cidade Universitária Zeferino Vaz, Distrito de Barão Geraldo,
Campinas

Cidade: Campinas

Estado: SP

CEP:

País: BRASIL

Telefone:

Fax:

Email: patentes@inova.unicamp.br

Inventor 8 de 8

Nome: MARCELO FALSARELLA CARAZZOLLE

CPF: 28464839812

Nacionalidade: Brasileira

Qualificação Física: Pesquisador

Endereço: Cidade Universitária Zeferino Vaz, Distrito de Barão Geraldo

Cidade: Campinas

Estado: SP

CEP:

País: BRASIL

Telefone:

Fax:

Email: patentes@inova.unicamp.br

Documentos anexados

Tipo Anexo	Nome
Comprovante de pagamento de GRU 200	1 - Depósito PI - 29409161948459875.pdf
Portaria	2 - Portaria 2195-2020 - Prof. Gilberto UFMG.pdf
Procuração	3 - Procuração UNICAMP.pdf
Comprovação de Poderes	4 - Comprovação de poderes UNICAMP.pdf
Relatório Descritivo	5 - Relatório Descritivo.pdf
Reivindicação	6 - Reivindicações.pdf
Desenho	7 - Desenhos.pdf
Resumo	8 - Resumo.pdf

Sequências Biológicas

- Declaro que a informação contida na 'Listagem de Sequências' apresentada em formato eletrônico está limitada ao conteúdo da matéria revelada pelas sequências de aminoácidos e/ou de nucleotídeos divulgadas no pedido de patente, conforme depositado

Tipos de Sequências Biológicas	Nome
Listagem de Sequências Biológicas em formato XML	Listagem de sequências.xml

Acesso ao Patrimônio Genético

- Declaração Positiva de Acesso - Declaro que o objeto do presente pedido de patente de invenção foi obtido em decorrência de acesso à amostra de componente do Patrimônio Genético Brasileiro, realizado a partir de 30 de junho de 2000, e que foram cumpridas as determinações da Lei 13.123 de 20 de maio de 2015, informando ainda:

Número da Autorização de Acesso: A7CF7A1

Acesso:

Data da Autorização de Acesso: 04/11/2018

Origem do material genético e do conhecimento tradicional associado, quando for o caso

Vide Cadastro

Declaração de veracidade

- Declaro, sob as penas da lei, que todas as informações acima prestadas são completas e verdadeiras.

INSTRUÇÕES:

A data de vencimento não prevalece sobre o prazo legal. O pagamento deve ser efetuado antes do protocolo. Órgãos públicos que utilizam o sistema SIAFI devem utilizar o número da GRU no campo Número de Referência na emissão do pagamento. Serviço: 200-Pedido nacional de Invenção, Modelo de Utilidade, Certificado de Adição de Invenção e entrada na fase nacional do PCT

Clique aqui e pague este boleto através do Auto Atendimento Pessoa Física.

Clique aqui e pague este boleto através do Auto Atendimento Pessoa Jurídica.

Recibo do Pagador

BANCO DO BRASIL | 001-9 | 00190.00009 02940.916196 48459.875174 3 89740000007000

Nome do Pagador/CPF/CNPJ/Endereço
UNIVERSIDADE FEDERAL DE MINAS GERAIS CPF/CNPJ: 17217985000104
AV ANTONIO CARLOS 6627 UNIDADE ADMINISTRATIVA II 2 ANDAR SALA 2011, BELO HORIZONTE -MG CEP:31270901

Sacador/Avalista
Nosso-Número 29409161948459875 Nr. Documento 29409161948459875 Data de Vencimento 03/05/2022 Valor do Documento 70,00 (=) Valor Pago

Nome do Beneficiário/CPF/CNPJ/Endereço
INSTITUTO NACIONAL DA PROPRIEDADE INDUST CPF/CNPJ: 42.521.088/0001-37
RUA MAYRINK VEIGA 9 24 ANDAR ED WHITE MARTINS , RIO DE JANEIRO - RJ CEP: 20090910

Agência/Código do Beneficiário 2234-9 / 333028-1 Autenticação Mecânica

BANCO DO BRASIL | 001-9 | 00190.00009 02940.916196 48459.875174 3 89740000007000

Local de Pagamento **PAGÁVEL EM QUALQUER BANCO ATÉ O VENCIMENTO** Data de Vencimento 03/05/2022

Nome do Beneficiário/CPF/CNPJ INSTITUTO NACIONAL DA PROPRIEDADE INDUST CPF/CNPJ: 42.521.088/0001-37 Agência/Código do Beneficiário 2234-9 / 333028-1

Data do Documento 04/04/2022 Nr. Documento 29409161948459875 Espécie DOC DS Aceite N Data do Processamento 04/04/2022 Nosso-Número 29409161948459875

Uso do Banco 29409161948459875 Carteira 17 Espécie R\$ Quantidade xValor (=) Valor do Documento 70,00

Informações de Responsabilidade do Beneficiário
A data de vencimento não prevalece sobre o prazo legal.
O pagamento deve ser efetuado antes do protocolo.
Órgãos públicos que utilizam o sistema SIAFI devem utilizar o número da GRU n o campo Número de Referência na emissão do pagamento.
Serviço: 200-Pedido nacional de Invenção, Modelo de Utilidade, Certificado de Adição de Invenção e entrada na fase nacional do PCT

(-) Desconto/Abatimento
(+) Juros/Multa
(=) Valor Cobrado

Nome do Pagador/CPF/CNPJ/Endereço
UNIVERSIDADE FEDERAL DE MINAS GERAIS CPF/CNPJ: 17217985000104
AV ANTONIO CARLOS 6627 UNIDADE ADMINISTRATIVA II 2 ANDAR SALA 2011, BELO HORIZONTE-MG CEP:31270901

Código de Baixa Autenticação Mecânica - Ficha de Compensação

Sacador/Avalista



___ SIAFI2022-DOCUMENTO-CONSULTA-CONGRU (CONSULTA GUIA DE RECOLHIMENTO DA UNIAO
07/04/22 16:48 USUARIO : LUDMILA
DATA EMISSAO : 07Abr22 TIPO : 1 - PAGAMENTO NUMERO : 2022GR800162
UG/GESTAO EMITENTE : 153254 / 15229 - ADMINISTRACAO GERAL/UFMG
UG/GESTAO FAVORECIDA : 183038 / 18801 - INSTITUTO NACIONAL DA PROPRIEDADE INDU
RECOLHEDOR : 153254 GESTAO : 15229
CODIGO RECOLHIMENTO : 72200 - 6 COMPETENCIA: ABR22 VENCIMENTO: 07Abr22
DOC. ORIGEM: 153254 / 15229 / 2022NP000571 PROCESSO :
RECURSO : 1
(-)VALOR DOCUMENTO : 70,00
(-)DESCONTO/ABATIMENTO:
(-)OUTRAS DEDUCOES :
(+)MORA/MULTA :
(+)JUROS/ENCARGOS :
(+)OUTROS ACRESCIMOS :
(=)VALOR TOTAL : 70,00
NOSSO NUMERO/NUMERO REFERENCIA : 00029409161948459875
CODIGO DE BARRAS : 89610000000 0 70000001010 3 95523127220 9 00360640000 4
OBSERVACAO
Serviço: 200-Pedido nacional de Invenção, Modelo de Utilidade, Certificado de
Adição de Invenção e entrada na fase nacional do PCT
LANCADO POR : 09663457627 - LUDMILA UG : 153254 07Abr2022 16:41
PF1=AJUDA PF3=SAI PF2=DADOS ORC/FIN PF4=ESPELHO PF12=RETORNA



UNIVERSIDADE FEDERAL DE MINAS GERAIS

PORTARIA Nº 2195, DE 06 DE ABRIL DE 2020

A REITORA DA UNIVERSIDADE FEDERAL DE MINAS GERAIS, no uso de suas atribuições legais e estatutárias, considerando o disposto nos artigos 11 e 12 do Decreto-Lei nº 200, de 25 de fevereiro de 1967,

RESOLVE:

Art. 1º Delegar competência ao Diretor da Coordenadoria de Transferência e Inovação Tecnológica (CTIT), Professor Gilberto Medeiros Ribeiro, Inscrição UFMG nº 247405 e SIAPE nº 1964486, e a seu substituto eventual para, no âmbito desse Órgão,

- a) assinar, por meio eletrônico ou físico, documentos ou instrumentos jurídicos, concernentes ao exercício das atividades de competência da CTIT, no âmbito da Lei 10.973/04 – Lei de Inovação Tecnológica, da Política de Inovação da UFMG e suas resoluções específicas, tais como Contrato de Transferência de *Know-How*, Contrato de Licenciamento de Tecnologia, Contrato de Partilhamento de Titularidade de Tecnologia, Acordos de Confidencialidade e Termos de Sigilo, Termos de Autorização de Teste e documentos afins;
- b) assinar, por meio eletrônico ou físico, documentação necessária para depósito, processamento, adição, retificação, substituição, modificação, ampliação e resposta de relatórios referentes a objeto de proteção de propriedade intelectual junto aos órgãos competentes, em âmbito nacional e internacional;
- c) autorizar a realização de despesas dentro dos limites orçamentários da CTIT;
- d) autorizar a concessão de suprimento de fundos a servidores da Unidade, bem como determinar a baixa de responsabilidade;
- e) requisitar passagens e transportes em geral, por quaisquer vias, nos limites da dotação orçamentária da CTIT;
- f) autorizar viagens de servidores, a serviço da Unidade, arbitrando-lhes as respectivas diárias, obedecidas as disposições legais pertinentes;
- g) assinar contratos, decorrentes de licitação, de dispensa de licitação ou inexigibilidade, no âmbito da CTIT;
- h) prover arrecadação de receitas em geral, no âmbito da CTIT; e
- i) apurar dívidas de terceiros para com a Universidade, oriundas de contratos de cotitularidade, licenciamento, transferência, dentre outros, adotando as medidas necessárias à regularização delas, no âmbito da CTIT.

Art. 2º Com base no disposto no Decreto nº 10.193, de 27 de dezembro de 2019, e no inciso II do art. 1º e art. 3º da Portaria nº 243, de 12 de fevereiro de 2020, do Ministério da Educação (MEC), subdelegar

competência ao supracitado Diretor e a seu substituto eventual para, no âmbito da CTIT,

I - celebrar novos contratos administrativos decorrentes de licitação, de dispensa de licitação e de inexigibilidade, ou prorrogar contratos em vigor relativos às atividades de custeio cujos valores sejam inferiores a R\$500.000,00 (quinhentos mil reais); e

II - autorizar a realização de despesas relativas às atividades de custeio cujos valores sejam inferiores a R\$500.000,00 (quinhentos mil reais).

Art. 3º Tornar sem efeito a Portaria nº 010, de 24 de janeiro de 2019.

Art. 4º A presente Portaria entra em vigor nesta data.

Belo Horizonte, 6 de abril de 2020.

Profa. Sandra Regina Goulart Almeida
Reitora



Documento assinado eletronicamente por **Sandra Regina Goulart Almeida, Reitora**, em 09/04/2020, às 17:17, conforme horário oficial de Brasília, com fundamento no art. 6º, § 1º, do [Decreto nº 8.539, de 8 de outubro de 2015](#).



A autenticidade deste documento pode ser conferida no site https://sei.ufmg.br/sei/controlador_externo.php?acao=documento_conferir&id_orgao_acesso_externo=0, informando o código verificador **0096203** e o código CRC **04D898C8**.

PROCURAÇÃO

Por este instrumento particular de Procuração, a **UNIVERSIDADE ESTADUAL DE CAMPINAS**, autarquia estadual em regime especial, inscrita no CNPJ sob nº 46.068.425/0001-33, com sede na Cidade Universitária “Zeferino Vaz”, Distrito de Barão Geraldo, Campinas, Estado de São Paulo, neste ato representada por seu Reitor Professor Doutor Antonio José de Almeida Meirelles, confere poderes especiais à **UNIVERSIDADE FEDERAL DE MINAS GERAIS - UFMG**, com sede na Avenida Antônio Carlos, nº 6.627, Belo Horizonte, Minas Gerais, inscrita no CNPJ sob o nº 17.217.985/0001-04, representada neste ato pelo Professor Gilberto Medeiros Ribeiro, Diretor da Coordenadoria de Transferência e Inovação Tecnológica – CTIT, para representá-la perante o Instituto Nacional da Propriedade Industrial – INPI, para o fim de requerer e processar direitos de propriedade intelectual face ao pedido de patente intitulado “INICIADORES, KIT E MÉTODO PARA IDENTIFICAÇÃO DE ASPERGILLUS WELWITSCHIAE E DIAGNÓSTICO MOLECULAR DA PODRIDÃO VERMELHA DE AGAVE SISALANA E SEUS HÍBRIDOS, E USOS”, a ser depositado junto ao INPI, para mantê-lo em vigor com amplos poderes para assinar petições e documentos, pagar taxas, anotar transferências, fazer prova de uso da invenção patenteada, apresentar oposições, recursos, réplicas, anotar, elaborar notificações extrajudiciais, e praticar para os fins mencionados todos os atos necessários perante as autoridades administrativas competentes no Brasil e no exterior, em benefício da Outorgante.

Esta procuração terá vigência de 10 (dez) anos, a partir da data de sua assinatura, que corresponderá à data da realização da assinatura digital.

UNIVERSIDADE ESTADUAL DE CAMPINAS

Antonio José de Almeida Meirelles

Reitor

(assinado digitalmente)

Documento assinado eletronicamente por **ANTONIO JOSÉ DE ALMEIDA MEIRELLES, REITOR**, em 19/08/2022, às 15:47 horas, conforme Art. 10 § 2º da MP 2.200/2001 e Art. 1º da Resolução GR 54/2017.



A autenticidade do documento pode ser conferida no site:
sigad.unicamp.br/verifica, informando o código verificador:
A282E5EE 613E46E2 92EA7874 9BBEDEC1



**“INICIADORES, KIT E MÉTODO PARA IDENTIFICAÇÃO DE
ASPERGILLUS WELWITSCHIAE E DIAGNÓSTICO MOLECULAR DA
PODRIDÃO VERMELHA DE AGAVE SISALANA E SEUS HÍBRIDOS, E
USOS”**

[01] A presente tecnologia trata de dois iniciadores, definidos pelas SEQ ID N° 1 e 2, um kit contendo os iniciadores e um método para detecção molecular de *Aspergillus welwitschiae*, agente etiológico da podridão vermelha da espécie vegetal *Agave sisalana* e seus híbridos, conhecidos como sisal, baseado na técnica de reação em cadeia da polimerase (PCR). A tecnologia se refere ainda ao uso dos iniciadores e do kit para o diagnóstico da podridão vermelha do sisal.

[02] O Brasil é o maior produtor de fibras naturais provenientes da espécie *Agave sisalana*, também chamada de sisal, estando os cultivos da planta concentrados majoritariamente no estado da Bahia e, em menor proporção, na Paraíba e outros estados do Nordeste. Um dos mais relevantes fatores que limitam o cultivo de sisal nestes locais e a consequente produção de fibras naturais é uma doença que afeta os caules da planta, caracterizado por uma coloração vermelha intensa nas regiões afetadas deste órgão, seguido por clorose (amarelamento das folhas) e pela morte da planta.

[03] A podridão vermelha do caule de sisal é uma doença causada pelo fungo filamentoso *Aspergillus welwitschiae*, e é uma das grandes responsáveis pela queda na produção de fibras de sisal desde 2012, ainda que o Brasil se mantenha como maior produtor deste material.

[04] Nas condições atuais, a doença só pode ser percebida quando a planta mostra sintomas visíveis em seu exterior (como a clorose, supramencionada), e nesta etapa, a extração das fibras (que agrega valor econômico à planta) já seria inviável, assim como a propagação de

bulbilhos (brotos que surgem após a floração em grandes pendões) infectados com a doença.

[05] *A. welwitschiae* é uma espécie críptica de *Aspergillus niger*, e atualmente o único método que pode ser aplicado ao diagnóstico da doença, ainda que este não seja seu propósito inicial, se dá por meio de uma associação de técnicas microbiológicas com PCR e sequenciamento de DNA, o que possui altíssimo custo, além de tratar-se de um processo moroso e dependente de mão-de-obra altamente especializada, o que praticamente impossibilita sua execução. A podridão vermelha do caule de sisal afeta também a propagação deste cultivo, feita inteiramente de forma assexuada, seja por mudas (plantas-filhas ligadas à planta matriz por um caule subterrâneo, o rizoma) ou por bulbilhos.

[06] Partindo desta premissa, a presente tecnologia se refere a um método para realizar o diagnóstico molecular rápido e preciso da podridão vermelha, possibilitando manejo fitossanitário do cultivo e propagação de *Agave sisalana* e outras variedades associadas, também afetadas por esta condição, garantindo mudas saudáveis e um diagnóstico precoce.

[07] O documento de patente CN109369280, intitulado “*Inhibit the preparation method of the slow released fertilizer of sisal hemp stem rot and chlorotic mottle*”, depositado em 17 de dezembro de 2017, trata de um método para inibir ou evitar o desenvolvimento da podridão vermelha em sisal. A presente tecnologia se difere, pois descreve um método para diagnóstico da podridão vermelha em plantas possivelmente já infectadas.

[08] A presente tecnologia trata de dois iniciadores, um kit contendo os iniciadores e um método para detecção molecular baseado de *Aspergillus welwitschiae*, agente etiológico da podridão vermelha da

espécie vegetal *Agave sisalana* e seus híbridos, conhecidos como sisal. A tecnologia consiste em um método simples, prático e de custo reduzido para a detecção da doença.

BREVE DESCRIÇÃO DAS FIGURAS

[09] A **Figura 1** apresenta o gel de eletroforese contendo da esquerda para a direita, o marcador molecular da KASVI de 1Kb (1), reação negativa do par de iniciadores AWF/AWF (2), banda da amplificação de CCMB 674 (3), banda de amplificação de CCMB 663 (4), e banda de amplificação de *A. niger* CCT 4026 (5). Em seguida, a banda da amplificação de CCMB 674 (6), banda de amplificação de CCMB 663 (7), e banda de amplificação de *A. niger* CCT 4026 (8) e reação negativa (9) do par de iniciadores awaspec/cmd6. Por último, marcador da KASVI de 1Kb (10).

[10] A **Figura 2** mostra o gel de eletroforese contendo, sempre na mesma ordem, da esquerda para a direita, a banda da amplificação de CCMB 674, banda de amplificação de CCMB 663, e banda de amplificação de *A. niger* CCT 4026 dos iniciadores de Aw1 (1-3), Aw2 (4-6), Aw3 (7-9), Aw4 (10-12), Aw5 (13-15), e Aw6 (16-18). Marcador molecular KASVI (19).

[11] A **Figura 3** mostra o gel de eletroforese contendo, sempre na mesma ordem, da esquerda para a direita, a banda da amplificação de CCMB 674, banda de amplificação de CCMB 663, e banda de amplificação de *A. niger* CCT 4026 dos iniciadores de Aw7 (1-3), Aw8 (4-6), Aw9 (7-9), e Aw10 (10-12). Em seguida, banda da amplificação de CCMB 674 (13), banda de amplificação de CCMB 663 (14), não amplificação de *A. niger* CCT 4026 (15) com a reação de Aw8 otimizada. Marcador molecular KASVI (16).

[12] A **Figura 4** representa o gel de eletroforese contendo, na parte superior os resultados obtidos a partir da reação A, onde da esquerda

para a direita; Marcador molecular KASVI (1), banda da amplificação de CCMB 674 nas temperaturas de anelamento de 57,7 °C (2), 60 °C (3), e 64°C (4). Banda da amplificação de CCMB 663 nas temperaturas de anelamento de 57,7 °C (5), 60 °C (6), e 64°C (7). Banda da amplificação de *A. niger* CCT 4026 nas temperaturas de anelamento de 57,7 °C (8), 60 °C (9), e 64°C (10). Marcador molecular KASVI (11). Na parte inferior estão os resultados obtidos a partir da reação B, onde da esquerda para a direita; Marcador molecular KASVI (1), banda da amplificação de CCMB 674 nas temperaturas de anelamento de 57,7 °C (2), 60 °C (3), e 64°C (4). Banda da amplificação de CCMB 663 nas temperaturas de anelamento de 57,7 °C (5), 60 °C (6), e 64°C (7). Banda da amplificação de *A. niger* CCT 4026 nas temperaturas de anelamento de 57,7 °C (8), 60 °C (9), e 64°C (10). Marcador molecular KASVI (11).

[13] A **Figura 5** apresenta o gel de eletroforese apresentando da esquerda para a direita, banda da amplificação de CCMB 674 e banda de amplificação de CCMB 663, primeiro em sua concentração (1-2) inicial e depois em sequência para suas respectivas diluições de 2 (3-4), 5 (5-6), 10 (7-8), 50 (9-10), 100 (11-12) e 1000 vezes (13-14). Marcador molecular KASVI (15).

DESCRIÇÃO DETALHADA DA TECNOLOGIA

[14] A presente tecnologia trata de dois iniciadores, um kit contendo os iniciadores e um método para detecção molecular de *Aspergillus welwitschiae*, agente etiológico da podridão vermelha da espécie vegetal *Agave sisalana* e seus híbridos, conhecidos como sisal, baseado na técnica de reação em cadeia da polimerase (PCR). A tecnologia se refere ainda ao uso dos iniciadores e do kit para o diagnóstico da podridão vermelha do sisal.

[15] Mais especificamente, os iniciadores são definidos pelas SEQs ID N° 1 e 2.

[16] O kit para identificação de *Aspergillus welwitschiae* diagnóstico molecular da podridão vermelha de *Agave sisalana* e seus híbridos compreende um par de iniciadores definidos pelas SEQ ID N° 1 e 2.

[17] O kit otimizado pode compreender até 60% v/v de H₂O complementar, 10 a 30% v/v de tampão de reação, 0,3 a 10 µM de cada iniciador, 100 a 500 µM de desoxirribonuclotídeos fosfatados (dNTP), 0,02 a 0,1 U/µl de enzima DNA polimerase, 0 a 10% v/v de dimetilsulfóxido (DMSO) e de 0,75 a 500 ng de DNA total extraído de plantas do gênero *Agave* ou do fungo a ser identificado.

[18] O método para identificação de *Aspergillus welwitschiae* e diagnóstico molecular da podridão vermelha de *Agave sasilana* e seus híbridos compreende as seguintes etapas:

- a) Coleta e preparo da amostra biológica;
- b) Extração e dosagem do DNA da amostra preparada em “a”;
- c) Realização da PCR utilizando os iniciadores definidos pelas SEQ ID N°s 1 e 2;
- d) Obtenção do resultado em gel de eletroforese.

[19] Na etapa “a”, o material biológico pode ser amostra de caule ou folhas ou fungo a ser identificado e o preparo da amostra pode ser realizado através das etapas de seccionamento e partição da amostra biológica em frascos estéreis livres de ácidos nucleicos e posterior refrigeração.

[20] Na etapa “b”, a extração do DNA pode ser realizada utilizando qualquer procedimento padrão de lise de células que considere a complexidade de rompimento das células vegetais e fúngicas, podendo ser químico, físico ou biológico, com subsequente purificação de DNA e a dosagem do DNA ser realizada por fluorometria, espectrofotometria ou outro método de quantificação.

[21] Na etapa “c”, a amplificação das amostras positivas pode ser realizada sob os seguintes parâmetros de corrida em termociclador: desnaturação inicial a 98°C por 30 s, seguido de 25 a 35 ciclos de desnaturação a 98°C por 5 a 10 s com anelamento de 60 a 64°C por 10 a 30 s e extensão de 72°C por 30 s/kb, e extensão final de 5 a 10 min, sendo que, com exceção da temperatura de anelamento, as temperaturas e tempos podem variar de acordo com as especificações do fabricante da enzima DNA polimerase.

[22] Na etapa “d”, o resultado positivo para podridão vermelha na amostra pode ser detectado mediante a presença de uma banda de aproximadamente 409 pb correspondente à espécie em questão no gel, e caso a amostra seja negativa não haverá amplificação de nenhuma banda.

[23] Os iniciadores e o kit da presente tecnologia podem ser utilizados para o diagnóstico da podridão vermelha de *Agave sisalana* e seus híbridos ou identificação de *Aspergillus welwitschiae*.

[24] A presente tecnologia pode ser mais bem compreendida através dos exemplos que se seguem, não limitantes da tecnologia.

EXEMPLO 1 - ANÁLISES COMPUTACIONAIS PARA SELEÇÃO E DESENVOLVIMENTO DE INICIADORES EXCLUSIVOS PARA CEPAS FITOPATOGÊNICAS DE *ASPERGILLUS WELWITSCHIAE*

[25] Para desenvolver um teste diagnóstico específico para a doença, utilizamos métodos computacionais para seleção de iniciadores e posterior validação deles. Foi realizada uma análise de ortólogos utilizando o software OrthoFinder v. 2.4 (Emms & Kelly, 2018) com o parâmetro “-d”, para utilizar sequências de DNA como entrada. Para a análise foram utilizados 40 genomas de *Aspergillus* e mais 2 *outgroups* (**Tabela 1**), sendo que, dentre esses, há a montagem de 2 genomas de haplótipos de *A. welwitschiae* isolados da região sisaleira da Bahia;

CCMB 663 e CCMB 674. As sequências de DNA codificantes (CDS) foram obtidas a partir do site do NCBI (<https://www.ncbi.nlm.nih.gov/>).

Tabela 1 - Genomas utilizados (conjuntos de CDS) para a análise de ortólogos.

Seção	Espécie	Linhagem	Número de acesso no GenBank
Flavi	<i>Aspergillus alliaceus</i>	CBS 536.65	GCF_009176365.1
	<i>Aspergillus avenaceus</i>	IBT 18842	GCA_009193465.1
	<i>Aspergillus bombycis</i>	NRRL 26010	GCF_001792695.1
	<i>Aspergillus caelatus</i>	CBS 763.97	GCF_009193585.1
	<i>Aspergillus flavus</i>	AF13	GCA_014117485.1
	<i>Aspergillus leporis</i>	CBS 151.66	GCA_009176345.1
	<i>Aspergillus oryzae</i>	RIB40	GCF_000184455.2
	<i>Aspergillus pseudonomiae</i>	IBT 12657	GCA_009176395.1
Fumigati	<i>Aspergillus fumigatus</i>	Af293	GCF_000002655.1
Nidulantes	<i>Aspergillus nidulans</i>	FGSC A4	GCF_000149205.2
Nigri	<i>Aspergillus aculeatinus</i>	CBS 121060	GCA_003184765.1
	<i>Aspergillus aculeatus</i>	ATCC 16872	GCA_001890905.1

<i>Aspergillus brasiliensis</i>	CBS 101740	GCA_001889945.1
<i>Aspergillus brunneoviolaceus</i>	CBS 621.78	GCA_003184695.1
<i>Aspergillus carbonarius</i>	ITEM 5010	GCA_001990825.1
<i>Aspergillus ellipticus</i>	CBS 707.79	GCA_003184645.1
<i>Aspergillus eucalypticola</i>	CBS 122712	GCA_003184535.1
<i>Aspergillus heteromorphus</i>	CBS 117.55	GCA_003184545.1
<i>Aspergillus homomorphus</i>	CBS 101889	GCA_003184865.1
<i>Aspergillus ibericus</i>	CBS 121593	GCA_003184845.1
<i>Aspergillus indologenus</i>	CBS 114.80	GCA_003184685.1
<i>Aspergillus luchuensis</i>	RIB 2604	GCA_001602395.1
<i>Aspergillus luchuensis</i>	IFO4308	GCA_000239835.2
<i>Aspergillus neoniger</i>	CBS 115656	GCA_003184625.1
<i>Aspergillus niger</i>	FDAARGOS_311	GCA_002211485.2
<i>Aspergillus niger</i>	N402 (ATCC 64974)	GCA_900248155.1
<i>Aspergillus niger</i>	CBS 101883	GCA_003184595.1
<i>Aspergillus niger</i>	ATCC 1015	GCA_000230395.2
<i>Aspergillus niger</i>	CBS 513.88	GCA_000002855.2

	<i>Aspergillus piperis</i>	CBS 112811	GCA_003184755.1
	<i>Aspergillus saccharolyticus</i>	JOP 1030-1	GCA_003184585.1
	<i>Aspergillus sclerotioniger</i>	CBS 115572	GCA_003184525.1
	<i>Aspergillus tubingensis</i>	WU-2223L	GCA_013340325.1
	<i>Aspergillus tubingensis</i>	CBS 134.48	GCA_001890745.1
	<i>Aspergillus uvarum</i>	CBS 121591	GCA_003184745.1
	<i>Aspergillus vadensis</i>	CBS 113365	GCA_003184925.1
	<i>Aspergillus welwitschiae</i>	CBS 139.54	GCA_003344945.1
	<i>Aspergillus welwitschiae</i>	CCMB 663	Ainda não disponível
	<i>Aspergillus welwitschiae</i>	CCMB 674	Ainda não disponível
Outros	<i>Neurospora crassa</i>	OR74A	GCF_000182925.2
	<i>Penicillium rubens</i>	Wisconsin 54-1255	GCF_000226395.1
Ustus	<i>Aspergillus calidoustus</i>	SF006504	GCA_001511075.1

[26] A partir do resultado, selecionamos famílias gênicas que continham apenas genes pertencentes às linhagens de *Aspergillus welwitschiae* (CBS 139.54, CCM 663 e CCB 674), ou seja, famílias exclusivas dessas

linhagens. A partir desse conjunto de 34 famílias gênicas, desenhamos iniciadores utilizando o software PrimerBlast (disponível em <https://www.ncbi.nlm.nih.gov/tools/primer-blast/>) com os parâmetros padrão e com “*Aspergillus welwitschiae*” na opção “organism”. Os iniciadores foram escolhidos com base no tamanho do amplicon, favorecendo maiores produtos de PCR (**Tabela 2**).

Tabela 2 - Iniciadores candidatos selecionados após análise de ortólogos e filtragem por tamanho de amplicon.

Nome	Cluster	Sequencia (5'->3')	Fita	Comprimento	Início	Parada	GC%	TM	
Aw_1	OG003 1004	<i>iniciador</i>	CACCGTCCA	+	20	48	67	55	60,11
		<i>senso</i>	ATTTTCCGC AG						
		<i>iniciador</i>	AGTCATGCC	-	20	888	869	50	59,96
		<i>anti-senso</i>	CAGCACAAT GA						
	<i>tamanho do produto</i>	841							
Aw_2	OG003 1008	<i>iniciador</i>	TGCTGCCCT	+	20	780	799	55	60,04
		<i>senso</i>	CCATTACAC AG						
		<i>iniciador</i>	TGGCCCGCA	-	20	1609	1590	50	60,03
		<i>anti-senso</i>	TACTCACAA AT						
	<i>tamanho do produto</i>	830							
Aw_3	OG003 0965	<i>iniciador</i>	TGGCGTACC	+	20	481	500	55	59,96
		<i>senso</i>	TGGAAGAGA GA						
		<i>iniciador</i>	GGATCCCCA	-	20	1212	1193	60	60,04
		<i>anti-senso</i>	TGAGAGCGA TG						
	<i>tamanho do produto</i>	732							

Aw_4	OG003 0964	<i>iniciador</i>	TGGCTCAGG	+	20	895	914	55	59,96
		<i>senso</i>	TTCCATCCC TA						
		<i>iniciador</i>	CCTGTTGCC						
		<i>anti-</i>	CAGATCCCA	-	20	1586	1567	55	60,03
		<i>senso</i>	AT						
		<i>tamanho</i>	692						
		<i>do</i>							
		<i>produto</i>							
Aw_5	OG003 1380	<i>iniciador</i>	CTTCATTTTCG	+	20	69	88	55	60,11
		<i>senso</i>	CCACTGGCA C						
		<i>iniciador</i>	CCCATCATC						
		<i>anti-</i>	GCCGTGTTC	-	20	663	644	55	59,9
		<i>senso</i>	TA						
		<i>tamanho</i>	595						
		<i>do</i>							
		<i>produto</i>							
Aw_6	OG003 0969	<i>iniciador</i>	AGAAGTACG	+	20	269	288	55	60,04
		<i>senso</i>	TGTGGGAAG CG						
		<i>iniciador</i>	GGTGCGGAT						
		<i>anti-</i>	AATGTCGGT	-	20	753	734	55	59,9
		<i>senso</i>	CT						
		<i>tamanho</i>	485						
		<i>do</i>							
		<i>produto</i>							
Aw_7	OG003 0966	<i>iniciador</i>	GAAGCCTGG	+	20	461	480	55	59,97
		<i>senso</i>	TGACGTTCT CA						
		<i>iniciador</i>	TTGCCCGTG						
		<i>anti-</i>	GAAATACCC	-	20	944	925	55	60,03
		<i>senso</i>	TC						
		<i>tamanho</i>	484						
		<i>do</i>							
		<i>produto</i>							
Aw_8 (SEQs	OG003 1003	<i>iniciador</i>	CACCTGATC	+	20	358	377	60	60,03
		<i>senso</i>	CTGGAGGGA GA						
		<i>iniciador</i>	AGCCACCTG						
IDs N°1		<i>anti-</i>	GAGAAGCAA	-	20	766	747	55	60,03
e 2)		<i>senso</i>							
		<i>produto</i>							

		senso	TC							
		tamanho								
		do	409							
		produto								
Aw_9	OG003 0687	iniciador	CAGCTCGCA	+	20	49	68	55	59,9	
		senso	GACATACTC							
			GT							
		iniciador	GACCACCGA	-	20	401	382	55	59,96	
anti-senso	TGTCCTGGT									
		TT								
		tamanho								
		do	353							
		produto								
Aw_10	OG003 1086	iniciador	TGGATCACC	+	20	94	113	55	59,96	
		senso	ACCACTGCT							
			TC							
		iniciador	CACAGCGAT	-	20	403	384	55	59,83	
anti-senso	TCACTCCGG									
		TA								
		tamanho								
		do	310							
		produto								

EXEMPLO 2 - VALIDAÇÃO EXPERIMENTAL E OTIMIZAÇÃO DAS REAÇÕES PARA DETECÇÃO DE *ASPERGILLUS WELWITSCHIAE*

[27] De modo a validar os 10 pares de iniciadores candidatos selecionados (denominados de AW 1 a 10 na **Tabela 2**), foram utilizados os seguintes controles: DNA extraído de isolado de duas cepas patogênicas de *Aspergillus welwitschiae*, a amostra identificada como CCMB 674, advinda de um haplótipo brasileiro e a amostra CCMB 663 advinda de uma cepa modelo de haplótipo geral. Para os testes de especificidade, como controle negativo, utilizou-se amostra de DNA extraído da cepa de *Aspergillus niger* CCT 4026, oriunda da coleção de microrganismos da UFMG. Iniciadores previamente descritos na literatura como capazes de segregar *A. welwitschiae* e *A. niger* também foram utilizados como controles externos. Foram escolhidos um par de

iniciadores descrito por Palumbo & O’Keeffe, (2015) (Aw F e Aw R) e o outro por Gherbawy et al., (2015) (awaspec e cmd6), conforme **Tabela 3**.

Tabela 3 - Conjuntos de iniciadores usados como controles externos neste exemplo. Adaptado de Palumbo & O’Keeffe, 2015 (Aw F e Aw R) e Gherbaway et al., 2015 (awaspec e cmd6).

Aw F	GGGATTTTCGACAGCATTctCAGAAAtt
Aw R	GATAAAACCATTGTTGTTCGCGGTCa
awaspec	ATTTTCGACAGCATTCTCAGAATTA
cmd6	CCGATAGAGGTCATAACGTGG

[28] As reações em cadeia da polimerase (PCR) foram realizadas com o kit ECRA HIFI DNA Polimerase (ECRA Biotec; EB1-17) seguindo o procedimento estabelecido pelo fabricante. Como temperatura de anelamento foi utilizada 58 °C para os iniciadores Aw_1-10, 56 °C para awaspec/cmd6 (Gherbaway et al., 2015) e 62 °C para AwF/AwR (Palumbo & O’Keeffe, 2015). Todos os produtos de PCR foram visualizados através de eletroforese em gel de agarose 1,5% com brometo de etídio.

[29] Testes iniciais com iniciadores descritos na literatura (Palumbo & O’Keeffe, 2015 e Gherbaway et al., 2015) atestaram a incapacidade destes em diferenciarem *A. welwitschiae* de *A. niger*. As bandas geradas podem ser observadas na **Figura 1**.

[30] Em seguida foram avaliados os iniciadores Aw_1-10 (**Figuras 2 e 3**). Apenas o par de iniciadores Aw_8 (SEQs IDs N° 1 e 2) apresentou polimorfismo capaz de diferenciar e detectar a presença de *A. niger* e de *A. welwitschiae*.

[31] Para aumentar a especificidade da reação, as condições de reação para o par de iniciadores Aw_8 (SEQs IDs N°1 e 2) foram testadas com variações de temperatura e adição de DMSO. Para tal, duas reações

foram montadas: A e B, colocadas em três temperaturas de anelamento, descritas na **tabela 4**, a seguir:

Tabela 4 - Condições de reação testadas neste exemplo.

Reação A	Reação B	Ciclos do termociclador
H ₂ O – 12,4 µL	H ₂ O – 11,8 µL	98°C - 30seg
Tampão – 5 µL	Tampão – 5 µL	98°C - 10seg
Iniciador senso – 0,5 µL	Iniciador senso – 0,5 µL	*** - 30seg
Iniciador anti-senso – 0,5 µL	Iniciador anti-senso –	72°C - 30seg
dNTP – 0,4 µL	0,5 µL	72°C - 10min
Enzima – 0,2 µL	dNTP – 0,4 µL	** Tm 1: 57,7 °C
DNA - 1µL	Enzima – 0,2 µL	** Tm 2: 60 °C
	DMSO - 0,6 µL	** Tm 3: 64 °C
	DNA – 1 µL	

[32] Como observado na **Figura 4**, a reação B com a adição de DMSO e com temperatura de anelamento de 60°C se apresentou como a melhor condição de reação para a detecção do *A. welwitschiae*, com o aumento da especificidade do iniciador, e desaparecimento das bandas inespecíficas na amostra ATCC.

[33] Uma vez ajustadas as condições ótimas de reação, foram realizados testes de sensibilidade com o par de iniciadores Aw_8 (SEQs IDs N°1 e 2), onde avaliou-se a capacidade do iniciador em gerar produtos de PCR com concentrações mínimas de DNA (Oliveira & Urashima, 2018). Para isso, foram utilizadas amostras diluídas de DNA em 2, 5, 10, 50, 100 e 1000 vezes. A partir da quantificação em Nanodrop, a amostra CCMB 674 partiu de uma concentração de 35 ng/µL, enquanto a amostra CCMB 663 teria 30 ng/µL. Foi possível

detecção do DNA do patógeno com até 0,75 ng/μL (diluição de 50x), de acordo com as bandas presentes na **Figura 5**.

[34] Em resumo, a partir das técnicas de biologia molecular aplicadas, comprovou-se a ineficiência do material disponível na literatura para a detecção de *A. welwitschiae*, espécie críptica de *A. niger*. Foi possível desenvolver e validar um marcador molecular, composto do conjunto de iniciadores (Aw_8, correspondendo as SEQs IDs N° 1 e 2)) e sua respectiva reação, capaz de detectar de modo qualitativo cepas patogênicas de *A. welwitschiae* em até 0,75 ng/μL DNA por amostra.

REIVINDICAÇÕES

1. **INICIADORES, caracterizados por** serem definidos pelas SEQ ID N^{os} 1 e 2.
2. **KIT PARA IDENTIFICAÇÃO DE *ASPERGILLUS WELWITSCHIAE* E DIAGNÓSTICO MOLECULAR DA PODRIDÃO VERMELHA DE *AGAVE SISALANA* E SEUS HÍBRIDOS** compreendendo os iniciadores definidos na reivindicação 1, **caracterizado por** compreender o par de iniciadores definidos pelas SEQ ID N^{os} 1 e 2.
3. **KIT PARA IDENTIFICAÇÃO DE *ASPERGILLUS WELWITSCHIAE* E DIAGNÓSTICO MOLECULAR DA PODRIDÃO VERMELHA DE *AGAVE SISALANA* E SEUS HÍBRIDOS, de acordo com a reivindicação 2, caracterizado por** compreender até 60% v/v de H₂O complementar, 10 a 30% v/v de tampão de reação, 0,3 a 10 µM de cada iniciador, 100 a 500 µM de desoxirribonuclotídeos fosfatados (dNTP), 0,02 a 0,1 U/µl de enzima DNA polimerase, 0 a 10% v/v de dimetilsulfóxido (DMSO) e de 0,75 a 500 ng de DNA total extraído de plantas do gênero *Agave* ou do fungo a ser identificado.
4. **MÉTODO PARA IDENTIFICAÇÃO DE *ASPERGILLUS WELWITSCHIAE* E DIAGNÓSTICO MOLECULAR DA PODRIDÃO VERMELHA DE *AGAVE SASILANA* E SEUS HÍBRIDOS, caracterizado por** compreender as seguintes etapas:
 - a) Coleta e preparo da amostra biológica;
 - b) Extração e dosagem do DNA da amostra preparada em “a”;
 - c) Realização da PCR utilizando os iniciadores definidos pelas SEQ ID N^{os} 1 e 2;
 - d) Obtenção do resultado em gel de eletroforese.
5. **MÉTODO PARA IDENTIFICAÇÃO DE *ASPERGILLUS WELWITSCHIAE* E DIAGNÓSTICO MOLECULAR DA PODRIDÃO**

VERMELHA DE AGAVE SASILANA E SEUS HÍBRIDOS, de acordo com a reivindicação 4, caracterizado por, na etapa “a”, a amostra ser de caule ou folhas ou o fungo a ser identificado e o preparo da amostra ser realizado através das etapas de seccionamento e partição da amostra biológica em frascos estéreis livres de ácidos nucleicos e posterior refrigeração.

6. MÉTODO PARA IDENTIFICAÇÃO DE *ASPERGILLUS WELWITSCHIAE* E DIAGNÓSTICO MOLECULAR DA PODRIDÃO VERMELHA DE AGAVE SASILANA E SEUS HÍBRIDOS, de acordo com a reivindicação 4, caracterizado por, na etapa “b”, a dosagem do DNA ser realizada por fluorometria, espectrofotometria ou outro método de quantificação.

7. MÉTODO PARA IDENTIFICAÇÃO DE *ASPERGILLUS WELWITSCHIAE* E DIAGNÓSTICO MOLECULAR DA PODRIDÃO VERMELHA DE AGAVE SASILANA E SEUS HÍBRIDOS, de acordo com a reivindicação 4, caracterizado por, na etapa “c”, a amplificação das amostras positivas ocorrer sob os parâmetros de corrida em termociclador de desnaturação inicial a 98°C por 30 s, seguido de 25 a 35 ciclos de desnaturação a 98°C por 5 a 10 s com anelamento de 60 a 64°C por 10 a 30 s e extensão de 72°C por 30 s/kb, e extensão final de 5 a 10 min, sendo que, com exceção da temperatura de anelamento, as temperaturas e tempos podem variar de acordo com as especificações do fabricante da enzima DNA polimerase.

8. MÉTODO PARA IDENTIFICAÇÃO DE *ASPERGILLUS WELWITSCHIAE* E DIAGNÓSTICO MOLECULAR DA PODRIDÃO VERMELHA DE AGAVE SASILANA E SEUS HÍBRIDOS, de acordo com a reivindicação 4, caracterizado por, na etapa “d”, o resultado positivo para podridão vermelha na amostra ser detectado mediante a presença de uma banda de aproximadamente 409 pb correspondente à

espécie em questão no gel, e caso a amostra seja negativa não haverá amplificação de nenhuma banda.

9. USO dos iniciadores definidos na reivindicação 1, caracterizado por ser no diagnóstico da podridão vermelha de *Agave sisalana* e seus híbridos ou na identificação de *Aspergillus welwitschiae*.

10. USO do kit definido na reivindicação 2, caracterizado por ser no diagnóstico da podridão vermelha de *Agave sisalana* e seus híbridos ou na identificação de *Aspergillus welwitschiae*.

DESENHOS

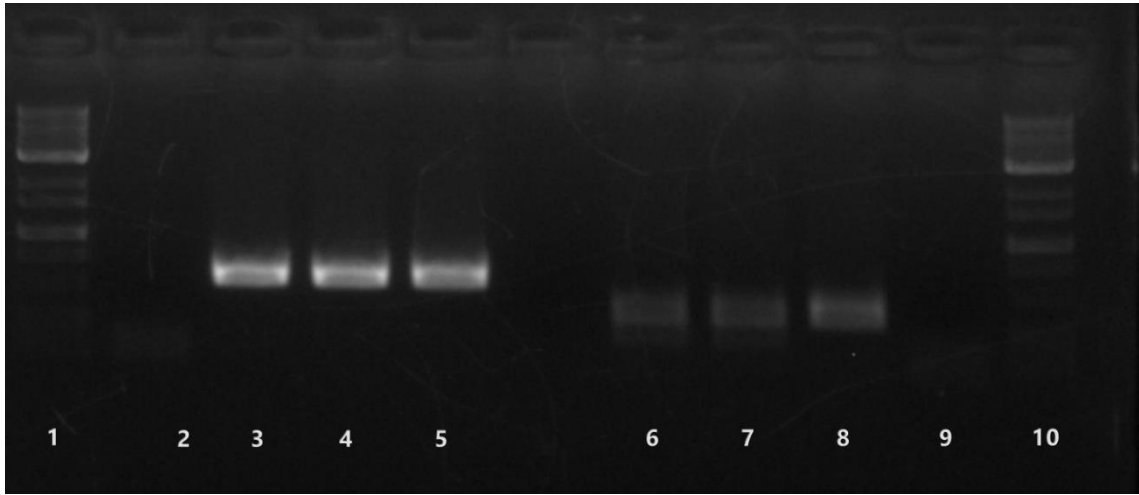


Figura 1

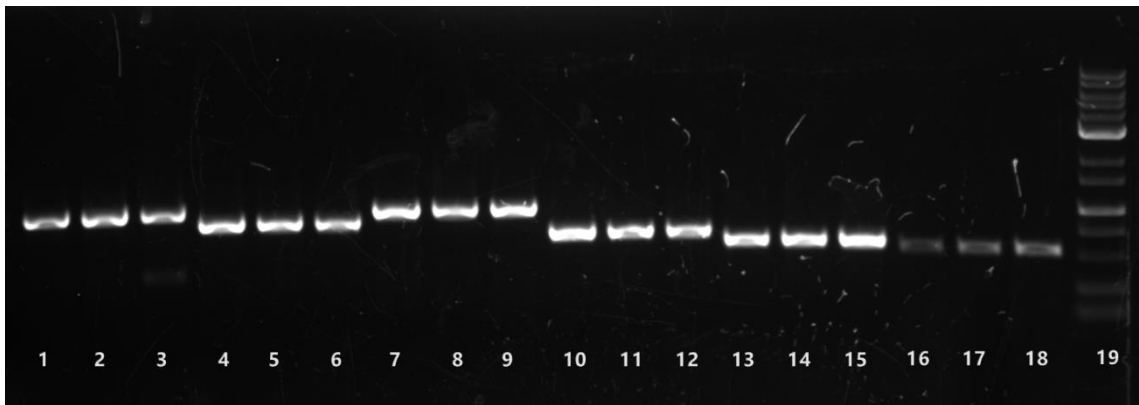


Figura 2

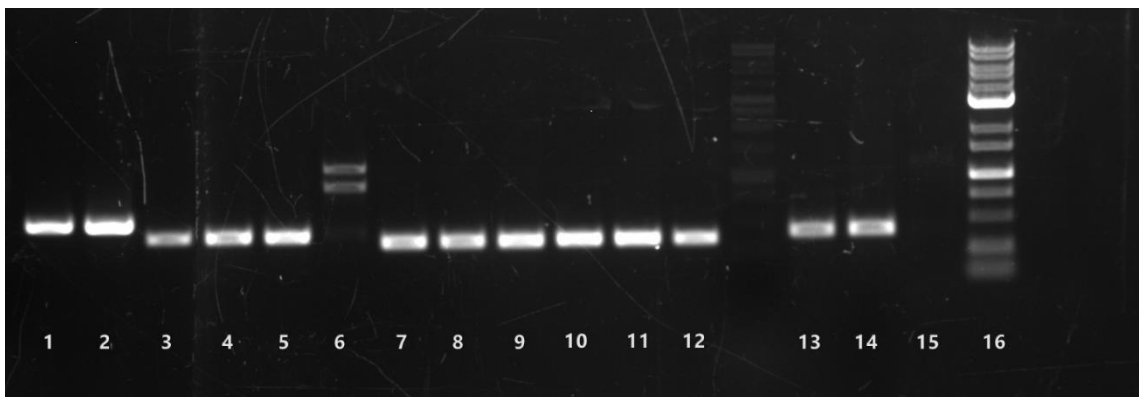


Figura 3

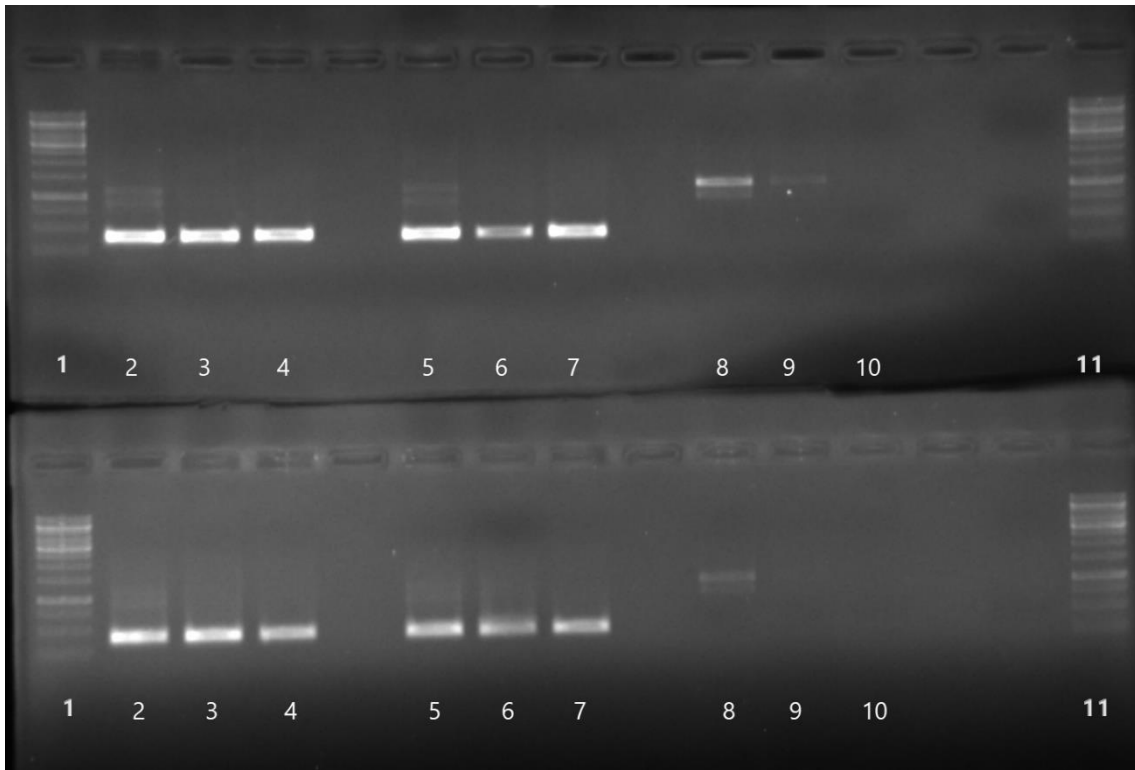


Figura 4

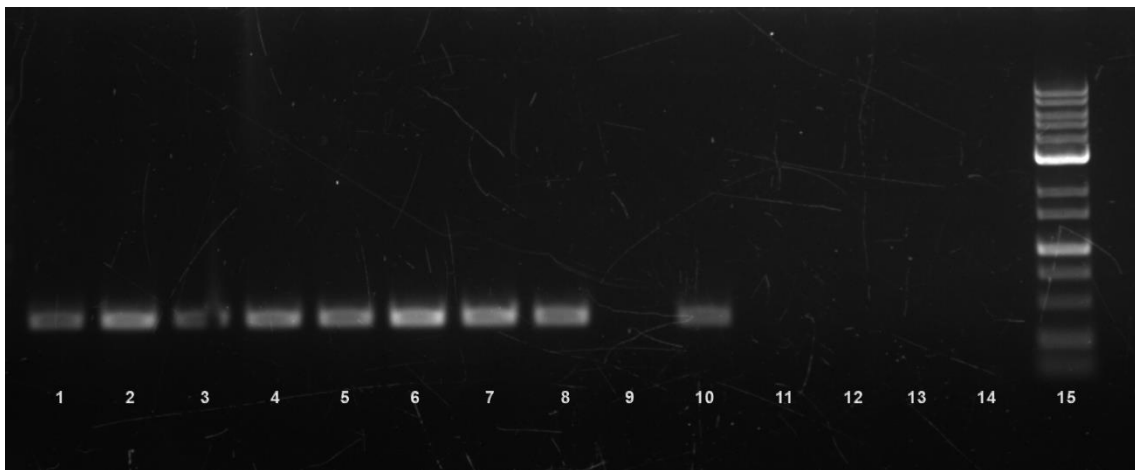


Figura 5

RESUMO**“INICIADORES, KIT E MÉTODO PARA IDENTIFICAÇÃO DE
ASPERGILLUS WELWITSCHIAE E DIAGNÓSTICO MOLECULAR DA
PODRIDÃO VERMELHA DE *AGAVE SISALANA* E SEUS HÍBRIDOS, E
USOS”**

A presente tecnologia trata de dois iniciadores, definidos pelas SEQ ID N° 1 e 2, um kit contendo os iniciadores e um método para detecção molecular de *Aspergillus welwitschiae*, agente etiológico da podridão vermelha da espécie vegetal *Agave sisalana* e seus híbridos, conhecidos como sisal, baseado na técnica de reação em cadeia da polimerase (PCR). A tecnologia se refere ainda ao uso dos iniciadores e do kit para o diagnóstico da podridão vermelha do sisal.

Este anexo apresenta o código de controle da listagem de sequências biológicas.

Código de Controle

Campo 1



Campo 2



Outras Informações:

- Nome do Arquivo: Listagem de sequências.xml
- Data de Geração do Código: 09/09/2022
- Hora de Geração do Código: 17:56:20
- Código de Controle:
 - Campo 1: FA969C41861C0C51
 - Campo 2: 8A93F5D670776BA5






Chapter V – Calm Before the Storm: A Glimpse into the Secondary Metabolism of *Aspergillus welwitschiae*, the Etiologic Agent of the Sisal Bole Rot.

RESUMO: *Aspergillus welwitschiae* é uma espécie da seção Nigri do gênero *Aspergillus*. Na natureza, é geralmente um saprófito, decompondo material vegetal. No entanto, causa a doença de podridão do caule em *Agave sisalana* (sisal), uma espécie de planta usada para a extração de fibras naturais resistentes, causando grandes perdas econômicas para essa cultura. Neste estudo, isolamos e sequenciamos um genoma de *A. welwitschiae* (isolado CCMB 674 - Coleção de Culturas de Microrganismos da Bahia) a partir de tecidos do caule do sisal e realizamos estratégias experimentais *in silico* e em laboratório para descrever sua capacidade de produzir micotoxinas. O isolado CCMB 674 possui 64 grupos de genes de metabolismo secundário (SMGCs) e, em condições normais, produz compostos de metabolismo secundário que podem perturbar o ciclo celular do sisal ou induzir anormalidades no crescimento da planta, como a malformina C. Esse isolado também produz um pigmento que pode explicar a cor vermelha característica dos tecidos afetados. Além disso, esse isolado é defeituoso na produção de fumonisina B1 e, apesar de possuir o agrupamento completo para a síntese do composto, não produziu ocratoxina A. Em conjunto, esses resultados fornecem novas informações sobre possíveis estratégias usadas pelos fungos durante a podridão do caule do sisal, ajudando a compreender melhor essa doença e como controlá-la.

Palavras-chave: fitotóxico; micotoxina; podridão vermelha do sisal.

Article

Calm before the Storm: A Glimpse into the Secondary Metabolism of *Aspergillus welwitschiae*, the Etiologic Agent of the Sisal Bole Rot

Gabriel Quintanilha-Peixoto ^{1,†}, Rosimére Oliveira Torres ^{2,†}, Isabella Mary Alves Reis ², Thiago Alves Santos de Oliveira ³, Dener Eduardo Bortolini ¹, Elizabeth Amélia Alves Duarte ⁴, Vasco Ariston de Carvalho Azevedo ¹, Bertram Brenig ⁵, Eric Roberto Guimarães Rocha Aguiar ^{1,6}, Ana Cristina Fermino Soares ⁴, Aristóteles Góes-Neto ^{1,*} and Alexandro Branco ²

¹ Instituto de Ciências Biológicas, Universidade Federal de Minas Gerais, 31270-901 Belo Horizonte, Minas Gerais, Brazil; gabrielnilha@gmail.com (G.Q.-P.); gigatonn@gmail.com (D.E.B.); vascoariston@gmail.com (V.A.d.C.A.); ericgdp@gmail.com (E.R.G.R.A.)

² Laboratório de Fitoquímica, Universidade Estadual de Feira de Santana, 44036-900 Feira de Santana, Bahia, Brazil; roseoliveiratorres@gmail.com (R.O.T.); isabella.alvesreis@gmail.com (I.M.A.R.); branco@uefs.br (A.B.)

³ Departamento de Ciências Biológicas, Universidade Estadual de Feira de Santana, 44036-900 Feira de Santana, Bahia, Brazil; dcbio@uefs.br

⁴ Centro de Ciências Agrárias, Ambientais e Biológicas, Universidade Federal do Recôncavo da Bahia, 44380-000 Cruz das Almas, Bahia, Brazil; elizabethaad@gmail.com (E.A.A.D.); ferminosoares@gmail.com (A.C.F.S.)

⁵ Institute of Veterinary Medicine, University of Göttingen, 37073 Göttingen, Germany; bbrenig@gwdg.de

⁶ Instituto de Ciências da Saúde, Universidade Federal da Bahia, 40231-300 Salvador, Bahia, Brazil

* Correspondence: arigoesneto@icb.ufmg.br

† G.Q.-P. and R.O.T. should be considered joint first author.

Received: 30 September 2019; Accepted: 28 October 2019; Published: 30 October 2019



Abstract: *Aspergillus welwitschiae* is a species of the Nigri section of the genus *Aspergillus*. In nature, it is usually a saprotroph, decomposing plant material. However, it causes the bole rot disease of *Agave sisalana* (sisal), a plant species used for the extraction of hard natural fibers, causing great economic loss to this culture. In this study, we isolated and sequenced one genome of *A. welwitschiae* (isolate CCMB 674 (Collection of Cultures of Microorganisms of Bahia)) from the stem tissues of sisal and performed in silico and wet lab experimental strategies to describe its ability to produce mycotoxins. CCMB 674 possesses 64 secondary metabolite gene clusters (SMGCs) and, under normal conditions, it produces secondary metabolism compounds that could disturb the cellular cycle of sisal or induce abnormalities in plant growth, such as malformin C. This isolate also produces a pigment that might explain the characteristic red color of the affected tissues. Additionally, this isolate is defective for the production of fumonisin B1, and, despite bearing the full cluster for the synthesis of this compound, it did not produce ochratoxin A. Altogether, these results provide new information on possible strategies used by the fungi during the sisal bole rot, helping to better understand this disease and how to control it.

Keywords: phytotoxic; mycotoxin; red rot of sisal

Key Contribution: Sixty-four secondary metabolites gene clusters (SMGCs) were predicted for isolate CCMB 674; and 65 for isolate CBS 139.54. Both isolates are genetically defective for fumonisin production and contain the full cluster for ochratoxin production. The malformin C cluster was described for both isolates, and this compound was detected in the HPLC-MS analysis, with other 10 compounds. Catenarin is hypothesized to be responsible for the red color of the bole rot.

1. Introduction

Aspergillus welwitschiae is a filamentous fungus, belonging to the Nigri section of the genus *Aspergillus* [1], and it is also the closest phylogenetic taxon of *Aspergillus niger* [2], a species used in diverse activities in the biotechnology industry. *A. welwitschiae* was first isolated from *Welwitschia mirabilis* in the Namib Desert, where it infects the plant's reproductive structures. In Brazil, *A. welwitschiae* is a serious threat to the sisal (*Agave sisalana*) cultivation in the Brazilian semi-arid region, causing bole rot (or red rot) disease [3], with an incidence of 35% [4]. According to Duarte et al. [3], in this pathosystem, *A. welwitschiae* invades the plant through wounds between the leaf basis and the stem. Leaf excision is a natural part of sisal cultivation, as this is the source of the natural fibers for which the plant is valued. As the disease progresses, the stem is degraded with a clear red margin, dividing dead tissue from the soon-to-be infected tissue. In the literature, phytopathogenic fungi are usually categorized into biotrophs, which depends on living tissue for feeding [5]; hemibiotrophs, which require living tissue, but kill the host plant at some stage [6]; and necrotrophs, which feed on dead plant tissue [7]. In both hosts, *A. sisalana* and *W. mirabilis*, *A. welwitschiae* initially feeds on dead tissue, but faces living tissues (and the host defenses) at some point during colonization. Fungal species commonly rely on secondary metabolites in order to facilitate invasion and colonization of plant tissues. Those compounds are produced as part of the fungal metabolism, but are generally not essential for their survival [8], which makes characterizing its functions very difficult [9]. Nonetheless, secondary metabolites represent an important evolutionary advantage for fungi because they might act either in silencing plant defense system [10] or over-activating it, such as, for instance, causing programmed cell death and making nutrients available for the fungus [11]. Therefore, assessing the fungal potential to produce secondary metabolites could provide important information in the understanding of plant–pathogen interactions and help the development of new strategies to avoid or manage the bole rot of sisal.

Our approach to studying the secondary metabolism of *A. welwitschiae* included (i) characterizing *in silico* secondary metabolite gene clusters (SMGCs) in the genomes of *Aspergillus welwitschiae* isolates CCMB 674 (isolated from the stem tissues of *Agave sisalana*) and CBS 139.54 (isolated from *W. mirabilis*), and (ii) identifying the secondary metabolites (specifically phenolic compounds) produced under normal conditions on isolate CCMB 674 through an HPLC-MS (High-Performance Liquid Chromatography coupled to a Mass Spectrometer) analysis.

2. Results

2.1. Secondary Metabolites Gene Clusters (SMGCs) Analysis

We sequenced and assembled the genome of *Aspergillus welwitschiae* isolate CCMB 674. The genome is 38.5 Mbp long, in which 64 secondary metabolite-associated genomic regions were found with antiSMASH v 5.0 [12] while 65 regions were identified for isolate CBS 139.54, which is 37.5 Mbp long. In order to describe the conservation and synteny of those regions between the two genomes, we verified their similarity with BLASTn v 2.5.0 [13], showing the results in a Fruchterman–Reingold layout network. As seen in Figure 1, our results show that even though CBS 139.54 possesses only one SMGC-predicted region more than CCMB 674, the latter contains two exclusive SMGCs (that is, did not show similarity with any other region of the other genome) in its genome (NODE_13_001 and NODE_15_001), while CBS 139.54 contains six exclusive SMGCs (scaffold_10_002, scaffold_49_001,

scaffold_80_001, scaffold_14_001, scaffold_27_001, and scaffold_41_001). Most of the other regions have only one large correspondent similar SMGC in the other genome, with some regions sharing short similarities with other regions.

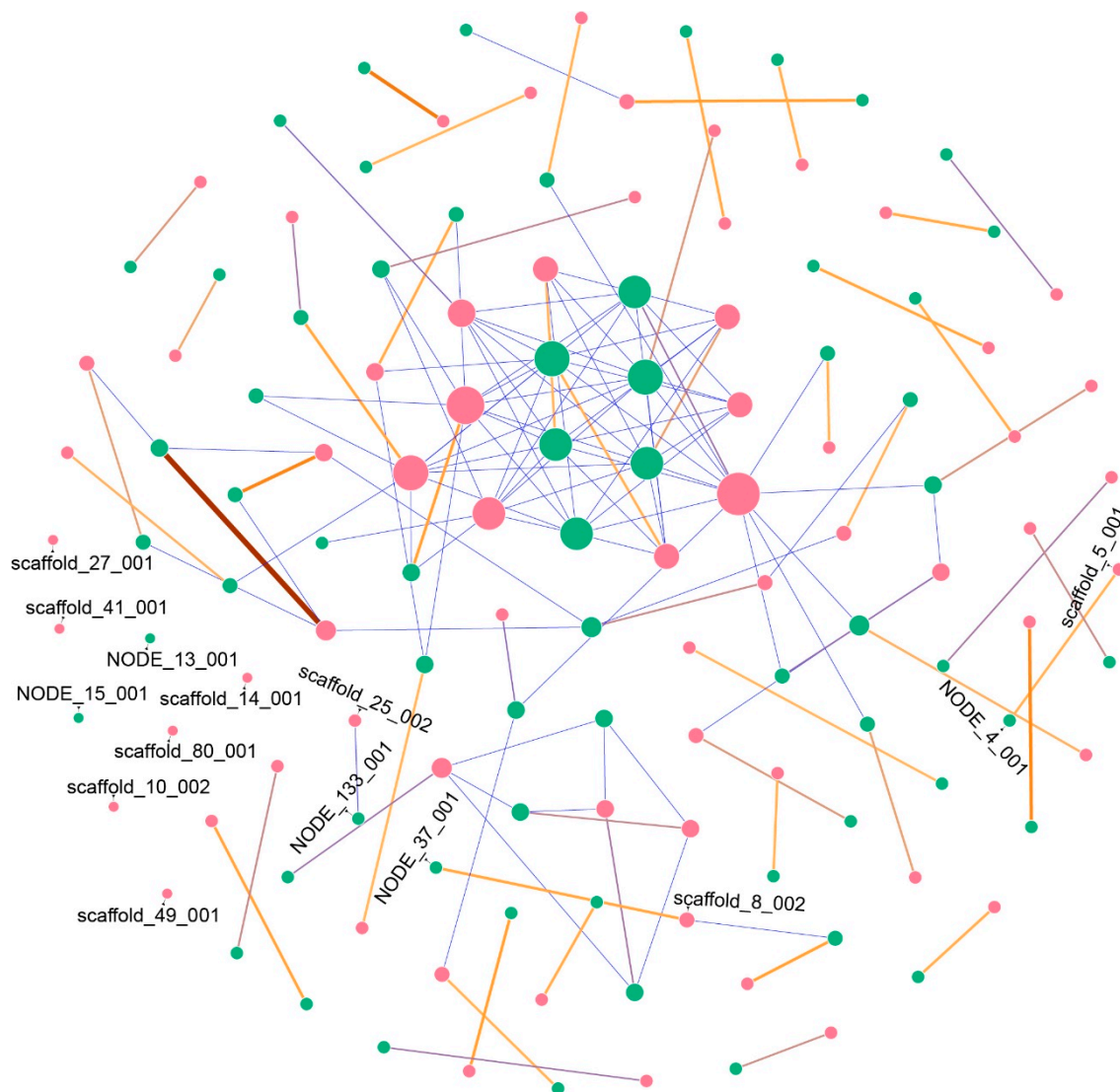


Figure 1. Fruchterman–Reingold layout network showing the similarity between CCMB 674 secondary metabolites predicted clusters (in green) and CBS 139.54 clusters (in pink) as nodes, and alignment scores as edges. Heat colors represent higher scores, while short alignments, presenting lower scores, are seen in blue. Regions with more hits are larger in node size. Exclusive regions (no hits) are labeled.

The antiSMASH web tool also categorizes predicted genes in SMGCs. Our results also show that biosynthetic protein composition is similar in the two genomes (Figure 2A), presenting type 1 polyketide synthases (T1PKS); non-ribosomal polyketide synthases (NRPS); NRPS-like proteins; terpenes; and, less frequently, indole and β -lactone associated proteins. Nonetheless, the similarity of those predicted proteins to previously known biosynthetic genes is divergent in the two isolates (Figure 2B) with some compounds predicted only in CCMB 674 or CBS 139.54, and vice-versa.

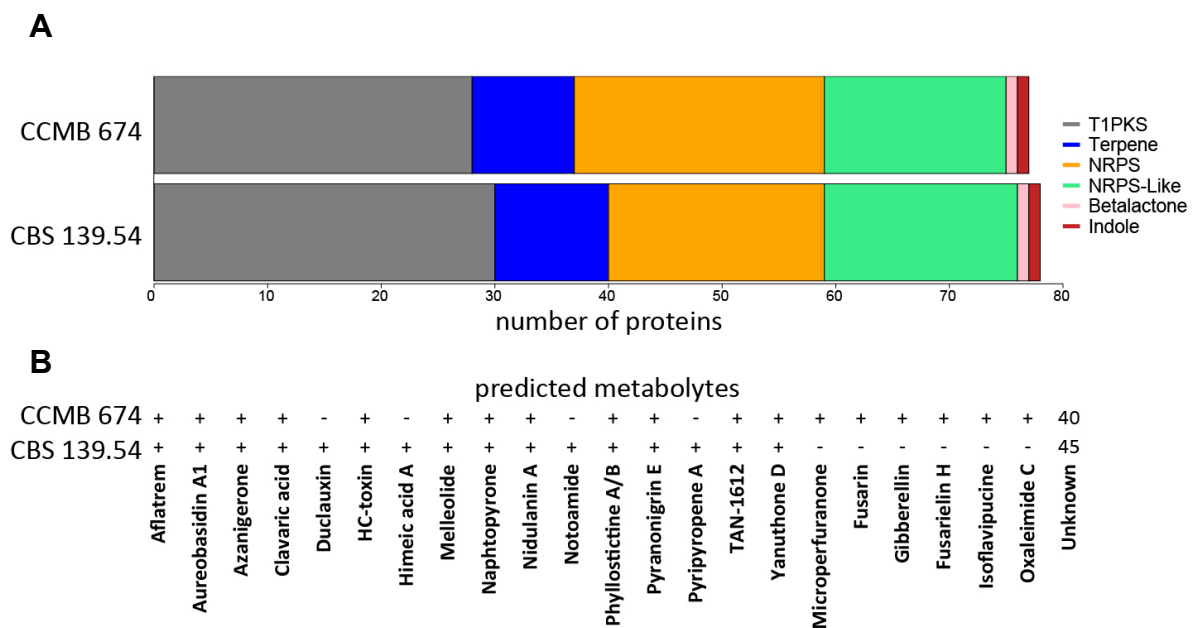


Figure 2. AntiSMASH results for *Aspergillus welwitschiae* CCMB 674 and *A. welwitschiae* CBS 139.54. (A) Stacked bar plot of biosynthetic protein distribution. Color scheme and quantities are detailed in the figure. (B) Presence–absence scheme of predicted compounds, and the number of clusters with no predicted products (unknown). T1PKS, presenting type 1 polyketide synthases; NRPS, non-ribosomal polyketide synthases.

2.2. Fungal Extract HPLC-MS Analysis and Compound Similarity

Associated with the sequencing, assembly, and functional annotation of SMGCs in the genome of isolate CCMB 674, we also investigated the production of secondary metabolites (especially phenolic compounds) produced by this fungus that might play a role in plant infection and colonization using a strategy similar to that described in Abu (2017) and Reis (2018) [14,15]. Briefly, we filtrated mycelia off the liquid culture, followed by a primary extraction in methanol. This extract was subjected to a solvent–solvent extraction using ethyl acetate. The methanol phase was discarded, and the ethyl acetate phase was concentrated using a rotary evaporator, with a final mass of 0.87 g. In the subsequent open chromatography column, 24 fractions were obtained (Table S1) and analyzed in HPLC coupled to a photodiode array, out of which 7 fractions were chosen as representative and combined into 4 fractions (FrA composed of fractions 2 and 4; FrB composed of fractions 6, 7, and 8; FrC composed of fraction 10; and FrD composed of fraction 13), which were later analyzed in HPLC coupled to a mass spectrometer. In this analysis, 11 peaks could be identified into compounds, as seen in Table 1, with ten of them being part of the secondary metabolism, and the other one being riboflavin, a common vitamin found in fungi related to aerobic respiration.

Table 1. Compounds per fraction identified in *Aspergillus welwitschiae* isolate CCMB 674 and their chemical properties. Columns represent retention time (RT), pseudo-molecular ion mass-to-charge ratio ($[M + H]^+$), sodium adducts mass-to-charge ratio ($[M+Na]^+$), liquid chromatography in positive mode mass-to-charge ratio (LC-MS m/z), and the identified molecule. * Identifies isomer compounds.

	Peak #	R _T (min)	[M + H] ⁺	[M+Na] ⁺	LC-MS m/z (Positive Mode)	Metabolite
Fraction A	1	28.5	287	309	[287]: 287;595	Catenarin
	2	29.6	571	-	[571]: 556	Aurasperone A
	3	33.3	530	-	[530]: 513;417;277;175	Malformin C
	4	34.9	377	-	[377]: 377;253;197;171	Riboflavin
	5	35.4	391	-	[391]: 253;197;159	Compactin
Fraction B	6	26.8	607	-	[607]: 589;574;531;505	Aurasperone B
	7	28.1	589	-	[589]:571;531	Aurasperone E
	8	29.9	571	-	[571]: 556;531;498	Nigerone
Fraction C	9	21.1	288	-	[288]: 246;575	Pyrophen
	10	30.9	349	-	[349]: 349;291;237	Clerocidin
	5	34.5	391	413	[391]: 279;149	Compactin *
Fraction D	9	21	288	310	[288]: 246;597	Pyrophen
	7	27.8	589	-	[589]: 531;505	Aurasperone E *
	3	29.6	571	593	[571]: 556	Aurasperone A
	11	30	533	555	[533]: 267;211	Roridin A

In order to prospect for similarities between the compounds predicted with antiSMASH and compounds detected in the HPLC-MS analysis, we used a cheminformatics approach based on the molecular fingerprints of those compounds (that is, binary data that encode the molecule's structure), available in public databases PubChem (<https://pubchem.ncbi.nlm.nih.gov/>) and ChEBI (<https://www.ebi.ac.uk/chebi/>). Data were analyzed with ChemmineR and ChemmineOB packages for R [16]. Figure 3 shows that there is no especially similar structure between predicted and detected compounds, except for the aurasperones (A, B, and E) and nigerone, both detected in the HPLC-MS analysis.

2.3. Fumonisin, Ochratoxin, and Malformin C Clusters' Characterization

In an effort to better describe the secondary metabolites' gene clusters for specific mycotoxins, known to be produced in the *Aspergillus welwitschiae/niger* clade, we obtained curated proteins and cluster sequences for the fumonisin, ochratoxin, and malformin C gene clusters, from selected references (Table S2), and compared those sequences with the genomes of isolates CCMB 674 and CBS 139.54. The sequence similarity results showed a similar profile of the presence of these secondary metabolites in both isolates, whose high synteny was confirmed by our network approach (Figure 1). Therefore, we generated a graphical visualization of those clusters that is representative of both genomes (Figure 4). Our results show that isolates CCMB 674 and CBS 139.54 are defective for the production of fumonisin (Figure 4A, NODE_4_001 and scaffold_5_001 in Figure 1), in a deletion pattern similar to previously described by Susca et al. in 2016 [17]. The ochratoxin cluster is complete, except for the protein OTA4, which has not been analyzed (Figure 4B, NODE_133_001 and scaffold_25_002 in Figure 1). However, this cluster, which has also been studied by Susca et al. [17], does not exhibit deletion patterns in which all proteins are present, but not *ota4*. We observed a similar profile for malformin C; the only protein known to be essential to the cluster is *mlfA*, as described by Theobald et al. [18]. In order to point out which of the antiSMASH predicted clusters corresponds to malformin C (Figure 4C), we used MLFA protein sequences from different species of *Aspergillus* (Table S2). Our results show that, in CCMB 674, the MLFA protein is in the contig NODE_37_001, while on CBS 139.54, the protein is in contig scaffold_8_002. This result is confirmed by our network, in which NODE_37_001 and scaffold_8_002 share a long region of similarity (Figure 1). Nevertheless, antiSMASH prediction did not correctly identify the compound in the case of region NODE_4_001, part of the *fum* cluster, predicted instead to

produce fusarin, as well as in the cases of NODE_133_001 and scaffold_25_002, which correspond to the *ota* cluster, but were annotated as melleolide by antiSMASH.

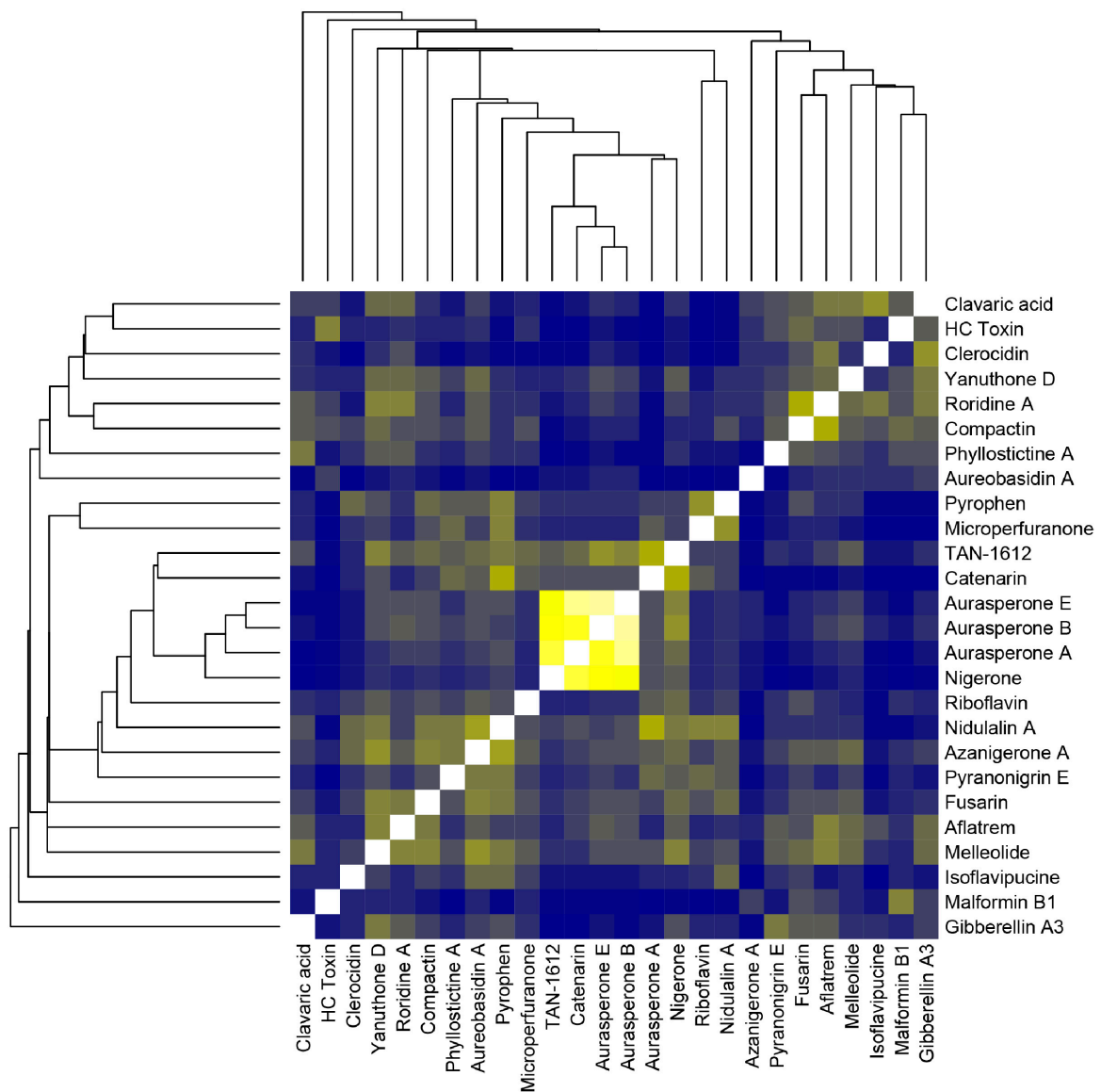


Figure 3. Structure comparison based on molecular fingerprints for predicted and detected compounds for isolate CCMB 674 with the Chemminer package. In the color matrix, blue indicates low similarity, yellow indicates medium to high similarity, and white indicates the structure’s similarity to itself. The attached dendrogram indicates the hierarchical clustering based on molecular fingerprints.

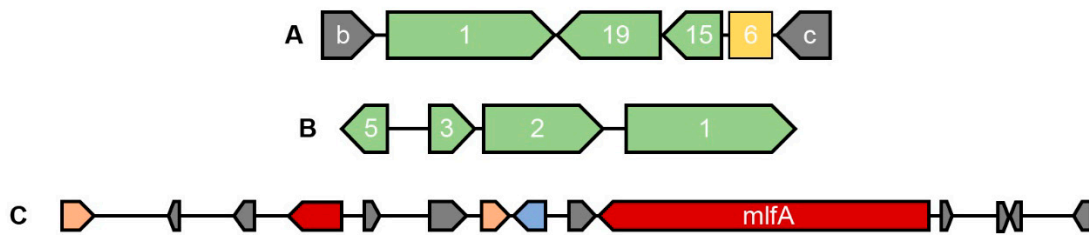


Figure 4. Representative genomic organization for CCMB 674 and CBS 139.54. (A) Fumonisin cluster. Flanking genes b and c in grey; viable genes *fum1*, *fum19*, and *fum15* in green; and truncated gene *fum6* in yellow. (B) Ochratoxin cluster including *ota1*, *ota2*, *ota3*, and *ota5*. (C) Malformin C gene cluster predicted by antiSMASH. Core biosynthetic genes, including *mlfA* in red, other biosynthetic genes in pink, transport-related genes in blue, and other genes (uncategorized) in grey.

3. Discussion

Aspergillus welwitschiae's strategies for infection in *Agave sisalana* resemble in many forms that of necrotrophic phytopathogenic fungi. It attacks damaged plants [19], possesses a broad host range [20], and contains a large arsenal of carbohydrate degrading enzymes [21]. However, necrotrophs also rely on the heavy production of toxins in order to induce cell death and make nutrients available for the fungus [22]. In this work, we used in silico and wet bench methods to describe compounds and genes associated with the secondary metabolism in *A. welwitschiae*, which could play a role in its colonization of *Agave sisalana* stem tissues [3]. As a first peek of this species potential, our general characterization of SMGCs is consistent with that described by Vesth et al. [21], who have analyzed different aspects of all species in the Nigri section of the genus *Aspergillus*, to which *A. welwitschiae* belongs. Nonetheless, Vesth et al. [21] could not find any compound associated with the clusters of *A. welwitschiae* CBS 139.54, which we used in our analysis for comparison purposes. That is very likely because the methods for SMGC prediction used by Vesth et al. [21] are slightly different, using the web application SMURF and complementation with antiSMASH, our single predictor. Nevertheless, even though we identified different compounds with this resource, compound prediction with antiSMASH relies on alignment-based similarity with known SMGCs. This might be the reason that none of the predicted compounds were detected in the HPLC-MS analysis. The “unknown” category of Figure 2B includes more than 40 clusters (>60%) in both isolates. As malformin C and roridine A are the only compounds seen in the HPLC-MS analysis that contain any genomic information, it is likely that compounds described in the HPLC-MS analysis fit as clusters with “unknown” compounds, which is corroborated by the color matrix in Figure 3, which shows no high similarity between any of the predicted and detected compounds, discarding the possibility of a detected compound being misidentified during prediction. In summary, the compounds described with antiSMASH and the ones detected with the HPLC-MS analysis are not directly related. Furthermore, the antiSMASH database could certainly be improved to include other compounds, such as malformin. Another reason is the context of the fungus. Owing to the cultivation conditions, in a nutrient-rich environment with no stresses found on the host plant, the fungus is unlikely to show its full potential for producing secondary metabolites. Our work is a first step towards a better understanding of the functioning of fungal metabolism, which is why we favor a nutrient-rich culture medium, as we believe this would yield secondary compounds produced under normal conditions. Similar strategies are described for the description of mycotoxins. Yassin et al. (2011 and 2012) and Soares et al. (2013) [23–25] describe the production of mycotoxins in fungal species associated with maize (including species of the genus *Aspergillus*) in a nutrient-rich medium, except for the quantification of aflatoxin, a very well-known compound, which requires a specific culture medium. This would not be adequate for our study because *A. welwitschiae* is not an aflatoxin producer. Discovery of new mycotoxins in the genus *Aspergillus* are also described with the use of nutrient-rich medium, as seen in Xu et al. [26]. While our bioinformatics assays fulfilled our first aim, our objective (ii) is solely related to the identification of secondary metabolites produced under

normal conditions, which were not directly related to the predicted compounds, according to Figure 3. The traditional HPLC-MS approach is suited for the detection of compounds mainly produced in large amounts and, in our study, non-stressful conditions. This is also one of the reasons that we decided to prospect for mycotoxins known to be produced in this species, such as malformin C, fumonisin B2, and ochratoxin A.

Malformin C has been previously detected in isolates of *Aspergillus niger* [27,28] and *A. tubingensis* [29,30], but not in *A. welwitschiae*. Genomics-wise, a single protein has been described as essential for the synthesis of this compound [18], which we used as a reference in our analysis. Thus, we were able to unite manually curated results with the predicted output of antiSMASH. The malformin C SMGC did not have any predicted compound in either one of the isolates (described as “unknown” in Figure 1), and our network corroborates with the results of the alignment with mlfA proteins, showing a strong similarity between the malformin C cluster in CCMB 674 (NODE_37_001) and CBS 139.54 (scaffold_8_002). Malformin C is known to have phytotoxic effects. Curtis was the first to isolate this class of metabolite [31] and also did an extensive study on its phytotoxic effects, showing malformations in plants (where the name originated), such as changes in curvatures in bean plants and corn roots [32], responses to abscission [33], and growth of onions [34].

The other two SMGCs we manually searched for in the genomes of isolate CCMB 674 and CBS 139.54 were fumonisin B1 (*fum*) and ochratoxin A (*ota*). Although neither one of these compounds were found in the HPLC-MS analysis, we are now able to add a further explanation on this result. The *fum* cluster is defective in both isolates, displaying a genomic organization very similar to that described by Susca et al. in 2014 [35] and 2016 [17]. Those works describe that there is a single cluster pattern for fumonisin producers in *Aspergillus niger* and *A. welwitschiae* (Type 1), while there are two patterns of deletion in non-producers (Type 2 and Type 3). Our isolate’s pattern is very similar to Type 2 of the *fum* cluster, in which *fum1*, *fum19*, *fum15*, *fum21*, and *fum6* proteins are present, in their complete or truncated form. However, in our results, *fum21* is not present in the *fum* cluster at all, with short similar regions located upstream of protein b, a flanking gene of the *fum* cluster. As for *ota*, the cluster seems to be complete, as described in the results (Figure 4B), suggesting that the regulation of this compound depends on factors other than gene viability, which corroborates the results from the literature, describing *A. welwitschiae* as a rare ochratoxin producer, if compared with *A. niger* [36–38].

Other compounds detected through our HPLC-MS analysis have little to no genomic information. In two cases, clusters are described in full, but for species very phylogenetically distant from the genus *Aspergillus*. For compactin, the full cluster has been described in *Penicillium citrinum* [39]. This compound belongs to the class of statins and was first isolated from cultures of *Penicillium brevicompactum*, determined by a combination of spectroscopic, chemical, and X-ray crystallography methods by Brown et al. in 1976 [40]. Abe [39] also mentions the inhibition effect of compactin over 3-hydroxy-3-methylglutaryl-coenzyme A (HMG-CoA) reductase. In plants, this protein is crucial for the synthesis of isoprenoids and steroids [41,42], without which cell metabolism is inviable. Thus, compactin is likely one of the mycotoxins used during plant infection by *A. welwitschiae* to kill host cells. Likewise, clerocidin, which has no genomic information in the literature, also affects the cell cycle to cause cell death. It has been described as attacking DNA gyrase in bacteria [43] and mammalian topoisomerase II [44]. Both proteins, however, are also present in plants, and their disturbance would cause DNA cleavage. Roridine A is considered the best-known toxin among the large and diversified group of macrocyclic trichothecenes, with known phytotoxic activity in different species [45]. Its structure was elucidated in 1965 in cellulose-degrading species *Myrothecium roridum* and *M. verrucaria* [46], and a full gene cluster for trichothecenes was described for *Fusarium sporotrichoides* and *Gibberella zeae* [47].

As for mycotoxins with no genetic information, catenarin is a very interesting compound in the context of the bole rot of sisal. This compound is a type of anthraquinone, with an orange to red color [48]. It has been described as a secondary metabolite produced by *Aspergillus glaucus* [49], which belongs to the same genus as our fungal model of study, as well as *Pyrenophora tritici-repentis*

and *Pyrenophora catenaria* [50]. This compound is mainly studied for its role in the tan spot of wheat, a foliar disease that affects this culture, even though antimicrobial activity has also been described [48]. In this pathosystem, the accumulation of catenarin in kernels and leaves of wheat, followed by PCD (programmed cell death) induced by necrotrophic fungus *P. tritici-repentis*, produces a red discoloration of the wheat infected tissues. Bouras and Strelkov have found catenarin production to be more abundant in a higher concentration of sugars and complex mediums. The stems of sisal are known to be rich in polysaccharides, a characteristic that gives economic value to related species *Agave tequilana*. Our research group also verified that the bole rot of sisal is restricted to this part of the plant, not spreading to leaves or other plant organs [3]. Wakulinski shows that, in melanin-deficient mutants of *P. tritici-repentis*, the absence of melanin is compensated with the accumulation of catenarin, giving the fungi a characteristic orange to red color, which is also seen in the bole rot. We hypothesize that a similar process occurs in *A. welwitschiae*, in which melanin production would be decreased during the infection of the plant (the fungus is dark-grey under normal conditions), and the following accumulation of catenarin would then create the dark red shade seen in the field. Other pigments were detected besides catenarin, such as Aurasperone A, B, and E, which are yellow pigments. These are common secondary metabolites of the genus *Aspergillus* [51]. These compounds belong to the group of naphtho- γ -pyrones [52]. Even though their presence is common in the genus, the biological function associated with this compound remains largely undescribed. Similarly to nigerone, which also belongs to the group of naphtho- γ -pyrones, as well as pyrophen, which belongs to another pyrone group [53], those secondary metabolites have been described in phytopathogenic fungi, but their role in disease progression is yet unknown [52].

The verification of the mentioned compounds in planta requires further study, in which the extraction and HPLC-MS methods are adapted for analysis of the plant tissue on infected and healthy plants. However, the results of the present work help to determine differences between fungal exposure to different environments, as well as to define toxins produced under normal conditions that could be necessary during plant–pathogen interaction. In addition, the findings of our work can help to uncover the whole repertoire of toxins produced by the fungus, as well as those that are essential to the pathogenesis.

4. Materials and Methods

4.1. Biological Samples and Computational Resources

Aspergillus welwitschiae isolate CCMB 674 (CCMB – Collection of Cultures of Microorganisms of Bahia) (Sequence Read Archive accession code SRR6793083) was isolated from *Agave sisalana* stem tissues presenting typical symptoms of bole rot in Conceição do Coité, State of Bahia, Brazil. This culture was kindly ceded by the Laboratory of Microbiology of the Universidade Federal do Recôncavo da Bahia. *Aspergillus welwitschiae* isolate CBS 139.54 was obtained from the Joint Genome Institution (Project ID 1060061). Bioinformatics analyses were carried out on the LGCM/Aquacen server and the Sarapalha server, both at the Universidade Federal de Minas Gerais, or at the application server, in the case of web tools.

4.2. Genome Sequencing and Assembly

The mycelium of isolate CCMB 674 was grown on potato dextrose agar medium (PDA; Sigma-Aldrich, St. Louis, MS, USA) and incubated at 25 °C for five days, after which it was scrapped for genomic DNA extraction, performed with FastDNA™ for Soil kit (MP Biomedicals, Santa Ana CA, USA). Genomic DNA quality and quantity were assessed by agarose gel electrophoresis and fluorometric analysis, respectively. A 450 bp library was prepared with NEBNext Fast DNA Fragmentation and Library Preparation Kit (New England Biolabs, Ipswich, NE, USA) following the instructions of the manufacturer. Library quality was evaluated with a 2100 Bioanalyzer (Agilent, Santa Clara, CA, USA), and whole-genome sequencing was performed on a HiSeq 2500 platform with

paired-end strategy and estimated fragment size of 450 bp (Illumina, San Diego, CA, USA). Raw reads were trimmed (Phred score >20) with BBDuk, and normalized with BBNorm, with both forms of software being components of the BBTools v.36.86 software kit [54]. Normalized reads were assembled with SPAdes v. 3.11.1, and assembly metrics were assessed using the Perl script *scaffold_stats.pl* (Table S3) and BUSCO v. 3.1. Contigs <1000 bp were removed, without an impact on ORF (open reading frame, coding) content (according to BUSCO results). Non-annotated scaffolds of *A. welwitschiae* CBS 139.54 were obtained from the Joint Genome Institute portal (JGI; <https://jgi.doe.gov/>).

4.3. Secondary Metabolites Gene Cluster Prediction and Network Construction

To describe all putative secondary metabolites gene clusters (SMGCs), we submitted both isolates CCMB 664 and CBS 139.54 to antiSMASH (<https://fungismash.secondarymetabolites.org/>). On the other hand, to describe specific mycotoxin clusters, we obtained curated sequences from GenBank and JGI and searched for similar sequences in our genomes with BLAST. Accession codes and references can be found in Table S2. SMGCs were obtained from antiSMASH and compared with BLASTn, with 1×10^{-5} E-value as a cutoff parameter. The resulting matrix was processed on Excel 2016 and with python script *soma_rede.py* plotted with Gephi v. 0.9.2, using the Fruchterman–Reingold layout and default parameters.

4.4. HPLC Analysis

Aspergillus welwitschiae CCMB 674 was cultured in potato-dextrose agar medium (PDA) containing chloramphenicol 50 mg/L and incubated at 25 °C for seven days. Five plugs (discs containing mycelium and agar) of approximately 0.5 cm in diameter were made out of the culture plates and transferred to 2 L Erlenmeyer flasks containing 1 L potato-dextrose medium and placed in an orbital shaker at 240 RPM and 25 °C for 28 days under a light shield, with experiments carried out in duplicate. Subsequently, the culture was vacuum filtered in a Büchner funnel, separating mycelia from the liquid. To extract phenolic compounds, the mycelia were macerated and 100 mL of methanol was added. Ethyl acetate was added to the methanol extract, creating a solvent–solvent partitioning process. The methanol phase was discarded, and the ethyl acetate phase was concentrated with a rotary evaporator. This extract was processed on HPLC coupled to a photodiode array producing 24 fractions, out of which 7 fractions were chosen as representative and combined into 4 fractions (FrA, FrB, FrC, and FrD; spectra can be found in Figure S1) that were later analyzed in HPLC coupled to a mass spectrometer.

4.5. Compound Chemical Structure Comparison

Chemical structures (SDF, structure-data file format) for predicted compounds (Figure 2B) and detected compounds (Table 1) of isolate CCMB 674 were obtained from PubChem (<https://pubchem.ncbi.nlm.nih.gov/>) and chEBI (<https://www.ebi.ac.uk/chebi/>). The structures for “naphtopyrone”, which is a large group of compounds; Fusarielin H; and Oxaleimide C were not available. The data were analyzed on the R programming language, with packages ChemmineR and ChemmineOB [16].

Supplementary Materials: The following are available online at <http://www.mdpi.com/2072-6651/11/11/631/s1>, Figure S1: Chromatograms for Fractions A–D, Table S1: Fractions were obtained (Table S1) and analyzed in HPLC coupled to a photodiode array. Yield value refers to initial 0.87 g, Table S2: References used for BLAST analysis, Table S3: Assembly metrics, generated with *scaffold_stats.pl*, for *Aspergillus welwitschiae* isolates CCMB674 and CBS 139.54, Script: *soma_rede.py*.

Author Contributions: Conceptualization, E.A.A.D., A.C.F.S., A.G.-N., and A.B.; Data curation, R.O.T.; Formal analysis, R.O.T., E.R.G.R.A., A.G.-N., and A.B.; Funding acquisition, A.C.F.S.; Investigation, R.O.T., E.R.G.R.A., A.G.-N., and A.B.; Methodology, G.Q.-P., R.O.T., E.R.G.R.A., and A.B.; Project administration, A.C.F.S.; Resources, V.A.d.C.A. and B.B.; Software, G.Q.-P., D.E.B., and E.R.G.R.A.; Supervision, A.G.-N. and A.B.; Validation, R.O.T., I.M.A.R., and T.A.S.d.O.; Writing—original draft, G.Q.-P., R.O.T., and A.B.; Writing—review & editing, G.Q.-P. and E.R.G.R.A.

Funding: This work was supported by the CNPq (Nexus Project: Integration Caatinga-Sisal n. 441625/2017-7), CAPES, FAPESB, and SECTI foundations. The funders had no role in study design, data collection and analysis,

decision to publish, or preparation of the manuscript. A.G.-N. receives a research grant for productivity from the National Council for Scientific and Technological Development (CNPq), Brazil (no. 310764/2016-5).

Acknowledgments: The authors would like to thank all the colleagues that contributed directly or indirectly to this work, as well as the Graduate Program in Biotechnology of the State University of Feira de Santana (UEFS); the Graduate Programs in Microbiology and in Bioinformatics of Federal University of Minas Gerais (UFMG); and the Center for Agricultural, Environmental, and Biological Sciences, Federal University of Recôncavo da Bahia (UFRB).

Conflicts of Interest: The authors declare that they have no financial or non-financial competing interests.

References

1. Varga, J.; Frisvad, J.C.; Kocsubé, S.; Brankovics, B.; Tóth, B.; Szigeti, G.; Samson, R.A. New and Revisited Species in *Aspergillus* Section *Nigri*. *Stud. Mycol.* **2011**, *69*, 1–17. [[CrossRef](#)] [[PubMed](#)]
2. Palumbo, J.D.; O’Keeffe, T.L. Detection and Discrimination of Four *Aspergillus* Section *Nigri* Species by PCR. *Lett. Appl. Microbiol.* **2015**, *60*, 188–195. [[CrossRef](#)] [[PubMed](#)]
3. Duarte, E.A.; Damasceno, C.L.; Oliveira, T.A.; Barbosa, L.D.; Martins, F.M.; Silva, J.R.; Lima, T.E.; Silva, R.M.; Kato, R.B.; Bortoline, D.E.; et al. Putting the Mess in Order: *Aspergillus Welwitschiae* (and Not *A. Niger*) Is the Etiologic Agent of the Sisal Bole Rot Disease. *Front. Microbiol.* **2018**, *9*, 1227. [[CrossRef](#)] [[PubMed](#)]
4. Abreu, K.C.L.D.M. Epidemiologia da Podridão Vermelha do Sisal No Estado da Bahia. Ph.D. Dissertation, Universidade Federal do Recôncavo da Bahia, Cruz das Almas, Brazil, 2010.
5. Selin, C.; de Kievit, T.R.; Belmonte, M.F.; Fernando, W.G.D. Elucidating the Role of Effectors in Plant-Fungal Interactions: Progress and Challenges. *Front. Microbiol.* **2016**, *7*, 600. [[CrossRef](#)]
6. Koeck, M.; Hardham, A.R.; Dodds, P.N. The Role of Effectors of Biotrophic and Hemibiotrophic Fungi in Infection. *Cell. Microbiol.* **2013**, *13*, 1849–1857. [[CrossRef](#)]
7. Horbach, R.; Navarro-Quesada, A.R.; Knogge, W.; Deising, H.B. When and How to Kill a Plant Cell: Infection Strategies of Plant Pathogenic Fungi. *J. Plant Physiol.* **2011**, *168*, 51–62. [[CrossRef](#)]
8. Bräse, S.; Encinas, A.; Keck, J.; Nising, C.F. Chemistry and Biology of Mycotoxins and Related Fungal Metabolites. *Chem. Rev.* **2009**, *109*, 3903–3990. [[CrossRef](#)]
9. Reverberi, M.; Ricelli, A.; Zjalic, S.; Fabbri, A.A.; Fanelli, C. Natural Functions of Mycotoxins and Control of Their Biosynthesis in Fungi. *Appl. Microbiol. Biotechnol.* **2010**, *87*, 899–911. [[CrossRef](#)]
10. Zvereva, A.S.; Pooggin, M.M. Silencing and Innate Immunity in Plant Defense against Viral and Non-Viral Pathogens. *Viruses* **2012**, *4*, 2578–2597. [[CrossRef](#)]
11. Expert, D.; Patrit, O.; Shevchik, V.E.; Perino, C.; Boucher, V.; Creze, C.; Wenes, E.; Fagard, M. Dickeya Dadantii Pectic Enzymes Necessary for Virulence Are Also Responsible for Activation of the Arabidopsis Thaliana Innate Immune System. *Mol. Plant Pathol.* **2018**, *19*, 313–327. [[CrossRef](#)]
12. Blin, K.; Shaw, S.; Steinke, K.; Villebro, R.; Ziemert, N.; Lee, S.Y.; Medema, M.H.; Weber, T. AntiSMASH 5.0: Updates to the Secondary Metabolite Genome Mining Pipeline. *Nucleic Acids Res.* **2019**, *47*, W81–W87. [[CrossRef](#)] [[PubMed](#)]
13. Camacho, C.; Coulouris, G.; Avagyan, V.; Ma, N.; Papadopoulos, J.; Bealer, K.; Madden, T.L. BLAST+: Architecture and Applications. *BMC Bioinform.* **2009**, *10*, 421. [[CrossRef](#)] [[PubMed](#)]
14. Abu, F.; Mat Taib, C.N.; Mohd Moklas, M.A.; Mohd Akhir, S. Antioxidant Properties of Crude Extract, Partition Extract, and Fermented Medium of *Dendrobium Sabin* Flower. *Evid. Based Complement. Altern. Med.* **2017**, *2017*. [[CrossRef](#)] [[PubMed](#)]
15. Reis, I.M.A.; Ribeiro, F.P.C.; Almeida, P.R.M.; Costa, L.C.B.; Kamida, H.M.; Uetanabaro, A.P.T.; Branco, A. Characterization of the Secondary Metabolites from Endophytic Fungi *Nodulisporium* Sp. Isolated from the Medicinal Plant *Mikania Laevigata* (Asteraceae) by Reversed-Phase High-Performance Liquid Chromatography Coupled with Mass Spectrometric Multistage. *Pharmacogn. Mag.* **2018**, *14*, S495–S498. [[CrossRef](#)]
16. Cao, Y.; Charisi, A.; Cheng, L.C.; Jiang, T.; Girke, T. ChemmineR: A Compound Mining Framework for R. *Bioinformatics* **2008**, *24*, 1733–1734. [[CrossRef](#)]
17. Susca, A.; Proctor, R.H.; Morelli, M.; Haidukowski, M.; Gallo, A.; Logrieco, A.F.; Moretti, A. Variation in Fumonisin and Ochratoxin Production Associated with Differences in Biosynthetic Gene Content in *Aspergillus Niger* and *A. Welwitschiae* Isolates from Multiple Crop and Geographic Origins. *Front. Microbiol.* **2016**, *7*. [[CrossRef](#)]

18. Theobald, S.; Vesth, T.C.; Rendsvig, J.K.; Nielsen, K.F.; Riley, R.; de Abreu, L.M.; Salamov, A.; Frisvad, J.C.; Larsen, T.O.; Andersen, M.R.; et al. Uncovering Secondary Metabolite Evolution and Biosynthesis Using Gene Cluster Networks and Genetic Dereplication. *Sci. Rep.* **2018**, *8*, 1–12. [[CrossRef](#)]
19. Struck, C.; Cooke, B.M.; Jones, D.G.; Kaye, B. Infection Strategies of Plant Parasitic Fungi. In *The Epidemiology of Plant Diseases*; Springer: Berlin, Germany, 2006; pp. 117–137. [[CrossRef](#)]
20. Brown, D.W.; Butchko, R.A.E.; Proctor, R.H. Identification of Genes and Gene Clusters Involved in Mycotoxin Synthesis. In *Determining Mycotoxins and Mycotoxigenic Fungi in Food and Feed*; Woodhead Publishing Limited: Cambridge, UK, 2011; pp. 332–348. [[CrossRef](#)]
21. Vesth, T.C.; Nybo, J.L.; Theobald, S.; Frisvad, J.C.; Larsen, T.O.; Nielsen, K.F.; Hoof, J.B.; Brandl, J.; Salamov, A.; Riley, R.; et al. Investigation of Inter- and Intraspecies Variation through Genome Sequencing of *Aspergillus* Section Nigri. *Nat. Genet.* **2018**, *50*, 1688–1695. [[CrossRef](#)]
22. Kavanagh, K. *Fungi—Biology and Applications*; Kavanagh, K., Ed.; John Wiley & Sons: County Kildare, Ireland, 2011.
23. Yassin, M.A.; Moslem, M.A.; El-Samawaty, A.E.-R.M.A. Mycotoxins and Non-Fungicidal Control of Corn Grain Rotting Fungi. *J. Plant Sci.* **2012**, *7*, 96–104. [[CrossRef](#)]
24. Yassin, M.A.; Moslem, M.; Bahkali, A.; Abd-elsalam, K. Fungal Biota and Occurrence of Aflatoxigenic *Aspergillus* in Postharvest Corn grains. *Fresenius Environ. Bull.* **2011**, *20*, 903–909.
25. Soares, C.; Calado, T.; Venâncio, A. Mycotoxin Production by *Aspergillus Niger* Aggregate Strains Isolated from Harvested Maize in Three Portuguese Regions. *Rev. Iberoam. Micol.* **2013**, *30*, 9–13. [[CrossRef](#)] [[PubMed](#)]
26. Xu, X.; He, F.; Zhang, X.; Bao, J.; Qi, S. New Mycotoxins from Marine-Derived Fungus *Aspergillus* Sp. SCSGAF0093. *Food Chem. Toxicol.* **2013**, *53*, 46–51. [[CrossRef](#)] [[PubMed](#)]
27. Kobbe, B.; Cushman, M.; Wogan, G.N.; Demain, A.L. Production and Antibacterial Activity of Malformin C, a Toxic Metabolite of *Aspergillus Niger*. *Appl. Environ. Microbiol.* **1977**, *33*, 996–997. [[PubMed](#)]
28. Blumenthal, C.Z. Production of Toxic Metabolites in *Aspergillus Niger*, *Aspergillus Oryzae*, and *Trichoderma Reesei*: Justification of Mycotoxin Testing in Food Grade Enzyme Preparations Derived from the Three Fungi. *Regul. Toxicol. Pharmacol.* **2004**, *39*, 214–228. [[CrossRef](#)] [[PubMed](#)]
29. Tan, Q.W.; Gao, F.L.; Wang, F.R.; Chen, Q.J. Anti-TMV Activity of Malformin A1, a Cyclic Penta-Peptide Produced by an Endophytic Fungus *Aspergillus Tubingensis* FJBJ11. *Int. J. Mol. Sci.* **2015**, *16*, 5750–5761. [[CrossRef](#)]
30. Wang, J.; Jiang, Z.; Lam, W.; Gullen, E.A.; Yu, Z.; Wei, Y.; Wang, L.; Zeiss, C.; Beck, A.; Cheng, E.C.; et al. Study of Malformin C, a Fungal Source Cyclic Pentapeptide, as an Anti-Cancer Drug. *PLoS ONE* **2015**, *10*, e0140069. [[CrossRef](#)]
31. Takahashi, N.; Curtis, R.W. Isolation and Characterization of Malformin. *Plant Physiol.* **1960**, 30–36. [[CrossRef](#)]
32. Curtis, R.W. Studies on Response of Bean Seedlings & Corn Roots to Malformin. *Plant Physiol.* **1961**, *36*, 37–43. [[CrossRef](#)]
33. Curtis, R.W. Phytochrome Involvement in the Induction of Resistance to Dark Abscission by Malformin. *Planta* **1978**, *141*, 311–314. [[CrossRef](#)]
34. Curtis, R.W.; Stevenson, W.R.; Tuite, J. Malformin in *Aspergillus Niger* Infected Onion Bulbs (*Allium cepa*). *J. Appl. Microbiol.* **1974**, *28*, 362–365.
35. Susca, A.; Proctor, R.H.; Butchko, R.A.E.; Haidukowski, M.; Stea, G.; Logrieco, A.; Moretti, A. Variation in the Fumonisin Biosynthetic Gene Cluster in Fumonisin-Producing and Nonproducing Black *Aspergilli*. *Fungal Genet. Biol.* **2014**, *73*, 39–52. [[CrossRef](#)] [[PubMed](#)]
36. Massi, F.P.; Sartori, D.; de Souza Ferranti, L.; Iamanaka, B.T.; Taniwaki, M.H.; Vieira, M.L.C.; Fungaro, M.H.P. Prospecting for the Incidence of Genes Involved in Ochratoxin and Fumonisin Biosynthesis in Brazilian Strains of *Aspergillus Niger* and *Aspergillus Welwitschiae*. *Int. J. Food Microbiol.* **2016**, *221*, 19–28. [[CrossRef](#)] [[PubMed](#)]
37. Gherbawy, Y.; Elhariry, H.; Kocsubé, S.; Bahobial, A.; El Deeb, B.; Altalhi, A.; Varga, J.; Vágvolgyi, C. Molecular Characterization of Black *Aspergillus* Species from Onion and Their Potential for Ochratoxin A and Fumonisin B2 Production. *Foodborne Pathog. Dis.* **2015**, *12*, 414–423. [[CrossRef](#)] [[PubMed](#)]
38. Varga, J.; Kocsubé, S.; Szigeti, G.; Baranyi, N.; Vágvolgyi, C.; Despot, D.J.; Magyar, D.; Meijer, M.; Samson, R.A.; Klarić, M.Š. Occurrence of Black *Aspergilli* in Indoor Environments of Six Countries. *Arh. Hig. Rada Toksikol.* **2014**, *65*, 219–223. [[CrossRef](#)] [[PubMed](#)]

39. Abe, Y.; Suzuki, T.; Ono, C.; Iwamoto, K.; Hosobuchi, M.; Yoshikawa, H. Molecular Cloning and Characterization of an ML-236B (Compactin) Biosynthetic Gene Cluster in *Penicillium Citrinum*. *Mol. Genet. Genom.* **2002**, *267*, 636–646. [[CrossRef](#)] [[PubMed](#)]
40. Brown, B.A.G.; Smale, T.C.; King, T.J.; Hasenkamp, R.; Thompson, R.H. Crystal and Molecular Structure of Compactin, a New Antifungal Metabolite from *Penicillium Brevicompactum*. *J. Chem. Soc. Perkin Trans. 1* **1976**, *11*, 1165–1170. [[CrossRef](#)]
41. Akhtar, N.; Gupta, P.; Sangwan, N.S.; Sangwan, R.S.; Trivedi, P.K. Cloning and Functional Characterization of 3-Hydroxy-3-Methylglutaryl Coenzyme A Reductase Gene from *Withania Somnifera*: An Important Medicinal Plant. *Protoplasma* **2013**, *250*, 613–622. [[CrossRef](#)]
42. Doblaz, V.G.; Amorim-Silva, V.; Posé, D.; Rosado, A.; Esteban, A.; Arró, M.; Azevedo, H.; Bombarely, A.; Borsani, O.; Valpuesta, V.; et al. The SUD1 Gene Encodes a Putative E3 Ubiquitin Ligase and Is a Positive Regulator of 3-Hydroxy-3-Methylglutaryl Coenzyme a Reductase Activity in *Arabidopsis*. *Plant Cell* **2013**, *25*, 728–743. [[CrossRef](#)]
43. McCullough, J.E.; O'sullivan, J.; Summerill, R.S.; Parker, W.L.; Wells, J.S.; Bonner, D.P.; Fernandes, P.B.; Muller, M.T.; Howells, A.J.; Maxwell, A. Clerocidin, A Terpenoid Antibiotic, Inhibits Bacterial Dna Gyrase. *J. Antibiot.* **1993**, *46*, 526–530. [[CrossRef](#)]
44. Gatto, B. The Topoisomerase II Poison Clerocidin Alkylates Non-Paired Guanines of DNA: Implications for Irreversible Stimulation of DNA Cleavage. *Nucleic Acids Res.* **2001**, *29*, 4224–4230. [[CrossRef](#)]
45. Vey, A.; Hoagland, R.E.; Tariq, M.B. Toxic Metabolites of Fungal Biocontrol Agents. *Fungal Divers.* **2001**, *311–346*. [[CrossRef](#)]
46. Burkin, A.A.; Kononenko, G.P. Mycotoxin Contamination of Meadow Grasses in European Russia. *Agric. Biol.* **2015**, *50*, 503–512. [[CrossRef](#)]
47. Brown, D.W.; McCormick, S.P.; Alexander, N.J.; Proctor, R.H.; Desjardins, A.E. A Genetic and Biochemical Approach to Study Trichothecene Diversity in *Fusarium Sporotrichioides* and *Fusarium Graminearum*. *Fungal Genet. Biol.* **2001**, *32*, 121–133. [[CrossRef](#)] [[PubMed](#)]
48. Wakuliński, W.; Kachlicki, P.; Sobiczewski, P.; Schollenberger, M.; Zamorski, C.; Łotocka, B.; Šarova, J. Catenarin Production by Isolates of *Pyrenophora Tritici-Repentis* (Died.) Drechsler and Its Antimicrobial Activity. *J. Phytopathol.* **2003**, *151*, 74–79. [[CrossRef](#)]
49. Anke, H.; Kolthoum, I.; Zähler, H.; Laatsch, H. Metabolic Products of Microorganisms. 185. The Anthraquinones of the *Aspergillus Glaucus* Group. I. Occurrence, Isolation, Identification and Antimicrobial Activity. *Arch. Microbiol.* **1980**, *126*, 223–230. [[CrossRef](#)]
50. Bouras, N.; Strelkov, S.E. The Anthraquinone Catenarin Is Phytotoxic and Produced in Leaves and Kernels of Wheat Infected by *Pyrenophora Tritici-Repentis*. *Physiol. Mol. Plant Pathol.* **2008**, *72*, 87–95. [[CrossRef](#)]
51. Lu, S.; Tian, J.; Sun, W.; Meng, J.; Wang, X.; Fu, X.; Wang, A.; Lai, D.; Liu, Y.; Zhou, L. Bis-Naphtho- γ -Pyrone from Fungi and Their Bioactivities. *Molecules* **2014**, *19*, 7169–7188. [[CrossRef](#)]
52. Nielsen, K.F.; Mogensen, J.M.; Johansen, M.; Larsen, T.O.; Frisvad, J.C. Review of Secondary Metabolites and Mycotoxins from the *Aspergillus Niger* Group. *Anal. Bioanal. Chem.* **2009**, *395*, 1225–1242. [[CrossRef](#)]
53. Reber, K.P.; Burdge, H.E. Total Synthesis of Pyrophen and Campyrones A-C. *J. Nat. Prod.* **2018**, *81*, 292–297. [[CrossRef](#)]
54. Bushnell, B. *BBTools: A Suite of Fast, Multithreaded Bioinformatics Tools Designed for Analysis of DNA and RNA Sequence Data*; Joint Genome Institute: Walnut Creek, CA, USA, 2018. Available online: <https://jgi.doe.gov/data-and-tools/bbtools> (accessed on 20 September 2019).



Supplementary Material: Calm Before the Storm: A Glimpse into the Secondary Metabolism of *Aspergillus welwitschiae*, the Etiologic Agent of the Sisal Bole Rot

Gabriel Quintanilha-Peixoto, Rosimére Oliveira Torres, Isabella Mary Alves Reis, Thiago Alves Santos de Oliveira, Dener Eduardo Bortolini, Elizabeth Amélia Alves Duarte, Vasco Ariston de Carvalho Azevedo, Bertram Brenig, Eric Roberto Guimarães Rocha Aguiar, Ana Cristina Fermino Soares, Aristóteles Góes-Neto and Alessandro Branco

Table S1. Fractions were obtained (Table S1) and analyzed in HPLC coupled to a photodiode array. Yield value refers to initial 0.87 g.

Fraction	Solvent System (%)	Mass (g)	Yield (%)
Fr-1	Hexane (100)	0,0139	1,61%
Fr-2	Hexane (100)	0,0273	3,15%
Fr-3	Hexane: Ethyl acetate (80:20)	0,0998	11,52%
Fr-4	Hexane: Ethyl acetate (70:30)	0,0374	4,32%
Fr-5	Hexane: Ethyl acetate (60:40)	0,0175	2,02%
Fr-6	Hexane: Ethyl acetate (50:50)	0,0155	1,79%
Fr-7	Hexane: Ethyl acetate (50:50)	0,0234	2,70%
Fr-8	Hexane: Ethyl acetate (50:50)	0,0134	1,55%
Fr9-10	Hexane: Ethyl acetate (40:60)	0,0101	1,17%
Fr-11	Hexane: Ethyl acetate (30:70)	0,0089	1,03%
Fr-12	Hexane: Ethyl acetate (10:90)	0,0133	1,54%
Fr-13	Ethyl acetate (100)	0,0170	1,96%
Fr-14	Ethyl acetate: Methanol (80:20)	0,0204	2,36%
Fr15-16	Ethyl acetate: Methanol (70:30)	0,0197	2,27%
Fr-17	Ethyl acetate: Methanol (50:50)	0,0123	1,42%
Fr18-19	Ethyl acetate: Methanol (30:70)	0,0489	5,65%
Fr-20	Ethyl acetate: Methanol (20:80)	0,0080	0,92%
Fr-21	Methanol (100)	0,0055	0,64%
Fr-22	Methanol: H ₂ O (50:50)	0,0042	0,48%
Fr-23	Methanol: H ₂ O (50:50)	0,0041	0,47%
Fr-24	H ₂ O (100)	0,0076	0,88%

Table S2. References used for BLAST analysis.

Compound	Gene	Situation	Organism	Accession	Reference	Seq
Compactin	mlcH, mlcG, mlcF, mlcA, mlcC, mlcB, mlcD, mlcE, mlcR	Full Cluster	<i>Penicillium citrinum</i>	AB072893.1	10.1007/s00438-002-0697- y	NT
Malformin C	mlfA	CDS	<i>Aspergillus vadensis</i> CBS 113365	A0A319BQC1.1	10.1038/s41598-018- 36561-3	NT
			<i>Aspergillus niger</i> CBS 115656	A0A318Z3U0.1	10.1038/s41598-018- 36561-3	NT
			<i>Aspergillus niger</i> CBS 513.88	A2QYX4.1	10.1038/s41598-018- 36561-3	NT
			<i>Aspergillus niger</i> ATCC 1015	G3XUF0.1	10.1038/s41598-018- 36561-3	NT
			<i>Aspergillus luchuensis</i> CBS 106.47	A0A1M3T4K3.1	10.1038/s41598-018- 36561-3	NT
			<i>Aspergillus lacticoffeatus</i> CBS 101883	A0A319A6V2.1	10.1038/s41598-018- 36561-3	NT
			<i>Aspergillus kawachii</i> IFO 4308	G7XQ31.1	10.1038/s41598-018- 36561-3	NT
			<i>Aspergillus homomorphus</i> CBS 101889	A0A395I3F8.1	10.1038/s41598-018- 36561-3	NT
Trichothecene	TRI8, TRI7, TRI3, TRI4, TRI6, TRI5, TRI10, TRI9, TRI11, TRI12, TRI13, TRI14,	Full Cluster	<i>Fusarium sporotrichioides</i>	AF359360.3	10.1006/fgbi.2001.1256	NT
	TRI8, TRI7, TRI3, TRI4, TRI6, TRI5, TRI10, TRI9, TRI11, TRI12, TRI13, TRI14,		<i>Gibberella zeae</i> GZ3639	AF359361.3	10.1006/fgbi.2001.1256	NT
	TRI13	CDS	<i>Gibberella zeae</i> HKM136	AY057841.1	10.1006/fgbi.2001.1256	NT
Ochratoxin	ota1-5	Full Cluster	<i>Aspergillus welwitschiae</i> ITEM 7468	KX267735	10.3389/fmicb.2016.01412	NT
			<i>Aspergillus welwitschiae</i> ITEM 11945	KX267737	10.3389/fmicb.2016.01412	NT
			<i>Aspergillus niger</i> ITEM 10355	KX267736	10.3389/fmicb.2016.01412	NT
	ota1	CDS	<i>Aspergillus niger</i> CBS 513.88	ANI_1_1826134	10.3389/fmicb.2016.01412	AA

	ota2	CDS	<i>Aspergillus niger</i> CBS 513.88	An15g07890	10.3389/fmicb.2016.01412	AA
	ota3	CDS	<i>Aspergillus niger</i> CBS 513.88	ANI_1_1830134	10.3389/fmicb.2016.01412	AA
	ota4	CDS	<i>Aspergillus niger</i> CBS 513.88	ANI_1_1832134	10.3389/fmicb.2016.01412	AA
	ota5	CDS	<i>Aspergillus niger</i> CBS 513.88	ANI_1_1836134	10.3389/fmicb.2016.01412	AA
Fumonisin	fum6	CDS	<i>Aspergillus niger</i> CBS 513.88	ANI_1_2654014	10.3389/fmicb.2016.01412	AA
	fum10	CDS	<i>Aspergillus niger</i> CBS 513.88	ANI_1_2658014	10.3389/fmicb.2016.01412	AA
	fum7	CDS	<i>Aspergillus niger</i> CBS 513.88	ANI_1_2660014	10.3389/fmicb.2016.01412	AA
	fum3	CDS	<i>Aspergillus niger</i> CBS 513.88	ANI_1_892014	10.3389/fmicb.2016.01412	AA
	fum8	CDS	<i>Aspergillus niger</i> CBS 513.88	ANI_1_894014	10.3389/fmicb.2016.01412	AA
	fum13	CDS	<i>Aspergillus niger</i> CBS 513.88	ANI_1_2662014	10.3389/fmicb.2016.01412	AA
	fum14	CDS	<i>Aspergillus niger</i> CBS 513.88	ANI_1_2664014	10.3389/fmicb.2016.01412	AA
	fum15	CDS	<i>Aspergillus niger</i> CBS 513.88	ANI_1_2668014	10.3389/fmicb.2016.01412	AA
	fum1	CDS	<i>Aspergillus niger</i> CBS 513.88	ANI_1_2672014	10.3389/fmicb.2016.01412	AA
	fum19	CDS	<i>Aspergillus niger</i> CBS 513.88	205909	10.3389/fmicb.2016.01412	AA
	fum21	CDS	<i>Aspergillus niger</i> CBS 513.88	225717	10.3389/fmicb.2016.01412	AA
	sdr1	CDS	<i>Aspergillus niger</i> CBS 513.88	51907	10.3389/fmicb.2016.01412	AA
	gene B	CDS	<i>Aspergillus niger</i> CBS 513.88	35994	10.3389/fmicb.2016.01412	AA
	gene C	CDS	<i>Aspergillus niger</i> CBS 513.88	171442	10.3389/fmicb.2016.01412	AA
gene D	CDS	<i>Aspergillus niger</i> CBS 513.88	171846	10.3389/fmicb.2016.01412	AA	

Table S3. Assembly metrics, generated with scaffold_stats.pl, for *Aspergillus welwitschiae* isolates CCMB674 and CBS 139.54.

FileNames	CCMB 674	CBS 139.54
Longest Scaffold	2008406	2162797
Num	244	396
Span	38188994	37511876
Min	1046	1010
Mean	156512	94726
N50	456288	757052
NumN50	23	17
GC	0.483	0.497
For Runs of Ns (≥ 10 Ns):		
Num	9	118
Span	436	33835
N50	96	1190

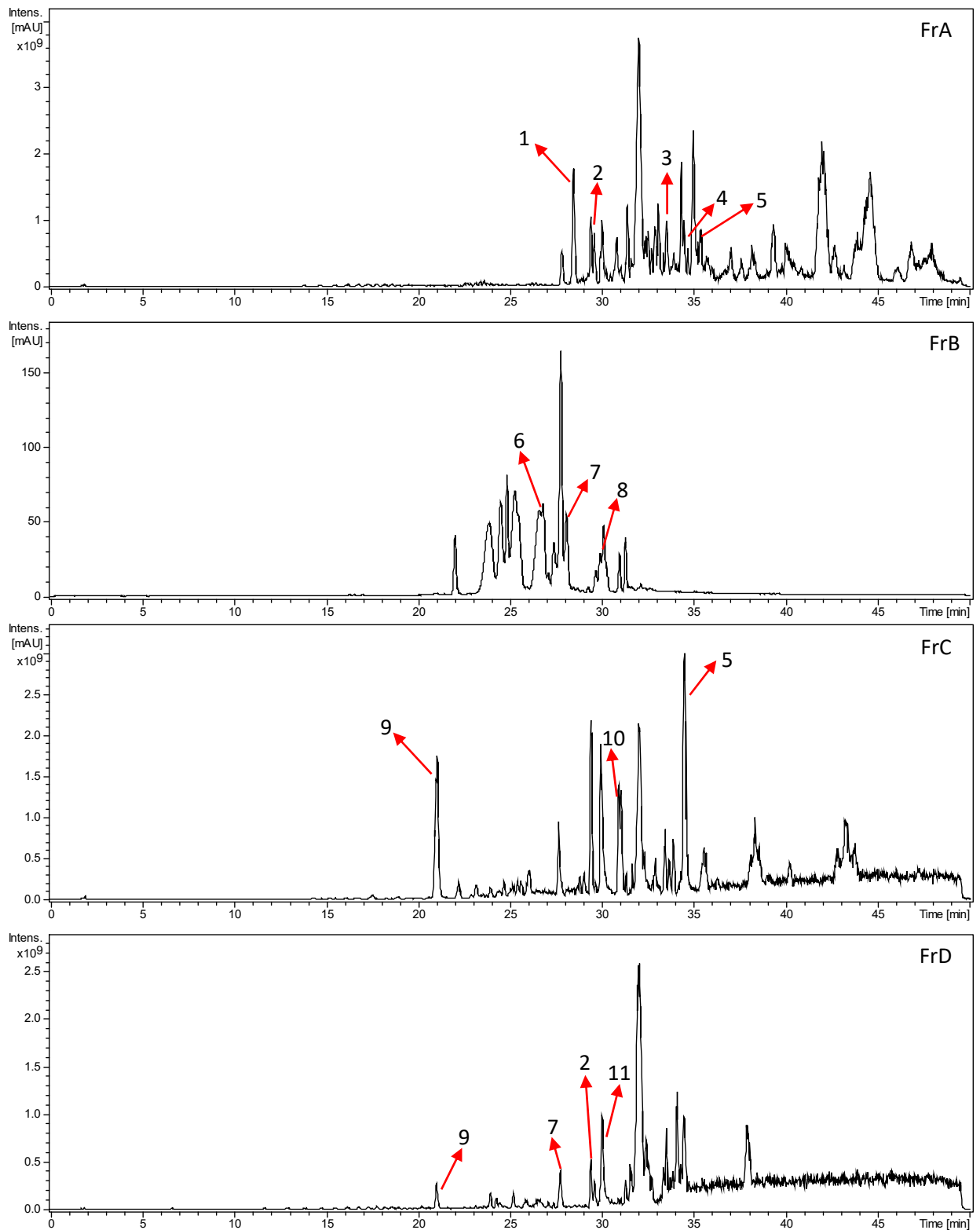


Figure S1. Chromatograms for Fractions A-D.

Mass Spectrometer: Amazon Speed ETD - Bruker

Nebulizer: 27 Psi

HV: 4500V

Dry gas: 12 L/min

ESI+

Temp: 300 °C

HPLC:

Controler: CBM-20A- Shimadzu

Solvent B: Methanol

Pump: LC-20AD Shimadzu

Column: Phenomenex Luna C18 (250x4.6mm
– 5um)

Detector: SPD-20A - Shimadzu

Oven Temp: environment

Oven: CTO-20A - Shimadzu

Flux: 1 ml/min

Autosampler: SIL 20AC – Shimadzu

Solvent A: H2O 0,1% Acetic Acid

Gradient: 0 min A:B (100:0) 30 min A:B (0:100) 46 min A:B (0:100) 47 min A:B (80:20) 50 min A:B (80:20)

Soma_rede.py

```
# -*- Coding: UTF-8 -*-
```

```
#coding: utf-8
```

```
import sys
```

```
if (len(sys.argv)!=2):
```

```
    print ("Please enter file name (Ex: python somaRede.py rede.txt)")
```

```
    sys.exit()
```

```
nomeArquivo=sys.argv[1]
```

```
# nomeArquivo="rede.txt"
```

```
arquivoRede=open(nomeArquivo, 'r')
```

```
resultado=[]
```

```
for linha in arquivoRede:
```

```
    index=linha.rfind(";")
```

```
    nome=linha[0:index]
```

```
    achou=0
```

```
    for item in resultado:
```

```
        if (item[0].find(nome)!=-1):
```

```
            item[1]=item[1]+float(linha[index+1:].rstrip())
```

```
            achou=1
```

```
            break
```

```
    if (achou==0):
```

```
        aux=[nome, float(linha[index+1:])]
```

```
        resultado.append(aux)
```

```
arqSaida=open(nomeArquivo[0:nomeArquivo.find(".")]+"_rst.txt", 'w')
```

```
for item in resultado:
```

```
    arqSaida.write(item[0]+";"+str(item[1])+"\n")
```

```
    print(item[0]+";"+str(item[1]))
```

```
arqSaida.close()
```

```
arquivoRede.close()
```

Chapter VI – CONCLUSIONS AND PERSPECTIVES

Over the three research publications and the patent discussed in the previous chapters, we have brought to light more information about the bole rot disease of sisal through the perspective of its main pathogen, *Aspergillus welwitschiae*, as well as a collection of cryptical viral species associated with sisal either directly or through its associated microbiota. Over the next paragraphs, we will bind those publications under the context of disease susceptibility in sisal and the larger context of opportunistic fungal pathogens in plants. We also bring the context of field observations that do not always fit the scope of scientific publications but might shape the next steps in sisal research.

Chapter II, our 2021 publication on the virome (QUINTANILHA-PEIXOTO et al., 2021), described 25 viral species associated with three varieties of sisal: *Agave sisalana*, *Agave* Hybrid 11648, and *Agave fourcroydes* (aka henequén). To the best of our knowledge, this was the first unbiased virome study in the genus *Agave*, the first virology study in henequén and *Agave* Hybrid 11648, as well as the first virology study in *A. sisalana* since 1995 (IZAGUIRRE-MAYORAL et al., 1995), when high-throughput sequencing was not yet available. This article makes little reference to the bole rot in its discussion, which is a gap we are now more able to fill, considering the broader prospect of the publications in this thesis. In that publication, we have found that henequén (*Agave fourcroydes*) roots harbor the greatest diversity of cryptical viral species of all tested samples (containing 18 out of the 25 species described in this publication), likely through the association of the plant host with fungi, since various viral species share similarity with mycoviruses and a high proportion of fungal transcripts was described latter with the same dataset (MARONE et al., 2022). The work by Marone et al. also reinforces our hypothesis that *A. welwitschiae* might be part of the regular microbiota of sisal-like species, causing disease in stressed or weakened plants. From field observations, we also know that the bole rot disease (or at least similar symptoms) is highly incident in mature sisal plants, during the blooming stage. That might also be connected with the florigen-like effector included in our 2022 publication (QUINTANILHA-PEIXOTO et al., 2022).

The tissues of *A. sisalana*, the main fiber-producing variety in Brazil, have a higher dominance of a single viral species (*Sisal-associated Closterovirus A*) throughout its roots, stem, and leaves (Figure 5E). Although no scientific article has ever been published on the disease incidence across the different sisal varieties, our research group knows from field works that henequén and the Hybrid 11648 are more resistant to the bole rot of sisal. Even though

henequén is a relevant crop in the Yucatán peninsula (which is also where *A. sisalana* originates) for fiber and mezcal production (GONZÁLEZ-ITURBE; OLMSTED; TUN-DZUL, 2002), the scientific literature on crop disease is very scarce for this species, which also reaffirms our publication as a breakthrough for sisal and henequén research. A single publication (QUIJANO RAMAYO et al., 2002) references research describing fungal pathogens in this crop during the late 1980s, not mentioning the bole rot, but a *pole* dry rot caused by *Cercospora*. It is not clear if this disease is equivalent or the same thing as bole rot, especially considering the techniques for fungal identification used at the time of this study. Henequén and Hybrid 11648 are less used for fiber extraction in Brazil due to higher lignification that damages the machinery in the fields (especially for henequén), which RAYA et al. (RAYA et al., 2021) believe to be a relevant factor for disease resistance. During field works we have also learned that some farmers are exchanging the cultivation of the traditional *A. sisalana* for the cultivation of Hybrid 11648, which is more resistant to the disease and not as “hard” (lignified) as *A. fourcroydes*.

On the other hand, it is also known from the literature that beneficial microbial species might help plant hosts fight diseases by antagonizing pathogenic microbes and by producing antimicrobial molecules (HASHIM et al., 2016; SINGH; SINGH; SINGH, 2018; YAN et al., 2019). Since our publication, other research has described plant viromes reflecting the plant host and associated microbial diversity (REDILA; PRAKASH; NOURI, 2021), and how that might be used as a tool when breeding for disease resistance (ALCALÁ BRISEÑO et al., 2023). It could be interesting to understand if bole rot susceptibility is also linked with the microbial composition of sisal plants, which could be achieved through a metagenomics study, especially considering the rise of Hybrid 11648 as a resistant alternative to *A. sisalana*. Our research group has taken steps toward understanding the plant gene expression in healthy *versus* affected individuals, which could give us a glimpse into microbial diversity and disease susceptibility associated with those plants. This was proven especially difficult, considering the lignification of the stem tissue in *A. sisalana* plants, which yields low RNA content as a consequence. Our experimental design includes 6 affected and 5 healthy plants, sequenced in triplicates. The early results were not included in this document precisely because of the low yield and specificity obtained; further analysis is required to understand if this is a reliable dataset for further transcriptome studies (CONESA et al., 2016). Nonetheless, because this is the current dataset at hand, it is the most concrete foreseeable perspective for our research group’s studies on the bole rot of sisal.

In Chapter IV we were able to produce a method for detecting the pathogen in plant tissues without the need to kill the plant, based on the PCR amplification of a marker gene, a Δ^1 -pyrroline-5-carboxylate reductase (PC5R). We understand that this method could be particularly useful for companies like Embrapa, which distributes sisal bulbils to farmers. By applying our method, such companies could make sure not to spread pathogen-infected bulbils, and keep a simple control when breeding for bole rot resistance. Although our technology has solid results seen throughout the patent, it has an important limitation; *A. niger* strain CCT 4026, which we used as a negative control for the P5CR, lacks molecular identification through markers like ITS or Calmodulin (CaM). Nonetheless, further testing performed by Dr. Fábio Raya has confirmed and expanded those results by using another certified strain of *A. niger* and various other certified *Aspergillus* species (the manuscript is currently under review at *Frontiers in Chemical Engineering*).

In the 2019 and 2022 publications on the fungal pathogen's genomics, we brought relevant information on the strategies that *A. welwitschiae* disposes to infect and colonize sisal plants. Chapter V corresponds to an effort to integrate wet bench and *in silico* approaches to the study of mycotoxins and other secondary metabolites (QUINTANILHA-PEIXOTO et al., 2019). In this research, the extraction of aromatic compounds was carried out only in strain CCMB 674, obtaining 13 different compounds. An *in silico* analysis aiming to describe the Secondary Metabolites Gene Clusters in this isolate obtained 64 clusters. Even though our focus has been the interaction of *A. welwitschiae* and sisal since the beginning of this research, this publication is particularly relevant considering the role of *A. welwitschiae* as an opportunistic human pathogen (TAKEDA et al., 2020); we studied the fungal ability to produce fumonisins and ochratoxins, which affect both plant hosts and animals feeding off contaminated produce (PFLIEGLER et al., 2020). Our results show that sisal strains are not capable of producing fumonisins, and even though a full cluster for the detection of ochratoxin was found, this compound was not detected in the wet bench analysis. The detected profile of secondary metabolites is expected to change under plant-pathogen interactions since mycotoxins are known to be activated under stress conditions (REVERBERI et al., 2010). Thus, a special experimental design would be required for further affirmations regarding mycotoxins production in the bole rot of sisal. In this research, we also discuss the gap between the chromatography detection of the secondary metabolites and the molecular knowledge about their production at the molecular level. That became an obstacle to our discussion and one of

the reasons why we devised a broader discussion of SMGCs in *Aspergillus* in our phylogenomics publication (QUINTANILHA-PEIXOTO et al., 2022).

The 2022 publication included in Chapter III describes the evolutionary relationships of *A. welwitschiae* with the other species in the genus *Aspergillus* and some evolutionary traits in protein-coding genes in the three strains available at that time (a new genome for strain BCSIR_imrd1 was made available in 2023), summing up to 40 *Aspergillus* genomes. The most impactful discovery in that publication is certainly the polyphyly of *A. welwitschiae*; while strain CBS 139.54 (from *Welwitschia mirabilis*) forms a monophyletic clade with strain CCMB 663 (isolated from *A. sisalana*), strain CCMB 674 (from *A. sisalana*) appears in a separate clade from both *A. welwitschiae* and *A. niger*, indicating that this could be a new species. Indeed, in the 2018 publication by Duarte et al. (DUARTE et al., 2018), which confirms *A. welwitschiae* as the causative agent of bole rot, strain CCMB 674 appears in a separate clade in a CaM-based phylogenetic tree of all *A. welwitschiae* sequences available at that time. But this clade is not an outlier, but rather fully incorporated with other *A. welwitschiae* strains. The remaining positive selection analysis performed in this publication confirms *A. welwitschiae* as an opportunistic pathogen/saprophytic species. The affected molecular functions (two membrane transporters and one effector protein) are classical traits of this niche of pathogens. Even though membrane transporters are present in all cellular organisms, the referred transporters have important links with pathogenicity in other species. Meanwhile, effector proteins are one of the typical strategies of necrotrophs to modulate the host plant response and cause cell death.

In summary, our results helped bring more information about the viral species and the main pathogen of *A. sisalana*. Specifically, we identified 25 viral species in sisal and henequén, 24 of which are new. We also describe that one of the *A. welwitschiae* genomes might correspond to a new species, in which 13 aromatic compounds were identified through HPLC-MS. Even though this was detected as a polyphyletic species, we have developed a PCR method for the identification of this fungus in sisal plants, in a marker gene that is conserved throughout all *A. welwitschiae* isolates. We sincerely hope that these findings might help advance the research on bole rot and other fungal diseases in crops and that it might lay a strong basis for the research that might follow.

REFERENCES

- ALCALÁ BRISEÑO, R. I. et al. Translating virome analyses to support biosecurity, on-farm management, and crop breeding. **Frontiers in Plant Science**, v. 14, n. March, p. 1–14, 2023.
- ANANDJIWALA, R. D.; JOHN, M. Sisal – Cultivation, Processing and Products. In: **Industrial Applications of Natural Fibres**. Chichester, UK: John Wiley & Sons, Ltd, 2010. p. 181–195.
- ARAÚJO, E. R. M. C. et al. First report of Colletotrichum agaves causing anthracnose in Agave angustifolia in Brazil. **New Disease Reports**, v. 44, n. 2, p. 1–5, 2021.
- BASHEER, S. M. et al. Lipase from marine Aspergillus awamori BTMFW032: Production, partial purification and application in oil effluent treatment. **New Biotechnology**, v. 28, n. 6, p. 627–638, 2011.
- BEULE, L. et al. Changes of scots pine phyllosphere and soil fungal communities during outbreaks of defoliating Insects. **Forests**, v. 8, n. 9, p. 316, 2017.
- BOTELLA, C. et al. Hydrolytic enzyme production by Aspergillus awamori on grape pomace. **Biochemical Engineering Journal**, v. 26, n. 2–3, p. 100–106, 2005.
- BOWSHER, A. W.; KEARNS, P. J.; SHADE, A. 16S rRNA/rRNA Gene Ratios and Cell Activity Staining Reveal Consistent Patterns of Microbial Activity in Plant-Associated Soil. **mSystems**, v. 4, n. 2, 2019.
- CANARINI, A. et al. Root exudation of primary metabolites: Mechanisms and their roles in plant responses to environmental stimuli. **Frontiers in Plant Science**, v. 10, n. February, 2019.
- CEN, K. et al. Divergent LysM effectors contribute to the virulence of Beauveria bassiana by evasion of insect immune defenses. **PLoS Pathogens**, v. 13, n. 9, p. 1–21, 2017.
- CHENG, Y. T.; ZHANG, L.; HE, S. Y. Plant-Microbe Interactions Facing Environmental Challenge. **Cell Host and Microbe**, v. 26, n. 2, p. 183–192, 2019.
- CHIAPELLO, M. et al. Analysis of the virome associated to grapevine downy mildew lesions reveals new mycovirus lineages. **Virus Evolution**, 2020.
- CIPRIANO, A. K. A. L. et al. Proteomic analysis of responsive stem proteins of resistant and susceptible cashew plants after Lasiodiplodia theobromae infection. **Journal of Proteomics**, v. 113, p. 90–109, 2015.
- CLEVELAND, T. E. et al. Potential of Aspergillus flavus genomics for applications in biotechnology. **Trends in Biotechnology**, v. 27, n. 3, p. 151–157, 2009.
- COETZEE, B. et al. Deep sequencing analysis of viruses infecting grapevines: Virome of a vineyard. **Virology**, v. 400, n. 2, p. 157–163, 2010.
- COLOU, J. et al. Role of membrane compartment occupied by Can1 (MCC) and eisosome subdomains in plant pathogenicity of the necrotrophic fungus Alternaria brassicicola. **BMC Microbiology**, v. 19, n. 1, p. 1–14, 2019.
- COLUNGA-GARCÍAMARÍN, P. The Domestication of Henequen (Agave fourcroydes Lem.). In: **The Lowland Maya Area: Three Millennia at the Human-Wildland Interface**. [s.l.: s.n.]. p. 439–446.
- CONESA, A. et al. A survey of best practices for RNA-seq data analysis. **Genome Biology**, v.

17, n. 1, p. 1–19, 2016.

CORREA, A. M. S. et al. Revisiting the rules of life for viruses of microorganisms. **Nature Reviews Microbiology**, v. 19, n. 8, p. 501–513, 2021.

DAAMI-REMADI, M. et al. Comparative Aggressiveness of *Verticillium dahliae*, *V. albo-atrum* and *V. tricorpus* on Potato as Measured by their Effects on Wilt Severity, Plant Growth and Subsequent Yield Loss. **Functional Plant Science and Biotechnology**, v. 5, n. 1, p. 1–8, 2011.

DAMASCENO, C. L. et al. *Penicillium citrinum* as a Potential Biocontrol Agent for Sisal Bole Rot Disease. **Journal of Agricultural Science**, v. 11, n. 10, p. 206, 2019.

DE AZEVEDO, S. C. et al. Analysis of the 2012–2016 drought in the northeast Brazil and its impacts on the Sobradinho water reservoir. **Remote Sensing Letters**, v. 9, n. 5, p. 438–446, 2018.

DE RIJK, T. C. et al. A study of the 2013 Western European issue of aflatoxin contamination of maize from the Balkan area. **World Mycotoxin Journal**, v. 8, n. 5, p. 641–651, 2015.

DEBNATH, M. et al. Biotechnological intervention of *Agave sisalana*: A unique fiber yielding plant with medicinal property. **Journal of Medicinal Plants Research**, v. 4, n. 3, p. 177–187, 2010.

DELAYE, L.; GARCÍA-GUZMÁN, G.; HEIL, M. Endophytes versus biotrophic and necrotrophic pathogens—are fungal lifestyles evolutionarily stable traits? **Fungal Diversity**, v. 60, n. 1, p. 125–135, 2013.

DEMOOR, A.; SILAR, P.; BRUN, S. Appressorium: The breakthrough in *Dikarya*. **Journal of Fungi**, v. 5, n. 3, 2019.

DISKIN, S. et al. Microbiome alterations are correlated with occurrence of postharvest stem-end rot in mango fruit. **Phytobiomes Journal**, v. 1, n. 3, p. 117–127, 2017.

DUARTE, E. A. A. et al. Putting the mess in order: *Aspergillus welwitschiae* (and not *A. niger*) is the etiologic agent of the sisal bole rot disease. **Frontiers in Microbiology**, v. 9, n. 1227, 2018.

DUTTA, D. et al. Endophytes: Exploitation as a Tool in Plant Protection. **Braz. Arch. Biol. Technol.**, v. 57, n. 5, p. 621–629, 2014.

ESPERSCHÜTZ, J. et al. Microbial response to exudates in the rhizosphere of young beech trees (*Fagus sylvatica* L.) after dormancy. **Soil Biology and Biochemistry**, v. 41, n. 9, p. 1976–1985, 2009.

FESEL, P. H.; ZUCCARO, A. Dissecting endophytic lifestyle along the parasitism/mutualism continuum in *Arabidopsis*. **Current Opinion in Microbiology**, v. 32, p. 103–112, 2016.

FONSECA, P. L. C. et al. Virome analyses of *Hevea brasiliensis* using small RNA deep sequencing and PCR techniques reveal the presence of a potential new virus. **Virology Journal**, v. 15, n. 1, p. 1–9, 2018.

GAO, J. et al. AFLP analysis and zebra disease resistance identification of 40 sisal genotypes in China. **Molecular Biology Reports**, v. 39, n. 5, p. 6379–6385, 2012.

GAO, J. et al. Expression of a hevein-like gene in transgenic *Agave* hybrid No. 11648 enhances tolerance against zebra stripe disease. **Plant Cell, Tissue and Organ Culture**, v. 119, n. 3, p.

579–585, 2014.

GARCÍA-GUZMÁN, G.; HEIL, M. Life histories of hosts and pathogens predict patterns in tropical fungal plant diseases. **New Phytologist**, v. 201, n. 4, p. 1106–1120, 2014.

GIESS, W. *Welwitschia mirabilis* Hook. fil. **Dinteria**, p. 3–14, 1969.

GONZÁLEZ-ITURBE, J. A.; OLMSTED, I.; TUN-DZUL, F. Tropical dry forest recovery after long term Henequen (*sisal*, *Agave fourcroydes* Lem.) plantation in northern Yucatan, Mexico. **Forest Ecology and Management**, v. 167, n. 1–3, p. 67–82, 2002.

GUL, H. et al. *Aspergillus welwitschiae* BK Isolate Ameliorates the Physicochemical Characteristics and Mineral Profile of Maize under Salt Stress. **Plants**, v. 12, n. 8, 2023.

HASHEM, A. et al. The interaction between arbuscular mycorrhizal fungi and endophytic bacteria enhances plant growth of *Acacia gerrardii* under salt stress. **Frontiers in Microbiology**, v. 7, n. JUL, p. 1–15, 2016.

HORBACH, R. et al. When and how to kill a plant cell: Infection strategies of plant pathogenic fungi. **Journal of Plant Physiology**, v. 168, n. 1, p. 51–62, 2011.

HUSNA et al. Heavy metal tolerant endophytic fungi *Aspergillus welwitschiae* improves growth, ceasing metal uptake and strengthening antioxidant system in *Glycine max* L. **Environmental Science and Pollution Research**, v. 29, n. 11, p. 15501–15515, 2022.

IZAGUIRRE-MAYORAL, M. L. et al. Effect of seasonal drought and cactus x virus infection on the crassulacean acid metabolism of *Agave sisalana* plants growing in a neotropical savanna. **Journal of Experimental Botany**, v. 46, n. 6, p. 639–646, 1995.

JO, Y. et al. The pepper virome: Natural co-infection of diverse viruses and their quasispecies. **BMC Genomics**, v. 18, n. 1, p. 1–12, 2017.

KIMARO, D. N.; MSANYA, B. M. Review of sisal production and research in Tanzania. **African Study Monographs**, v. 15, n. 4, p. 227–242, 1994.

KUBICEK, C. P.; STARR, T. L.; GLASS, N. L. Plant Cell Wall–Degrading Enzymes and Their Secretion in Plant-Pathogenic Fungi. **Annual Review of Phytopathology**, v. 52, n. 1, p. 427–451, 2014.

LAMBONI, Y. et al. Diversity in secondary metabolites including mycotoxins from strains of *aspergillus* section *nigri* isolated from raw cashew nuts from benin, west africa. **PLoS ONE**, v. 11, n. 10, p. 1–14, 2016.

LEBEIS, S. L. Greater than the sum of their parts: Characterizing plant microbiomes at the community-level. **Current Opinion in Plant Biology**, v. 24, p. 82–86, 2015.

LEWIS, D. H. CONCEPTS IN FUNGAL NUTRITION AND THE ORIGIN OF BIOTROPHY. **Biol. Rev.**, v. 48, p. 261–278, 1973.

LI, C. et al. Expression and characterization of α -L-arabinofuranosidase derived from *Aspergillus awamori* and its enzymatic degradation of corn byproducts with xylanase. **Bioresource Technology**, v. 384, n. June, p. 129278, 2023a.

LI, J. et al. Isolation, identification, and host range of *Aspergillus welwitschiae* causing postharvest rot on Chinese cabbage in China. **Canadian Journal of Plant Pathology**, p. 1–9, 2023b.

- LI, Z. et al. Candidate effector proteins of the necrotrophic apple canker pathogen *Valsa mali* can suppress BAX-induced PCD. **Frontiers in Plant Science**, v. 6, n. July, p. 1–9, 2015.
- LIU, C. et al. A novel double-stranded RNA mycovirus isolated from *Trichoderma harzianum*. **Virology Journal**, v. 16, n. 1, p. 1–10, 2019a.
- LIU, C. Q. et al. Polygalacturonase gene *pgxB* in *Aspergillus Niger* is a virulence factor in apple fruit. **PLoS ONE**, v. 12, n. 3, p. 43, 2017.
- LIU, Y. et al. Evaluation of the biocontrol potential of *Aspergillus welwitschiae* against the root-knot nematode *Meloidogyne graminicola* in rice (*Oryza sativa* L.). **Journal of Integrative Agriculture**, v. 18, n. 11, p. 2561–2570, 2019b.
- LORANG, J. Necrotrophic exploitation and subversion of plant defense: a lifestyle or just a phase, and implications in breeding resistance. *Phytopathology*. **Phytopathology**, v. 109, n. 3, p. 332–346, 2019.
- MADRIZ-ORDEÑANA, K. et al. Prevalence of soil-borne diseases in *Kalanchoe blossfeldiana* reveals a complex of pathogenic and opportunistic fungi. **Plant Disease**, v. 103, n. 10, p. 2634–2644, 2019.
- MARONE, M. P. et al. Fungal communities represent the majority of root-specific transcripts in the transcriptomes of *Agave* plants grown in semiarid regions. **PeerJ**, v. 10, p. e13252, maio 2022.
- MASSI, F. P. et al. Prospecting for the incidence of genes involved in ochratoxin and fumonisin biosynthesis in Brazilian strains of *Aspergillus niger* and *Aspergillus welwitschiae*. **International Journal of Food Microbiology**, v. 221, p. 19–28, 2016.
- MASSI, F. P. et al. Molecular analysis of *Aspergillus* section *Nigri* isolated from onion samples reveals the prevalence of *A. welwitschiae*. **Brazilian Journal of Microbiology**, 2020.
- MEENA, K. K. et al. Abiotic stress responses and microbe-mediated mitigation in plants: The omics strategies. **Frontiers in Plant Science**, v. 8, n. February, p. 1–25, 2017.
- MENDONÇA, J. O. SECA NA BAHIA: PREJUÍZOS PARA O SETOR AGRÍCOLA (2012-2016). **Conj. & Planej.**, v. 192, p. 91–109, 2017.
- MITTAL, V. et al. Stimulatory effect of phosphate-solubilizing fungal strains (*Aspergillus awamori* and *Penicillium citrinum*) on the yield of chickpea (*Cicer arietinum* L. cv. GPF2). **Soil Biology and Biochemistry**, v. 40, n. 3, p. 718–727, 2008.
- MPUNAMI, A. **Purification and Partial Characterization of a Virus Associated with Korogwe Leaf Spot Disease of Sisal**. [s.l.] Oregon State University, 1986.
- MTUNG'E, O. G. et al. **Prevalence and fungal isolates associated with Korogwe leaf spot disease (KLS) of sisal**. 2014 APS-CPS Joint Meeting. **Anais...**Minneapolis, Minnesota: 2014
- MUÑOZ-ADALIA, E. J.; FERNÁNDEZ, M. M.; DIEZ, J. J. The use of mycoviruses in the control of forest diseases. **Biocontrol Science and Technology**, v. 26, n. 5, p. 577–604, 2016.
- NEGI, S.; BANERJEE, R. Characterization of amylase and protease produced by *Aspergillus awamori* in a single bioreactor. **Food Research International**, v. 42, n. 4, p. 443–448, 2009.
- PEKAREK, E.; JACOBSON, K.; DONOVAN, A. High levels of genetic variation exist in *Aspergillus niger* populations infecting *Welwitschia mirabilis* hook. **Journal of Heredity**, v. 97, n. 3, p. 270–278, 2006.

- PERERA, D. et al. Occurrence of fumonisin-producing black aspergilli in Australian wine grapes: effects of temperature and water activity on fumonisin production by *A. niger* and *A. welwitschiae*. **Mycotoxin Research**, v. 37, n. 4, p. 327–339, 2021.
- PFLIEGLER, W. P. et al. The Aspergilli and Their Mycotoxins: Metabolic Interactions With Plants and the Soil Biota. **Frontiers in Microbiology**, v. 10, n. February, 2020.
- PRITSCH, K.; GARBAYE, J. Enzyme secretion by ECM fungi and exploitation of mineral nutrients from soil organic matter. **Annals of Forest Science**, v. 68, n. 1, p. 25–32, 2011.
- QUEIROGA, V. DE P. et al. **Sisal (Agave sisalana, Perrine) TECNOLOGIAS DE PLANTIO E UTILIZAÇÃO**. Campina Grande: AREPB, 2021.
- QUIJANO RAMAYO, A. et al. Microbial diseases affecting henequen (*Agave fourcroydes* Lem.) in Yucatan, Mexico. **Revista mexicana de fitopatología**, v. 20, n. 1, p. 18–23, 2002.
- QUINTANILHA-PEIXOTO, G. et al. Calm Before the Storm: A Glimpse into the Secondary Metabolism of *Aspergillus welwitschiae*, the Etiologic Agent of the Sisal Bole Rot. **Toxins**, v. 11, n. 11, p. 1–14, out. 2019.
- QUINTANILHA-PEIXOTO, G. et al. The Sisal Virome: Uncovering the Viral Diversity of Agave Varieties Reveals New and Organ-Specific Viruses. **Microorganisms**, v. 9, n. 1704, p. 1–21, 2021.
- QUINTANILHA-PEIXOTO, G. et al. Phylogenomics and gene selection in *Aspergillus welwitschiae*: Possible implications in the pathogenicity in *Agave sisalana*. **Genomics**, v. 114, n. 6, 2022.
- RAYA, F. T. et al. Extreme physiology: Biomass and transcriptional profiling of three abandoned Agave cultivars. **Industrial Crops and Products**, v. 172, n. September, 2021.
- REDILA, C. D.; PRAKASH, V.; NOURI, S. Metagenomics analysis of the wheat virome identifies novel plant and fungal-associated viral sequences. **Viruses**, v. 13, n. 12, 2021.
- REDKAR, A. et al. Determinants of endophytic and pathogenic lifestyle in root colonizing fungi. **Current Opinion in Plant Biology**, v. 67, p. 102226, 2022.
- REIS, A.; HENRIQUE, I. M. *Phytophthora nicotianae* e *Rhizoctonia solani*: dois novos patógenos da vinca no Brasil. p. 19, 2007.
- REN, Z.-Q. Q. A.-Z.-Q. Q. A.-B.-L. Q. A.-J.-H. W. A.-A. G. S. C. A.-S.-X. Effect of temperature on the life history of *Dysmicoccus neobrevipes* (Hemiptera: Pseudococcidae): An invasive species of gray pineapple mealybug in South China. **Crop protection**, v. v. 45, p. 141–146–2013 v.45, 2013.
- REVERBERI, M. et al. Natural functions of mycotoxins and control of their biosynthesis in fungi. **Applied Microbiology and Biotechnology**, v. 87, n. 3, p. 899–911, 2010.
- RIBEIRO, S. et al. Transcriptome profiling in susceptible and tolerant rubber tree clones in response to cassiicolin Cas1, a necrotrophic effector from *Corynespora cassiicola*. **PLoS ONE**, v. 16, n. 7 July, p. 1–23, 2021.
- RODRIGUEZ-MORENO, L. et al. Tools of the crook- infection strategies of fungal plant pathogens. **Plant Journal**, v. 93, n. 4, p. 664–674, 2018.
- ROJAS, C. M. et al. Regulation of primary plant metabolism during plant-pathogen interactions and its contribution to plant defense. **Frontiers in Plant Science**, v. 5, n. February, p. 1–12,

2014.

SALEH, A. A. et al. Effects of Feeding *Aspergillus Awamori* and *Aspergillus Niger* on Growth Performance and Meat Quality in Broiler Chickens. **Journal of Poultry Science**, v. 48, n. 3, p. 201–207, 2011.

SALEH, A. A. et al. Beneficial effects of *Aspergillus awamori* in broiler nutrition. **World's Poultry Science Journal**, v. 70, n. 4, p. 857–864, 2014.

SANTOS, Á. F. DOS; LUZ, E. D. M. N.; SOUZA, J. T. DE. *Phytophthora nicotianae*: agente etiológico da gomose da acácia-negra no Brasil. **Fitopatologia Brasileira**, v. 30, n. 1, p. 81–84, 2005.

SANTOYO, G. et al. Plant growth-promoting bacterial endophytes. **Microbiological Research**, v. 183, p. 92–99, 2016.

SEEKLES, S. J. et al. Genome sequences of 24 *Aspergillus niger* sensu stricto strains to study strain diversity, heterokaryon compatibility, and sexual reproduction. **G3: Genes, Genomes, Genetics**, v. 12, n. 7, 2022.

SHAO, D. et al. Effectors of Plant Necrotrophic Fungi. **Frontiers in Plant Science**, v. 12, n. June, p. 1–14, 2021.

SHIN, H. Y. et al. Solid-state fermentation of black rice bran with *Aspergillus awamori* and *Aspergillus oryzae*: Effects on phenolic acid composition and antioxidant activity of bran extracts. **Food Chemistry**, v. 272, n. July 2018, p. 235–241, 2019.

SIEBER, T. N. Endophytic fungi in forest trees: are they mutualists? **Fungal Biology Reviews**, v. 21, n. 2–3, p. 75–89, 2007.

SINGH, N.; SINGH, J.; SINGH, K. Small at size, big at impact: Microorganisms for sustainable development. **Microbial Bioprospecting for Sustainable Development**, p. 3–28, 2018.

SOLÍS-GARCÍA, I. A. et al. *Phytophthora* Root Rot Modifies the Composition of the Avocado Rhizosphere Microbiome and Increases the Abundance of Opportunistic Fungal Pathogens. **Frontiers in Microbiology**, v. 11, n. January, p. 1–15, 2021.

SOLÓRZANO LEMOS, J. L. et al. Thermal stability of xylanases produced by *Aspergillus awamori*. **Brazilian Journal of Microbiology**, v. 31, n. 3, p. 206–211, 2000.

SPERSCHNEIDER, J.; DODDS, P. EffectorP 3.0: prediction of apoplastic and cytoplasmic effectors in fungi and oomycetes. **Molecular Plant-Microbe Interactions®**, p. 1–28, 2021.

STONE, J. M. et al. Simulation of Fungal-Mediated Cell Death by Fumonisin B1 and Selection of Fumonisin B1-Resistant (fbr) *Arabidopsis* Mutants. **The Plant Cell**, v. 12, n. 10, p. 1811, 2000.

SUINAGA, F. A.; COUTINHO, W. M.; SILVA, O. R. R. F. DA. **Sisal - Pragas e Doenças**. Disponível em: <<https://www.embrapa.br/agencia-de-informacao-tecnologica/cultivos/sisal/producao/pragas-e-doencas>>. Acesso em: 21 jul. 2023.

SUSCA, A. et al. Comparison of species composition and fumonisin production in *Aspergillus* section *Nigri* populations in maize kernels from USA and Italy. **International Journal of Food Microbiology**, v. 188, p. 75–82, 2014.

TAHERI, P.; KAKOOEE, T. Reactive oxygen species accumulation and homeostasis are involved in plant immunity to an opportunistic fungal pathogen. **Journal of Plant Physiology**,

v. 216, n. April, p. 152–163, 2017.

TAKEDA, K. et al. Species identification, antifungal susceptibility, and clinical feature association of *Aspergillus* section *Nigri* isolates from the lower respiratory tract (Medical Mycology (2019) 58 (e3) DOI: 10.1093/mmy/myz072). **Medical Mycology**, v. 58, n. 3, p. E3, 2020.

TAYI, L. et al. Identification of pectin degrading enzymes secreted by *Xanthomonas oryzae* pv. *Oryzae* and determination of their role in virulence on rice. **PLoS ONE**, v. 11, n. 12, p. 1–15, 2016.

VARGA, J. et al. *Aspergillus*: Sex and Recombination. **Mycopathologia**, v. 178, n. 5–6, p. 349–362, 2014.

VAZ, A. B. M. et al. Foliar mycoendophytome of an endemic plant of the Mediterranean biome (*Myrtus communis*) reveals the dominance of basidiomycete woody saprotrophs. **PeerJ**, v. 8, n. e10487, p. 1–25, 2020.

WANG, G. et al. Development of a Specific Nested PCR Assay for the Detection of 16SrI Group Phytoplasmas Associated with Sisal Purple Leafroll Disease in Sisal Plants and Mealybugs. **Plants**, v. 11, n. 21, 2022.

WANG, G. et al. Detection and molecular identification of a 16SrI group phytoplasma associated with sisal purple leafroll disease. **Plant Protection Science**, v. 59, n. 1, p. 19–30, 2023.

WANG, P. L. Yellow pigments of *Aspergillus niger* and *Aspergillus awamori*. **Agricultural and Biological Chemistry**, v. 30, n. 7, p. 683–687, 1966.

WHITAKER, C.; PAMMENTER, N. W.; BERJAK, P. Infection of the cones and seeds of *Welwitschia mirabilis* by *Aspergillus niger* var. *phoenicis* in the Namib-Naukluft Park. **South African Journal of Botany**, v. 74, n. 1, p. 41–50, 2008.

WU, Q. et al. Metabolic Pathways of Ochratoxin A. **Current Drug Metabolism**, v. 12, n. 1, p. 1–10, 2011.

XIANG, C. et al. $\alpha\beta$ -Dehydrocurvularin isolated from the fungus *Aspergillus welwitschiae* effectively inhibited the behaviour and development of the root-knot nematode *Meloidogyne graminicola* in rice roots. **BMC Microbiology**, v. 20, n. 1, p. 1–10, 2020.

XIE, H. H. et al. First Report of Black Spot Caused by *Neoscytalidium dimidiatum* on Sisal in Guangxi, China. **Plant Disease**, v. 105, n. 3, p. 701–701, 2021.

YAN, L. et al. Beneficial effects of endophytic fungi colonization on plants. **Applied Microbiology and Biotechnology**, v. 103, p. 3327–3340, 2019.

ZHAO, Z. et al. Comparative analysis of fungal genomes reveals different plant cell wall degrading capacity in fungi. **BMC Genomics**, v. 14, n. 274, 2013.



Gabriel Quintanilha Peixoto

Endereço para acessar este CV: <http://lattes.cnpq.br/9614546264344691>

ID Lattes: **9614546264344691**

Última atualização do currículo em 31/05/2023

(QUINTANILHA-PEIXOTO, G.) É Técnico em Meio Ambiente pelo Instituto Federal Fluminense (IFF) (2013), Licenciado em Ciências Biológicas pela Universidade Estadual do Norte Fluminense Darcy Ribeiro (UENF) com período sanduíche na Miami University (EUA) (2017), Mestre (2019) e estudante de doutorado em Bioinformática pela Universidade Federal de Minas Gerais (UFMG) com período sanduíche na Texas A&M University (EUA). Tem experiência em bioinformática, biologia molecular e microbiologia e atua nas áreas de genômica de fungos, metagenômica e interação planta-microrganismo. Está alocado no Laboratório de Biologia Molecular e Computacional de Fungos, sob orientação do Prof. Dr. Aristóteles Góes Neto. **(Texto informado pelo autor)**

Identificação

Nome	Gabriel Quintanilha Peixoto
Nome em citações bibliográficas	QUINTANILHA, G.; PEIXOTO, G. Q.; QUINTANILHA-PEIXOTO, G.; QUINTANILHA-PEIXOTO, GABRIEL
Lattes iD	http://lattes.cnpq.br/9614546264344691
Orcid iD	https://orcid.org/0000-0002-7476-5845

Endereço

Endereço Profissional	Universidade Federal de Minas Gerais, Instituto de Ciências Biológicas. Av. Pres. Antônio Carlos, 6627 Pampulha 31270901 - Belo Horizonte, MG - Brasil Telefone: (31) 34093050 URL da Homepage: https://sites.icb.ufmg.br/lbmc/index.html
------------------------------	--

Formação acadêmica/titulação

2019	Doutorado em andamento em Bioinformática (Conceito CAPES 7). Universidade Federal de Minas Gerais, UFMG, Brasil. com período sanduíche em Texas A&M University (Orientador: Libo Shan). Título: Transcritômica da Podridão Vermelha do Sisal Orientador: Aristóteles Góes Neto. Coorientador: Eric Roberto Guimarães Rocha Aguiar. Bolsista do(a): Fundação de Amparo à Pesquisa do Estado de Minas Gerais, FAPEMIG, Brasil.
2017 - 2019	Mestrado em Bioinformática (Conceito CAPES 7). Universidade Federal de Minas Gerais, UFMG, Brasil. Título: The Death Is Red: Analysis of the Predicted Secretome of <i>Aspergillus welwitschiae</i> , with Emphasis in Pathogenicity and Carbohydrate Metabolism , Ano de Obtenção: 2019. Orientador: Aristóteles Góes Neto. Coorientador: Eric Roberto Guimarães Rocha Aguiar & Fernanda Badotti. Bolsista do(a): Fundação de Amparo à Pesquisa do Estado de Minas Gerais, FAPEMIG, Brasil.
2013 - 2017	Graduação em Ciências Biológicas. Universidade Estadual do Norte Fluminense Darcy Ribeiro, UENF, Brasil. com período sanduíche em Miami University, Ohio (Orientador: CAPES). Título: Caracterização de um Mutante de resposta Imune e Identificação do Gene na Planta Modelo <i>Arabidopsis thaliana</i> . Orientador: Aline Chaves Intorne. Bolsista do(a): Fundação Carlos Chagas Filho de Amparo à Pesquisa do Estado do RJ, FAPERJ, Brasil.
2010 - 2013	Curso técnico/profissionalizante em Técnico em Meio Ambiente. Instituto Federal Fluminense, IFF, Brasil.

Formação Complementar

2021 - 2021	Phylogenetic Orthology Inference for Comparative Genomics. (Carga horária: 4h). 2nd Women in Bioinformatics and Data Science LA, WBDS LA, Brasil.
2021 - 2021	Oficina Moodle. (Carga horária: 15h). Universidade Federal de Minas Gerais, UFMG, Brasil.
2020 - 2020	Virus Research and Surveillance: Bioinformatics, Genetics and Public Health. (Carga horária: 32h). Fundação Oswaldo Cruz, FIOCRUZ, Brasil.
2020 - 2020	Formação de bolsistas da Diretoria de Inovação e Metodologias de Ensino. (Carga horária: 45h). Universidade Federal de Minas Gerais, UFMG, Brasil.
2019 - 2019	Investigação Temporal e Epidemiologia de Surto de Dengue. (Carga horária: 96h). Universidade Federal de Minas Gerais, UFMG, Brasil.
2019 - 2019	Análise de Transcritomas e MicroRNAs. (Carga horária: 36h). Laboratório Nacional de Computação Científica, LNCC, Brasil.
2018 - 2018	Vigilância genômica de Flavivírus emergentes e identificação de novos vírus. (Carga horária: 80h). Universidade Federal de Minas Gerais, UFMG, Brasil.
2017 - 2017	I Curso de Verão em Bioinformática. (Carga horária: 24h). Universidade Federal de Minas Gerais, UFMG, Brasil.
2017 - 2017	Introdução à Programação. (Carga horária: 3h). Universidade Federal de Minas Gerais, UFMG, Brasil.
2017 - 2017	Unidade Potencialmente Significativa sobre Magnetismo. (Carga horária: 8h). Instituto Federal Fluminense, IFF, Brasil.
2017 - 2017	Bioinformática em Epidemiologia Molecular e Evolução Viral. (Carga horária: 60h). Universidade Federal de Minas Gerais, UFMG, Brasil.
2017 - 2017	Ecologia e Coleta de Dados em Praias Arenosas. (Carga horária: 8h). Universidade Estadual do Norte Fluminense Darcy Ribeiro, UENF, Brasil.
2017 - 2017	Theoretical and Practical Approaches to Metagenomics and Viral Discovery. (Carga horária: 30h). Universidade de São Paulo, USP, Brasil.
2017 - 2017	Effects of Global Change on Photosynthesis and Plant Respiration. (Carga horária: 8h). Universidade Estadual do Norte Fluminense Darcy Ribeiro, UENF, Brasil.
2016 - 2016	Coleta e Identificação de Plantas do Norte e Noroeste Fluminense. (Carga horária: 20h). Universidade Estadual do Norte Fluminense Darcy Ribeiro, UENF, Brasil.
2015 - 2015	Busca Eletrônica em Bases Bibliográficas. (Carga horária: 2h). Universidade Estadual do Norte Fluminense Darcy Ribeiro, UENF, Brasil.
2014 - 2014	O Mundo Microbiano e Você. (Carga horária: 4h). Universidade Estadual do Norte Fluminense Darcy Ribeiro, UENF, Brasil.
2014 - 2014	Microbiologia e Meio Ambiente. (Carga horária: 4h). Universidade Estadual do Norte Fluminense Darcy Ribeiro, UENF, Brasil.
2014 - 2014	Microbiologia na Agricultura. (Carga horária: 4h). Universidade Estadual do Norte Fluminense Darcy Ribeiro, UENF, Brasil.
2011 - 2011	Recomposição de Mata Ciliar. (Carga horária: 4h). Instituto Federal Fluminense, IFF, Brasil.
2011 - 2011	Energia renovável: Introdução à energia fotovoltaica. (Carga horária: 4h). Instituto Federal Fluminense, IFF, Brasil.
2010 - 2011	Informática. (Carga horária: 126h). DATAFOX Cursos Técnicos, DATAFOX, Brasil.
2010 - 2010	Imagens de satélite: Obtenção e visualização. (Carga horária: 3h). Instituto Federal Fluminense, IFF, Brasil.

Atuação Profissional

Universidade Federal de Minas Gerais, UFMG, Brasil.

Vínculo institucional

2019 - Atual

Vínculo: Bolsista, Enquadramento Funcional: Estudante de Doutorado, Carga horária: 40, Regime: Dedicção exclusiva.

Vínculo institucional

2021 - 2022

Vínculo: Colaborador, Enquadramento Funcional: Representante Discente (Titular)

Vínculo institucional

2020 - 2022

Vínculo: Bolsista, Enquadramento Funcional: Bolsista de Incentivo à Formação Docente, Carga horária: 8

Vínculo institucional

2020 - 2021

Vínculo: Colaborador, Enquadramento Funcional: Representante Discente (Suplente)

Vínculo institucional

2019 - 2019

Vínculo: Bolsista, Enquadramento Funcional: Bolsista de Incentivo à Formação Docente, Carga horária: 8

Vínculo institucional

2017 - 2019

Vínculo: Bolsista, Enquadramento Funcional: Estudante de Mestrado, Carga horária: 40, Regime: Dedicção exclusiva.

Texas A&M University, TAMU, Estados Unidos.

Vínculo institucional

2016 - 2016

Vínculo: Bolsista, Enquadramento Funcional: Estagiário, Carga horária: 40, Regime: Dedicção exclusiva.

Universidade Estadual do Norte Fluminense Darcy Ribeiro, UENF, Brasil.

Vínculo institucional

2014 - 2017

Vínculo: Bolsista, Enquadramento Funcional: Bolsista de Iniciação Científica, Carga horária: 20, Regime: Dedicção exclusiva.

Vínculo institucional

2013 - 2014

Vínculo: Bolsista, Enquadramento Funcional: Iniciação Profissional, Carga horária: 12, Regime: Dedicção exclusiva.

Instituto Federal Fluminense, IFF, Brasil.

Vínculo institucional

2010 - 2012

Vínculo: Bolsista, Enquadramento Funcional: Iniciação Profissional, Carga horária: 20, Regime: Dedicção exclusiva.

Membro de corpo editorial

2020 - 2020

Periódico: V CIM CONGRESSO DE INOVAÇÃO E METODOLOGIAS DE ENSINO SUPERIOR E TECNOLÓGICO

Revisor de periódico

2018 - Atual

Periódico: PLANT AND SOIL

2020 - 2020

Periódico: REVISTA DOCENCIA DO ENSINO SUPERIOR

Áreas de atuação

1. Grande área: Ciências Biológicas / Área: Microbiologia.
2. Grande área: Ciências Biológicas / Área: Bioquímica / Subárea: Biologia Molecular.
3. Grande área: Ciências Biológicas / Área: Biotecnologia / Subárea: Bioinformática.

Idiomas

Inglês

Compreende Bem, Fala Bem, Lê Bem, Escreve Bem.

Espanhol

Compreende Bem, Fala Bem, Lê Bem, Escreve Bem.

Francês

Compreende Razoavelmente, Fala Razoavelmente, Lê Bem, Escreve Razoavelmente.

Português

Compreende Bem, Fala Bem, Lê Bem, Escreve Bem.

Italiano

Compreende Razoavelmente, Fala Pouco, Lê Bem, Escreve Pouco.

Prêmios e títulos

2019

Destaque Acadêmico - Inovação e melhorias na qualidade do Ensino de Graduação da UFMG - GIZ, Semana do Conhecimento - UFMG.

2014

Menção Honrosa - XIV Encontro Nacional de Microbiologia Ambiental: O manganês e a glutatona na resposta ao estresse por metal em *Gluconacetobacter diazotrophicus*, Sociedade Brasileira de Microbiologia.

Produções

Produção bibliográfica


Artigos completos publicados em periódicos

Ordenar por

Ordem Cronológica

1. DE MENEZES, THAÍS ALMEIDA ; ABURJAILE, FLÁVIA FIGUEIRA ; **QUINTANILHA-PEIXOTO, GABRIEL** ; TOMÉ, LUIZ MARCELO RIBEIRO ; FONSECA, PAULA LUIZE CAMARGOS ; MENDES-PEREIRA, THAIRINE ; ARAÚJO, DANIEL SILVA ; MELO, TARCISIO SILVA ; Kato, Rodrigo Bentes ; DELABIE, JACQUES HUBERT CHARLES ; RIBEIRO, SÉRVIO PONTES ; BREINIG, BERTRAM ; AZEVEDO, VASCO ; DRECHSLER-SANTOS, ELISANDRO RICARDO ; ANDRADE, BRUNO SILVA ; GÓES-NETO, ARISTÓTELES . Unraveling the Secrets of a Double-Life Fungus by Genomics: *Ophiocordyceps australis* CCMB661 Displays Molecular Machinery for Both Parasitic and Endophytic Lifestyles. *JOURNAL OF FUNGI* **JCR**, v. 9, p. 110, 2023.
Citações: **WEB OF SCIENCE**™ 1
2. FONSECA, PAULA LUIZE CAMARGOS ; SKALTSAS, DEMETRA ; DA SILVA, FELIPE FERREIRA ; Kato, Rodrigo Bentes ; DE CASTRO, GIOVANNI MARQUES ; GARCÍA, GLEN JASPER YUPANQUI ; **QUINTANILHA-PEIXOTO, GABRIEL** ; MENDES-PEREIRA, THAIRINE ; DO CARMO, ANDERSON OLIVEIRA ; AGUIAR, ERIC ROBERTO GUIMARÃES ROCHA ; DE CARVALHO, DANIEL SANTANA ; COSTA-REZENDE, DIOGO HENRIQUE ; DRECHSLER-SANTOS, ELISANDRO RICARDO ; BADOTTI, FERNANDA ; FERREIRA-SILVA, ALICE ; OLIVEIRA, GUILHERME ; CHAVERRI, PRISCILA ; VAZ, ALINE BRUNA MARTINS ; GÓES-NETO, ARISTÓTELES . An Integrative View of the Phyllosphere Mycobiome of Native Rubber Trees in the Brazilian Amazon. *JOURNAL OF FUNGI* **JCR**, v. 8, p. 373, 2022.
Citações: **WEB OF SCIENCE**™ 4
3. **QUINTANILHA-PEIXOTO, GABRIEL** ; MARONE, MARINA PÜPKE ; RAYA, FÁBIO TRIGO ; JOSÉ, JULIANA ; OLIVEIRA, ADRIELE ; FONSECA, PAULA LUIZE CAMARGOS ; TOMÉ, LUIZ MARCELO RIBEIRO ; BORTOLINI, DENER EDUARDO ; Kato, Rodrigo Bentes ; ARAÚJO, DANIEL S. ; DE-PAULA, RUTH B. ; CUESTA-ASTROZ, YESID ; DUARTE, ELIZABETH A.A. ; BADOTTI, FERNANDA ; DE CARVALHO AZEVEDO, VASCO ARISTON ; BREINIG, BERTRAM ; SOARES, ANA CRISTINA FERMINO ; CARAZZOLLE, MARCELO FALSARELLA ; PEREIRA, GONÇALO AMARANTE GUIMARÃES ; AGUIAR, ERIC ROBERTO GUIMARÃES ROCHA ; GÓES-NETO, ARISTÓTELES . Phylogenomics and gene selection in *Aspergillus welwitschiae*: Possible implications in the pathogenicity in *Agave sisalana*. *GENOMICS* **JCR**, v. 114, p. 110517, 2022.
4. ★ de ARAUJO, D. ; de PAULA, R. B. ; TOME, L. M. R. ; **QUINTANILHA-PEIXOTO, G** ; SALVADOR-MONTOYA, C. A. ; DEL-BEM, L. ; BADOTTI, FERNANDA ; AZEVEDO, VASCO ; BREINIG, B. ; AGUIAR, E. R. G. R. ; DRECHSLER-SANTOS, E. R. ; FONSECA, P. L. C. ; GOES NETO, A. . Comparative mitogenomics of Agaricomycetes: diversity, abundance, impact and coding potential of putative open-reading frames. *MITOCHONDRION* **JCR**, v. 1, p. 1, 2021.
Citações: **WEB OF SCIENCE**™ 7
5. ADELINO, TALITA ÉMILE RIBEIRO GIOVANETTI, MARTA FONSECA, VAGNER XAVIER, JOILSON DE ABREU, ÁLVARO SALGADO DO NASCIMENTO, VALDINETE ALVES DEMARCHI, LUIZ HENRIQUE FERRAZ OLIVEIRA, MARLUCE APARECIDA ASSUNÇÃO DA SILVA, VINÍCIUS LEMES DE MELLO, ARABELA LEAL E. SILVA CUNHA, GABRIEL MURICY SANTOS, ROSELENE HANS DE OLIVEIRA, ELAINE CRISTINA JÚNIOR, JORGE ANTÔNIO CHAMON DE MELO IANI, FELIPE CAMPOS DE FILIPPIS, ANA MARIA BISPO DE ABREU, ANDRÉ LUIZ DE JESUS, RONALDO DE ALBUQUERQUE, CARLOS FREDERICO CAMPELO RICO, JAIRO MENDES DO CARMO SAID, RODRIGO FABIANO SILVA, JOSCELIO AGUIAR DE MOURA, NOELY FABIANA OLIVEIRA LEITE, PRISCILA FRUTUOSO, LÍVIA CARLA VINHAL , *et al.* ; Field and classroom initiatives for portable sequence-based monitoring of dengue virus in Brazil. *Nature Communications* **JCR**, v. 12, p. 1, 2021.
Citações: **WEB OF SCIENCE**™ 5
6. ★ **QUINTANILHA-PEIXOTO, GABRIEL** ; FONSECA, PAULA LUIZE CAMARGOS ; RAYA, FÁBIO TRIGO ; MARONE, MARINA PUPKE ; BORTOLINI, DENER EDUARDO ; MIECZKOWSKI, PIOTR ; OLMO, ROENICK PROVETI ; CARAZZOLLE, MARCELO FALSARELLA ; VOIGT, CHRISTIAN A. ; SOARES, ANA CRISTINA FERMINO ; PEREIRA, GONÇALO AMARANTE GUIMARÃES ; GÓES-NETO, ARISTÓTELES ; AGUIAR, ERIC ROBERTO GUIMARÃES ROCHA . The Sisal Virome: Uncovering the Viral Diversity of *Agave* Varieties Reveals New and Organ-Specific Viruses. *Microorganisms* **JCR**, v. 9, p. 1704, 2021.
Citações: **WEB OF SCIENCE**™ 4
7. da Silva, Alessandra Lima ; ABREU, ANA PAULA DE ; Mariano, Diego ; Caixeta, Felipe ; Santos, Fenícia Brito ; LAGE, FERNANDA STUSSI D. ; **QUINTANILHA-PEIXOTO, GABRIEL** ; HILÁRIO, HERON. O. ; XAVIER, JOICYMARA. S. ; QUEIROZ, LUCIO. R. ; DE TOLEDO, NAYARA EVELIN ; TAVARES, RAPHAEL ; Kato, Rodrigo Bentes ; DOS SANTOS, ROSELANE GONÇALVES ; SOARES, STELLAMARIS ; GOES, WANESSA. M. ; NOGUEIRA, WYLERSON. G. ; BATISTA, THIAGO M. ; ORTEGA, JOSÉ MIGUEL ; DE CARVALHO, VASCO ARISTON AZEVEDO ; FRANCO, GLÓRIA. REGINA ; MELO-MINARDI, RAQUEL. C. DE ; GÓES-NETO, ARISTÓTELES . From In-Person to the Online World: Insights Into Organizing Events in Bioinformatics. *Frontiers in Bioinformatics*, v. 1, p. 711463, 2021.
8. VAZ, ALINE BRUNA M. ; FONSECA, PAULA LUIZE C. ; SILVA, FELIPE F. ; **QUINTANILHA-PEIXOTO, GABRIEL** ; SAMPEDRO, INMACULADA ; SILES, JOSE A. ; CARMO, ANDERSON ; KATO, RODRIGO B. ; AZEVEDO, VASCO ; BADOTTI, FERNANDA ; OCAMPO, JUAN A. ; ROSA, CARLOS A. ; GÓES-NETO, ARISTÓTELES . Foliar mycoendophytome of an endemic plant of the Mediterranean biome (*Myrtus communis*) reveals the dominance of basidiomycete woody saprotrophs. *PeerJ* **JCR**, v. 8, p. e10487, 2020.
Citações: **WEB OF SCIENCE**™ 2
9. ★ **QUINTANILHA-PEIXOTO, G** ; TORRES, R. O. ; REIS, I. M. A. ; BORTOLINI, D. E. ; DUARTE, E. A. A. ; AZEVEDO, V. A. C. ; BREINIG, B. ; AGUIAR, E. R. G. R. ; SOARES, A. C. F. ; GOES NETO, A. ; BRANCO, A. . Calm Before the Storm: A Glimpse into the Secondary Metabolism of *Aspergillus welwitschiae*, the Etiologic Agent of the Sisal Bole Rot. *Toxins* **JCR**, v. 11, p. 631, 2019.
Citações: **WEB OF SCIENCE**™ 5

Capítulos de livros publicados

1. Mariano, Diego ; Nogueira, Wylerson G. ; Goes, Wanessa M. ; dos Santos, Roselane G. ; Kato, Rodrigo Bentes ; Toledo, Nayara ; Queiroz, Lucio R. ; Hilário, Heron O. ; **QUINTANILHA-PEIXOTO, GABRIEL** ; Lage, Fernanda S. D. ; Santos, Fenícia Brito ; Caixeta, Felipe ; de Abreu, Ana Paula ; da Silva, Alessandra Lima ; Xavier, Joicymara S. . Uma estratégia para engajamento de participantes de eventos online. *BIOINFO - Revista Brasileira de Bioinformática e Biologia Computacional*. 1ed.: Alfahelix, 2021, v. 1, p. 1-.
2.  Mothé, Geórgia Peixoto Bechara ; **QUINTANILHA-PEIXOTO, GABRIEL** ; de Souza, Glacielen Ribeiro ; Ramos, Alessandro Coutinho ; Intorne, Aline Chaves . Overview of the Role of Nitrogen in Copper Pollution and Bioremediation Mediated by Plant&Microbe Interactions. In: Cruz C.; Vishwakarma K.; Choudhary D.K.; Varma A.. (Org.). *Soil Biology*. 1ed.: Springer International Publishing, 2021, v. 62, p. 249-264.

Trabalhos completos publicados em anais de congressos

1. **QUINTANILHA-PEIXOTO, G**; CARVALHO, A. O. ; INTORNE, A. C. . Extração de peptídeos antimicrobianos da planta biondicadora *Salvinia auriculata* Aubl.. In: II Simpósio de Recursos Hídricos da Bacia do Rio Paraíba do Sul, 2014, São José dos Campos - SP. Transposição das águas: conflitos, desafios e oportunidades, 2014.

Resumos expandidos publicados em anais de congressos

1. SOUZA, M. F. ; **PEIXOTO, G. Q.** ; SOUZA FILHO, G. A. ; INTORNE, A. C. . O manganês e a resposta a estresses ambientais na bactéria *Gluconacetobacter diazotrophicus*. In: XIV Congresso Brasileiro de Ecotoxicologia, 2016, Curitiba - PR. XIV Congresso Brasileiro de Ecotoxicologia, 2016.
2. SOUZA, M. F. ; **PEIXOTO, G. Q.** ; SOUZA FILHO, G. A. ; INTORNE, A. C. . A glutatona na resposta ao estresse por metais em *Gluconacetobacter diazotrophicus*. In: XIV Congresso Brasileiro de Ecotoxicologia, 2016, Curitiba - PR. XIV Congresso Brasileiro de Ecotoxicologia, 2016.

Resumos publicados em anais de congressos

1. GOULART, J. T. S. S. ; **QUINTANILHA-PEIXOTO, G** ; SUZUKI, M. S. ; INTORNE, A. C. . Screening Plant Growth-Promoting Bacteria for *Salvinia*-mediated bioremediation of aquatic environments. In: *Water Daze 2023*, 2023, College Station, Texas. EUA. *Water Daze 2023*, 2023.
2. **QUINTANILHA-PEIXOTO, GABRIEL**; OLIVEIRA, H. B. ; BARBOSA, K. P. ; DURAES, W. Q. B. ; XAVIER, J. S. . Nucleotide mutations and protein stability of SARS-CoV-2: A brief experience with Machine Learning. In: 2nd Women in Bioinformatics and Data Science LA, 2021, (Online). 2nd Women in Bioinformatics and Data Science LA, 2021.
3. FONSECA, P. L. C. ; de PAULA, R. B. ; de ARAUJO, D. ; BORTOLINI, D. E. ; **PEIXOTO, G. Q.** ; AZEVEDO, V. A. C. ; BRENIG, B. ; BADOTTI, F. ; AGUIAR, E. R. G. R. ; GOES-NETO, A. . IMPACTO DOS ÍNTRONS E HOMING ENDONUCLEASES NA EVOLUÇÃO DO GENOMA MITOCONDRIAL DE FUNGOS. In: VI SIMPÓSIO DE MICROBIOLOGIA DA UFMG, 2019, Belo Horizonte - MG. VI SIMPÓSIO DE MICROBIOLOGIA DA UFMG, 2019.
4. de ARAUJO, D. ; **QUINTANILHA-PEIXOTO, G** ; FONSECA, P. L. C. ; de PAULA, R. B. ; BRENIG, B. ; AZEVEDO, V. A. C. ; DRECHSLER-SANTOS, E. R. ; GOES-NETO, A. . MONTAGEM E ANOTAÇÃO DO GENOMA MITOCONDRIAL DE *Phellinotus piptadeniae* (BASIDIOMYCOTA, HYMENOCHEATALES). In: VI SIMPÓSIO DE MICROBIOLOGIA DA UFMG, 2019, Belo Horizonte - MG. VI SIMPÓSIO DE MICROBIOLOGIA DA UFMG, 2019.
5. FONSECA, P. L. C. ; de PAULA, R. B. ; de ARAUJO, D. ; BORTOLINI, D. E. ; **QUINTANILHA-PEIXOTO, G** ; AZEVEDO, V. A. C. ; BRENIG, B. ; Del BEM, L. E. V. ; BADOTTI, F. ; GOES-NETO, A. ; AGUIAR, E. R. G. R. . Introns and homing endonucleases shape mitochondrial genomes of fungal species from Hypocreales order (Ascomycota). In: X-Meeting 2019, 2019, Campos do Jordão - SP. X-Meeting 2019, 2019.
6. de ARAUJO, D. ; FONSECA, P. L. C. ; **QUINTANILHA-PEIXOTO, G** ; de PAULA, R. B. ; BRENIG, B. ; AZEVEDO, V. A. C. ; DRECHSLER-SANTOS, E. R. ; GOES-NETO, A. . Characterization of the mitochondrial genome of *Phellinotus piptadeniae* (Basidiomycota, Hymenochaetales) and insights on the phylogeny of Agaricomycetes through comparative mitogenomics. In: X-Meeting 2019, 2019, Campos do Jordão - SP. X-Meeting 2019, 2019.
7. **QUINTANILHA-PEIXOTO, G**; de ARAUJO, D. ; KATO, R. B. ; FONSECA, P. L. C. ; TOME, L. M. R. ; MIRANDA, F. M. ; RAMOS, R. T. J. ; BRENIG, B. ; AZEVEDO, V. A. C. ; BADOTTI, F. ; AGUIAR, E. R. G. R. ; GOES-NETO, A. . The Death Is Red: Analysis of the Predicted Secretome of *Aspergillus welwitschiae*, with Emphasis in Pathogenicity and Carbohydrate Metabolism. In: X-Meeting 2019, 2019, Campos do Jordão - SP. X-Meeting 2019, 2019.
8. TOME, L. M. R. ; SANTOS, M. ; FONSECA, P. L. C. ; **PEIXOTO, G. Q.** ; TOLEDO, A. T. Z. ; de ARAUJO, D. ; GOES-NETO, A. ; BADOTTI, F. . CARACTERIZAÇÃO IN SILICO E FILOGENIA DE HEME-PEROXIDASES DE CLASSE II DE *Trametes versicolor*. In: X-Meeting 2019, 2019, Campos do Jordão - SP. X-Meeting 2019, 2019.
9. **QUINTANILHA-PEIXOTO, G**; SOUZA, M. F. ; VESPOLI, L. S. ; SOUZA FILHO, G. A. ; INTORNE, A. C. . A defesa antioxidante da bactéria *Gluconacetobacter diazotrophicus* em resposta a metais. In: IX Congresso Fluminense de Iniciação Científica e Tecnológica, 2017, Campos dos Goytacazes. IX CONFICT - Ciência, tecnologia e informação no Brasil: Desafios e Transformações, 2017.
10. VESPOLI, L. S. ; SOUZA, S. A. ; LEANDRO, M. R. ; SANTOS, T. ; **QUINTANILHA, G.** ; INTORNE, A. C. ; OLIVEIRA, M. V. V. ; SOUZA FILHO, G. A. . Functional characterization of *acrA* and *acrB* genes (*acrAB*-OprM pump) in *Gluconacetobacter diazotrophicus* PAI 5 reveals its essential role for response to toxic compounds and for plant growth promoting. In: Brazilian-International Congress of Genetics, 2017, Águas de Lindoia - SP. Brazilian-International Congress of Genetics, 2017.
11. BARROSO, L. M. ; **QUINTANILHA, G.** ; GOMES, P. H. ; GRANATO, T. M. ; INTORNE, A. C. . Isolation of plant growth promoting bacteria associated *Typha domingensis*, an emergent aquatic macrophyte. In: 28º Congresso Brasileiro de Microbiologia, 2015, Florianópolis - SC. 28º Congresso Brasileiro de Microbiologia, 2015.
12. **QUINTANILHA, G.**; de SOUZA, T. G. ; VESPOLI, L. S. ; SOUZA FILHO, G. A. ; INTORNE, A. C. . O papel da glutatona na resposta ao estresse por metal em *Gluconacetobacter diazotrophicus*. In: VII Congresso Fluminense de Iniciação Científica e Tecnológica, 2015, Campos dos Goytacazes - RJ. VII Congresso Fluminense de Iniciação Científica e Tecnológica, 2015.
13. de SOUZA, T. G. ; **QUINTANILHA, G.** ; VESPOLI, L. S. ; SOUZA FILHO, G. A. ; INTORNE, A. C. . O papel do manganês na resposta ao estresse por metal na bactéria *Gluconacetobacter diazotrophicus*. In: VII Congresso Fluminense de Iniciação

14. **QUINTANILHA, G.;** VESPOLI, L. S. ; SOUZA FILHO, G. A. ; INTORNE, A. C. . O manganês e a glutatona na resposta ao estresse por metal em *Gluconacetobacter diazotrophicus*. In: XIV Encontro Nacional de Microbiologia Ambiental - ENAMA, 2014, João Pessoa - PB. XIV Encontro Nacional de Microbiologia Ambiental - ENAMA, 2014.
15. **QUINTANILHA-PEIXOTO, G;** CARVALHO, A. O. ; INTORNE, A. C. . Extração de peptídeos antimicrobianos da macrófita aquática flutuante *Salvinia auriculata* Aubl.. In: VI Congresso Fluminense de Iniciação Científica e Tecnológica, 2014, Campos dos Goytacazes. VI Congresso Fluminense de Iniciação Científica e Tecnológica, 2014.
16. **QUINTANILHA, G.;** CARVALHO, A. O. ; INTORNE, A. C. . Isolamento de Peptídeos Antimicrobianos da Macrófita Aquática *Salvinia auriculata* Aubl.. In: XIV Encontro Nacional de Microbiologia Ambiental - ENAMA, 2014, João Pessoa - PB. XIV Encontro Nacional de Microbiologia Ambiental - ENAMA, 2014.

Apresentações de Trabalho

1. **QUINTANILHA-PEIXOTO, GABRIEL;** GOES-NETO, A. ; AGUIAR, E. R. G. R. . Desvendando o Viroma do Sisal. 2021. (Apresentação de Trabalho/Seminário).
2. **QUINTANILHA-PEIXOTO, G.** Introdução à Metagenômica. 2020. (Apresentação de Trabalho/Conferência ou palestra).
3. **QUINTANILHA-PEIXOTO, G.** Bioinformática: Tudo que você precisa saber em 2 horas. 2020. (Apresentação de Trabalho/Conferência ou palestra).
4. **QUINTANILHA-PEIXOTO, GABRIEL;** ALCANTARA, L. C. J. . Virus Research and Surveillance: Bioinformatics, Genetics and Public Health. 2020. (Apresentação de Trabalho/Outra).
5. **QUINTANILHA-PEIXOTO, G;** FONSECA, P. L. C. ; TOME, L. M. R. ; SIERRA, L. A. B. . Fungi-ômicas: um estudo abrangente do mundo dos fungos. 2019. (Apresentação de Trabalho/Conferência ou palestra).
6. **QUINTANILHA-PEIXOTO, G;** BADOTTI, F. ; AGUIAR, E. R. G. R. ; GOES-NETO, A. . Avaliação de Diferentes Estratégias para a Montagem de Genomas Mitocondriais de Fungos. 2019. (Apresentação de Trabalho/Seminário).
7. **QUINTANILHA-PEIXOTO, G.** O maravilhoso mundo dos fungos: heróis e vilões. 2019. (Apresentação de Trabalho/Outra).
8. **QUINTANILHA-PEIXOTO, G;** GOES-NETO, A. . Estudios Multidimensionales en Micología. 2019. (Apresentação de Trabalho/Conferência ou palestra).
9. **QUINTANILHA-PEIXOTO, G;** GOES-NETO, A. . Identificação Bacteriana: Coloração de Gram. 2018. (Apresentação de Trabalho/Conferência ou palestra).
10. **QUINTANILHA-PEIXOTO, G;** VAZ, A. B. M. ; GOES-NETO, A. . Produtos e Serviços Biotecnológicos Utilizando Microorganismos. 2017. (Apresentação de Trabalho/Seminário).
11. **QUINTANILHA-PEIXOTO, G;** TOME, L. M. R. ; VAZ, A. B. M. ; GOES-NETO, A. . Identificação Molecular de Microorganismos. 2017. (Apresentação de Trabalho/Seminário).

Produção técnica

Entrevistas, mesas redondas, programas e comentários na mídia

1. **QUINTANILHA-PEIXOTO, G.** Impactos da biotecnologia na agricultura - estudando a interação planta e microrganismos. 2017. (Programa de rádio ou TV/Entrevista). 📺

Demais tipos de produção técnica

1. **QUINTANILHA-PEIXOTO, G;** HILARIO, H. O. . Montagem e Análises de Genomas. 2020. (Curso de curta duração ministrado/Outra).
2. **QUINTANILHA-PEIXOTO, G;** HILARIO, H. O. . Montagem e Análise de Genomas. 2019. (Curso de curta duração ministrado/Extensão).
3. **QUINTANILHA-PEIXOTO, G;** FONSECA JUNIOR, N. J. . Introdução à Programação. 2019. (Curso de curta duração ministrado/Extensão).
4. **QUINTANILHA-PEIXOTO, G.** X Percuso Formativo em Docência do Ensino Superior. 2019. (Curso de curta duração ministrado/Extensão).
5. **QUINTANILHA-PEIXOTO, G.** Grupo de Colaboração - Tecnologias e Gamificação. 2019. (Curso de curta duração ministrado/Outra).

Patentes e registros

Patente

A Confirmação do status de um pedido de patentes poderá ser solicitada à Diretoria de Patentes (DIRPA) por meio de uma Certidão de atos relativos aos processos

1. **QUINTANILHA-PEIXOTO, GABRIEL;** RAYA, FÁBIO TRIGO ; MARONE, MARINA PUPKE ; CARAZZOLLE, MARCELO FALSARELLA ; PEREIRA, GONÇALO AMARANTE GUIMARÃES ; OLIVEIRA, A. B. ; AGUIAR, E. R. G. R. ; GOES-NETO, A. . INICIADORES, KIT E MÉTODO PARA IDENTIFICAÇÃO DE ASPERGILLUS WELWITSCHIAE E DIAGNÓSTICO MOLECULAR DA PODRIDÃO VERMELHA DE AGAVE SISALANA E SEUS HÍBRIDOS, E USOS. 2022, Brasil.
Patente: Privilégio de Inovação. Número do registro: BR1020220181268, título: "INICIADORES, KIT E MÉTODO PARA

Bancas

Participação em bancas de comissões julgadoras

Outras participações

1. **QUINTANILHA, G..** EDUCAÇÃO AMBIENTAL E CARTOGRAFIA SOCIAL: HORIZONTES PARA PENSAR A EXTENSÃO A PARTIR DO PERTENCIMENTO. 2021. Universidade Federal de Alfenas.
2. **QUINTANILHA, G..** DIALOGANDO COM JOVENS SOBRE AS PRÁTICAS SEXUAIS E A PREVENÇÃO DE INFECÇÕES SEXUALMENTE TRANSMISSÍVEIS. 2021. Universidade Federal de Alfenas.
3. **QUINTANILHA, G..** SEMEANDO QUIZ NAS MÍDIAS SOCIAIS: UMA FORMA DE COMUNICAÇÃO INTERATIVA COM A COMUNIDADE EM MOMENTOS DE PANDEMIA. 2021. Universidade Federal de Alfenas.
4. **QUINTANILHA, G..** DROPS DE FÍSICA NA PANDEMIA. 2021. Universidade Federal de Alfenas.
5. **QUINTANILHA, G..** COSMÉTICA SOCIAL. 2021. Universidade Federal de Alfenas.
6. **QUINTANILHA, G..** QUALIDADE MICROBIOLÓGICA DE AMBIENTES INTERNOS CLIMATIZADOS. 2018. Universidade Federal de Minas Gerais.
7. **QUINTANILHA, G..** ANÁLISE DA QUANTIDADE DE FLÚOR INGERIDA POR PRÉ-ESCOLARES DEVIDO À UTILIZAÇÃO DE DENTIFRÍCIOS E CONSUMO DE ÁGUA FLUORETADA. 2018. Universidade Federal de Minas Gerais.
8. **QUINTANILHA, G..** A PRODUÇÃO DE TEXTOS COMO FORMA DE ARTIGOS LITERÁRIOS: Uma leitura da sociedade pela palavra dos jovens. 2018. Universidade Federal de Minas Gerais.
9. **QUINTANILHA, G..** PREVALÊNCIA DE PESSOAS INFECTADAS COM VERMINOSES E ANÁLISE DA ÁGUA NA REGIÃO DA VÁRZEA DAS FLORES. 2018. Universidade Federal de Minas Gerais.

Eventos

Participação em eventos, congressos, exposições e feiras

1. 23rd Annual Ecological Integration Symposium. 2023. (Simpósio).
2. 9th Plant Breeding Symposium. 2023. (Simpósio).
3. Genome Editing Symposium. 2022. (Simpósio).
4. 1st Symposium of Fungal Diversity and Conservation in Cloud Forests. 2021. (Simpósio).
5. Brazilian Student Council Symposium: Omics and Data Science. 2021. (Simpósio).
6. HackAçu.RestinGO. 2021. (Outra).
7. Workshop de Avaliação Discente do Programa de Pós-Graduação em Bioinformática. 2020. (Outra).
8. X-Meeting 2019. 2019. (Encontro).
9. Darwin Day. 2018. (Outra).
10. 1ª Feira de Ciências da UENF. Atividades do Grupo de Microbiologia Ambiental - LFBM. 2017. (Feira).
11. XIII Semana Nacional de Ciência e Tecnologia. 2016. (Outra).
12. VII Congresso Fluminense de Iniciação Científica e Tecnológica. 2015. (Congresso).
13. II Simpósio de Recursos Hídricos do Rio Paraíba do Sul. 2014. (Simpósio).
14. VI Congresso Fluminense de Iniciação Científica e Tecnológica. 2014. (Congresso).
15. VI Workshop do Núcleo de Desenvolvimento de Insumos Biológicos para a Agricultura (NUDIBA). 2014. (Outra).
16. XIV Encontro Nacional de Microbiologia Ambiental - ENAMA. 2014. (Encontro).
17. I Encontro Científico da Estação Ecológica de Guaxindiba. 2013. (Encontro).
18. V Workshop do Núcleo de Desenvolvimento de Insumos Biológicos para a Agricultura (NUDIBA). 2013. (Outra).
19. III Semana do Meio Ambiente. 2010. (Feira).

Organização de eventos, congressos, exposições e feiras

1. **QUINTANILHA-PEIXOTO, GABRIEL;** FRANCO, GLÓRIA. REGINA ; GÓES-NETO, ARISTÓTELES . VI Curso de Verão em Bioinformática da UFMG. 2022. (Outro).
2. **QUINTANILHA, G..** I Workshop Online de Bioinformática. 2021. (Outro).
3. **QUINTANILHA, G..** IV Curso de Verão em Bioinformática da UFMG. 2020. (Outro).
4. **QUINTANILHA, G..** III Curso de Verão em Bioinformática da UFMG. 2019. (Outro).
5. **QUINTANILHA, G..** IV CIM - Congresso de Inovação e Metodologias no Ensino Superior. 2019. (Congresso).
6. **★ QUINTANILHA, G.;** ALCANTARA, L. C. J. ; AZEVEDO, V. A. C. . Uso de tecnologias de sequenciamento de nova geração na vigilância genômica de Flavivírus emergentes e identificação de novos vírus circulantes. 2018. (Outro).
7. **QUINTANILHA, G..** Ciência na Prática (2017). 2017. .
- 8.

